



TECHNICKÁ UNIVERZITA V LIBERCI
Fakulta textilní



Vlastnosti fotochromných textilií

Disertační práce

Studijní program: P3106 – Textile Engineering
Studijní obor: 3106V015 – Textile Technics and Materials Engineering
Autor práce: **Aravin Prince Periyasamy, M.Tech.**
Vedoucí práce: doc. Ing. Martina Víková, Ph.D.





TECHNICAL UNIVERSITY OF LIBEREC
Faculty of Textile Engineering



Properties of Photochromic Textiles

Dissertation

Study programme: P3106 – Textile Engineering
Study branch: 3106V015 – Textile Technics and Materials Engineering
Author: **Aravin Prince Periyasamy, M.Tech.**
Supervisor: doc. Ing. Martina Víková, Ph.D.



Prohlášení

Byl jsem seznámen s tím, že na mou disertační práci se plně vztahuje zákon č. 121/2000 Sb., o právu autorském, zejména § 60 – školní dílo.

Beru na vědomí, že Technická univerzita v Liberci (TUL) nezasahuje do mých autorských práv užitím mé disertační práce pro vnitřní potřebu TUL.

Užiji-li disertační práci nebo poskytnu-li licenci k jejímu využití, jsem si vědom povinnosti informovat o této skutečnosti TUL; v tomto případě má TUL právo ode mne požadovat úhradu nákladů, které vynaložila na vytvoření díla, až do jejich skutečné výše.

Disertační práci jsem vypracoval samostatně s použitím uvedené literatury a na základě konzultací s vedoucím mé disertační práce a konzultantem.

Současně čestně prohlašuji, že tištěná verze práce se shoduje s elektronickou verzí, vloženou do IS STAG.

Datum:

Podpis:

Contents

| | |
|--|------|
| Declaration..... | viii |
| Acknowledgement | ix |
| List of figures..... | xi |
| List of schemes | xv |
| List of tables..... | xvi |
| List of abbreviations | xvii |
| ABSTRACT..... | 1 |
| ANOTACE | 3 |
| Chapter-1 INTRODUCTION | 5 |
| Chapter-2 LITERATURE REVIEW | 9 |
| 2.1 Introduction and history of Photochromism..... | 9 |
| 2.1.1 Mechanisms of photochromism..... | 11 |
| 2.1.2 Kinetics of photochromism | 16 |
| 2.1.3 Classification of photochromic materials | 17 |
| 2.1.3.1 P-type photochromic materials | 17 |
| 2.1.3.2 T-type photochromic materials | 17 |
| 2.1.4 Photodegradation | 21 |
| 2.2 Interaction between light and matter | 22 |
| 2.2.1 Reflectance | 22 |
| 2.2.2 Transmittance | 22 |
| 2.2.3 Absorbance | 23 |
| 2.3 Kinetics behavior of photochromic materials | 23 |
| 2.3.1 Kinetic model for photochromic materials | 25 |
| 2.3.2 Half-life of color change for photochromic materials | 27 |
| 2.4 Color measurements..... | 28 |
| 2.4.1 Color measurement of photochromic textiles..... | 28 |

| | |
|---|----|
| 2.4.2 Color difference assessment of photochromic materials | 29 |
| 2.5 Conclusion..... | 30 |
| Chapter 3 MASS COLORED miPP FILAMENTS | 31 |
| 3.1 Introduction | 31 |
| 3.1.1 Mass coloration of miPP filament | 31 |
| 3.2 Experimental procedure | 32 |
| 3.2.1 Production of photochromic filaments | 33 |
| 3.2.2 Drawing process | 37 |
| 3.2.3 Winding process | 37 |
| 3.2.4 Measurement of Kinetic properties of photochromic materials | 38 |
| 3.2.5 Thermogravimetry analysis of miPP filaments | 39 |
| 3.2.6 Differential scanning calorimetry of miPP filaments | 39 |
| 3.2.7 Physical & Mechanical properties of miPP filaments | 40 |
| 3.2.8 Microscopic analysis of miPP filaments | 40 |
| 3.3 Results and Discussion of photochromic miPP filaments (circular cross-section)..... | 40 |
| 3.3.1 Effect of photochromic response on drawing ratio of photochromic filaments | 40 |
| 3.3.1.1 Effect of K/S Values on drawing ratio of photochromic filaments | 40 |
| 3.3.1.2 K/S (max) of photochromic miPP filaments during the exposure phase..... | 49 |
| 3.3.1.3 Changing in optical density of photochromic miPP filaments | 53 |
| 3.3.1.4 Half-life of color change for photochromic miPP filaments | 56 |
| 3.3.1.5 Color difference analysis of miPP filaments | 61 |
| 3.3.2 Physical and mechanical properties of photochromic miPP filaments..... | 64 |
| 3.3.2.1 Linear density of photochromic miPP filaments | 64 |
| 3.3.2.2 Tensile strength of photochromic miPP filaments..... | 65 |
| 3.3.2.3 Elongation at break of photochromic miPP filaments | 67 |
| 3.3.2.4 Elastic modulus of photochromic miPP filaments..... | 67 |
| 3.3.3 Thermogravimetric Analysis of miPP filaments | 69 |

| | |
|--|-----|
| 3.3.4 Differential scanning calorimetry analysis on miPP filaments | 70 |
| 3.3.5 Surface morphological analysis of miPP filaments | 76 |
| 3.4 Results and Discussion of photochromic miPP filaments (non-circular) | 78 |
| 3.4.1 Optical properties | 78 |
| 3.4.2 Surface morphological analysis of miPP non-circular filaments | 80 |
| 3.5 Conclusion..... | 82 |
| Chapter 4 SOL-GEL PHOTOCHROMIC FABRIC..... | 83 |
| 4.1 Introduction | 83 |
| 4.1.1 Sol-gel coating on PET fabric | 83 |
| 4.1.1.1 Dip coating method..... | 85 |
| 4.2 Experimental procedure for sol-gel coating | 85 |
| 4.2.1 Silica sol-gel synthesis and coating on fabrics | 86 |
| 4.2.2 Measurement of kinetic properties of photochromic PET fabric | 89 |
| 4.2.3 Effect of abrasion durability on photochromic response | 90 |
| 4.2.4 Effect of washing durability on photochromic response | 90 |
| 4.2.5 Uptake % of the coated fabric | 90 |
| 4.2.6 Effect of physical properties of sol-gel coated fabrics | 91 |
| 4.2.7 Surface morphological analysis of sol-gel coated fabric | 91 |
| 4.2.8 Surface roughness analysis of sol-gel coated fabrics | 92 |
| 4.3 Results and discussion on sol-gel coated photochromic fabrics | 92 |
| 4.3.1 Effect of photochromic response on the sol-gel coating | 92 |
| 4.3.1.1 Effect of K/S Values on drawing ratio of photochromic filaments | 92 |
| 4.3.1.2 K/S (max) functions on sol-gel coated fabrics under exposure phase | 96 |
| 4.3.1.3 Half-life of color change for sol-gel coated fabric..... | 99 |
| 4.3.1.4 Color difference analysis of sol-gel coated fabric | 103 |
| 4.3.1.5 Effect of silica sol networks on optical and physical properties..... | 104 |
| 4.3.1.6 Uptake % of the coated fabric and their photochromic response | 105 |

| | |
|--|-----|
| 4.3.2 Hypsochromic shift on sol-gel coated fabrics | 106 |
| 4.3.3 Effect of abrasion durability on photochromic response | 109 |
| 4.3.4 Effect of washing durability on photochromic response | 110 |
| 4.3.5 Effect of physical properties of sol-gel coated fabrics | 112 |
| 4.3.5.1 Thickness and areal density of coated fabrics..... | 112 |
| 4.3.5.2 Bending length, flexural rigidity and bending modulus of coated fabrics..... | 113 |
| 4.3.6 Surface morphological analysis on sol-gel coated fabric | 115 |
| 4.3.7 Surface roughness analysis on sol-gel coated fabrics..... | 116 |
| 4.4 Conclusion..... | 118 |
| Chapter-5 COMPARISON RESULTS OF BOTH THE TECHNIQUES | 119 |
| 5.1 Kinetics response of photochromic change on a different substrate | 119 |
| Chapter-6 CONCLUSION..... | 122 |
| 6.1 Photochromic miPP filaments..... | 122 |
| 6.2 Photochromic PET fabric | 125 |
| 6.3 Suggestion for future work..... | 130 |
| Chapter-7 NEW FINDINGS OF THE RESEARCH | 131 |
| Chapter-8..... | 134 |
| 8.1 Appendix | 134 |
| 8.2 References | 146 |
| List of Publications | 157 |
| Research Manuscripts | 157 |
| Book Chapter..... | 157 |
| Book | 158 |
| International Conferences / Workshops | 158 |
| Curriculum Vitae..... | 159 |

Declaration

I hereby declare that the material in this thesis, herewith I now submit for the assessment of PhD defense is entirely my own work, that I have taken precautionary measures to ensure that the work is original and does not to the best of my knowledge breach any copyright law and hasn't been extracted from the work of others save and to the extent that such work has been cited and acknowledged within the text of this work.

The core theme of this thesis is *Properties of Photochromic Textiles* and contains 3 original papers published in impact factor journals, 2 more papers are submitted and 2 papers is under preparation. Also, 2 book chapters and 5 papers published in conference proceedings. The idea, development and write up of all the published work related to this thesis were the principal responsibility of me (the candidate working in the Department of Material Engineering, Faculty of Textile engineering, Technical University of Liberec, Czech Republic), under the supervision of Assoc. Prof. Martina Vikova, M.Sc, PhD.

Name: Aravin Prince Periyasamy, M.Tech.

Signature:

Student Number: T14000558

Date: June, 2018

Acknowledgement

I take this opportunity with immense pleasure to express my deep sense of gratitude to my thesis supervisor, Assoc. Prof. Martina Vikova, M.Sc, PhD, Associate Professor, Laboratory of Color and Measurement, Department of Material Engineering, Technical University of Liberec, for the continuous support of my PhD study and related research, for her patience, motivation, and immense knowledge. Her dedication, keen interest and guidance which helped me in all the time of research and writing of this thesis. I could not have imagined having a better supervisor and mentor for my PhD study. I do sincerely acknowledge the freedom rendered to me by her for independent thinking, planning and executing the research.

I am profound gratitude to Assoc. Prof. Michal Vik, M.Sc, PhD, Associate Professor, Head of Laboratory of Color and Measurement, Department of Material Engineering, Technical University of Liberec, my study consultant, for his inspiration, valuable discussion, cooperation and constant encouragement, which resulted in this work, will remain a lifelong memory. I thank him for his excellent guidance, sincere advice, understanding and unstinted support during all the tough times of my PhD life. I consider very fortunately for my association with him, which has given a decisive turn and a significant boost in my career.

I would also like to thank to Prof. Tong Lin, M.Sc, PhD, Yan Zhao, M.Sc, PhD and Haito Niu, M.Sc, PhD, during our discussions especially during my stays in IFM, Deakin University-Geelong, Australia as visiting student.

I thank profusely all the staffs of the department of material engineering, the Technical University of Liberec for their kind help and co-operation throughout my study period. I also thank Miroslava Pechociakova, M.Sc, PhD for the initial training she gave me in using the TGA, DSC machines and Assoc. Prof. Pavel Pokorny, M.Sc, PhD for providing the syringe pump. I would like to say a big thank you to my work colleagues in the department especially Marcela Pechova, M.Sc and Marketa Kasparova, M.Sc who we always shared the perils of doctoral research. Also, I would like to express my gratitude to all my teachers who put their faith in me and urged me to do better.

Last but not least, I wouldn't be where I am today without the support from my family, you have been an inspiration. My wife and daughter, you always inspired me to move on.

In God I Trust

Aravin Prince Periyasamy

List of figures

| | |
|---|----|
| Figure 1: Application of photochromic materials in the various fields. | 6 |
| Figure 2: Graphic representation of a photochromic system (<i>A</i> -colorless; <i>B</i> -colored form)... | 11 |
| Figure 3: The Jablonski-diagram for the representation of electronic, radiative and non-radiative transitions (Adapted and modified from [17])..... | 12 |
| Figure 4: Typical behavior of a photochromic compound under UV radiation (Adopted and modified from [14, 22])...... | 16 |
| Figure 5: Various kinetic reactions of the photochromic system (adopted & modified from [25]). | 18 |
| Figure 6: Summary of substituent effects in 5-chloro-1,3,3-trimethylspiro[indoline-2,3'-(3H)naphtho(2,1-b) (1,4)-oxazine]..... | 19 |
| Figure 7: Structure modification on spirooxazine with its final color [12]. | 19 |
| Figure 8: Photodegradation yield of 1,3,3-trimethyloxindole (a), 3,3-dimethyloxindole (b) 1,2,3,4-tetrahydro-2,3-dioxo-4,4-dimethylquinoline (c) [21]. | 22 |
| Figure 9: A kinetic model of exposure & reversion phase of photochromic materials [16]. .. | 26 |
| Figure 10: Scheme of LCAM designed Spectrophotometer (Photochrom-3). | 29 |
| Figure 11: Chemical structure of three commercial photochromic pigments used for this study [74, 75]. | 33 |
| Figure 12: The process sequence of photochromic miPP filaments manufacturing..... | 35 |
| Figure 13: Schematic representation of drawing process (i.e. <i>V1</i> - feed roller; <i>V2</i> - take-off roller). | 37 |
| Figure 14: The reflectance spectrum of used photochromic pigments under UV-radiation,... | 41 |
| Figure 15: Produced photochromic miPP filaments (<i>A</i>); filament winded on cardboard <i>B</i> & <i>C</i> (<i>B</i> -UV off; <i>C</i> -UV on). | 41 |
| Figure 16: Kubelka-Munk characteristics miPP filaments (MPP-2.5 wt.%) under 5 minutes of exposure phase..... | 44 |
| Figure 17: Kubelka-Munk characteristics miPP filaments (MPP-2.5 wt.%) under 5 minutes of reversion phase. | 44 |
| Figure 18: Conversion of photochromic system (<i>A</i> → <i>B</i> - exposure) and (<i>B</i> → <i>A</i> - reversion) (MPP 2.5 wt.%). | 45 |
| Figure 19: Thickness of 6 layers of the produced filament in the card board (MPP-0 wt.%). .. | 46 |
| Figure 20: Reflectance spectra of photochromic miPP filaments (MPP-0.5 wt.%) | 47 |
| Figure 21: Effect of DR on <i>K/S</i> values of photochromic miPP filaments (MPP-0.25 wt.%).. | 47 |

| | |
|--|----|
| Figure 22: Effect of DR on K/S values of photochromic miPP filaments (MPP-0.50 wt.%). | 48 |
| Figure 23: Effect of DR on K/S values of photochromic miPP filaments (MPP-1.50 wt.%). | 48 |
| Figure 24: Effect of DR on K/S values of photochromic miPP filaments (MPP-2.50 wt.%). | 49 |
| Figure 25: Dependence of K/S (max) on the photochromic miPP filaments with MPP under exposure phase..... | 50 |
| Figure 26: Dependence of K/S (max) on the photochromic miPP filaments with MPB under exposure phase..... | 51 |
| Figure 27: Dependence of K/S (max) on the photochromic miPP filaments with MPY under exposure phase..... | 51 |
| Figure 28: Dependence of K/S (max) for various photochromic miPP filaments (DR-2) under exposure phase..... | 52 |
| Figure 29: Dependence of ΔOD on the photochromic miPP filaments with MPP..... | 54 |
| Figure 30: Dependence of ΔOD on the photochromic miPP filaments with MPB. | 55 |
| Figure 31: Dependence of ΔOD on the photochromic miPP filaments with MPY. | 55 |
| Figure 32: Dependence of ΔOD on the various photochromic miPP filaments (DR-2)..... | 56 |
| Figure 33: Half-life of color change on miPP filaments under exposure phase (DR-2)..... | 59 |
| Figure 34: Half-life of color change on miPP filaments under reversion phase (DR-2). | 59 |
| Figure 35: Half-life of color change on miPP filaments under exposure phase, | 60 |
| Figure 36: Half-life of color change on miPP filaments under reversion phase,..... | 60 |
| Figure 37: Residual ΔE^* values for photochromic miPP filament with MPP..... | 63 |
| Figure 38: Residual ΔE^* values for photochromic miPP filament with MPB. | 63 |
| Figure 39: Residual ΔE^* values for photochromic miPP filament with MPY. | 64 |
| Figure 40: Filament molecular model (Peterlin model) of structure transformation during the drawing process (adopted and modified from [86, 87]). | 66 |
| Figure 41: Effect of drawing ratio on various physical properties (MPP-0.25 wt.%). | 68 |
| Figure 42: Impact of pigment concentration on various physical properties (DR-1). | 69 |
| Figure 43: TGA analysis of photochromic pigments..... | 70 |
| Figure 44: DSC test of miPP filament (i.e. DR-1, MPB- 0 wt.%). | 72 |
| Figure 45: Normalized DSC curves for miPP filaments, (MPP=0.0 wt.%). | 74 |
| Figure 46: Normalized DSC curve of MPP incorporated miPP filament (DR-1). | 74 |
| Figure 47: Normalized DSC curve of MPP incorporated miPP filament (DR-4). | 75 |
| Figure 48: Effect of pigment concentration on T_m | 75 |
| Figure 49: Effect of drawing ratio on T_m | 76 |

| | |
|--|-----|
| Figure 50: Longitudinal view of Photochromic miPP filaments with a circular cross-section, | 77 |
| Figure 51: Cross-sectional view of photochromic miPP filaments with a circular cross-section, (A) unpigmented circular shape; (B) circular shape with 2.5 wt.% MPP; | 78 |
| Figure 52: Longitudinal view of non-circular Photochromic miPP filaments,..... | 80 |
| Figure 53: Cross-sectional view of non-circular photochromic miPP filaments,..... | 81 |
| Figure 54: Cross-sectional view of non-circular photochromic miPP filaments,..... | 82 |
| Figure 55: Schematic representation of Sol-gel coating method, | 84 |
| Figure 56: Chemical structure of PhTES, OTES, APS and TAS. | 86 |
| Figure 57: The sequencing process for the sol-gel coating process..... | 89 |
| Figure 58: Schematic representation of surface roughness analysis..... | 92 |
| Figure 59: Visible reflection spectrum of sol-gel (OTES) coated fabric with MPP pigment.. | 93 |
| Figure 60: Photochromic sol-gel coated fabric, (A) indicates the fabric coated with APS precursor and (B) indicates the fabric coated with OTES precursor (Colored portion indicates the influence of UV radiation)..... | 94 |
| Figure 61: Effect of the precursor on the K/S values of coated fabrics (MPP-2.0 wt.%). | 95 |
| Figure 62: K/S values of OTES coated fabric (MPP-2.50 wt.%) under 5 minutes of exposure phase (UV-on). | 95 |
| Figure 63: K/S values of OTES coated fabric (MPP-2.50 wt.%) under 5 minutes of reversion phase (UV-off)..... | 96 |
| Figure 64: Dependence of K/S (max) on the sol-gel coated fabric under exposure phase. | 98 |
| Figure 65: Dependence of ΔOD on the sol-gel coated fabric. | 98 |
| Figure 66: Dependence of K/S (max) on sol-gel coated fabric (MPP-2.50 wt.%) under exposure phase..... | 99 |
| Figure 67: Half-life of color change during exposure phase of coated fabric. | 100 |
| Figure 68: Half-life of color change during reversion phase of coated fabric..... | 101 |
| Figure 69: Impact of precursors on the half-life of color change (MPP-2.5 wt.%). | 101 |
| Figure 70: Residual ΔE^* for the sol-gel coated fabric..... | 104 |
| Figure 71: Reflectance spectra of coated fabric with different precursors (MPP-2.5%)..... | 107 |
| Figure 72: Schematic interpretation of hypsochromic shift on precursors polarity..... | 108 |
| Figure 73: Abrasion durability of coated fabrics on photochromic response (MPP-2.5 wt.%). | 110 |
| Figure 74: Washing durability of coated fabric on photochromic response (MPP-2.5 wt.%). | 111 |

| | |
|--|-----|
| Figure 75: Flexural rigidity of sol-gel coated fabric (MPP-2.5 wt.%) | 114 |
| Figure 76: Bending modulus of sol-gel coated fabric (MPP-2.5 wt.%) | 115 |
| Figure 77: Surface morphological characterization of sol-gel coated fabric | 116 |
| Figure 78: LSCM images photochromic fabrics with (A) control PET fabric and modified with (B) OTES; (C) O:P (2:1); (D) P:O (2:1) (E) APS and (F) PhTES precursors (MPP-2.5 wt.%) | 117 |
| Figure 79: K/S (max) of photochromic textiles with different technique with respect to their relative concentrations | 119 |
| Figure 80: Half-life of color change photochromic textiles (i.e. MPP-2.5 wt.%) | 120 |
| Figure 81: Rate constant of photochromic textiles (i.e. MPP-2.5 wt.%) | 121 |
| Figure 82: Reflectance spectra of MPP coated fabric with different precursors | 127 |

List of schemes

| | |
|--|----|
| Scheme 1: Photochromic reactions of pyrans with heterolytic cleavage [16]. | 14 |
| Scheme 2: Homolytic cleavage for hexaphenylbisimidazole (Adopted and modified [57])... | 15 |
| Scheme 3: Trans-Cis isomerization of azobenzene (Adopted and modified from [57]). | 15 |
| Scheme 4: Tautomerism in salicylidene anils [20]. | 15 |
| Scheme 5: The photochromic reaction of spiropyrans. | 17 |
| Scheme 6: Photochromic reaction of spirooxazines. | 20 |
| Scheme 7: Photochromic reaction of naphthopyrans, | 21 |
| Scheme 8: Possible pathway of photoisomerization of photochromic colorants (i.e. <i>A</i> -colorless; A^{SES} - singlet energy state; A^{TES} - triplet energy state; <i>Q</i> and <i>U</i> - short-lived intermediates; <i>B</i> - colored isomer (adopted and modified from [79]). | 62 |
| Scheme 9: Hydrolysis and condensation reaction of OTES. | 87 |
| Scheme 10: Hydrolysis and condensation reaction of APS. | 88 |
| Scheme 11: Hydrolysis and condensation reaction of PhTES. | 88 |

List of tables

| | |
|---|-----|
| Table 1: Commercial photochromic pigments used for the production of mass colored filaments. | 33 |
| Table 2: Parameters used in melt spinning for the production of miPP filaments. | 34 |
| Table 3: Details of photochromic miPP filaments with a circular cross-section. | 36 |
| Table 4: A details of the photochromic miPP filaments with non-circular cross-sections. | 36 |
| Table 5: Thermal and crystallinity properties of miPP filaments with respect to various drawing ratio (i.e. without the addition of photochromic pigment). | 71 |
| Table 6: Thermal and crystallinity properties of miPP filaments with respect to their photochromic pigments (i.e. DR-1). | 73 |
| Table 7: Thermal and crystallinity properties of miPP filaments with respect to their photochromic pigments (i.e. DR-4). | 73 |
| Table 8: The K/S (max) on the different cross-sections of the produced filament (DR-1) under exposure phase. | 79 |
| Table 9: The K/S (max) on the different cross-sections of the produced filament (DR-2) under exposure phase. | 79 |
| Table 10: Commercial photochromic pigment used to produce photochromic fabrics. | 85 |
| Table 11: Various physical properties of Raw PET fabric. | 86 |
| Table 12: Recipe and coating conditions. | 87 |
| Table 13: Comparison of optical properties of photochromic filaments and fabrics. | 102 |
| Table 14: Uptake %, and K/S (max) (MPP-2.50 wt.%) of coated fabrics. | 106 |
| Table 15: Physical properties of the sol-gel coated fabric (MPP-2.5 wt.%) | 112 |
| Table 16: Surface roughness characteristics of coated fabric (MPP-2.5 wt.%) | 117 |

List of abbreviations

| | |
|-----------------|---|
| Φ_v | : Radiometric power |
| Δa^* | : Difference in redness to greenness |
| Δb^* | : Difference in yellowness to blueness |
| ΔE^* | : Color difference |
| ΔL^* | : Difference in lightness |
| ΔH_m | : Change in melting enthalpy |
| ΔOD | : Changing in optical density |
| ΔS_m | : Change in entropy |
| λ_{max} | : Absorbance maximum in the absorption spectrum |
| A | : Colorless form of photochromic materials |
| APS | : Amino propyltriethoxy silane |
| ASTM | : American Society for Testing and Materials |
| B | : Colored form of photochromic materials |
| CC | : cis-cis |
| CIE | : International Commission on Illumination |
| CT | : cis-trans |
| DSC | : Differential scanning calorimetry |
| DR | : Drawing ratio |
| HALS | : Hindered amine light stabilizer |
| H_m | : Melting enthalpy |
| $h\nu_1$ | : UV radiations |
| $h\nu_2$ | : Without UV radiations |
| ISE | : Inter system conversion |
| ISO | : International Organization for Standardization |
| IUPAC | : International Union of Pure and Applied Chemistry |
| k | : Rate constant |
| K | : Absorption coefficient |
| K/S | : Kubelka-Munk functions |
| $K/S_{(max)}$ | : Kubelka-Munk functions maximum values at exposure phase |
| LCAM | : Laboratory of color and appearance measurement |
| L/D | : Length to diameter |

| | |
|-------------------|--|
| LSCM | : Laser scanning confocal microscope |
| MC | : Merocyanine |
| MFI | : Melt flow index |
| miPP | : Metallocene catalyst isotactic polypropylene |
| MPB | : Matsui Photopia Blue |
| MPP | : Matsui Photopia Purple |
| MPY | : Matsui Photopia Yellow |
| OTES | : Octyltriethoxysilane |
| O:P | : Octyltriethoxy silane: Phenyltriethoxy silane (67:33 mole ratio) |
| PA-6 | : Nylon 6 |
| PAN | : Polyacrylonitrile |
| PET | : Polyethylene terephthalate |
| PhTES | : Phenyltriethoxysilane |
| P:O | : Phenyltriethoxy silane: Octyltriethoxy silane (67:33 mole ratio) |
| PP | : Polypropylene |
| R _p | : Maximum peak height |
| R _v | : Maximum valley depth |
| R _z | : Maximum height profile |
| S ₀ | : Singlet ground state |
| S ₁ | : First singlet excited state |
| S ₂ | : Second singlet excited state |
| S | : Scattering coefficient |
| SCE | : Specular component excluded |
| SEM | : Scanning electron microscope |
| SP | : Spiropyran |
| SPD | : Spectral power distributions |
| SPO | : Spirooxazines |
| t ₀ | : Start of UV irradiation |
| t ₁ | : End of UV irradiation |
| t _{1/2} | : half-life |
| t _{1/2E} | : Half-life during exposure phase |
| t _{1/2R} | : Half-life during reversion phase |
| T ₁ | : First triplet excited state |
| T ₂ | : Second triplet excited state |

| | |
|----------------|--|
| TAS | : Triacetoxymethylsilane |
| TC | : trans-cis |
| T _d | : Drawing temperature |
| T _g | : Glass transition temperature |
| TGA | : Thermogravimetry analysis |
| T _m | : Melting temperature |
| TT | : trans-trans |
| UV | : Ultra violet radiation |
| Vis | : Visible region of electromagnetic spectrum |
| X _c | : Crystallinity |

ABSTRACT

Textile materials are one of the basic needs for the human life after food and shelter. It can be applied in various forms from clothing to high tech applications such as protective textiles, medical textiles, geo textiles and sports textiles. Due to the environmental changes, there is a high chance of getting skin cancer, eye damages and immune system damages due to ozone layer depletion. Skin cancer is one of the most effective threaten to the human being and everyone is cringed in these regards. Therefore, it gives immense inspiration to prepare the UV sensor based on incorporating the various photochromic pigments in to textile materials. In this regard, take more attention to prepare the mass colored polypropylene filaments and sol-gel coated with photochromic pigments and which can able to use as flexible UV-sensor. For the production of mass coloration, metallocene catalyst polypropylene (miPP) filaments were chosen due to many features. The mass colored filaments were produced with various concentrations as well as different color. Also, the filaments were produced with different cross-sections. On other hand, different precursors are used to preparing the sol-gel solution along with photochromic pigment which later applied to PET fabrics. After production, it applied to different drawing ratio, object of this research to investigate how the drawing ratio is affected the various optical properties like K/S functions, changes in optical density, color difference by ΔE^* (CIE 1976), half-life of color change in during exposure and reversion phase, rate constant, color intensity in beginning, at half of the cycle and color intensity at infinitive were studied. Apart from optical properties, it also investigated the various physical properties like tensile strength, elongation at break, flexural rigidity and bending modulus. In the case of sol-gel coating, since different precursors are used, therefore it is required to investigate the precursors impact on the various optical properties as like the same properties which above mentioned was analyzed. Thermal analysis was done with pigments by TGA to get an idea for the thermal properties and DSC analysis could be done with produced filaments to know the impact on drawing ratios. The laser scanning confocal microscope analysis helps to find the surface roughness after the coating process. Finally, SEM analysis could be done to understand the surface modifications of both filaments and fabrics. The overall photochromic response is depending on the drawing ratio on the filaments, whereas the fabric is depending on the precursors which used in the sol-gel coated fabric. The miPP filaments generally showed a good stability of photocoloration during the color measurement and the optical density have been reduced with increasing the fineness of the miPP filament. Thermal degradation is varied with respect to the photochromic pigments it can be confirmed by TGA results, it is due to their

structures, highest degraded pigment shows less photochromic response than another one. In fact, the thermal analysis can give an idea that how the drawing ratio changes its crystallinity % and melting temperature, however, the drawing ratio positively increased all these properties. The surface characterization confirms that there is no change in case of unpigmented and colored filaments. In some case, it shows some micro fibrils, which is due to their cross sections and nor on the pigment addition or process conditions. On other hand, the photochromic response for the fabric was depending on the precursor and its combinations, in some case the reflectance spectrum was shifted, which denoted as hypsochromic shift. This shift is due to the polarity of the precursors. Also, the precursors have a strong influence on the physical and handle properties. The surface characterization confirms that there is a deposition of precursors in the fabrics, laser scanning confocal microscopy analysis showed significant changes in the surface micro-roughness after coating.

ANOTACE

Textilní materiály jsou jednou ze základních potřeb lidského života po jídle a přístřeší. Tyto materiály mohou být využity v různých formách oděvů až po high-tech aplikace jako jsou ochranné textilie, textilie využívané v medicíně, geo-textilie nebo sportovní textilie. Vzhledem ke globálním změnám klimatu se zvyšuje možnost onemocnění rakoviny kůže, poškození očí a imunitního systému v důsledku snížení ozónové vrstvy. Rakovina kůže je jednou z nejefektivnějších rakovin, která ohrožuje lidské bytí a každý je v tomto ohledu ohrožen. Tento fakt poskytuje inspiraci pro přípravu UV senzorů/čidel založených na zabudování různých fotochromních pigmentů do textilních materiálů. Tato práce se věnuje především přípravě barvených polypropylenových filamentů ve hmotě a materiálům s povrchově nanesenými fotochromními pigmenty, které mohou být využity jako flexibilní UV-senzory. Pro barvení ve hmotě byly vybrány, vzhledem k mnoha svým vlastnostem, metalocen-katalycké-polypropylenové (miPP) filamenty. Výsledné filamenty byly vyrobeny s různou koncentrací a stejně tak i s různým odstínem, jakožto i s různým příčným řezem. Na druhou stranu, pro přípravu sol-gel roztoků byly použity různé prekursorů společně s fotochromními pigmenty, které byly následně aplikovány na polyesterové tkaniny. To bylo aplikováno s různým dlouhým poměrem. Cílem tohoto výzkumu je studium, jak dlouhý poměr ovlivňuje různou optické vlastnosti, např. Kubelka-Munkovu funkci, změnu optické propustnosti, barevný rozdíl ΔE^* vyjádření pomocí CIE 1976, poločas barevné změny během osvitové a reverzní fáze, rychlostní konstantu, intenzitu odstínu na začátku, v polovině a na konci cyklu. Vedle optických vlastností byly zkoumány různé fyzikální vlastnosti jako pevnost v tahu, prodloužení při přetržení, ohybová tuhost a pevnost v ohybu. V důsledku použití různých prekursorů u sol-gelů, bylo zkoumáno, jak tyto prekursorů ovlivňují optické vlastnosti, tak i fyzikální vlastnosti uvedené výše. Tepelná analýza byla provedena pomocí termogravimetrické metody ke zjištění tepelné degradace filamentů. Diferenční skenovací kalorimetrie byla použita pro zjištění, jak tepelná degradace ovlivňuje dlouhý poměr filamentů. Konfokální laserová skenovací mikroskopie (SEM) byla použita pro zjištění povrchových drsností způsobených nanásecím procesem. SEM analýza může být provedena pro pochopení povrchových modifikací filamentů a tkanin. U filamentů závisí celková fotochromní změna na dlouhým poměru, zatímco u tkanin s aplikovaným sol-gelem je tato změna závislá na použitém prekursoru. Polypropylenové filamenty obecně vykazovaly dobrou barevnou změnu během měření a optická hustota se snižovala se zvyšující se jemností použitých polypropylenových filamentů. Tepelná degradace se liší s ohledem na typ fotochromního pigmentu, což lze potvrdit výsledky TGA analýzy na základě jejich struktury. Více degradovaný pigment vykazuje nižší

fotochromní odvezu než ostatní. Na základě tepelné analýzy lze získat myšlenku, jak změna dloužícího poměru může ovlivnit krystalinitu a teplotu tání. Avšak dloužící poměr pozitivně zvyšuje všechny tyto vlastnosti. Povrchová analýza potvrdila, že v případě nepigmentovaných a barevných filamentů nedochází k žádným změnám. V některých případech se objevují mikrofibrily, které nemají díky svému příčnému řezu vliv na procesní podmínky. Povrchová analýza potvrdila, že není žádný rozdíl mezi nepigmentovanými a barvenými filamenty. V několika případech (8-cípe) se mikrofibrily objevily na povrchu filamentů. Avšak analýza prokázala, že neexistuje vztah mezi přidáním pigmentů a generací těchto mikrofibril. Na druhé straně lze říci, že fotochromní odpověď závisí na typu prekurzoru. V několika případech došlo k posunu maximální vlnové délky směrem k nižším vlnovým délkám. Hypsochromní posun je způsoben polaritou prekurzorů. Prekurzory mají velký vliv na fyzikální a povrchové vlastnosti. Povrchová analýza potvrdila, že v tkaninách dochází k ukládání prekurzorů. SEM analýza ukázala významné změny povrchové mikrostruktury po nanášení sol-gelů.

Chapter-1 INTRODUCTION

In our day to day life, for various application such as clothing, furnishing and for technical uses such as protective clothing, medical textiles and geotextiles, therefore, textile materials are essential. The creative idea of imparting colors into textiles has an extended application of these materials. In 2500 BC, ancient Egyptians who applied color to their clothing have delivered the pleasure of colors have been beyond the thinking of them, and the consequent development of colorants from natural dyes derived from the plants which are used for introduction of different colors on various textiles materials through the modern synthetic dyes. One of the well-established technologies is to introduce colors to textiles. Under the influence of external stimuli such as light, heat or chemical process, these particular colorants possess the ability to undergo reversible color change. Photochromic colorants are a class of unusual colorants which undergo reversible color change stimulated by applying light of different wavelengths which is an example of color changeable materials. Due to the color changing properties, it is shown that potential applications such as ophthalmic sun-screening applications, flexible sensors, security printing, optical recording and switching, solar energy storage, nonlinear optics and biological systems (Figure 1). However, the production of photochromic textiles offers color changeable fabrics which may be used as fashionable textiles, security prints and ultraviolet (UV) sensitive textiles such as a visual alarm for a signal indicating the high levels of UV radiation in specific areas. There are many photochromic materials, spirooxazines (SPO) having significant interest since it has good fatigue resistance and relative ease of synthesis towards to their intense color generation properties. Due to a ring-opening reaction, the existing range of products generally undergoes positive photochromism, a light-induced transition from colorless to color. The aim of this research work is to find the impact of different drawing ratio on physical, mechanical and optical properties of mass colored photochromic polypropylene filament as well as the impact of the precursor on optical and physical properties of sol-gel photochromic coated fabrics. For mass coloration, polypropylene (PP) was chosen since it is most versatile polymer available currently with the huge potential application, such as plastics, filaments, textile fabrics, medical devices and etc. The advantages of PP, it has good resistance to the chemicals, solvents, having good impact strength and excellent abrasion resistance. Since, non-polar in nature, and having the aliphatic structure, high stereoregularity and high crystallinity, therefore, coloration of polypropylene is very difficult on classical methods of dyeing as like other fibers. Nevertheless, mass coloration can solve such issues and helps to make coloration of PP textiles. However, this technique provides better dispergation and

homogenization properties of dyed PP textiles. Based on these advantages and the fact behind the dyeability of PP, it is decided to produce photochromic polypropylene filaments through mass coloration techniques. The end product of polypropylene is mainly depended on the degree of orientation, which can be obtained by the drawing process with different ratios. SPO based photochromic pigments were used for this study, the pigments are formulated with many additives which include, hindered amine light stabilizer (HALS). However, these additives are not only impaired the tensile strength but also show some significant changes in the optical and physical properties. The second technology which is used to produce the photochromic materials are sol-gel coating technology, by using this technology, photochromic pigments can be incorporated into textile fabrics. Polyethylene terephthalate (PET) was chosen for the sol-gel coating since it has many advantages as compared other synthetic fibers, particularly more resistant to wear and tear, good durability, good resistance to chemicals except strong alkalis. In this work, different types of precursors are used to study on their impact of optical, physical properties.

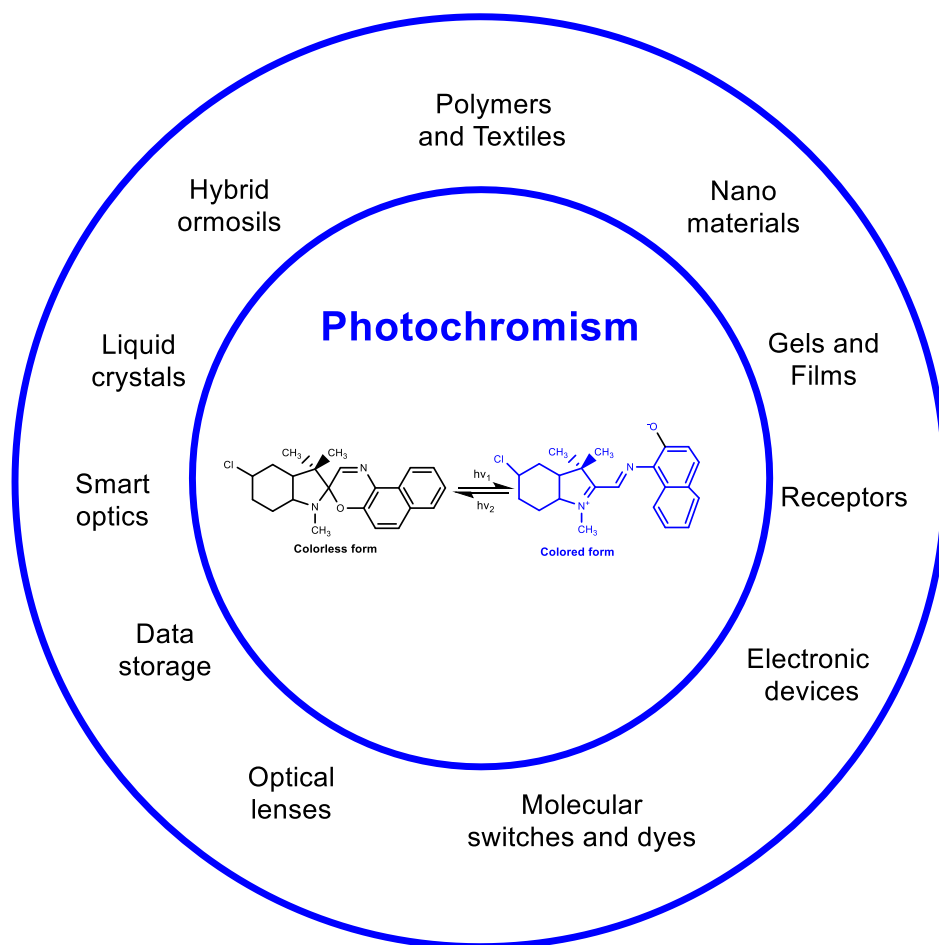


Figure 1: Application of photochromic materials in the various fields.

Structure of the Thesis

This thesis consists of eight chapters as follows.

Chapter 1 gives an introduction to the thesis which includes the specific aims and objectives of this study.

Chapter 2 contains a review of the literature on photochromism and its history, types, the mechanism involved. It also reviewed the basics of optics, color measurement of photochromic textile materials.

Chapter 3 provides the information on the materials and methods which involved to produce the mass coloration of polypropylene filaments. In this chapter, the deep discussion on characterization and analysis techniques which is used to determine the various properties like kinetic, physical and thermal properties of produced photochromic miPP filaments. Also, it describes on the basis of results which were obtained and discussion on the mass colored miPP filaments. This investigation carried out with photochromic properties of mass colored filaments with respect to the drawing ratio. The physical, thermal and mechanical properties also examined and how it influenced on the photochromic properties were discussed in this chapter.

Chapter 4 gives information on the materials, technological factors which are involved to produce photochromic fabrics via sol-gel coating technology. In this chapter, the deep discussion on characterization and analysis techniques which is used to determine the various properties like physical, handling and kinetic properties of produced photochromic fabrics. Also, it describes the results on photochromic properties of sol-gel coated fabric with respect to the precursor composition. The physical and mechanical properties also examined and how it influenced on the photochromic properties were discussed in this chapter.

Chapter 5 describes the combine results of mass coloration and sol-gel coating technology in terms of kinetic properties.

Chapter 6 covers the overall conclusion which drawn from this investigation in terms of two technologies and their influence on photochromic performance. Also, this chapter suggests the potential possibilities for the future work.

Chapter 7 provides the new finding from this work.

Chapter 8 provides the extensive list of reference which is used for this study. The various photochromic parameters like half-life, the rate constant, various stages of shade intensity, physical and mechanical properties of miPP filaments and PET fabrics were given as appendices, and the list of publications was provided at the end of the thesis.

Chapter-2 LITERATURE REVIEW

2.1 Introduction and history of Photochromism

One flourishing field in photochemistry is photochromism [1]. During the 1950's, Hirschberg suggested the use of the term photochromism to describe the phenomenon of color change on exposure to light, a word which is derived from two Greek words, $\Phi\omega\varsigma$ (phos) meaning light and $\chi\rho\omega\mu\alpha$ (chroma) meaning color, with the suffix (-ism) which means phenomenon. Photochromism is defined by the international union of pure and applied chemistry (IUPAC) as a "*Light-induced reversible change of color*"; the reversible color change occurs on exposure to electromagnetic radiation (mainly on exposure to UV radiation). Photochromic compounds are a kind of chromic materials since chromic materials were divided into several types, photochromic and thermochromic materials are the most often used due to their wide scope of applications [2]. There are significant differences between photochromism and thermochromism; in photochromism, the color change is normally brought about by electromagnetic radiation, whereas it is the heat that is responsible for the change in color in thermochromism [3]. The presence of light alone is not sufficient to induce a photochemical reaction in photochromic materials: the light must also be of the correct wavelength to be absorbed by the reactant species; there needs to be a reversible change of a single chemical species between two states having distinguishably different absorption spectra and such change should be able to be induced in at least one direction by electromagnetic radiation. The two forms of the reactant species may differ in terms of other properties such as their redox potential [4, 5], fluorescent intensity, dipole moment [6, 7] and molecular shape. Von Grothus (1819) and Draper (1841) formulated the first law of photochemistry: "*When a molecule absorbs light, the light can produce photochemical changes in the respective molecule*". This law relates photochemical activity to the fact that each chemical substance absorbs certain wavelengths of light unique to that substance. A photochromic or color-changing chemical compound was observed by Fritzsche in 1867; he found that decoloration of an orange-colored solution of tetracene occurred on exposure to daylight and that the original color returned when it was replaced in darkness [6, 7]. Silver halide in borosilicate or aluminoborosilicate is perhaps the best example of an inorganic photochromic material becoming excited in the wavelength range of 200-400nm [8], but researchers mostly study organic rather than inorganic photochromic materials, due to the higher possibility of obtaining a photochromic response in the visible spectrum (400-700nm). Despite the only significant commercial applications being in

ophthalmic lenses [9], photochromic materials can be considered a growing domain of research with various applications like optical data storage, non-linear optics, photo-switching and molecular-phonic devices, polymeric membranes and photochromic polymers [10]. The most commonly available organic photochromic materials at present are the diarylethenes, fulgides, azobenzenes, spiropyrans (SP), spirooxazine and naphthopyrans, among it, azobenzenes, spiropyrans, spirooxazine and naphthopyrans are thermally unstable and return to their original form by the reversible photochromic reaction when left in darkness. In photochromism, the stable form of the photochromic compound *A* is converted on absorption of radiation at its absorption maximum into the thermodynamically-metastable form *B*, which reverts back to form *A* by the absorption of thermal energy or the absorption of radiation at the absorption maximum of form *B* (a process resulting in reversible color change) as shown Eq. 2.1. In order to achieve a useful photochemical process, a number of factors are involved, they are exposed to transmission spectra to generate the colored form, responsiveness to light, speed of recovery (fatigue resistance), and long-term stability (ability to withstand extended exposure to light and therefore to yield a high number of cycles) [11].



During UV radiation, the photochromic pigments were absorbing energy from the UV radiation which initiated to structural modification of the colorless molecules to a colored molecule through a process known as “photoisomerization”. These modifications vary and depending upon the photochromic colorant. Generally, the radiation within the UV region (naphthopyrans, for example, respond to radiation at wavelengths of 350-380nm), but for a few compounds such modifications occur on radiation with light in the visible region; SPO, for instance, are activated by radiation at a wavelength of 410nm. The excited state behavior of photochromic materials (each isomer) can decide its efficiency [12, 13]. Based on the color formation, it can be classified in to two types, positive and negative photochromism;

Positive photochromism

Figure 2 illustrates how optical density varies depending on wavelength in the case of so-called positive photochromism; the absorption maximum of form *A* is located at a shorter wavelength range than that of the thermodynamically metastable form *B*. The thermo-dynamically more-stable, colorless or slightly yellow form *A*, is transformed by radiation with UV-light to the colored, in this case, blue form *B*. The reverse reaction may either occur spontaneously if the

compound is left in the dark and/or photochemically by radiation with light of wavelength in the range of the absorption maximum of form *B*.

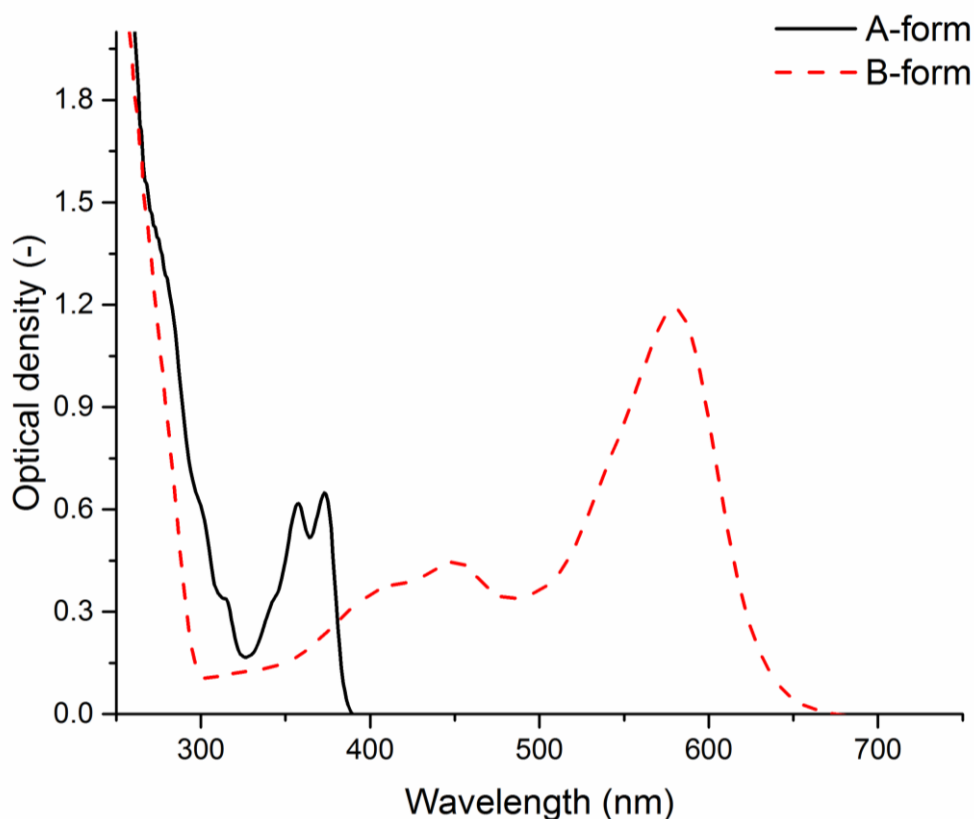


Figure 2: Graphic representation of a photochromic system (*A*-colorless; *B*-colored form).

Negative Photochromism

In the case of negative photochromism, instead of color development, decoloration takes place. The photochromic compound, which in this case is colored until it is exposed to UV radiation, becomes decolorized on exposure to UV radiation because the photoproducts absorb at shorter wavelengths than the original compound [7, 14].

2.1.1 Mechanisms of photochromism

There are many conformational changes that can take place in the excitation process, which lead to changes in electronic absorption spectra, resulting in a visible color change [15, 16]. The formation of a new absorption band, resulting from the transition from various vibrational levels in the excitation of a colorless molecule S_1^A is schematically described in Figure 3.

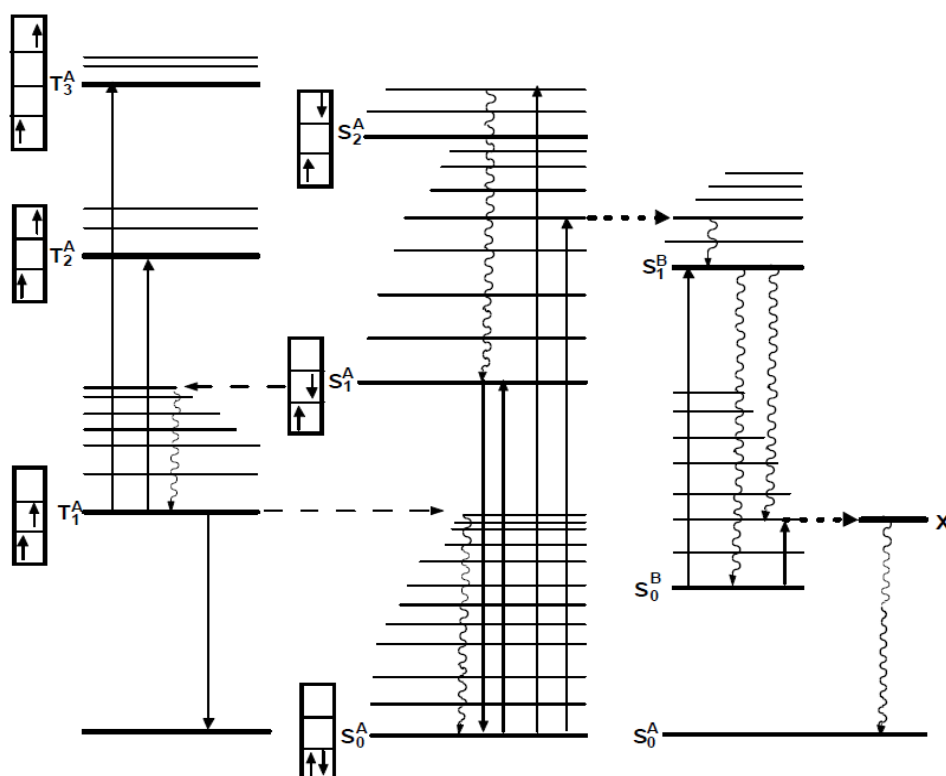


Figure 3: The Jablonski-diagram for the representation of electronic, radiative and non-radiative transitions (Adapted and modified from [17]).

After the molecule is in the excited state S_1^B the colored molecule is deactivated to the ground state S_1^B . Then there follows an exergonic process (i.e. a spontaneous reaction releasing energy) in which the regeneration of the colorless form occurs via a radiationless transition back to the original form in its ground state S_1^A (System B is not thermodynamically stable and therefore spontaneously returns to state A). Frequently the backward reaction $B \rightarrow A$ (the so-called thermal conversion from S_1^B to S_1^A), proceeds via a transition state X , whose energy is higher than the singlet state of the colored form S_1^B . The process is thermally activated. The reaction $B \rightarrow A$ may also be induced by long-wavelength light (infrared radiation) or by the light of wavelength near to the new absorption band. With regard to the energy difference $E(S_0^B) - E(S_0^A)$, the photochromic change can be used to provide energy accumulation. As with the yield from the light energy on conversion to thermal energy, so the accumulative capacity of thermodynamic difference between colored (B) and colorless (A) forms; which depends on the chemical structure of the meta-stable photoproduct, which has non-conventional bond lengths, angles, dissipation of resonance energy which involves to increase

stability caused by delocalization of π electrons. The limitation of the effect results is from the second law of thermodynamics, due to the overall reaction between temperatures T and T' , the photochemical reaction $A(S_0^A) \rightarrow A(S_1^A) \rightarrow (S_0^B)$ at temperature T and the exothermal reaction of $B(S_0^B) \rightarrow X \rightarrow A(S_0^B)$ at temperature T' the final yield of accumulative capacity increases at a temperature T' as does the energy of ground state of the “colored” molecule (S_0^B) [16, 18]. Six categories may be used to classify the mechanism of photochromic effects [16, 18, 19] as follows;

- Triplet-triplet photochromism
- Heterolytic cleavage
- Homolytic cleavage
- Trans-cis isomerization
- Photochromism based on tautomerism
- Photodimerization

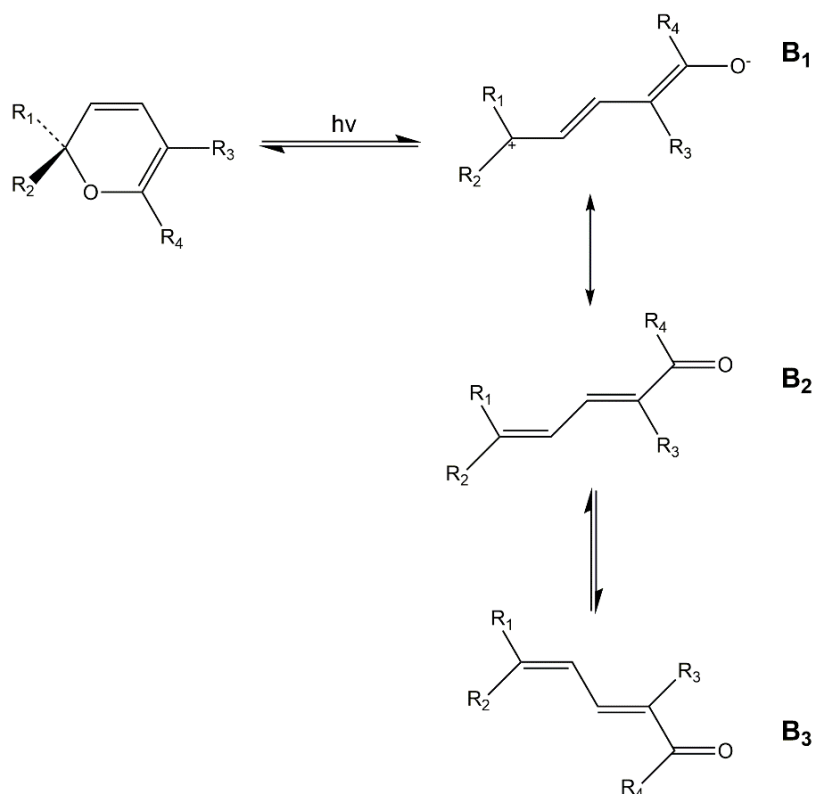
Triplet-triplet photochromism

In this system, the absorption band in the long wavelength region of the spectrum characterizes the colored form B (Eq. 2.1). In general, these chromophores can quickly absorb radiation to raise ground state molecules to an excited singlet state, then as a second step, the excited singlet state proceeds by a process known as intersystem crossing, to convert to a triplet state; in the third stage, triplet state molecules absorb incident radiation to convert from the first triplet state level to a higher level. Usually, materials exhibiting triplet-triplet photochromism respond very quickly with a bleaching time of less than one second for the reversion of photochromic change from colored to colorless. The concentration of oxygen in the system can decide the quantum yield of triplet-triplet photochromism, since oxygen cause triplet excitation, a good example is a pentacene [16, 20].

Heterolytic cleavage

Heterolytic cleavage can cause the formation of charged ions with absorption characteristics that differ from those of the parent photochromic compound. During the cleavage reaction, a covalent bond is broken in the excited molecule and new bonds are created with zwitterionic (dipolar) structures; typical examples exhibiting this photochromic mechanism are the pyrans.

During UV radiation, the bond between the carbon and oxygen atoms is broken and the pyran ring is opened, forming the ionic structure (B_1) as shown in Scheme 1. These ionic structures provide intense coloration through interconversion of the pyrans (colorless form) into merocyanines (colored form). In the latter, there is a resonance contribution from the neutral form (B_2) and the cis-trans conversion (isomer B_3) and triplet-triplet absorption can play a vital role in the photochromic process of pyrans. The thermal bleaching rate depends on the substituent's R_1 , R_2 , R_3 and R_4 [20].

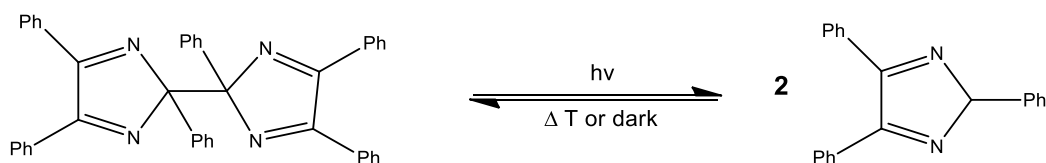


Scheme 1: Photochromic reactions of pyrans with heterolytic cleavage [16].

Homolytic cleavage

In this system, the bond is broken during UV radiation into two or more parts, which in the case of azo colorants contain the azo group electrons [18]. This dissociation is accompanied by changes in the spectral absorbance due to the formation of colored radicals which may be stable and persist for long periods of time. In the case of the heterolytic cleavage mechanism on the other hand, where the products have some ionic character, the paramagnetic radical products are formed by homolytic cleavage. The cleavage character depends on the type of bonding configuration accommodating the dissociation of electrons. Examples of this system are given in Scheme 2 which explains the formation of naphthoxy radicals from β -TCDHN-1 [57]. Hexa-

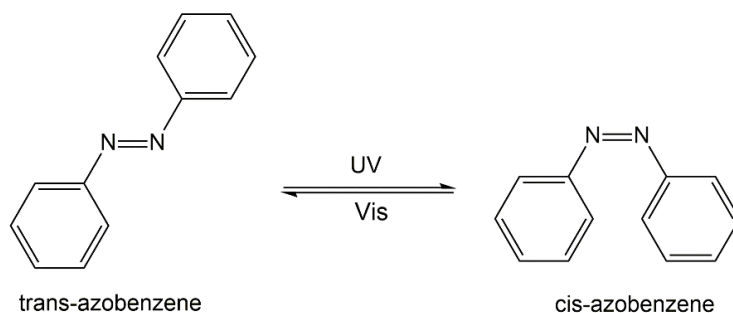
aryl ethanes and bisimidazoles also exhibit photochromism by homolytic cleavage (see Scheme 2, for hexaphenylbisimidazole).



Scheme 2: Homolytic cleavage for hexaphenylbisimidazole (Adopted and modified [57]).

Trans-cis isomerization

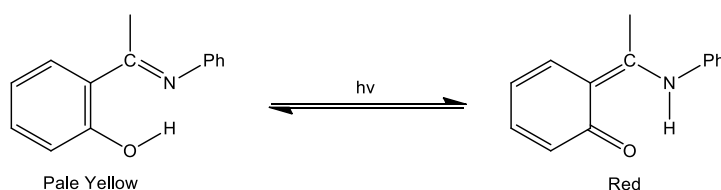
Most photochromic agents are capable of trans-cis isomerism around the carbon-carbon double bond. However, thermal energy can cause a change from the trans-state to cis-state [20]. The generalized trans-cis isomerization process is shown in the Scheme 3.



Scheme 3: Trans-Cis isomerization of azobenzene (Adopted and modified from [57]).

Tautomerism

Tautomerism based on interconversion of hydrogen atom transfer is the mechanism by which a number of organic compounds exhibit photochromism. Photochromic tautomerism results in a photochemical shift in the equilibrium between two tautomers having different absorption spectra, thereby giving rise to a reversible color change; light exposure can change the relative concentration of isomers which may or may not reach thermal equilibrium readily [21]. Examples of this mechanism are ortho-substituted phenyl ketones, aromatic nitro compounds and anils. Salicylidene anils (Scheme 4) are examples of compounds which are photochromic by virtue of tautomerism [20].



Scheme 4: Tautomerism in salicylidene anils [20].

2.1.2 Kinetics of photochromism

The dynamics of photochromism are shown in Figure 4, which describe the optical density of a photochromic compound under the influence of UV radiation, the numbers 1,2,3 and 4, positioned above the line which traces the changes in optical density with respect to the impact of UV radiation, the numbers 1 & 4 indicates the colorless (or weakly colored) and numbers 2 & 3 indicates the partially and fully colored compounds respectively. The sequence of the photochromic system could be like, before exposure to the UV radiation, the photochromic compound is colorless. On UV-exposure, the colorless form of photochromic compound rapidly begins to be converted into the colored form. After a sufficient period of exposure, the equilibrium is shifted to the furthest extent in favor of the colored form of the photochromic material. On terminating the UV-radiation stage, the (thermal or light-induced) back reaction occurs and the photochromic compound reverts to its original colorless state.

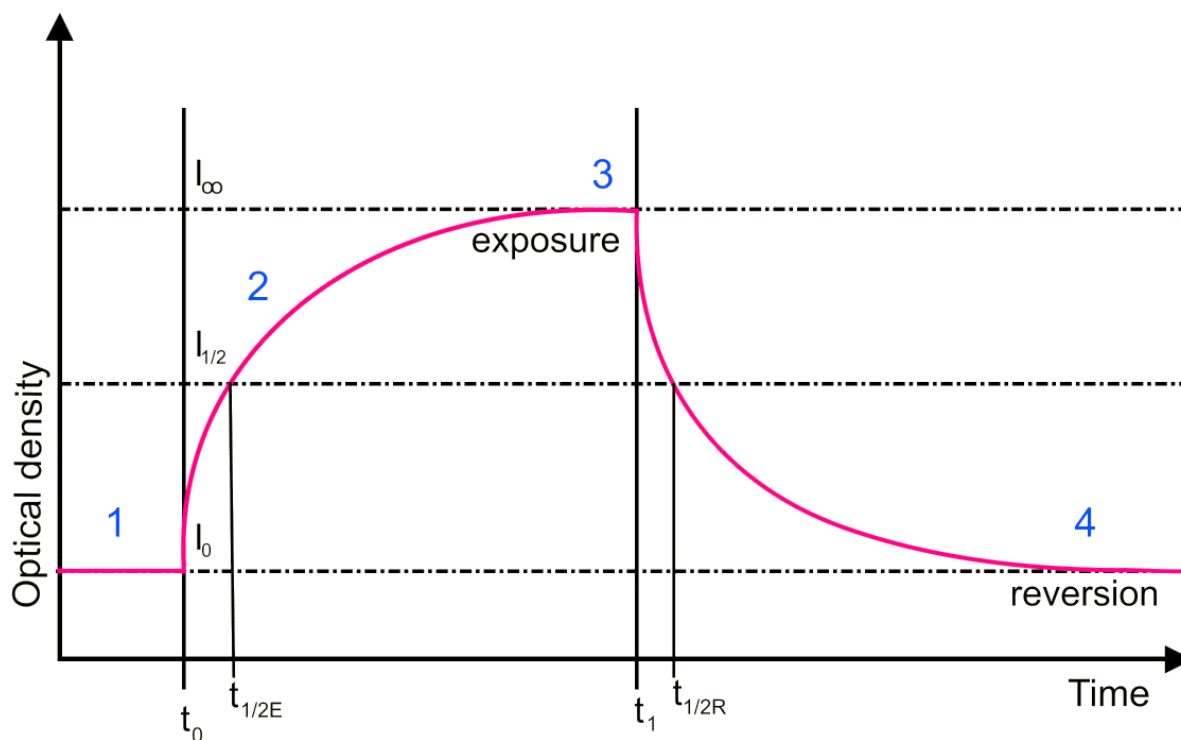


Figure 4: Typical behavior of a photochromic compound under UV radiation (Adopted and modified from [14, 22]).

where, t_0 - start of UV radiation; t_1 - end of the UV radiation; $t_{1/2E}$ - time taken to achieve half of the total photochromic response during exposure; $t_{1/2R}$ - time taken for half of the photochromic reversion to take place; I_0 - Optical density at beginning; $I_{1/2}$ - Half of optical density; I_∞ - Optical density at infinity.

2.1.3 Classification of photochromic materials

Photochromic materials can be classified based on the type of back reaction, if the back reaction occurs through irradiation with the light is called a P-type photochromic material, whereas back reaction is caused by thermal means T-type.

2.1.3.1 P-type photochromic materials

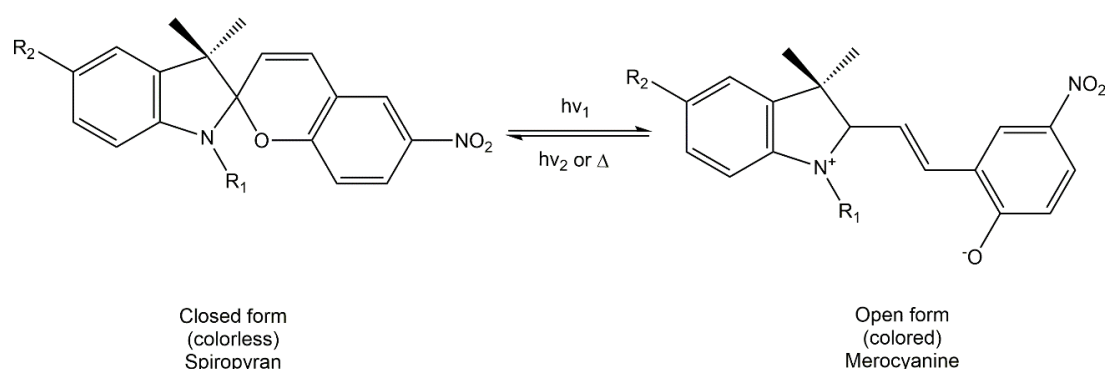
Last five decades, a significant amount of research could be conducted on the P-type photochromic materials, however, these materials are mostly used in molecular switches. The diarylethene, fulgide and fulgimide family constitute an important class of P-type photochromic compounds.

2.1.3.2 T-type photochromic materials

There are many T-type photochromic compounds have been investigated in the last five decades, some are commercialized such as spiropyran, spirooxazines and naphthopyrans [12, 23, 24].

Spiropyrans

Spiropyrans (SP) was the first commercialized T-type photochromic compounds, it was deeply studied in 1950. The general structure of photochromic SP contains a second ring system attached to a pyran core in a spiro manner [25]; the photochromic response is brought through ring opening which is caused by UV radiation (Scheme 5); removal of UV radiation causes reversal effect from colored to colorless.



Scheme 5: The photochromic reaction of spiropyrans.

During ring opening of pyrans under UV radiation, the merocyanine form is created. It exists as a cis-cis/trans-trans mixture in equilibrium and is responsible for the intensification of color [25]. Removal of UV source has the opposite effect; the equilibrium moves towards to the

colorless pyran form of the colorant, the result of which seen as a fading of the color. Generally, the thermal bleaching (Figure 5) rates for spiropyrans are low, since it is very sensitive to temperature, the photochromic effect will be weaker at a higher temperature. In terms of textile applications, the spiropyran are less due to the poorer photostability.

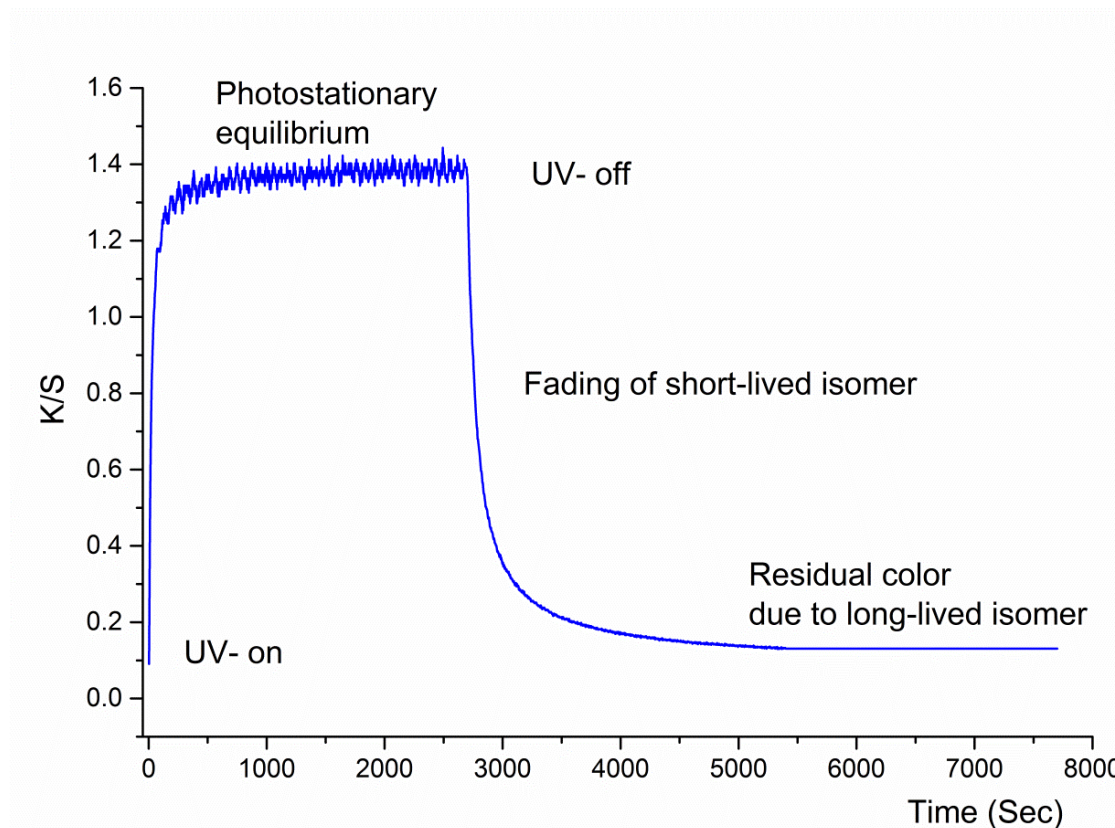


Figure 5: Various kinetic reactions of the photochromic system (adopted & modified from [25]).

Spirooxazines

The chemical structures of spirooxazines (SPO) are similar to those of spiropyrans except that the pyran core is replaced by an oxazine group, more specifically, a condensed ring substituted 2H-(1,4)oxazine in which it is the number two carbons of the oxazine ring that is involved in the spiro linkage. In 1970's, first SPO photochromic compounds were reported and patented by Ono and Osada [26], Arnold and Volmer [27], but were not subject to much research attention due to the growth of interest at that time in SP [28, 29]. In 1982, however, Hovey et al [29] reported SPO photochromic compounds having excellent resistance to photo-degradation. Generally, SPO provides a relatively fast-fading blue photo-coloration; with small adjustments in their structure can provide improved hue, intensity and half-life. The parent structure of indolinonaphthoxazine turns blue during UV-radiation on the absorption of a

dominant wavelength of 600nm (Scheme 6) which rapidly reverts and fades back to the colorless form on the removal of the activating radiation. The kinetic properties of SPO depends on the substituent's and its positions, the effects of substituent's and structure on various kinetic properties are summarized in Figure 6. However, placing bulky alkyl groups on the indoline nitrogen (*R* in Figure 7) helps to slow down fading and increase the color strength [12].

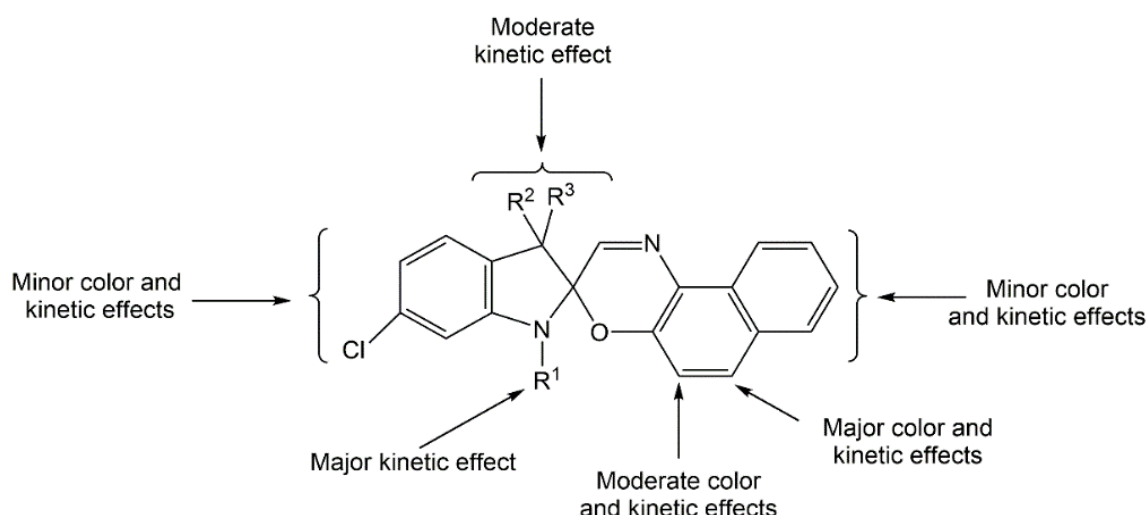


Figure 6: Summary of substituent effects in 5-chloro-1,3,3-trimethylspiro[indoline-2,3'-(3H)naphtho(2,1-b)(1,4)-oxazine].

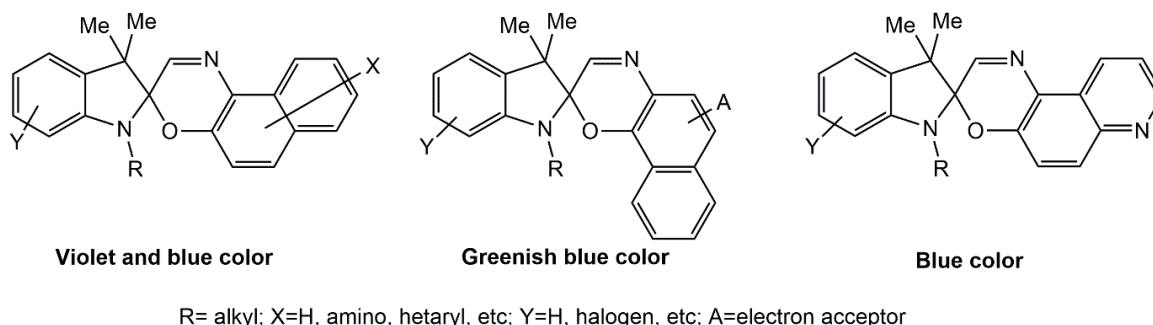
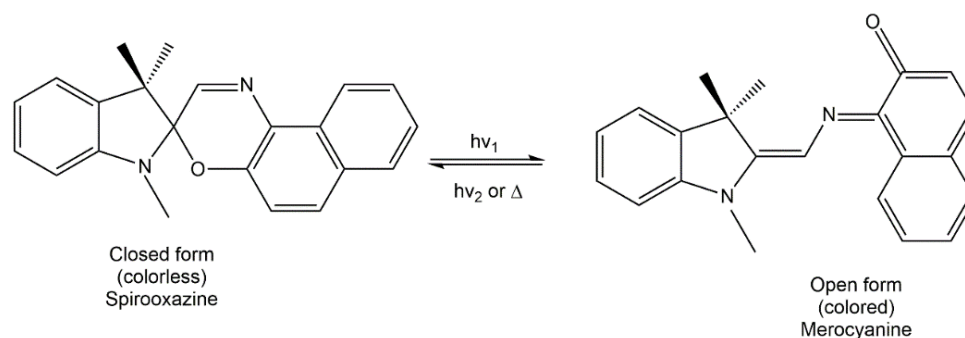


Figure 7: Structure modification on spirooxazine with its final color [12].

In the 1990's, plastic photochromic ophthalmic lenses were successfully produced using SPO as the photochromic agent and since then other applications following on from the synthesis of a large number of modified SPO have emerged in the form of photochromic inks, dyes and cosmetic products such as nail polish. While there is numerous example of more-complex SPO in the patent literature, most do not offer any advantages over simple derivatives [12]. Vikova et al.[30] produced the mass colored polypropylene filaments through melt spinning. The application of spiroindolinonaphthoxazines as disperse dyes on polyethylene terephthalate (PET), nylon-6 (PA-6) and polyacrylonitrile (PAN) fabric was studied by Billah et.al [31, 32],

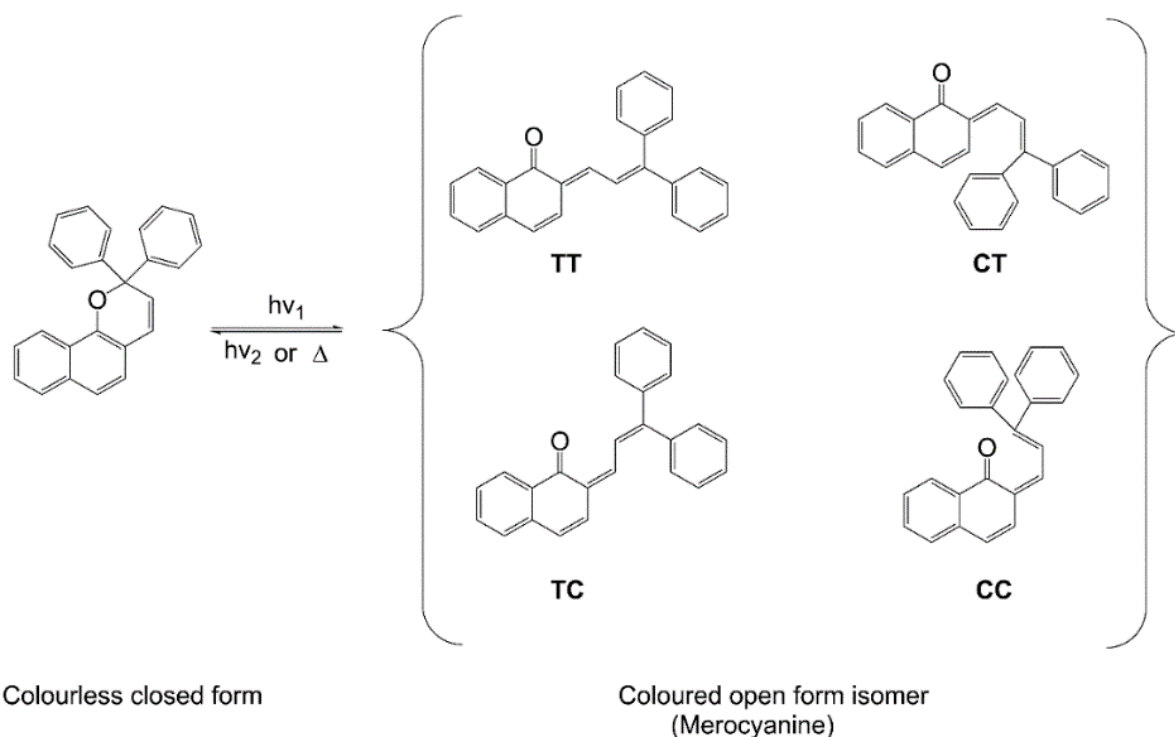
color build-up for the spiroindolinonaphthoxazines on PA-6 was significantly higher than PET and PAN (dyeing results for PAN and PET were similar). In another approach, Billah et al [33] dyed various textile substrates such as nylon, polyester and acrylic with spiroindolinonaphthoxazines, for detailed exploration of solvation effects. They wetted the photochromic dyed fabric samples in different solvents, namely acetonitrile, water, ethanol, dichloromethane and toluene. After wetting the samples were irradiated with UV light for two minutes. The solvent-treated samples invariably showed higher color build-up than the dry fabric. Among the five solvents, acetonitrile exhibited the highest effect on colorability, attributable to the fact that it was the most polar in nature, whereas the least-polar solvents such as toluene produced lower coloration; the reason for their effectiveness is that the polar solvents not only penetrate into the fibers to cause swelling but also provide a medium in which the photo-conversion is favored.



Scheme 6: Photochromic reaction of spirooxazines.

Naphthopyrans

Naphthopyrans used in the manufacture of plastic photochromic lenses, it also known as benzochromenes, chemically based on chromene, 2-H-1-benzopyran. The photochromism of SP, benzo- and naphthopyrans are similar in that all involve the breaking of the oxygen-carbon bond of the pyran core. The photochromic effects for naphthopyrans by light-induced ring opening of the structure described in Scheme 7 [14, 25].



Scheme 7: Photochromic reaction of naphthopyrans,

Note: (*TT*=trans-trans; *CT*= cis-trans; *TC*= trans-cis; *CC*=cis-cis).

2.1.4 Photodegradation

Generally, photochromism is a non-destructive process, but there is a possibility of side reaction. The degradation of chemicals lead to reduce the photochromic response with respect to the time is termed as "fatigue", the major cause of degradation by the oxidation process [34]. The fatigue resistance is depending upon the excited state reactivity of spiro/merocyanine (MC) forms. Previous literature confirms that the oxygen can react to the triplet state of SPO/SP, lead to photooxidation [35]. Generally, SPO is more stable than the SP, the previous literature shows that the photooxidation of SPO; mechanism wasn't clear although it was suggested due to the interaction of a biradical form of the merocyanine with oxygen or with singlet oxygen 1O_2 . Lenoble et al. [35] studied the photooxidation of SPO/SP, actually, it acts as the sensitizers by promoting the formation of singlet oxygen. Ayesha studied the degradation products of SPO yielded more 1,3,3-trimethyloxindole (Figure 8-a) whereas the SP yielded 3,3-dimethyloxindole (Figure 8-b) 1,2,3,4-tetrahydro-2,3-dioxo-4,4-dimethylquinoline (Figure 8-c).

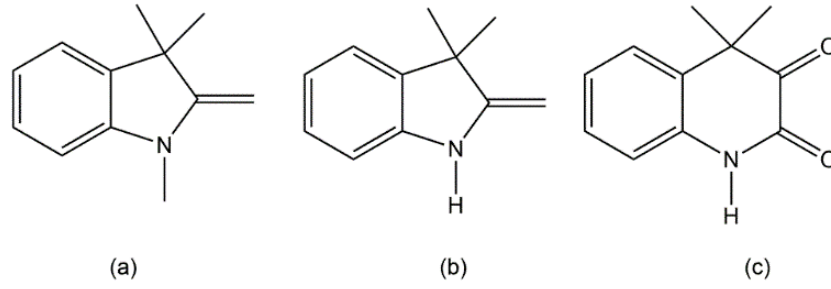


Figure 8: Photodegradation yield of 1,3,3-trimethyloxindole (a), 3,3-dimethyloxindole (b) 1,2,3,4-tetrahydro-2,3-dioxo-4,4-dimethylquinoline (c) [21].

2.2 Interaction between light and matter

2.2.1 Reflectance

It can be defined as the reflection of light at an object or an interface between the two media, it can be denoted as $R(\lambda)$ which is written in the Eq. 2.2.

$$R(\lambda) = \frac{I(\lambda)}{I_0(\lambda)} \quad (2.2)$$

where $I(\lambda)$ and $I_0(\lambda)$ are the reflected and incident intensities respectively.

Boundaries of all kinds of materials are applied by spectral reflectance's, including materials with opaque, transparent and translucent. In case of non-fluorescent materials, an intrinsic property of the material is a spectral reflectance is independent of the intensity of the incident light. The spectral linearity allows transformation of reflectance data to other illumination conditions is referred to as the spectral linearity.

2.2.2 Transmittance

It is the ratio between the transmitted and incident energy can be written in Eq. 2.3,

$$T(\lambda) = \frac{I(\lambda)}{I_0(\lambda)} \quad (2.3)$$

where $I(\lambda)$ and $I_0(\lambda)$ are the intensities of the transmitted and incident lights; for prediction of the result after a light ray passes through a thin, transparent layer such as a filter is also useful in predicting a spectral transmittance [36]. To compute the light intensity after the transmission the following relationship may be used. Based on spectral reflectance, a similar equation for computing the spectral power distribution of reflected light is allowed to use by this interpretation.

2.2.3 Absorbance

The concentration of an absorbing species is plotted by the transmittance, but the relationship is not linear. Transparent or translucent material within a unit path length (l) of light propagation absorbs the spectral absorptivity is the part of the light energy. General analytical description of spectral absorption is given by Eq. 2.4.

$$a(\lambda, r) = \frac{1}{I(\lambda, r)} \frac{dI(\lambda, r)}{dl} \quad (2.4)$$

Wavelength λ is not only depended on the spectral but in case of not homogenous material also on spatial location r . The SPD of a light after it travels from r_0 to r with $l=[r_0 - r]$ can be calculated with respect to the spectral linearity from [16],

$$I(\lambda, r) = I_0(\lambda, r) e^{-\int_0^l a(\lambda, r) dl} \quad (2.5)$$

where, $I_0(\lambda, r_0)$ is the initial SPD, the spectral absorptivity of homogenous material will be in independent location, therefore, simplification model can be used, which is $a(\lambda, r) = a(\lambda)$. So, the equation derived from Eq. 2.5 [16],

$$I(\lambda) = I_0(\lambda) e^{-a(\lambda)l} \quad (2.6)$$

We know this equation are Bouguer's law, however, there is another expression of this law can be,

$$T_{\text{internal}}(\lambda) = \frac{I(\lambda)}{I_0(\lambda)} = e^{-a(\lambda)l} \quad (2.7)$$

where spectral transmittance internal are $T_{\text{internal}}(\lambda)$, from the Eq. 2.7, optical effect of absorption can be described, however, it depends on the object thickness. Absorption can depend on the concentration of the homogeneous solution (transparent), it can describe through Beer's law [16],

$$T_{\text{internal}}(\lambda) = e^{-\varepsilon(\lambda)cl} \quad (2.8)$$

where $\varepsilon(\lambda)$ is the spectral functions (i.e. absorption coefficient), c is a concentration of the solution. However, Bouger's law is rigorous for all conditions, whereas Beer's law is not and only for low or moderate concentration, but for turbid media, both are valid [16].

2.3 Kinetics behavior of photochromic materials

In order to characterize the kinetic behavior of photochromic reaction, it is desirable to determine how the rate of reaction varies as the reaction progresses. The differential-rate law

relates to the rate of reaction for the concentrations of the various species in the system. Differential-rate laws can take on many forms but most of the chemical reactions obey one of three differential-rate laws [18, 37, 38], each rate law contains a constant (k). The kinetics of many chemical reactions are well-explained by the first order equation, it explains the conversion rate is directly proportional to the number (or concentration) of unreacted species. In previous studies, it has been well documented that thermal isomerization for the photochromic systems are follows the first-order kinetics [39–42], however, the behavior of commercial photochromic dyes can often be approximated by the first order kinetics and it derived from the following Eq. 2.9 [18, 43, 44];

$$n_R(t) = n_R(0)e^{-kt} \quad (2.9)$$

where $n_R(0)$ is the initial concentration and k represents the rate constant, typically it deviates from this simple relationship due to additional processes. Janus et al. [43] investigated the isomerization kinetics by monitoring the absorbance of the transforms of substituted azobenzenes at 350nm. Based on the Beer-Lambert law, the concentration ratio $n_R(t)/n_R(0)$ is given by the Eq. 2.10 [45],

$$\frac{n_R(t)}{n_R(0)} = \frac{A(\infty) - A(t)}{A(\infty) - A(0)} \quad (2.10)$$

In general, for photochromic compounds which show photo-induced conversion from the colorless to the colored form, the kinetics of the conversion can be observed by simple monitoring of absorbance bands. Therefore, the absorbance $A = -\log(T)$ or the Napierian absorbance $A_e = -\ln(T) = A(1/T)$, respectively, is determined from the measurement of transmission T , where;

$$T = I_d / I_0 \quad (2.11)$$

in which d is the thickness of the sample, I_0 is the intensity of light measured at the input face ($z=0$) of the sample and I_d is the transmitted light intensity measured behind its output face ($z=d$) [46, 47].

$$-\ln\left(\frac{\Delta A(t)}{\Delta A(0)}\right) = -\ln\left(\frac{\Delta A_e(t)}{\Delta A_e(0)}\right) - \ln\left(\frac{A_e(\infty) - A_e(t)}{A_e(\infty) - A_e(0)}\right) \quad (2.12)$$

So, the first order kinetic equation can be re-written as follows:

$$\frac{t}{\tau} = -\ln\left(\frac{n_R(t)}{n_R(0)}\right) - \ln\left(\frac{A(\infty) - A(t)}{A(\infty) - A(0)}\right) \quad (2.13)$$

In Eq. 2.18, the time constant (τ) is defined as $\tau = kR^{-1}$, and $A(0)$, $A(t)$ and $A(\infty)$ are the initial, momentary and final values of the absorbance respectively. It is very difficult to determine a value for $A(\infty)$, particularly for the long period relaxation processes where an instability in the measurement could play an essential role, and in those cases where there may be some UV degradation of the photochromic material [47].

$$\frac{t}{\tau} \propto \ln \frac{dn}{dt} \propto \ln \frac{dA}{dt} \quad (2.14)$$

Both methods, that shown by Eq. 2.12 and that in Eq. 2.13 give similar results for (τ) so Eq. 2.15 can be written in following form [46]:

$$A(t) = [A(0) - A(\infty)]e^{-kt} + A(\infty) \quad (2.15)$$

whereas,

$$-\ln \left(\frac{\Delta A(t)}{\Delta A(0)} \right) = k_0 t \quad \text{or} \quad (2.16)$$

$$\Delta A(t) = \Delta A(0)e^{-k_0 t} \quad (2.17)$$

In the case of translucent media, Lambertian absorption A can be replaced by the K/S function. Vikova and Vik [48] suggested that Eq. 2.13 & 2.15 could be suitable for calculating the kinetic data; shade intensity (I) can be used as the measure for absorbance A or a K/S function; [18, 22, 49];

$$I(t) = [I(0) - I(\infty)]e^{-kt} + I(\infty) \quad (2.18)$$

2.3.1 Kinetic model for photochromic materials

Gaughlitz [50] described the exponential decay (i.e. reversion) of light intensity in absorbing matters, and based on his conclusion, Vikova and Christie [57] proposed the first order kinetic model for photochromic compounds incorporated into textiles for their response during exposure as well as in the reversion. It provides a simplified way of describing the changes within a sample of an applied photochromic pigment from I_0 (color intensity at time t_0 , or sample without exposure), to I_∞ (the color intensity after an infinite exposure time t_∞) as illustrated in Figure 9.

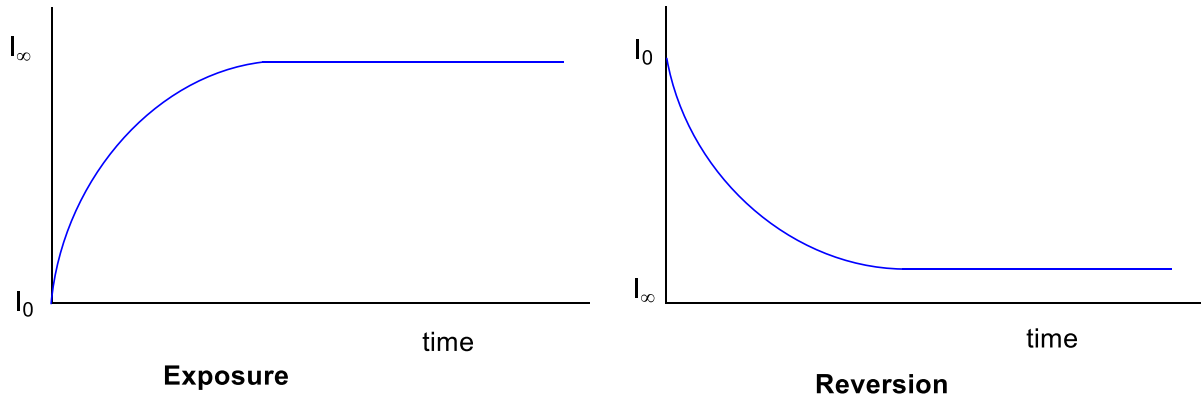


Figure 9: A kinetic model of exposure & reversion phase of photochromic materials [16].

The proposed model is based on the approximate view that the process follows first-order kinetics with the rate described by Eq. 2.19. The rate of color intensity development dI/dt is directly proportional to the difference of color intensity at time t and in equilibrium;

$$\frac{dI}{dt} = -k(I - I_{\infty}) \quad (2.19)$$

where I_0 is the color intensity of the sample at the time of t_0 .

$$\frac{dI}{I - I_{\infty}} = -k \cdot dt \quad (2.20)$$

where I is the color intensity of the sample at the time of t .

$$\int_{I_0}^I \left(\frac{dI}{I - I_{\infty}} \right) = -kt \quad (2.21)$$

where I_{∞} is the color intensity of the sample in time t_{∞} ,

After substituting $I - I_{\infty} = z \rightarrow dI = dz$, we obtain the following solution for the integral;

$$\int \frac{dz}{z} = \ln z \rightarrow \left[\ln(I - I_{\infty}) \right]_{I_0}^I = \frac{(I - I_{\infty})}{(I_0 - I_{\infty})} e^{-kt} \rightarrow I - I_{\infty} = (I_0 - I_{\infty}) e^{-kt} \quad (2.22)$$

So, the kinetic model for exposure is (I_E) ,

$$I_E = I_{\infty} + (I_0 - I_{\infty}) \cdot e^{-kt} \quad (2.23)$$

The kinetic model for reversion phase and change of color intensity I , for the photochromic pigment (photochromic response during reversion) is based on the fact that during reversion the change in color intensity as it reduces from I_{∞} to I_0 , is as shown in Figure 9.

$$\frac{dI}{dt} = -k(I_0 - I) \quad (2.24)$$

where I_0 is the color intensity of the sample at time t_0 ,

$$\frac{dI}{I_0 - I} = -k \cdot dt \quad (2.25)$$

where I is the color intensity of the sample in time t .

$$\int_{I_0}^I \left(\frac{dI}{I_0 - I} \right) = -kt \quad (2.26)$$

where I_∞ is the color intensity of the sample in time t_∞ .

After making the substitution $I_0 - I = z \rightarrow dI = dz$, the following solution of the integral is obtained;

$$\int \frac{dz}{z} = \ln z \rightarrow [\ln(I_0 - I)]_{(I_0)}^I = \frac{(I - I_0)}{(I_\infty - I_0)} e^{(-kt)} \rightarrow I - I_0 = (I_\infty - I_0) e^{(-kt)} \quad (2.27)$$

so, the kinetic model for reversion I_R is,

$$I_R = I_0 + (I_\infty - I_0) \cdot e^{-kt} \quad (2.28)$$

2.3.2 Half-life of color change for photochromic materials

In a first-order reaction, the half-life of the reactant (the photochromic material) may be used as the half-life of the reaction. Similarly, when more than one reactant is involved in the photochromic reaction at concentrations in their stoichiometric ratios, the half-life of each reactant is the same, and once again it may be used to give the half-life of the reaction. Using concentrations of a reactant which are not in stoichiometric ratios will not give the half-life of the reaction [16, 51–53]. Generally, the speed of the coloration and decoloration processes depend upon the type of photochromic materials, but apart from this the photochromic materials also require enough free space for the transformation of its structure by photo-induction to change from its colorless to colored form (Figure 4). The half-time for the color changing properties of photochromic materials can then be calculated through Eq. 2.29 and the rate constant can be calculated via the Eq.2.30.

$$t_{1/2} = \frac{\ln 2}{k} \quad (2.29)$$

$$k = \frac{\ln 2}{t_{1/2}} \quad (2.30)$$

where k is the rate constant.

2.4 Color measurements

2.4.1 Color measurement of photochromic textiles

It is difficult to analyze the kinetic behavior of photochromic materials with commercial spectrophotometers which require controlled exposure at selected irradiance levels [54]; a long time may be required between individual measurements (approximately 5s) or, if using a separate UV source any time delay between irradiation and measurement can allow thermal fading of the sample to affect the results [48, 55]. Also, the commercial spectrophotometer cannot measure the whole color change during UV exposure without interruption of illumination of the samples [48, 56]. The required experiments can be done by other researcher in Datacolor Spectraflash SF600 spectrophotometer with specular component excluded (SCE) and UV component included [32], if at first the fabric samples undergo UV-radiation and are then immediately transferred to the spectrophotometer to evaluate the fading behavior, but it will not give the required accuracy for kinetic data; the photochemical reaction can take place in times of the order of attoseconds to nanoseconds. To solve such issues, it is necessary to add an additional aperture to the spectrophotometer for the UV-radiation. Vik and Vikova [16, 54, 57, 58] developed such a spectrophotometer (Figure 10) to help to resolve the above issues and allow determination of the development of color during continuous irradiation to measure the behavior of photochromic textiles and other substrates [55]. Dual light source construction of the spectrophotometer with a shutter over an excitation light source makes a possible continuous measurement of photochromic color change during reversion after switching off the excitation light source [54, 59]. Due to control over excitation with light sources by using the shutter, it becomes possible to examine the photochromic properties of materials with respect to single or multiple cycles. The main feature of the instrument can measure continuously; it allows to study the color-changing photochromic kinetics, the influence of exposure time and thermal and spectral sensitivities of photo-chromic samples and can be used as a fatigue tester. The most of the photochromic materials are sensitive towards to temperature, so this instrument also offers control of temperature during the measurement [54, 59]. In this work, the produced photochromic materials are measured its kinetics by a special spectrophotometer (Photochrom-3).

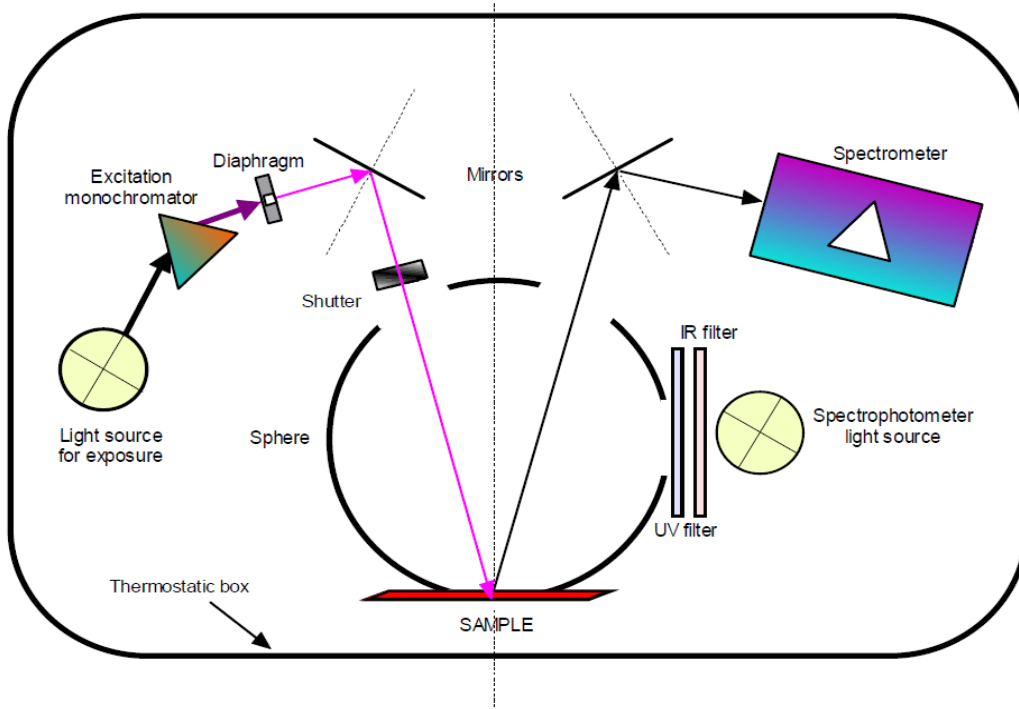


Figure 10: Scheme of LCAM designed Spectrophotometer (Photochrom-3).

2.4.2 Color difference assessment of photochromic materials

According to Berns [60], the color difference is a three dimensional space with approximately uniform visual spacing in terms of color difference judgments. To find the color difference, there are several formulae was developed by previous studies, but in this research $CIE L^*, a^*, b^*$ was used, it is a rectangular coordinate system which having the axes of L^*, a^* & b^* . It explains (ΔL^*) as the lightness, (Δa^*) as redness to greenness and (Δb^*) as yellowness to blueness of the color difference, the color difference of photochromic textile can be computed by the Eq.2.31.

$$\Delta E^* = \sqrt{(\Delta L^*)^2 + (\Delta a^*)^2 + (\Delta b^*)^2} \quad (2.31)$$

where $\Delta L^* = L_2^* - L_1^*$ (L_2 -batch and L_1 -standard, for Δa^* and Δb^* also the same).

On other hand, the color difference can be possible to calculate by using the CIELCH color space, which is similar with CIELAB. In this case the use of C^* & H^* (chroma and hue respectively) coordinates, which are colorimetric coordinates that clearly describe the change a shift the shade with respect to the change in color and purity, given that it is a cylindrical coordinate system and hue shift is described herein by shifting the hue angle h_0 . The both CIELAB and CIELCH color space on photochromic materials are studied [61] and concluded

as CIELCH has a certain problem that they pose cylindrical coordinates, however, CIELCH color space is not used in this thesis and there is no specific reason that.

2.5 Conclusion

In this chapter, the review of the history of photochromism, mechanism of photochromic materials, classification of photochromic materials, photo-degradation are discussed. Also, it reviewed other optical property's such as transmittance, reflectance, absorptivity, fundamental of color measurement and also the optical measurements of the photochromic system with respect to the issues associated from the previous works could be discussed in this chapter.

Chapter 3 MASS COLORED miPP FILAMENTS

3.1 Introduction

The polypropylene has been chosen for the mass coloration, in the section 3.1.1 reviewed elaborately about the mass coloration techniques. Commercially, there are three types of polypropylenes (i.e. based on its backbone structure) but metallocene catalyst based isotactic polypropylene (miPP) has been selected for this study to produce the filaments via melt spinning technology. In general, miPP having salient features like stereo-regularity and narrow molecular weight distributions, therefore it ensures the filament or fiber production with improved processing and mechanical characteristics of final product, therefore it is expected to get higher tensile strength, lower elongation, allow faster spinning with lower denier of the final filaments [62–65]. The mass colored photochromic miPP filaments was produced with the cooperation of STU-Bratislava, Slovakia Republic. Since, the end product of photochromic miPP filaments were depends on the degree of orientation, which can be obtained through drawing process with different drawing ratios. The main aim of this chapter is to discuss to the effect of drawing ratio on the optical, mechanical and physical properties of produced photochromic miPP filaments. Therefore, this chapter deals with the production of miPP filament with their obtained results and their discussions on the various properties. So, the various optical properties like color strength values (K/S functions), color strength maxima (K/S (max)), changing in optical density, color difference by residual ΔE^* values, half-life for color change of photochromic response during exposure and reversion phase, rate constant and various color intensity has been discussed. Also, it discusses the influence of drawing ratios and addition of pigment concentration on the various physical properties like linear density, tenacity, elongation at break, Young's modulus and several thermal properties like melting temperature, changing in enthalpy & entropy, crystallinity% has been discussed. For all the measurement, the error can be calculated through standard uncertainty measurement [66, 67].

3.1.1 Mass coloration of miPP filament

Polyolefins, a class of polymeric materials is exemplified by polypropylene (PP). For the past 60 years, there is a remarkable growth in this thermoplastic polymer, PP is one among [68]. Synthetic polymers having versatile, its ability to modify for specific applications arising from its overall balance of physical, mechanical, electrical, chemical and thermal properties and a competitive price are the reasons for this growth. In viewing to the applications, a large volume

of PP is utilized in the area classified as the fibers and fabrics in which carpet backing, upholstery fabrics, smart textiles, clothing, geotextiles, disposable diapers, medical fabric, and automotive interior fabrics are included. In the present century due to these reasons, PP fiber has a bright future as a smart material. The low specific gravity that is greater bulk per given weight, strength, chemical and stain resistance are the advantages offered by the PP filaments. The discovery of metallocene catalysts was opened frontier in the area of polymerization of polyolefin's, polymer synthesis and various processing of polymers. Before metallocene, polyolefin's were manufactured through Ziegler-Natta catalysts, in spite of this, it has few drawbacks which is not possible to produce the PP with the uniform molecular weight and tacticity and tacticity distributions, but metallocene catalyst based PP can ensure the homogeneous in molecular weight distributions, tacticity and tacticity distributions [68], nevertheless, this is not the main scope of this research work. Generally, as an olefin textile fiber from an aqueous dyebath the PP fibers are undyeable, polar groups are lacked by polypropylene and is regarded as a hydrophobic polymer with a moisture regain of less than 1%, also due to the aliphatic structure, high crystallinity and high stereo-regularity, which limit the accessibility of dye molecules. It is caused by factors such as;

- Chemical affinity is insufficient between the fibers and dyes due to the ionic absence or polar groups in the polymer chain, only due to the presence of weak Van der Waals' forces, the dye molecules are retented.
- Due to the high degree of crystallinity, the accessibility of dyes on the fibers is poor.

Therefore, polypropylene can be colored through mass or spin coloration techniques. In this technique, the colorants are added during or after polymerization but before the polymers are extruded through the spinneret. The mass coloration techniques offer a uniform coloration, good fastness properties, low coloration cost, negligible waste generation, reduce the consumption of water, heat and other resources for the subsequent treatments. Also, it ensures the sustainability. The factors deciding the pigment durability for spin coloration are heat stability, dispersibility, fastness properties especially light fastness and solubility in polymer melts and it depends on the pigment chemical structure [69–73].

3.2 Experimental procedure

Metallocene catalyst isotactic polypropylene: Metocene HM 562R (miPP) with melting flow rate (MFR) 2.66 g.min⁻¹ was procured from Lyondell Basell, Italy. In this study, three different

colors of photochromic pigments were used, these pigments are commercially available in the market, the list is given in Table 1, and the chemical structure has been given in Figure 11. Actually, the pigment is in the form of ink with 50% concentration of pure pigment and rest are formulated by the tetrakis (1,2,2,6,6-pentamethyl-1-4-piperdyl)-1,2,3,4-butanetetracarboxylate (HALS) and other additives, the formulated pigment was purchased from Matsui Shikiso Chemical Co., Ltd, Japan. However, these additives are not only impaired the tensile strength also show some significant changes in optical and physical properties of final products.

Table 1: Commercial photochromic pigments used for the production of mass colored filaments.

| Color | Abbreviation | CAS number | Chemical name |
|--------|--------------|------------|--|
| Blue | MPB | 27333-47-7 | 1,3,3-trimethylspiro [indolino-2,3'-(3H)naphtho(2,1-b)(1,4)-oxazine] [74, 75]. |
| Purple | MPP | 27333-50-2 | 5-chloro-1,3,3-trimethylspiro[indoline-2,3'-(3H) naphtho(2,1-b) (1,4)-oxazine] [74, 75]. |
| Yellow | MPY | 4222-20-2 | 3,3-diphenyl-3H-naphtho[2,1-b]pyran [74, 75]. |

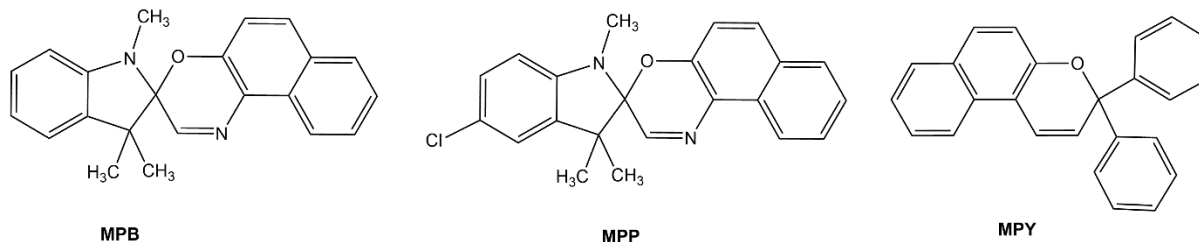


Figure 11: Chemical structure of three commercial photochromic pigments used for this study [74, 75].

3.2.1 Production of photochromic filaments

Two varieties of miPP filaments were produced (i.e. with and without pigment), during the production, miPP dried chips were used with standard conditions which could be specified by the manufacturer. For the production of colored filaments, first 100% colored miPP was produced like a tape/ribbon form, therefore photochromic pigments and miPP dried chips (un colored) were mechanically mixed before it melts, finally, it can be dried and converted into chips form. The single-screw tape extruder was used to produce the tape, although it has three different temperature zones, however, the same temperature was maintained in all the zones at 220°C (i.e. photochromic pigment is sensitivity towards temperature if more than 230°C), after

extruding the colored tapes passed through water bath immediately and then dried to make chips. Later, these air-dried colored chips were vacuum dried for 2 hours at 105 °C, then these chips (colored chips) were mixed to colorless chips with four different concentrations (0.25; 0.50; 1.50 and 2.50 on weight % of the chips (wt.%) to produce colored photochromic filaments. The filaments were produced by laboratory scale single-screw melt extruder (melt spinning) with the diameter of 16mm, L/D ratio of 30. The spinneret has 13 orifices and each having the diameter of 0.5mm (i.e. the spinneret designs are varied according to the shape of filament produced). The detailed process sequence is given in Figure 12, spinning temperature and the other process parameters were as illustrated in Table 2.

Table 2: Parameters used in melt spinning for the production of miPP filaments.

| | |
|---------------------------------------|-------------------------------|
| Temperature during melt spinning zone | 220 °C |
| Pigment concentration | 0.0; 0.25; 0.5; 1.5; 2.5 wt.% |
| Drawing temperature (T_d) | 120 °C |
| Melt flow index (MFI) | 2.66 g.min ⁻¹ |
| L/D ratio | 30 |
| Number of holes in the spinneret | 13 |

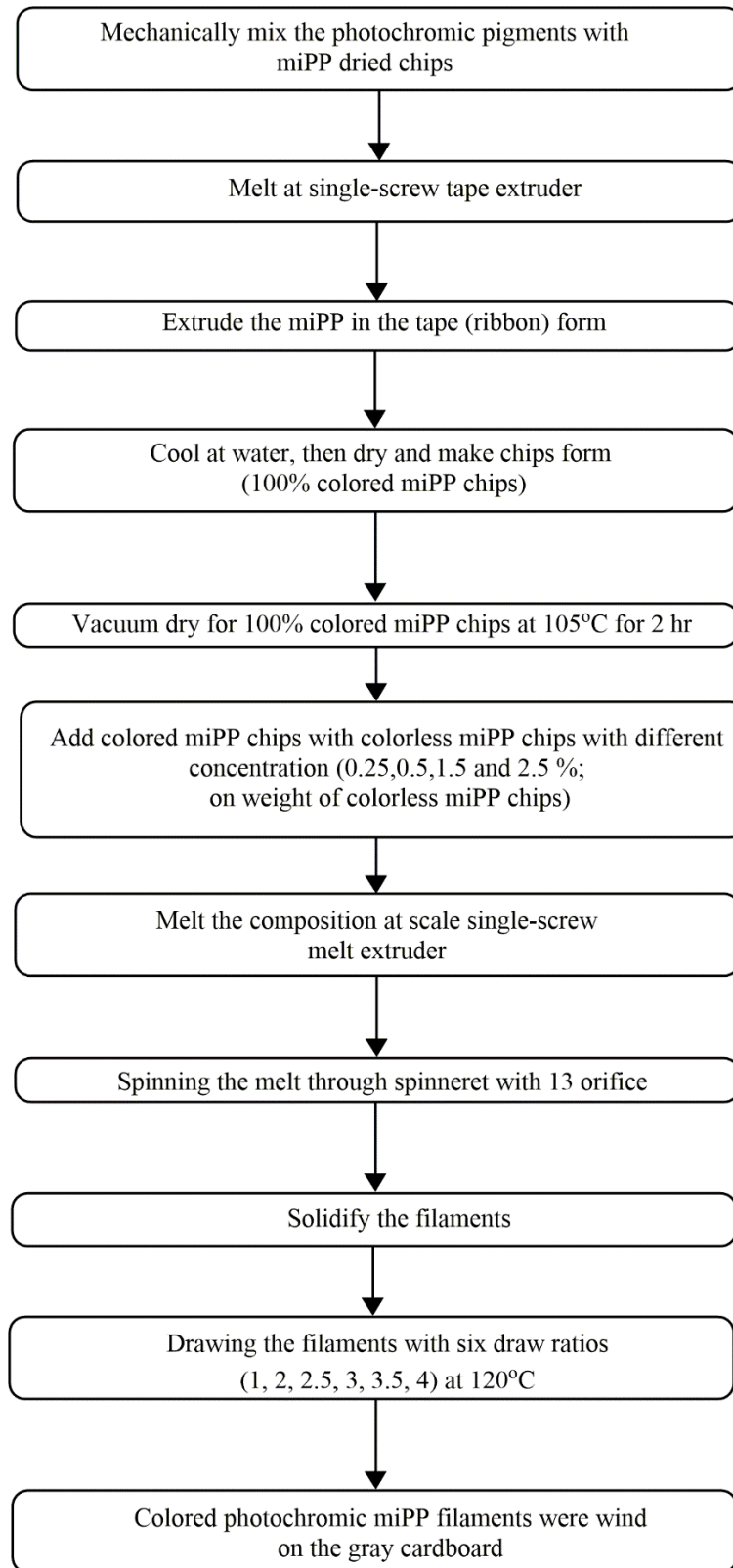


Figure 12: The process sequence of photochromic miPP filaments manufacturing.

Table 3: Details of photochromic miPP filaments with a circular cross-section.

| Pigment | Composition | Drawing ratio (DR) | | | | | |
|---------|--------------------------|--------------------|-----|-----|-----|-----|-----|
| MPB | miPP (without pigment) | 1.0 | 2.0 | 2.5 | 3.0 | 3.5 | 4.0 |
| | miPP + 0.25 wt.% pigment | 1.0 | 2.0 | 2.5 | 3.0 | 3.5 | 4.0 |
| | miPP + 0.5 wt.% pigment | 1.0 | 2.0 | 2.5 | 3.0 | 3.5 | - |
| | miPP + 1.5 wt.% pigment | 1.0 | 2.0 | 2.5 | 3.0 | 3.2 | - |
| | miPP + 2.5 wt.% pigment | 1.0 | 2.0 | 2.5 | 3.0 | 3.2 | - |
| MPP | miPP (without pigment) | 1.0 | 2.0 | 2.5 | 3.0 | 3.5 | 4.0 |
| | miPP + 0.25 wt.% pigment | 1.0 | 2.0 | 2.5 | 3.0 | 3.5 | 4.0 |
| | miPP + 0.5 wt.% pigment | 1.0 | 2.0 | 2.5 | 3.0 | 3.5 | - |
| | miPP + 1.5 wt.% pigment | 1.0 | 2.0 | 2.5 | 3.0 | 3.2 | - |
| | miPP + 2.5 wt.% pigment | 1.0 | 2.0 | 2.5 | 3.0 | 3.2 | - |
| MPY | miPP (without pigment) | 1.0 | 2.0 | 2.5 | 3.0 | 3.5 | 4.0 |
| | miPP + 0.25 wt.% pigment | 1.0 | 2.0 | 2.5 | 3.0 | 3.5 | 4.0 |
| | miPP + 0.5 wt.% pigment | 1.0 | 2.0 | 2.5 | 3.0 | 3.5 | - |
| | miPP + 1.5 wt.% pigment | 1.0 | 2.0 | 2.5 | 3.0 | 3.2 | - |
| | miPP + 2.5 wt.% pigment | 1.0 | 2.0 | 2.5 | 3.0 | 3.2 | - |

Table 4: A details of the photochromic miPP filaments with non-circular cross-sections.

| Cross-section | Composition | Drawing ratio (DR) | |
|---------------|------------------------|--------------------|-----|
| Triangle | miPP (without pigment) | 1.0 | 5.7 |
| | miPP + 3 wt.% MPY | 1.0 | 4.0 |
| | miPP + 3 wt.% MPB | 1.0 | 3.5 |
| | miPP + 3 wt.% MPP | 1.0 | 2.3 |
| 5-star | miPP (without pigment) | 1.0 | 3.5 |
| | miPP + 3 wt.% MPY | 1.0 | 2.0 |
| | miPP + 3 wt.% MPB | 1.0 | 2.5 |
| | miPP + 3 wt.% MPP | 1.0 | 2.0 |
| 10-star | miPP (without pigment) | 1.0 | 5.2 |
| | miPP + 3 wt.% MPY | 1.0 | 2.3 |
| | miPP + 3 wt.% MPB | 1.0 | 3.5 |
| | miPP + 3 wt.% MPP | 1.0 | 2.3 |

3.2.2 Drawing process

Generally, the drawing process is carried out to increase the molecular orientation for both crystalline and amorphous phase of the filaments. Drawing is the process carried out by simple stretching of the synthetic filament between the two set of rollers, often called feed and take-up rollers. Generally, the drawing process carried out at room temperature or at elevated temperature, selection of temperature is purely depended on the type of filaments and its applications. A typical drawing process is shown in the Figure 13, which was used for this study. The machine drawing ratio is defined as the ratio of surface speed between the take-up (V_2) and feed roller (V_1). After the drawing process, the filaments may get relaxed and recover to some extent, therefore, the ratio between the final length (i.e., after relaxation) and the original length is called actual drawing ratio. After drawing process, miPP filaments shows the improved physical, structural and mechanical properties. In this research, six different drawing ratios ($DR-1.0$; $DR-2$; $DR-2.5$; $DR-3$; $DR-3.5$ and $DR-4.0$) was applied under 120°C .

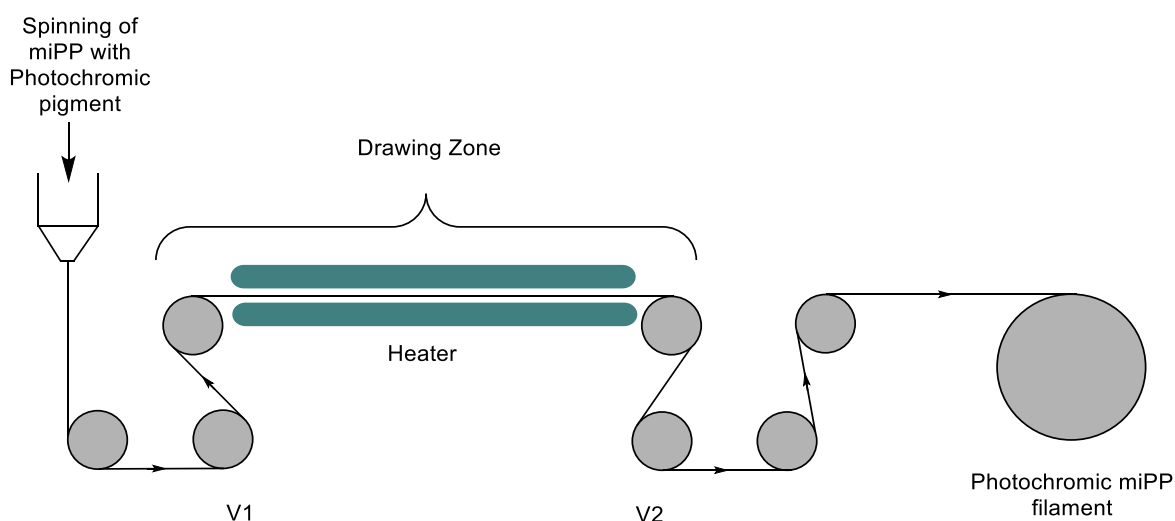


Figure 13: Schematic representation of drawing process (i.e. V_1 - feed roller; V_2 - take-off roller).

3.2.3 Winding process

After the drawing process, the filaments were winded on the gray cardboard with uniform tension as well as sufficient thickness, therefore six layers of the filaments can be winded on the cardboard. The color of the cardboard is gray and there no addition of fluorescing agents in the cardboard and it can be confirmed by subsequent tests.

3.2.4 Measurement of Kinetic properties of photochromic materials

As discussed in the section 2.4.1, Photochrom-3 has made with the activation light source of Edixeon UVLED EDEV-3LA1 with radiometric power (Φ_V)=350mW with adjustable minimum peak wavelength. The minimum peak wavelength for the pigment MPB and MPP incorporated filaments are measured at 385nm, whereas MPY incorporated filaments measured at 365nm, the minimum peak wavelength is based on the pigment characteristics, it can be seen in Figure 14. The Photochrom-3 having the construction of dual light source with the shutter over the exciting light source makes the continuous measurement of photochromic materials with the UV energy density of $675 \pm 50 \mu W.cm^{-2}$. Due to the easy control over excitation with light sources by using the shutter, it becomes possible to examine the photochromic properties of materials with respect to single or multiple cycles. The produced photochromic miPP filaments have been measured five cycles both exposure and reversion phase. One measurement cycle consists of 5 min exposure under UV and 5 min of reversion phase (i.e. without UV-radiation) and totally 10 min per cycle. Average value of the five repetitive measurements was used for statistical data treatment. Generally, photochromic colorants are sensitive towards the temperature, therefore a thermostat was used to maintain the temperature at $22 \pm 2^\circ C$ and the relative humidity is $45 \pm 10\%$. Figure 4 describes the simple process of changes within a sample of an applied photochromic colorants from I_0 (color intensity at time t_0 , or sample without exposure), I_∞ (color intensity after infinite time t_∞). A kinetic model for exposure and reversion phase can be developed based on the first order kinetics, it has been discussed in the section 2.3.1 and 2.3.2 After the kinetic measurement, the Photochrom-3 provides the reflectance value (i.e. reflectance factor) with an accuracy of $\pm 0.5nm$. The reflectance values can be utilized to find out the color strength and another related properties, the color strength (K/S function) values can be computed as following equation Eq. 3.1;

$$\frac{K}{S} = \frac{(1 - R)^2}{2R} \quad (3.1)$$

where R - reflectance factor, K -absorption; S -scattering of colorant. The changing in optical density (ΔOD) was calculated using the Eq. 3.2;

$$\Delta OD = K/S_{\lambda_{max} G_{max}} - K/S_{\lambda_{max} D_{min}} \quad (3.2)$$

where $K/S_{\lambda_{max} G_{max}}$ is the maximal value of K/S function at a wavelength of absorption maxima during exposure phase and $K/S_{\lambda_{max} D_{min}}$ is the minimal value of K/S function at a wavelength of absorption maxima during reversion phase. The color difference (ΔE^*) of drawn and undrawn filaments are computed through simple CIE lab formula in the Eq. 2.31. From the first order

kinetics, the half-life ($t_{1/2}$) of color change and rate constant (k) for the photochromic miPP filaments can be calculated by using the Eq. 2.29 & 2.30 respectively.

3.2.5 Thermogravimetry analysis of miPP filaments

To find out the thermo-chemical behavior of photochromic pigments, the thermogravimetry analysis could be done in Mettler Toledo TGA analyzer. Therefore, the samples weighing between 7-8mg were used for analysis to heat from 25°C to 300°C with a heating rate of 5°C.min⁻¹ under the nitrogen atmosphere.

3.2.6 Differential scanning calorimetry of miPP filaments

The thermal behavior of a material which undergoes to physical and chemical changes with the absorption or emission of heat as a function of the temperature is studied by differential scanning calorimetry (DSC). The function of temperature such as thermal transitions, phase changes, crystallization, melting glass transitions of a material is studied by it. In this analysis, the flow of heat either heat of absorption (endothermic) or heat of emissions (exothermic) is measured as a temperature's function or time of the sample and compared with that of a thermally inert reference. In this research work, the DSC analysis were performed on Perkin Elmer based on ASTM standard D3418-08, the reason for choosing the respective ASTM standard which is advised to start the experiment below 50°C. In the DSC analysis, the produced colored miPP filaments were heated at a rate of 10°C.min⁻¹ from 25°C to 200°C (melting phase), later it cooled from 200°C to 25°C (cooling phase). After the measurement the data was collected for both heating and cooling phase. The measurement can be done under the nitrogen atmosphere in the rate of 20 mL.min⁻¹. Based on the DSC data, the various thermal properties can be calculated such as melting temperature (T_m) and melting enthalpy (H_m), change in melting enthalpy (ΔH_m). Change in entropy (ΔS_m) can be calculated through Eq. 3.3.

$$\Delta S_m = \frac{\Delta H_m}{T_m} \quad (3.3)$$

The crystallinity ($X_c\%$) of the produced filaments were computed from the Eq. 3.4, where ΔH_m° is 209 J.g⁻¹ [76],

$$X_c(\%) = \frac{\Delta H_m}{\Delta H_m^\circ} \times 100 \quad (3.4)$$

3.2.7 Physical & Mechanical properties of miPP filaments

Before going to the mechanical properties, the linear density of produced filaments was analyzed. Later the mechanical properties have been determined through Instron instrument according to the international organization for standardization (ISO) standard 2062:1993. The various mechanical properties namely tenacity, elongation, Young's modulus was investigated and discussed in the section 3.3.2, the coefficients of variations for all these mechanical properties are tabulated in the Appendix- B. For each specimen, the above testing was repeated 20 times and the mean value has been plotted. During the testing, clamping length of 12.5cm was maintained with clamp speed of is 350 $m.min^{-1}$.

3.2.8 Microscopic analysis of miPP filaments

The surface morphology of control and photochromic miPP filaments were observed by using TS5130 Vega-Tescan scanning electron microscope (SEM). While preparing the filament for SEM analysis, first the razor blade is used to cut and used for the cross-sectional analysis. Before SEM analysis, the filaments were sputter-coated with gold by using of Sputter coater to avoid the accumulation of high static electric fields. In the measurement, the electron column was kept at vacuum and other following parameters were used; 20kV accelerating voltage and 500x magnification levels with a vacuum of $7.8 \times 10^{-3} Pa$. The working distance between the sample and objective lens can be adjusted according to the image resolution.

3.3 Results and Discussion of photochromic miPP filaments (circular cross-section)

3.3.1 Effect of photochromic response on drawing ratio of photochromic filaments

3.3.1.1 Effect of K/S Values on drawing ratio of photochromic filaments

In this study, three different photochromic pigments were used to produce the miPP filaments, the reflectance characteristics of these colored filaments were shown in Figure 14. To determine their reflectance characteristics of colored filaments, same concentrations pigments were used (i.e. 1.5 wt.%). During the measurement, it was subjected to exposure 5 minutes under UV-radiation. Photochromic materials are sensitive towards to the amount of UV energy; therefore, it is necessary to ensure the amount of UV energy during the measurement. So, amount of UV energy was measured under exposure and reversion phase, the value of energy

is $675 \pm 50 \mu W.cm^{-2}$, $2.26 \pm 0.8 \mu W.cm^{-2}$ respectively, the detailed measurement of UV energy data was given in Appendix- C.

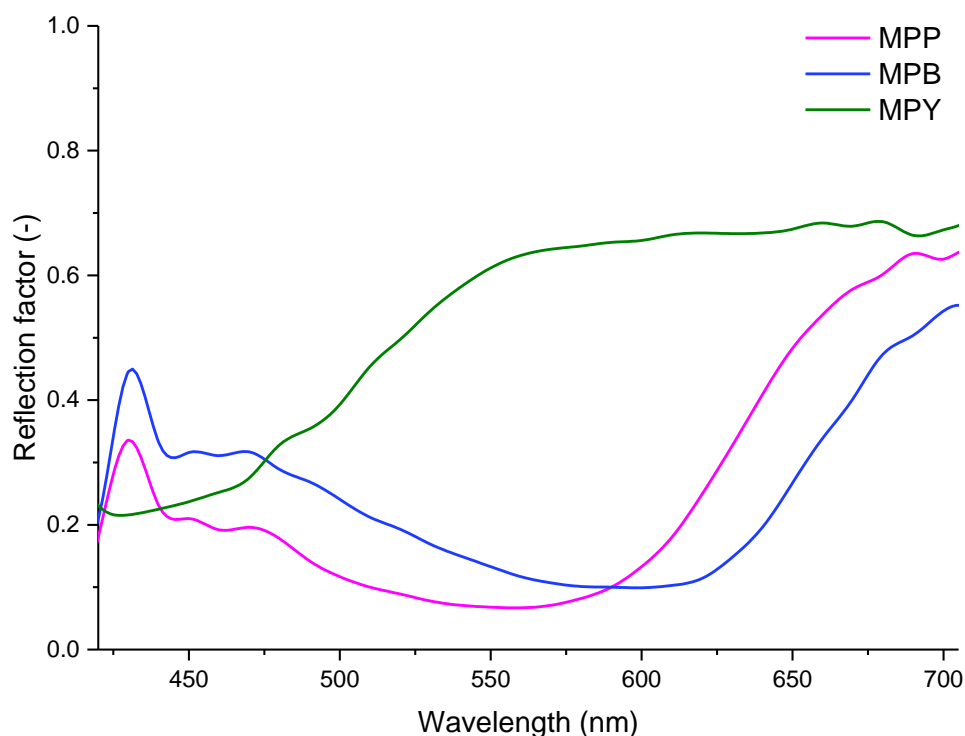


Figure 14: The reflectance spectrum of used photochromic pigments under UV-radiation, Note: MPB- Matsui Photopia Blue; MPP- Matsui Photopia Purple; MPY- Matsui Photopia Yellow.

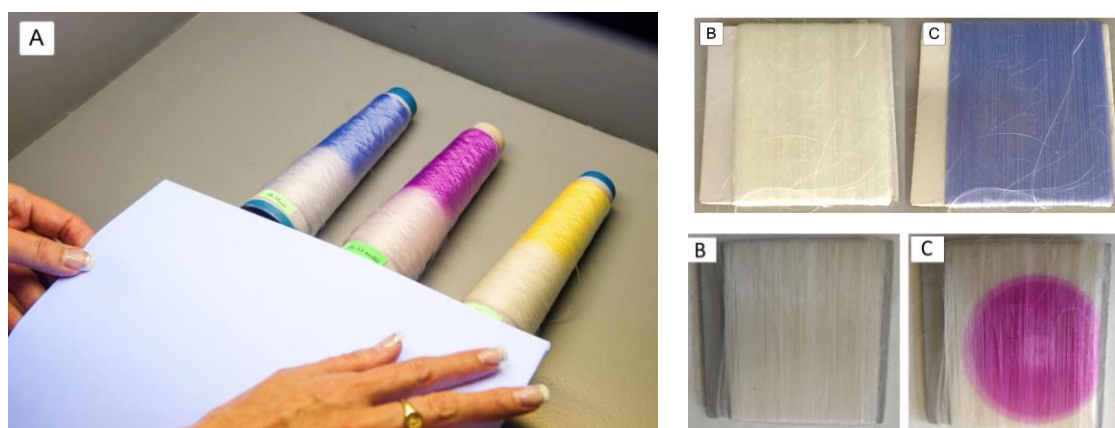


Figure 15: Produced photochromic miPP filaments (A); filament wound on cardboard B & C (B-UV off; C-UV on).

Figure 15 shows the photographs of original color (i.e. colorless) and developed the color of the filament under the UV exposure. These photographs were captured after removal of UV-

radiation and within 3s. Nevertheless, there are practical issues associated with the picture capturing, but it mostly with weakly developed color as well as the pigment having the fast decay (i.e. reversion). In case of color difference is not possible to capture within the specified time limit, due to the in presence of UV-radiations. For color measurement, the color human eye is the oldest techniques and it used for a long time, still some of the people used (i.e. visual assessment), however, it has specific drawbacks like the memory of colors and its related parameters such as hue, value and chroma. These drawbacks are solved by developing the instrument, research still has the growing and interest in the field of color measurement. The first spectrophotometer was developed by Hardy and Hunter in 1935 and 1948 respectively [77]. There are many assumptions on the color measurement, the theory of Kubelka and Munk is one among them. This theory corresponds to the ratio of the absorption (λ) and scattering S (λ) coefficient with respect to the dominant wavelength (λ). In simple words, it defines the spectral reflectance ($R\%$) of the colored substrate with its absorption (K) and scattering (S). In general, the K/S values can be calculated when the color measurement is carried out in the reflectance mode. To understand, the K/S values grow to infinity when the reflectance towards to zero. In other words, it is a ratio of absorption coefficient to the scattering coefficient, in purely it indicates the number of colored molecules absorbed in the filaments. Normally, the higher the K/S value, greater the dye uptake and deeper the color shades. In textile, paper and coating industries are mostly using this Kubelka-Munk equation to formulate the colors, since, it assumes the scattering coefficient (S) of colorants which depends on the type of substrate and its physical properties, on other hand, the absorption coefficient (K) of light depends on the colorants. Therefore, Kubelka-Munk (K/S) model is most suitable for the colored textiles since it included the higher scattering effects. The absorption property of colorants decides the strength of color, it is not only for the classical colored materials but also for the textiles colored with functional dyes. In simple explanations, the K/S values express the color strength, even for the photochromic colored textiles as like classical dyed textiles. However, the rate of shade change is a complex parameter indicating the rate of change achromatic shade to color shade where all three (i.e. reflectance, absorption & scattering) changes are present coordinate of the colorimetric system, it is better to express this parameter using the K/S values or Kubelka-Munk function, which is simultaneously the expression of spectral change characteristics- in other words, the remission properties with respect to the change of the photochromic conformation organic molecules, as described in section 2.3. The kinetic measurement of photochromic materials can be done in Photochrom-3 under the reflectance mode, finally, results are computed as K/S value by using of Eq. 3.1. Later on, the various optical properties

of photochromic materials are analyzed, namely, color build-up analysis through K/S function, K/S (max) at exposure phase, changing in the optical density (ΔOD), color difference analysis via L^* , a^* , b^* & ΔE^* (under CIELAB 1976), half-life of color change in both exposure and reversion phase, rate constant and color intensity at beginning, half and infinitive. This Photochrome-3 is used to find all these colorimetric properties photochromic miPP filament with respect to the spectral characteristics. Above mentioned properties were used to express the optical properties of a photochromic system with respect to the color difference and color buildup under UV & without UV-radiations. The K/S values of both exposure and reversion phase with respect to the time and wavelength interval are plotted in Figure 16 and Figure 17 respectively for the filament with MPP pigment. These graphs provide the information on the influence of K/S values with respect to the UV radiation. Figure 16 describes, K/S values are significantly increased some extent with respect to the time and in this case, it required 30s to reach the maximum value of K/S (i.e. 6.27), thereafter the systems get saturated with minor stabilization, in this position called photostationary state or photostationary equilibrium. There are many parameters which decide the time requirement to reach the maximum K/S values, such as the structure of colorants, amount of UV energy, measurement geometry and properties of the substrate. Figure 17 defines the idea of K/S values with respect to the time at reversion phase, time 0 second indicates the UV radiation was switched-off. After removal of UV radiation, it requires 128s to reach the minimum value of K/S from the maximum value of K/S . It is evident from these two graphs are, positive acceleration of K/S values under UV exposure required less time than the negative acceleration of K/S under reversion phase, it is due to the structure of photochromic pigment (MPP) which having the higher half-life. The results of half-life for color change can be discussed in deeply in section 3.3.1.4. In other words, conversion of colored form to the colorless form required more time, which is slightly depended on the time, whereas reverse phase is independent on the time. The reason behind this is, during the exposure phase, the photochromic compounds get faster reconversion of the original chemical structure (i.e. conversion of original form to merocyanine form), in case of reversion phase, it becomes slower reconversion of merocyanine form to original form.

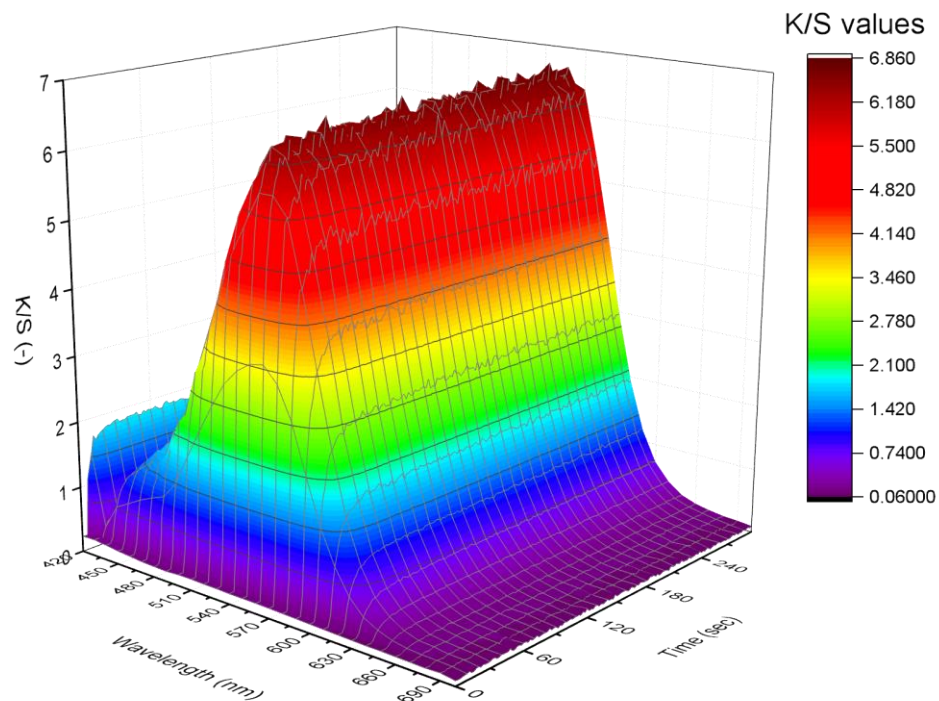


Figure 16: Kubelka-Munk characteristics miPP filaments (MPP-2.5 wt.%) under 5 minutes of exposure phase.

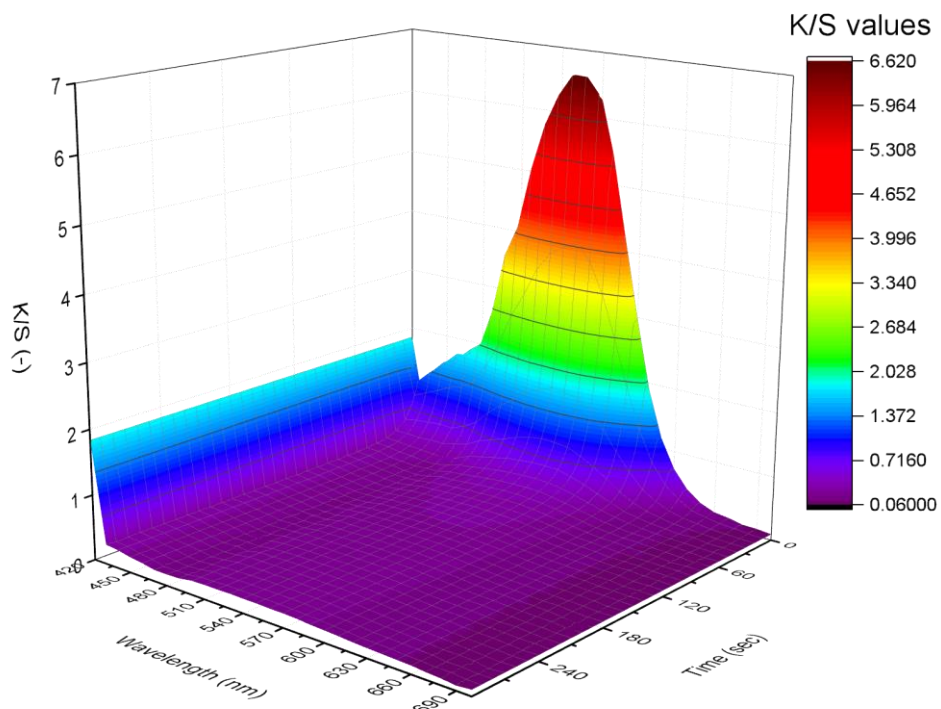


Figure 17: Kubelka-Munk characteristics miPP filaments (MPP-2.5 wt.%) under 5 minutes of reversion phase.

Figure 16 and Figure 17 gives the information on the individual spectra curves, in the case of exposure phase shows overlapping ($A \rightarrow B$), on the other hand, it gives good separation of spectra curves under reversion phase ($B \rightarrow A$). Figure 18 illustrates the result of photochromic miPP filaments with (MPP- 2.5 wt.%) exposure and reversion phase, this result is an average value of five measurements in both exposure and reversion phase. The span of measurement error in the exposure phase shows higher than the reversion phase, which means that the error from reversion phase is invisible, this is due to the higher variability in exposure phase and lower variability in reversion phase. However, the variability of measurement in the reversion phase shows higher at the initial stage and gradually reduced and to some extent it becomes invisible. The reason behind for these phenomena is, the molecular vibration in the excited state is generally higher than the opposite direction (i.e. excited state to ground state, also called as reversion), it can be confirmed by the results.

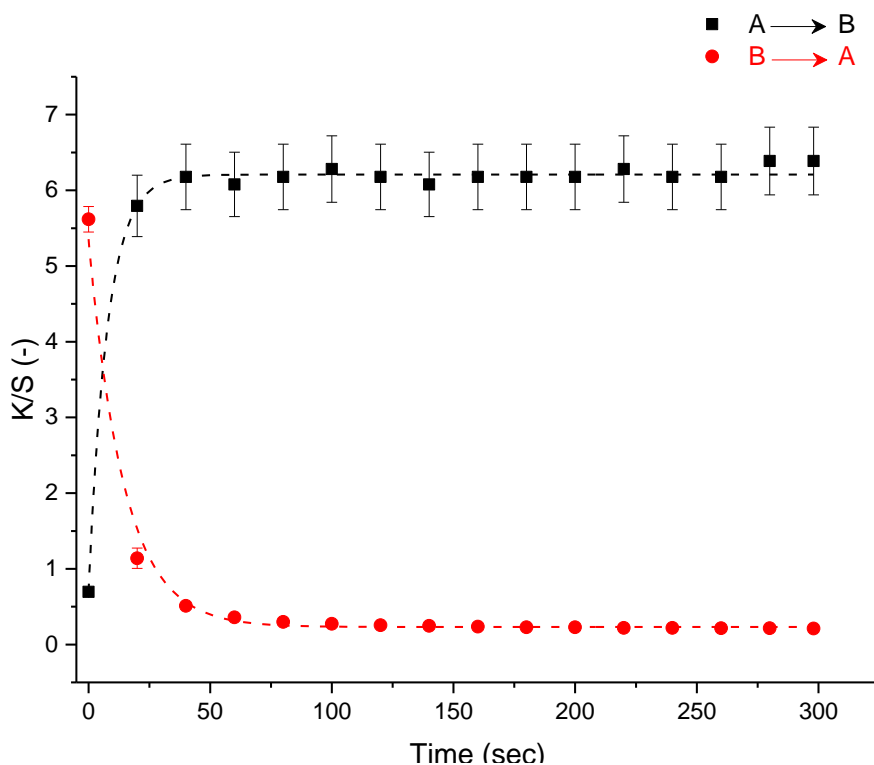


Figure 18: Conversion of photochromic system ($A \rightarrow B$ - exposure) and ($B \rightarrow A$ - reversion) (MPP 2.5 wt.%).

The results of K/S values for five cycles of exposure and reversion phase for the various concentration of photochromic miPP filaments with MPP pigments on circular cross-sections were plotted in Figure 21 to Figure 24. Results significantly show the reduction of K/S values with increasing the fineness of filament (i.e. increasing the drawing ratio). Therefore, K/S

values are depending on the drawing ratios of respective filaments, in a simple way, it could be, amount of light reflection during the color measurement is marginally depends on the presence of pigment in the filament with respect to the unit area. Therefore, light reflection is decreased with increasing the drawing ratio. During the drawing process, there is an extension of filaments towards to the drawing direction (i.e. lengthwise), in other word, increasing the length of filaments causes the reduction of the diameter. In the mass colorations, the pigments are mixed thoroughly with the polymer in the molten state, when it extrudes, the pigments are incorporated with the filaments since the amount of pigment per unit area could reduce according to the drawing ratio in the drawing process.

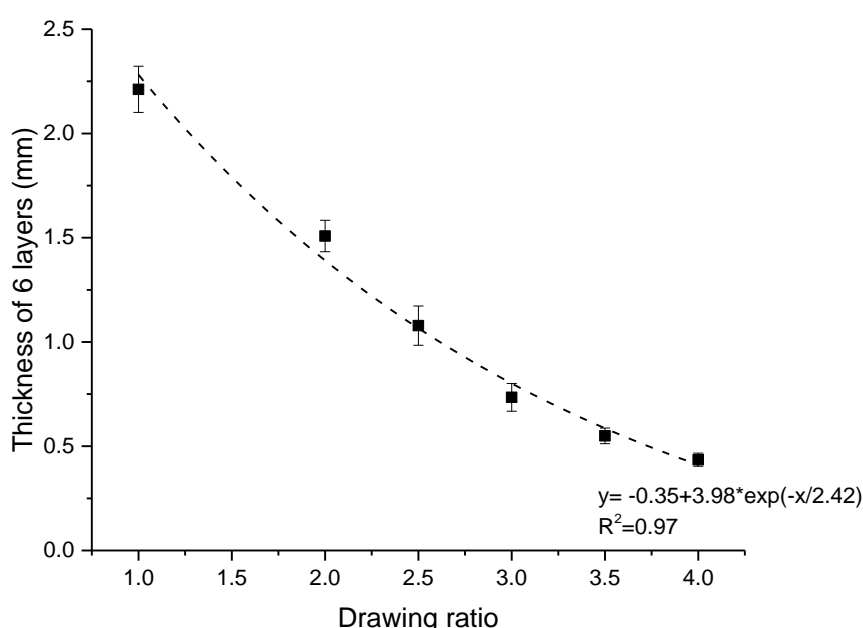


Figure 19: Thickness of 6 layers of the produced filament in the card board (MPP-0 wt.%).

Apart from this fact, the thickness of filament layers also influences the light reflection, for all drawing ratio, the filaments are wind uniform number of layers (i.e. six layers) on the gray board, which already explained in the section 3.2.3, the thickness of layers is decreased with increasing the drawing ratio, this is due to the reduction of filament fineness. The thickness of filament layers versus drawing ratio is plotted in Figure 19. The drawing ratio 1 shows the highest thickness and drawing ratio four indicates the lowest thickness of the layers. In this case, the drawing ratio 4 could not reflect all the light during the color measurement, due to the lowest thickness of the layers may cause that some part of light could be absorbed by the background, it can be confirmed in Figure 20.

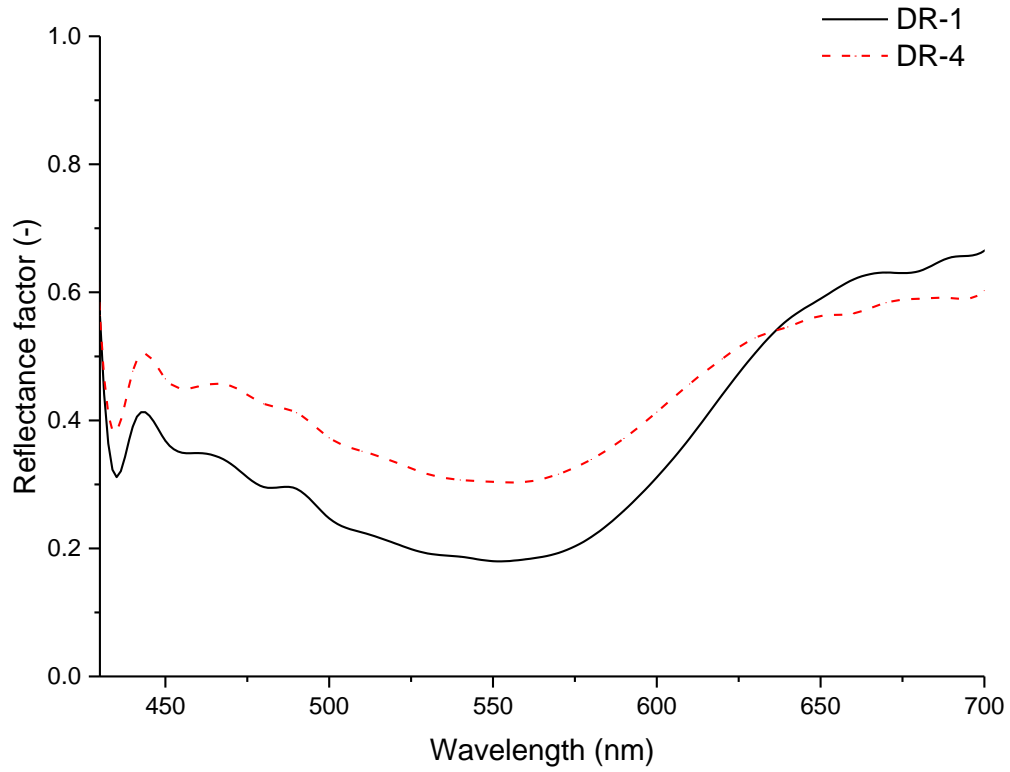


Figure 20: Reflectance spectra of photochromic miPP filaments (MPP-0.5 wt.%)

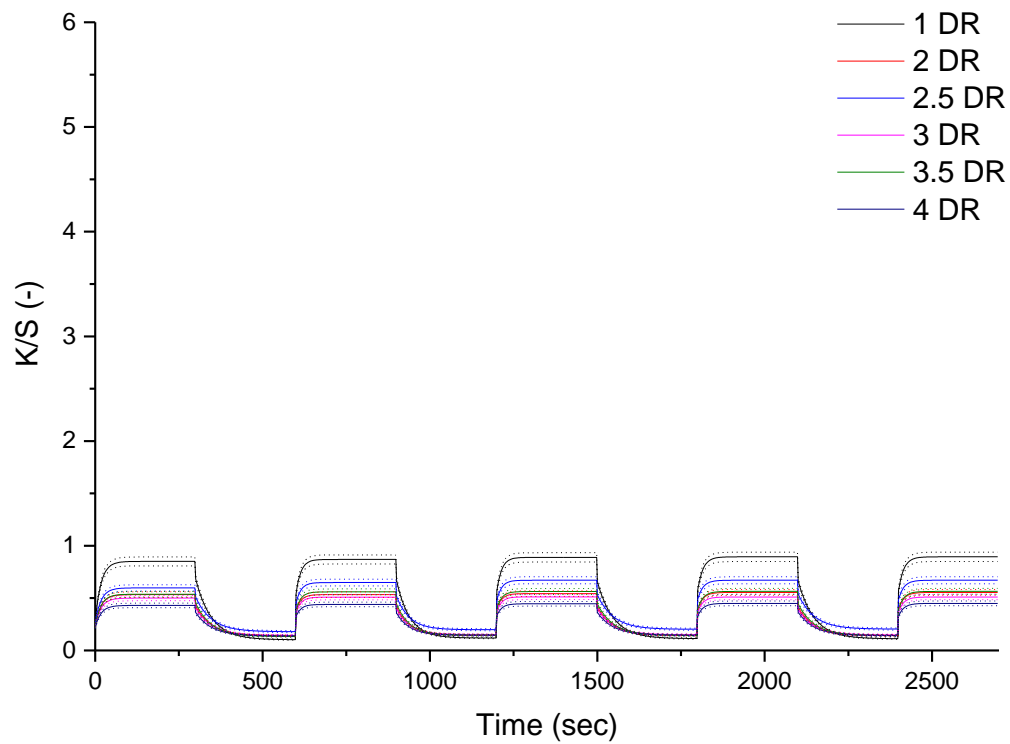


Figure 21: Effect of DR on K/S values of photochromic miPP filaments (MPP-0.25 wt.%).

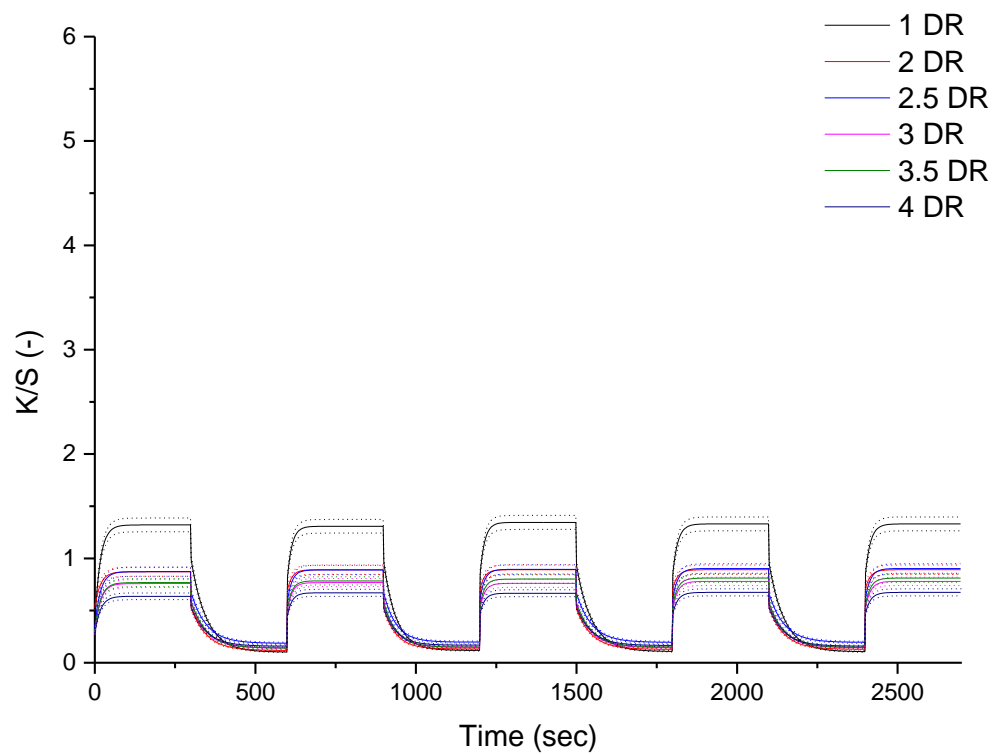


Figure 22: Effect of DR on K/S values of photochromic miPP filaments (MPP-0.50 wt.%).

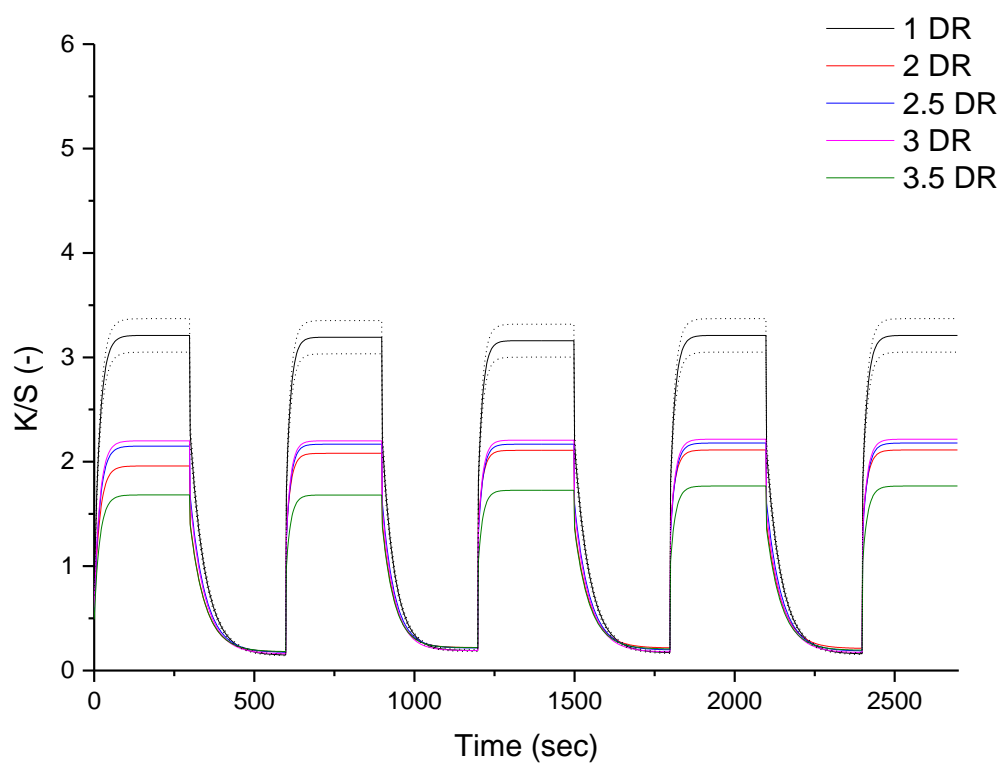


Figure 23: Effect of DR on K/S values of photochromic miPP filaments (MPP-1.50 wt.%).

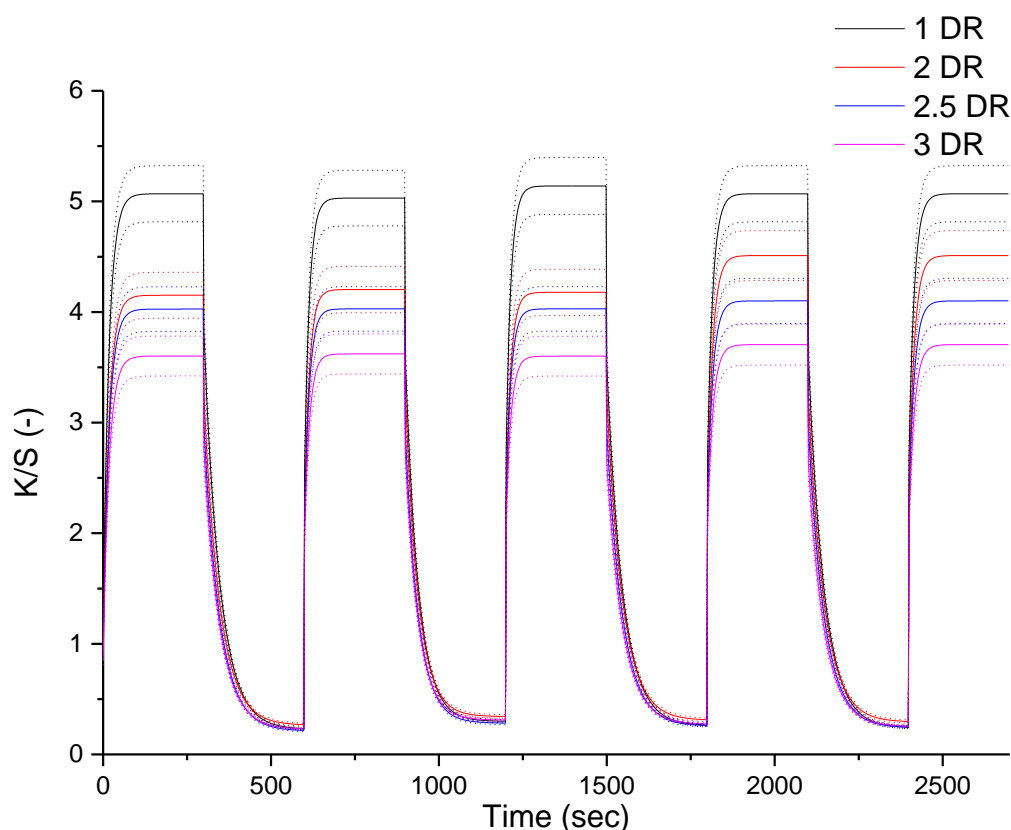


Figure 24: Effect of DR on K/S values of photochromic miPP filaments (MPP-2.50 wt.%).

Generally, it is the well-known effect of absorption coefficient (K), which express the absorption of light rays versus presence of colorant in the photochromic miPP filament during the color measurement, the absorption values could be modified with respect to the drawing ratio. Nevertheless, the opposite value of absorption coefficient (K) is the scattering co-efficient (S) and the value of scattering co-efficient also depends on the substrate (photochromic filament). Increasing the value of (S) is nothing but the amount of colorless reflection, which purely reduces the shade intensity or color buildup of photochromic filaments. Apart from these facts, there are some factors which influence the colorimetric analysis, which is, refraction coefficient of the filament with and without coloration, the cross-section of the filaments (i.e. closer to circle, triangle, 5-star, 8-star), filament surface and distribution of the photochromic pigments on the filament.

3.3.1.2 K/S (max) of photochromic miPP filaments during the exposure phase

K/S (max) for produced photochromic miPP filaments (circular cross-sections) under exposure phase were plotted in Figure 25 to Figure 27 with respect to the color of the pigment. Results were significantly reduced with increasing the drawing ratio. Therefore, K/S (max) values are

purely depending on the drawing ratio of the produced photochromic miPP filament. This is due to the changing of physical and geometrical properties of the filaments, the modifying physical and geometrical properties of the filaments could modify the light absorption/reflection properties of the colored filament. From these results, it is confirmed that negative correlation between fiber fineness & K/S (max). Therefore, the optical characteristics are decreased with increasing the drawing ratio.

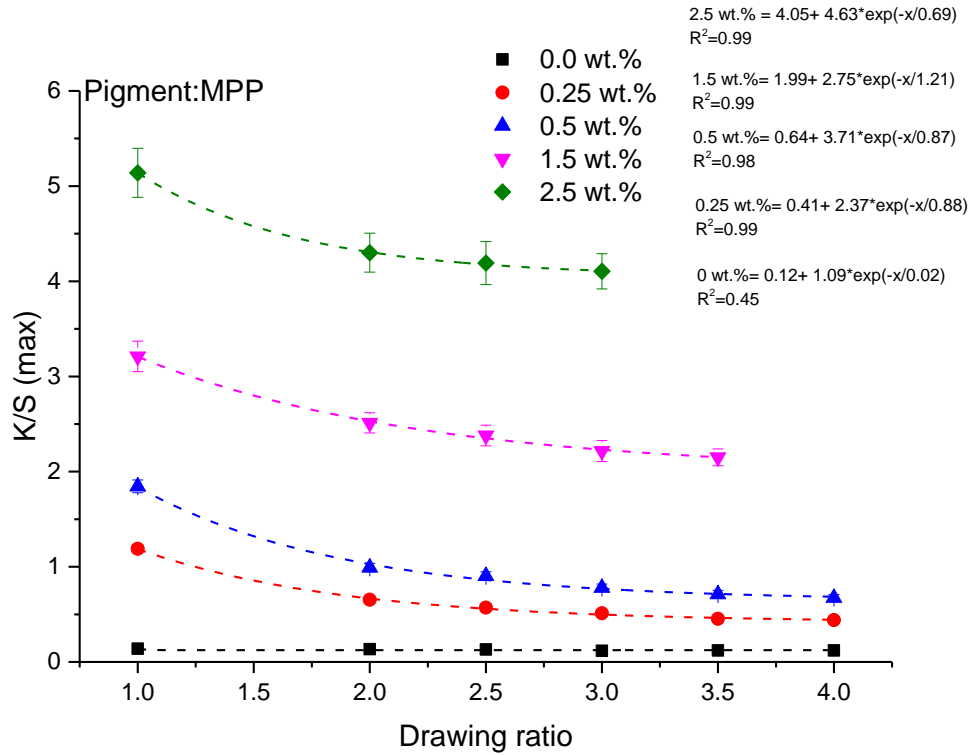


Figure 25: Dependence of K/S (max) on the photochromic miPP filaments with MPP under exposure phase.

The results of K/S (max) on drawing ratio was fitted with exponential functions to find the goodness of fit. For all drawing ratios, the photochromic miPP filaments with MPP shows $R^2=0.98$ and above, which conclude there is a strong relationship between the drawing ratio and concentration of MPP pigment. The same trend was observed in case of MPB, the goodness of fit was observed in all the cases $R^2=0.98$ and above. On other hand, filaments with MPY shows a linear relationship between drawing ratio and concentration of pigment. Also, it shows 220% less K/S (max) values than another pigment (i.e. MPP) in the same concentration. There are many possibilities for the reduction of K/S (max) values, one is the thermal degradation of the pigment during the melt spinning, it can be discussed in upcoming section.

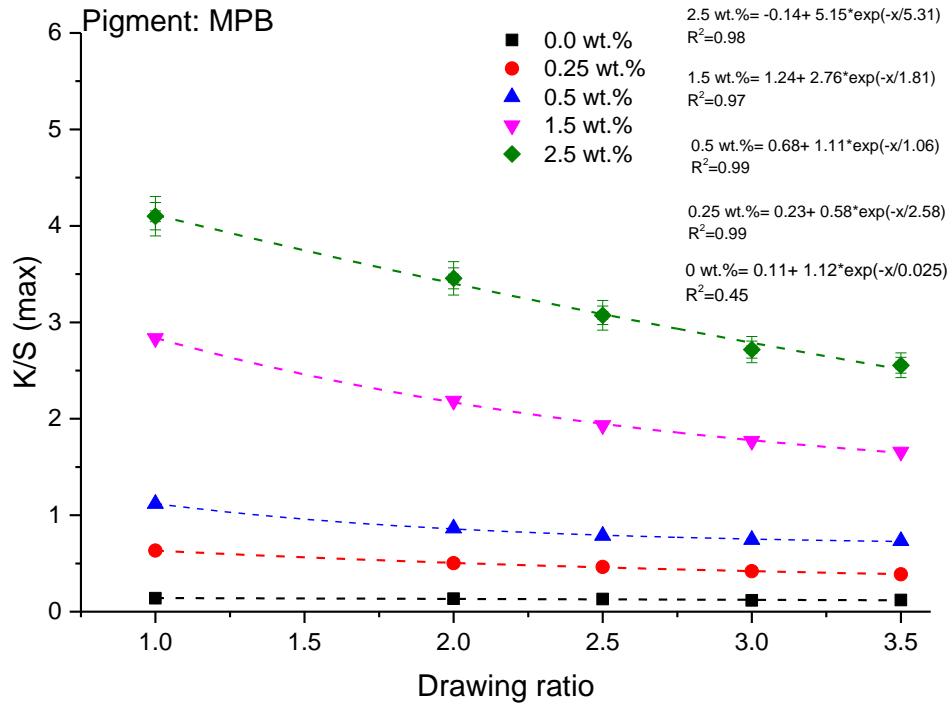


Figure 26: Dependence of K/S (max) on the photochromic miPP filaments with MPB under exposure phase.

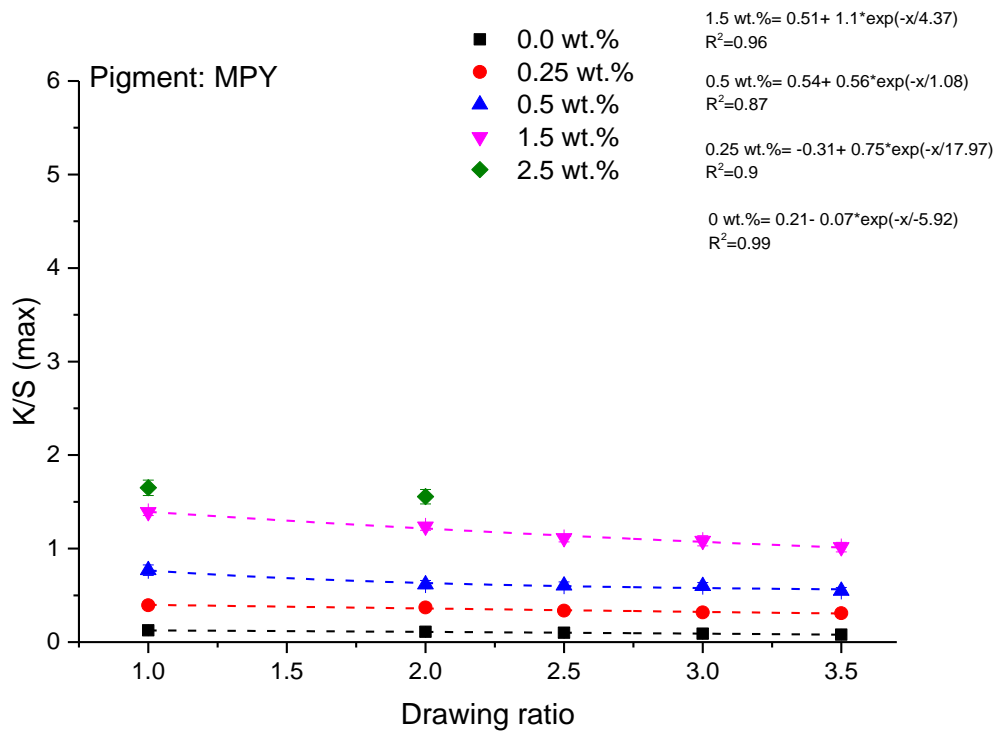


Figure 27: Dependence of K/S (max) on the photochromic miPP filaments with MPY under exposure phase.

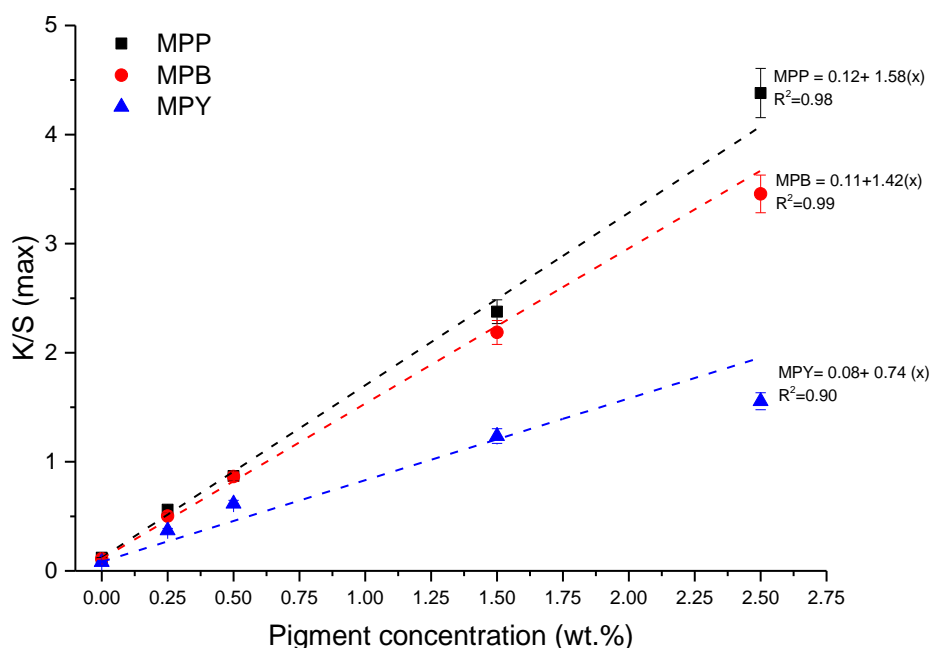


Figure 28: Dependence of K/S (max) for various photochromic miPP filaments (DR-2) under exposure phase.

Figure 28 shows the K/S (max) for all three pigments with same drawing ratio (i.e. DR-2), overall K/S (max) is increased with increasing the pigment concentration. The results of K/S (max) for all the data was used to fit with linear regression and MPP shows the $R^2=0.98$; MPB is $R^2=0.99$ and MPY provides $R^2=0.92$, it confirms there is a strong linear relationship between the pigment concentration and K/S (max) values. Among of three pigments, MPP shows highest and MPY shows lowest K/S (max) values, even in the same concentration. This purely depends on the dyeability of photochromic pigment with respect to the miPP filament, there are many parameters which influence the dyeability, namely, stability of pigment towards to the heat, chemical structure of pigments, adverse interactions between the additives like stabilizers (HALS and others), other impurities present in the pigments, these factors may have caused to reduction of dyeability. These unforeseen reactions will reduce the K/S values among the pigments. Figure 43 shows the thermal properties of three different photochromic pigments. Among three pigments, MPY shows the highest degradation in terms of weight loss towards to the specific temperature, it can be seen in TGA measurement. In the mass coloration, heat stability for the colorants decides the dyeability, if heat stability is good, which produce higher

dyeability and it is vice versa and the factors behind these phenomena could be well explained in the section 3.3.3.

3.3.1.3 Changing in optical density of photochromic miPP filaments

ΔOD of produced photochromic miPP filaments (circular cross-sections) were plotted in Figure 29 to Figure 31 and it can be calculated through the Eq.3.2. The changing in optical density can be measured on the undrawn filament (DR-1) with respect to the drawn filaments. Results significantly show the reduction ΔOD values with increasing the drawing ratio. Therefore, ΔOD were depending on the drawing ratio of produced photochromic miPP filaments. However, this is due to changing the physical and geometrical properties of the filaments, which change the ΔOD . From these results, it is confirmed that negative correlation between fiber fineness and ΔOD . It is due to the light absorption/reflection between the filament and optical characteristics are decreased with increasing the drawing ratio. The results of ΔOD with respect to the drawing ratio was fitted with exponential functions, which helps to find the goodness of fit. For all drawing ratio, the photochromic miPP filaments with MPP shows $R^2=0.95$ and above, which conclude there is a good relationship between the drawing ratio and the concentration of MPP pigment. The same trend was observed in case of MPB, the goodness of fit was observed in all the cases $R^2=0.98$ and above. On other hand, ΔOD for the filaments with MPY shows a linear relationship between drawing ratio and concentration of pigment. The goodness of fit was found $R^2=0.83$ in case of the concentration 1.5 wt.%, for other concentration shows above $R^2=0.92$. The results of ΔOD for three pigments shown in Figure 32 with same drawing ratio (i.e. DR-2), the ΔOD is increased with increasing the pigment concentration, the trend was observed for three pigments. The results of ΔOD for all the data was used to fit with linear regression and MPP shows the $R^2=0.98$; MPB is $R^2=0.99$ and MPY provides $R^2=0.89$, it confirms there is a strong linear relationship between the pigment concentration and ΔOD . Among of three pigments, MPP shows highest and MPY shows lowest ΔOD , even in the same concentration. These phenomena are purely depending on the dyeability of photochromic pigment with respect to the miPP filament, there are many parameters which influence the dyeability, namely, stability of pigment towards to the heat, chemical structure of pigments, adverse interactions between the additives like light stabilizers (HALS and others), other impurities present in the pigments, these factors may have caused to reduction of dyeability. These unforeseen reactions will reduce the ΔOD among the pigments. Figure 43 shows the thermal properties of three different photochromic pigments. Among three pigments, MPY shows the highest degradation in terms of weight loss towards to the specific temperature,

it can be seen in TGA measurement. In the mass coloration, heat stability for the colorants decides the dyeability, if heat stability is good, which produce higher dyeability and it is vice versa and the factors behind these phenomena could be well explained in the section 3.3.3. Generally, the absorption (K) and scattering (S) of produced photochromic miPP filaments are negatively correlated in photochromic pigment absorption bands, in other words, when the concentration of photochromic pigment is increase, the absorption (K) ascends and scattering (S) will descend, it is confirmed from K/S values and followed by K/S (max) and ΔOD . However, the miPP filament already have the property of scattering, once it has mass colored (i.e. filament contains the photochromic pigment) created many absorbing points. In most cases, we consider the refractive indexes of substrate, but it is necessary to consider the refractive indexes of colorants (in this case, photochromic pigment) and its effects on the filaments with respect to the scattering, but these scattering effects are very small and it is within tolerable and so it could be ignored. When the concentration of photochromic pigment is increased, the distance between scattering and absorption points of photochromic miPP filaments have bellowed the limit of incoherence, which is nothing but, the scattering and absorption points of photochromic miPP filaments are coherent [78].

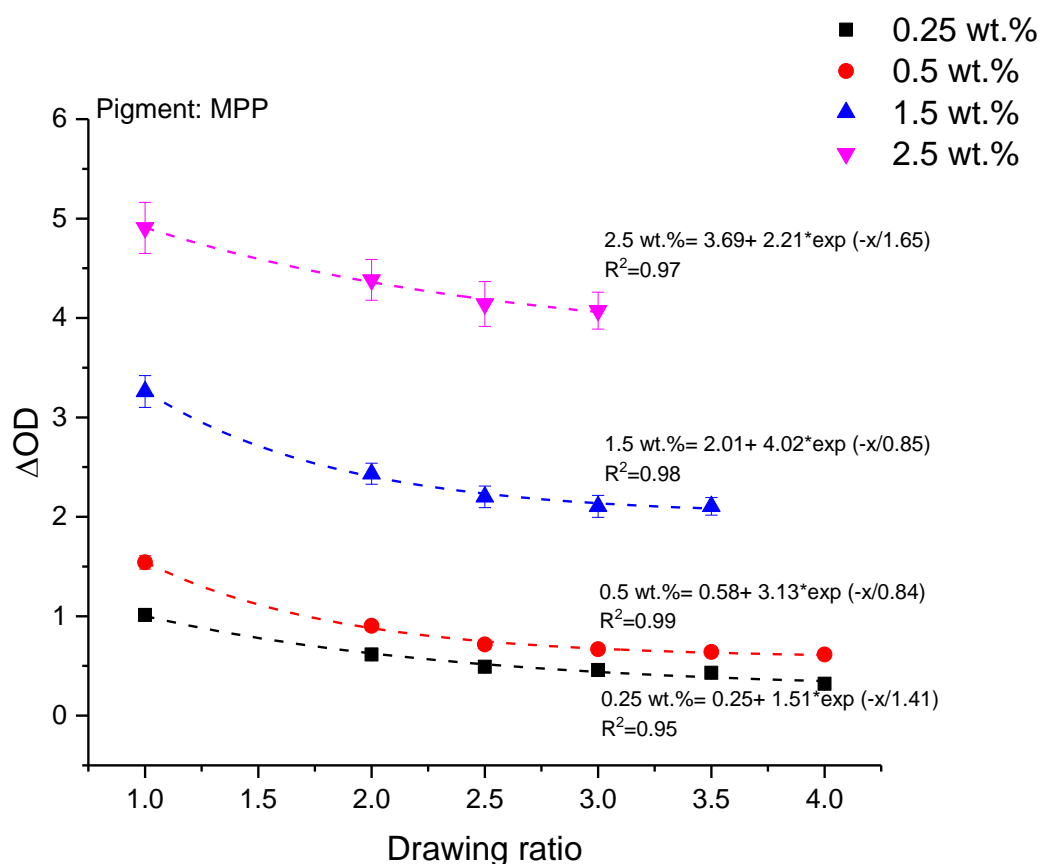


Figure 29: Dependence of ΔOD on the photochromic miPP filaments with MPP.

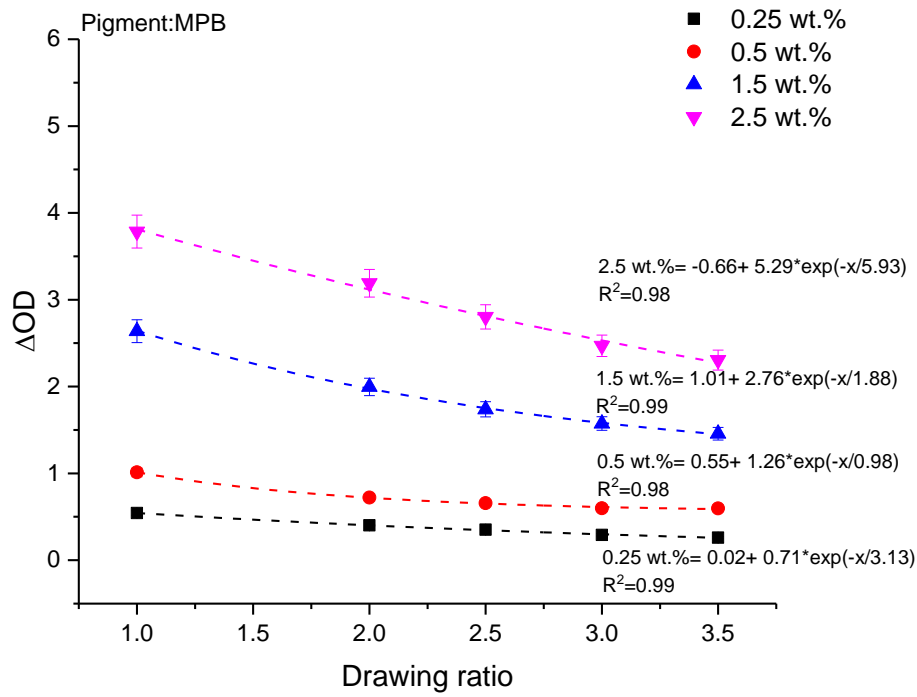


Figure 30: Dependence of ΔOD on the photochromic miPP filaments with MPB.

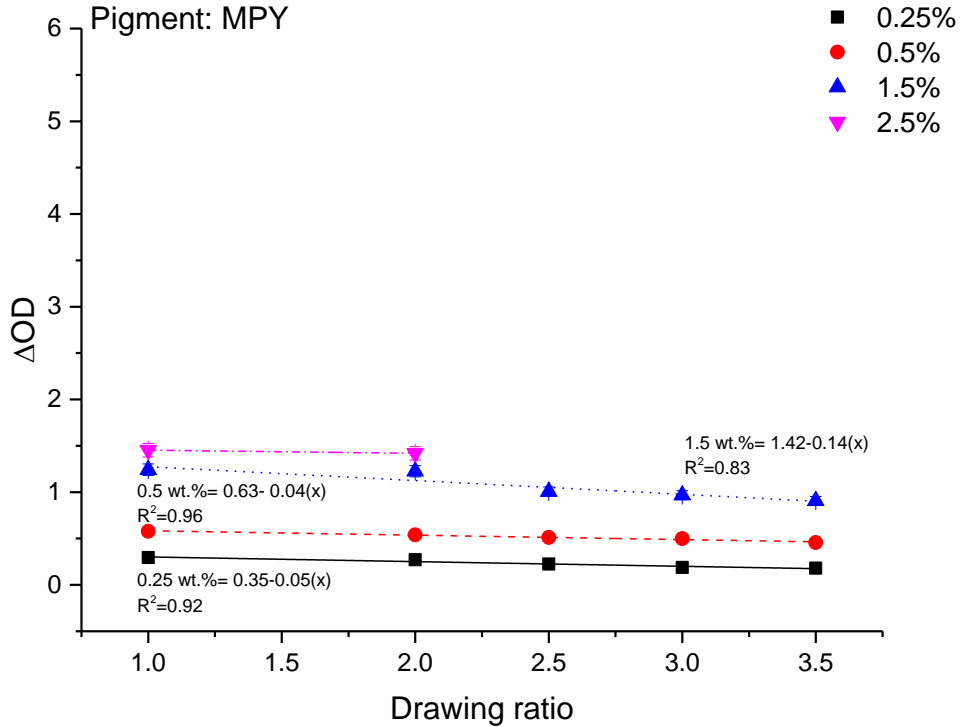


Figure 31: Dependence of ΔOD on the photochromic miPP filaments with MPY.

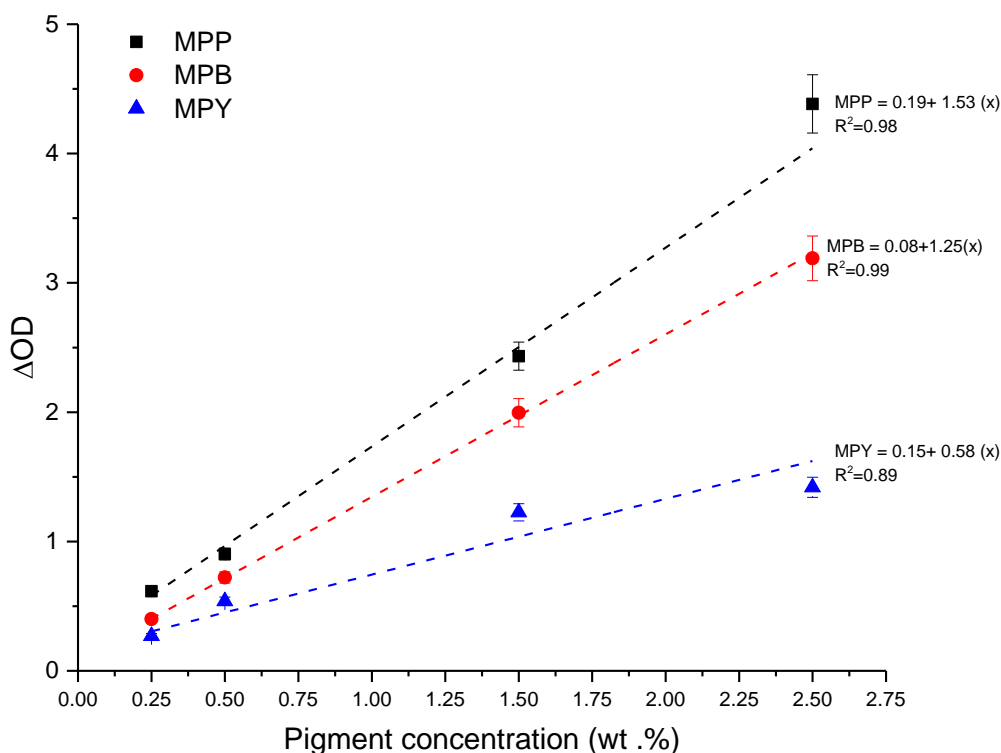


Figure 32: Dependence of ΔOD on the various photochromic miPP filaments (DR-2).

3.3.1.4 Half-life of color change for photochromic miPP filaments

The term 'half-life' is a rate of time taken for the photochromic colorants to fade back to original color or vice versa. The concept of half-life is important for the photochromic materials which explains the stability and rate of reaction of photochromic response of the materials. In this research work., the half-life of color change could be calculated as per the first-order kinetics, the equation is clearly described in the section 2.3.2. The reason for choosing the first order kinetics, to calculating the half-life is, the photochromic reaction is directly proportional to the concentration of photochromic pigments in other words the reaction is independent of the initial concentration of photochromic pigment since it is a unique aspect of first-order kinetics. The half-life of color change for the photochromic filaments could be calculated as per the Eq. 3.4. The relationship between in the half-life of color change during the exposure and reversion phase was studied with pigment concentration, the observed results show that there is a significant dependence of half-life of color change with respect to the pigment concentration, the trend is same for both exposure and reversion phase. Figure 33 shows the half-life of color change of photochromic miPP filaments with respect to the pigment concentration under the exposure phase, results are evident that purely depends on the concentration of pigments, the

trend of the result is same as for all the pigments. The half-life for color change during exposure is approximately two times less than the reversion phase. The results of the half-life of color change and rate of reaction varied with respect to the type of pigment, even though in same concentrations. In the concentration of 0.25 wt.%, results of the half-life of color change during the exposure phase shows 34s, 24s, 15s for the pigment MPP, MPB and MPY respectively. So, it confirmed that the filament with the pigment MPY shows faster reaction which is nothing but shorted half-life as compared to other pigments. Similarly, the pigment MPP provides the longer half-life color change, which denotes the slower reaction. During the exposure phase, all the pigments show half-life of color change has been reduced linearly with increasing the concentration of pigments from 0.25 to 2.5 wt.%. It was observed, miPP filament with MPP shows 34s when the concentration is 0.25 wt.%, the same filaments were reduced to 24s when the concentration has been increased to 2.5 wt.%, Similarly the lowest half-life of color change was found in filaments with MPY, 14s and 5s respectively with the above-mentioned concentration, these data were fitted with linear regression and the goodness of fit was found $R^2=0.91$. The observed linear trend is same for another pigment too. The goodness of fit for MPB and MPY shows $R^2=0.89$, $R^2=0.91$ respectively. The variability of error shows higher in case of filaments with MPP and lower with MPY. Overall the results conclude that filament with MPP shows longer half-life which denotes slower reaction, on other hand filaments with MPY shows shorter half-life of color change, which is nothing but faster reaction. The half-life of color change for all three pigments in the order of $MPP > MPB > MPY$. Figure 34 described the half-life of color change of photochromic miPP filaments under the reversion phase, it is clearly described that the results are depending on the pigment concentration, which is similar to the exposure phase. The results of the half-life of color change during reversion phase has been reduced linearly by increasing the concentration of pigment, it can be observed for all three pigments. In the concentration of pigments at 0.25 wt.%, MPP incorporated filament shows 71s, when the concentration is increased to 2.5 wt.%, the half-life of color change could be reduced to 45s. This trend is same for other pigments too, overall results during the reversion phase were found that filament with MPY shows the lowest half-life, 23s for 0.25 wt.%, in case of 11s for 2.5 wt.%. The results of the half-life of color change during reversion phase with respect to the pigments in the order is $MPP > MPB > MPY$. There are many parameters which influence the half-life of color change, such as, amount of UV radiation and its absorption rate of pigment, concentration of photochromic colorant, available form of colorant, chemical structure of the colorant, number or type of functional groups present in the colorant, position of functional group, surface area of reactant, temperature of the system, reaction rate and type

of substrate. However, it is generalizing the statement and it is difficult to articulate the specific parameter which influences on the half-life of color change. However, one conclusion can be proposed from these results, increasing concentration makes faster reconversion of the original form of photochromic pigment into merocyanine form. Based on the first order kinetics, the detailed kinetic parameters of photochromic miPP filaments are tabulated in the Appendix- A. Figure 35 shows the dependence of half-life of color change on the drawing ratio of miPP filaments under exposure phase, the graph is made with a constant concentration (i.e. pigment concentration- 1.5 wt.%) of all three pigments. From this graph, it is evident that increasing the drawing ratio of photochromic miPP filaments causes to increase the half-life of color change. Therefore, the half-life of color change is strongly depended on the drawing ratio too. To confirm these facts, data were fitted with linear regression, the R^2 values shows, 0.98, 0.90 for the filament with pigment MPP and MPB respectively. In the case of MPY shows 0.82, which means that moderate relationship between the parameters. Drawing ratio has a strong influence on the half-life, this effect is same in both exposure and reversion phase (Figure 36). The reason behind these phenomena is, increasing the drawing ratio will decrease the number of photochromic colorant per unit mass of the filaments which reduce the rate of reaction of conversion and reconversion of the original structure of photochromic pigments to merocyanine form and vice-versa, so, it increases the half-life of color change, it happened in both exposure and reversion phase. Even other photochromic properties like color strength values, changing in optical density and maximum color strength also reduced with increasing the drawing ratio. All these facts are described already elaborated at the section 3.3.1. The life time of colored merocyanine forms of MPP incorporated filaments found longer than other pigments, the reason might be the merocyanine group of MPP could be stabilized by the intermolecular interaction between the two spirooxazine photochromic groups.

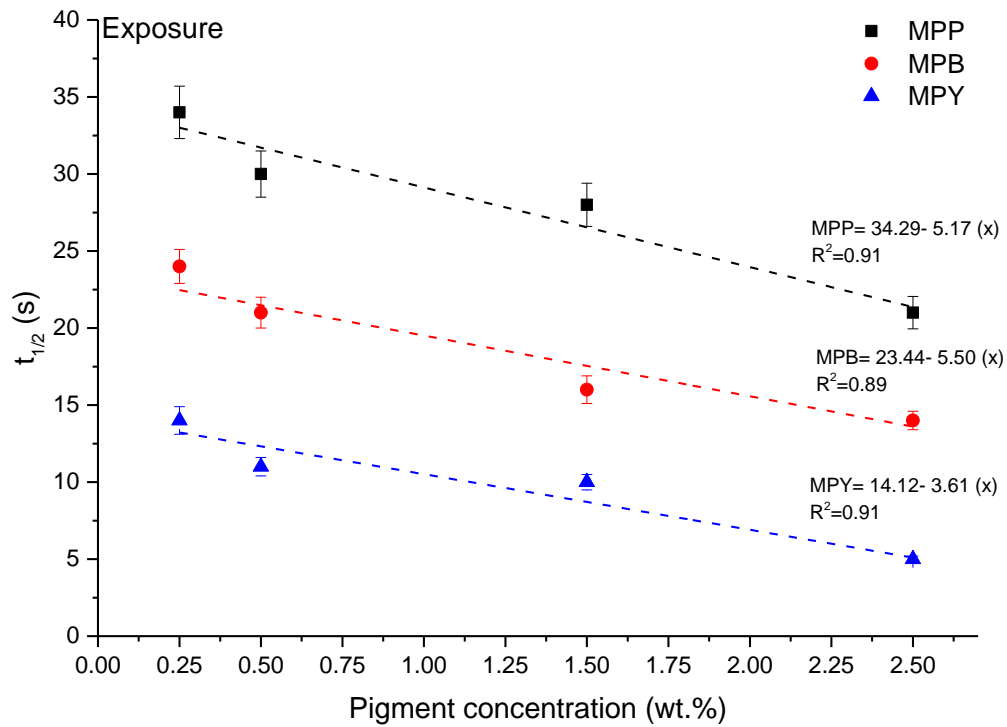


Figure 33: Half-life of color change on miPP filaments under exposure phase (DR-2).

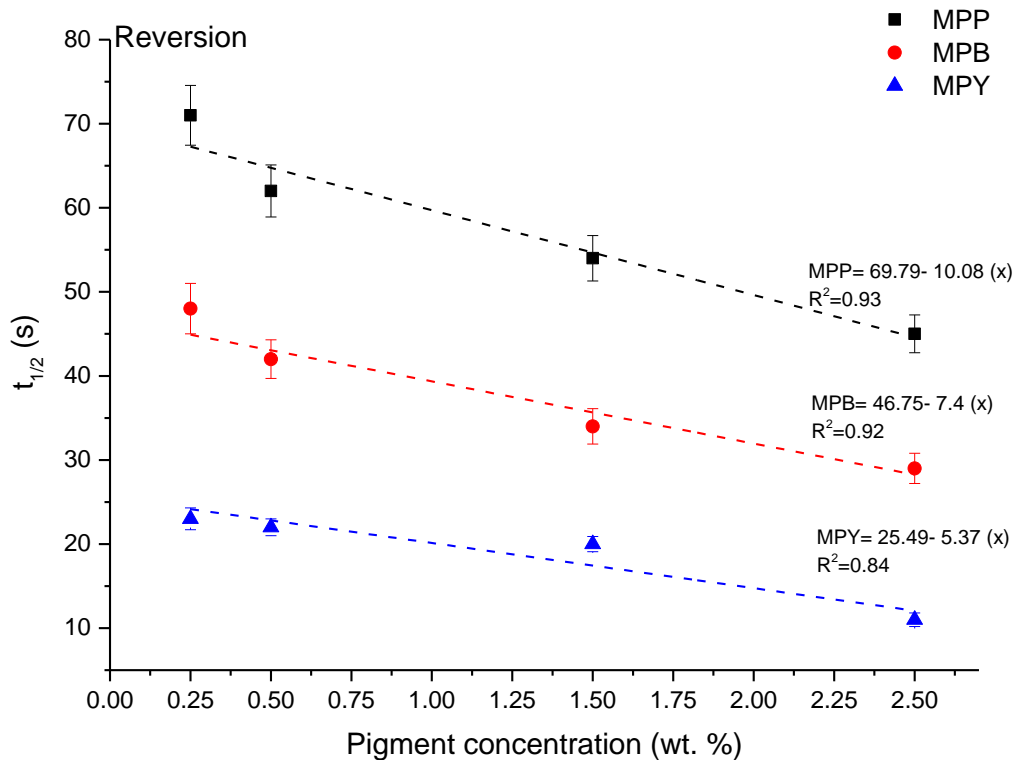


Figure 34: Half-life of color change on miPP filaments under reversion phase (DR-2).

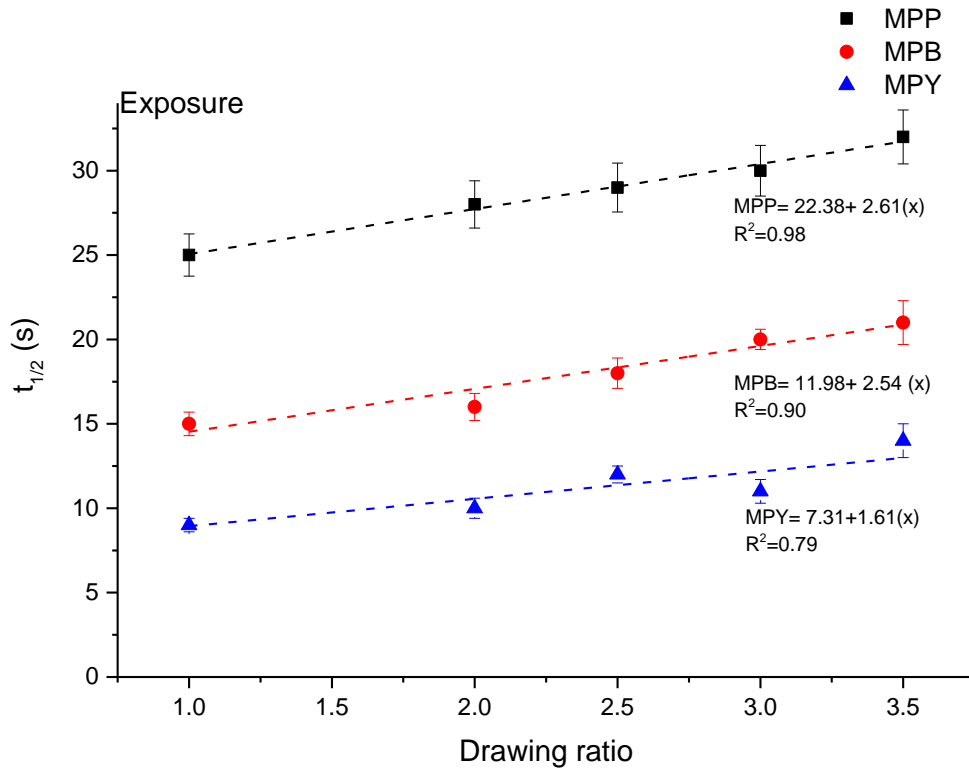


Figure 35: Half-life of color change on miPP filaments under exposure phase, (pigment concentration- 1.5 wt.%).

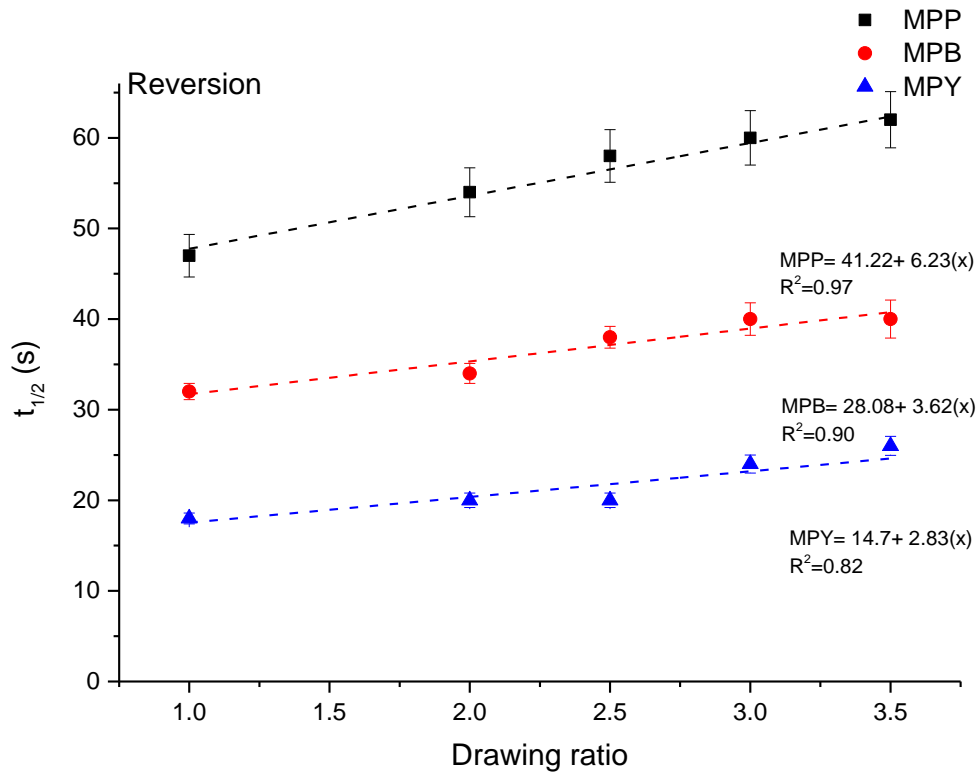
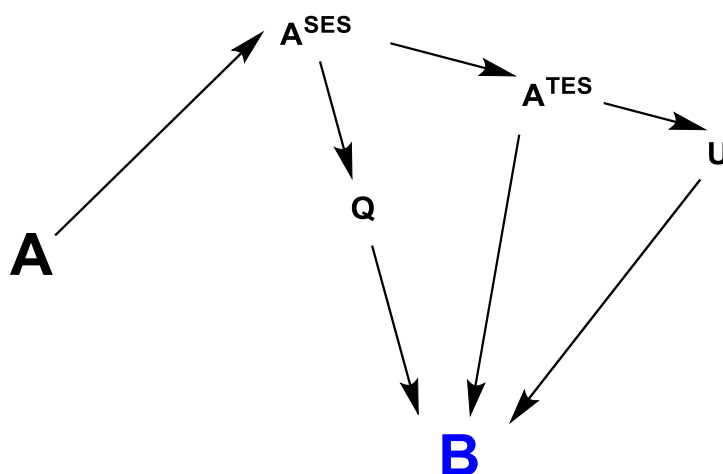


Figure 36: Half-life of color change on miPP filaments under reversion phase, (pigment concentration- 1.5 wt.%).

3.3.1.5 Color difference analysis of miPP filaments

The CIELAB color space (1976) is very well established for the determination of color changes by using different colorimetric properties, namely $L^*a^*b^*$. Based on these models, it is possible to identify the various level of color perceptual. However, the photochromic systems show the color or tint shift during the exposure phase (i.e. under UV irradiance) can be expressed different colorimetric properties such as reddish, yellowish, bluish and greenish. Therefore, the orthogonal three-axis system can be used to describe the color properties of photochromic materials, it can be discussed deeply in section 2.4.2 and the residual ΔE^* and the results are plotted in Figure 37 to Figure 39. The speed of coloration and discoloration for the photochromic materials mainly depends on the chemical structure and amount of UV energy, however, when it applied in to the other materials like textiles may create another parameter which influences the properties of the substrate. For all these parameters which could decide the coloration and discoloration, stability, fatigue resistance and discoloration of photochromic materials. Perhaps, the color difference ΔE^* can explain the changing of hue, shade intensity or shifting of the lightness of the color which is produced by the photochromic materials. These colorimetric properties were analyzed with respect to the residual ΔE^* values which explains the visible color difference on the photochromic filaments and it is depended on the physiology of the human vision, nevertheless, when these filaments are used as a sensorial application for the determination of UV (i.e. when it applied to the UV sensor) in the atmosphere, there is an important requirement which ability to recognize the specific color difference for the human visual evaluation. For human eyes can identify the discernible color differences, when the residual ΔE^* values is higher than 0.4. Overall the results found that the maximum residual ΔE^* values are ~2.5 units and minimum is ~0.02. Also, the maximum residual ΔE^* values are found for the lowest drawing ratios, however, these residuals ΔE^* values are a significantly nonlinear relationship with respect to the concentration of pigment and drawing ratio, the residual ΔE^* values are marginally increased with increasing the concentration of pigment, it can be observed for all three pigments. Among three photochromic miPP filaments, coloration with MPB shows higher residual ΔE^* values (~2.5 units) when the drawing ratio is 2. The data were fitted with an exponential function to find the goodness of fit, which show $R^2=0.95$. It conveys that there is a non-linear relationship between the residual ΔE^* and the concentration of pigment. The goodness of fit for another drawing ratio also shows above 0.95, which conveys that there is a non-linear relationship between the concentration and residual ΔE^* values. The photochromic miPP filament with MPY pigments observed lowest ΔE^* , it can be

seen in the lowest drawing ratio as well as in the highest concentration of pigment too. The reason behind in these phenomena is, first it provides the lower color strength values, also these colors is brighter, which shows the lower color differences. There are many reasons behind in this fact for the varying the residual ΔE^* values, first concentration of pigment, under the exposure, the same number of colored molecules affected for lower and higher (up to certain limit) concentration, on the other hand, it create big difference in the lowest concentration, this mechanism is similar to the light fastness of classical dyed textile goods, therefore it accelerate to change the residual ΔE^* values, second reason is the molecular structure and functional groups present in the photochromic pigment. Generally, it undergoes isomerization with the presence of UV radiations to form merocyanine groups or vice versa (i.e. without UV radiations), during these structural modifications, there is a possibility to form some side product, which may react thermally or photochemically to form short-lived isomers (Q and U) between the singlet energy state (A^{SES}) or triplet energy state (A^{TES}) to colored isomer (B), the detailed mechanism is described in Scheme 8. This effect is more apparent on the highest concentration of pigment (2.5 wt.%) and in case of lowest concentration (0.25 wt.%), the ΔE^* values are not perceptible by human eyes since the results show less than 1 unit.



Scheme 8: Possible pathway of photoisomerization of photochromic colorants (i.e. A -colorless; A^{SES} - singlet energy state; A^{TES} - triplet energy state; Q and U - short-lived intermediates; B - colored isomer (adopted and modified from [79]).

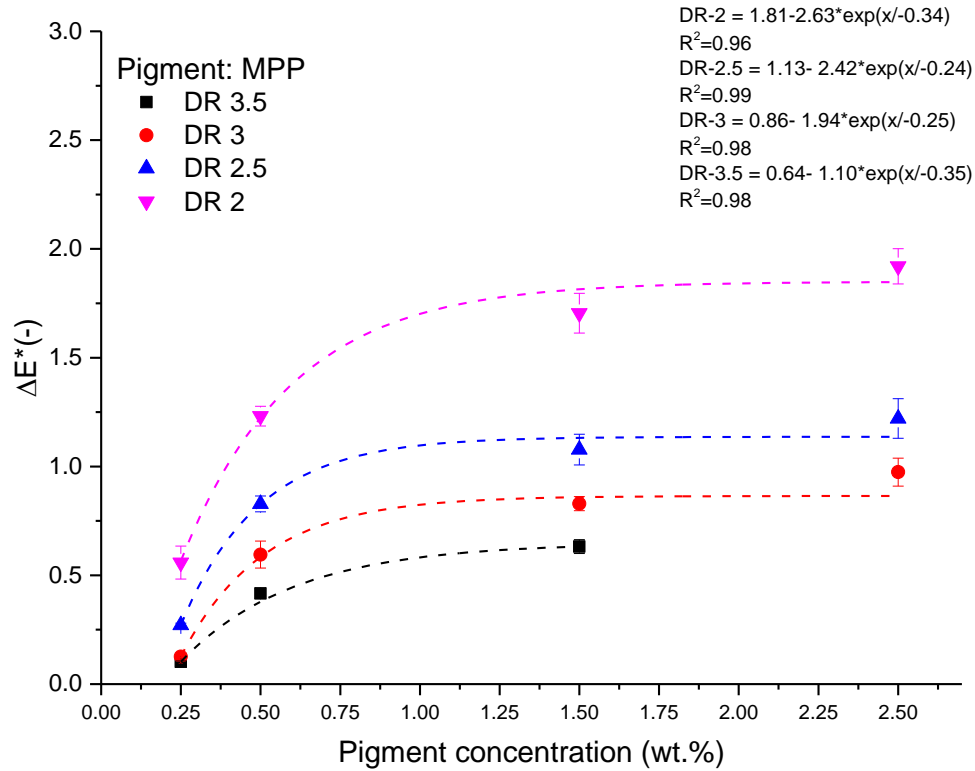


Figure 37: Residual ΔE^* values for photochromic miPP filament with MPP.

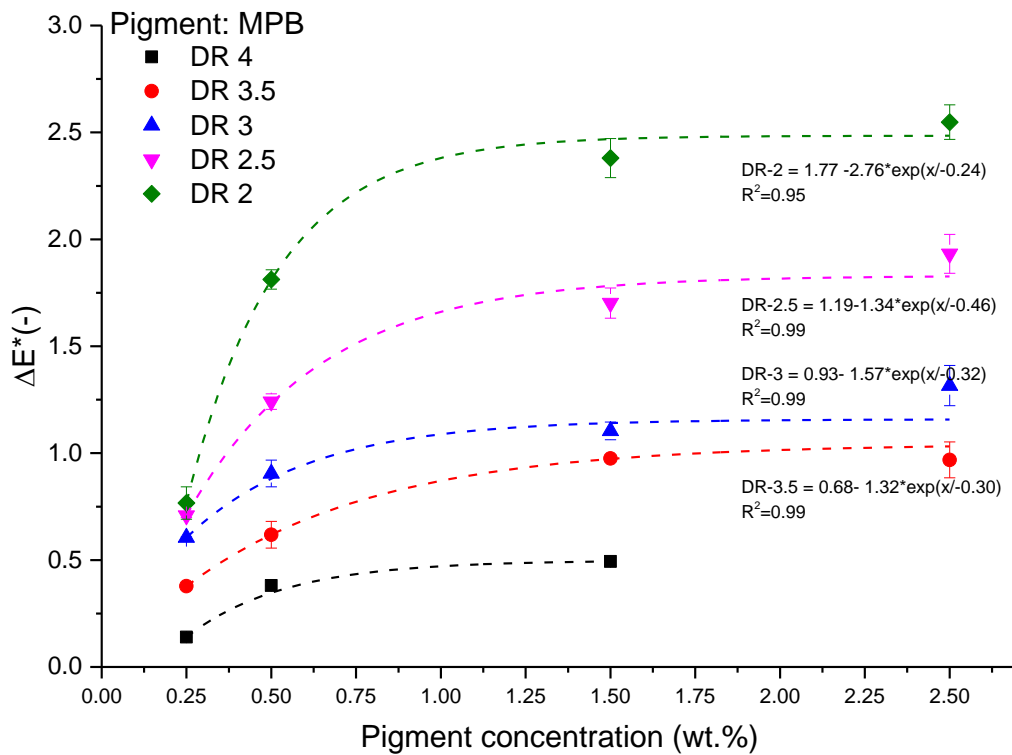


Figure 38: Residual ΔE^* values for photochromic miPP filament with MPB.

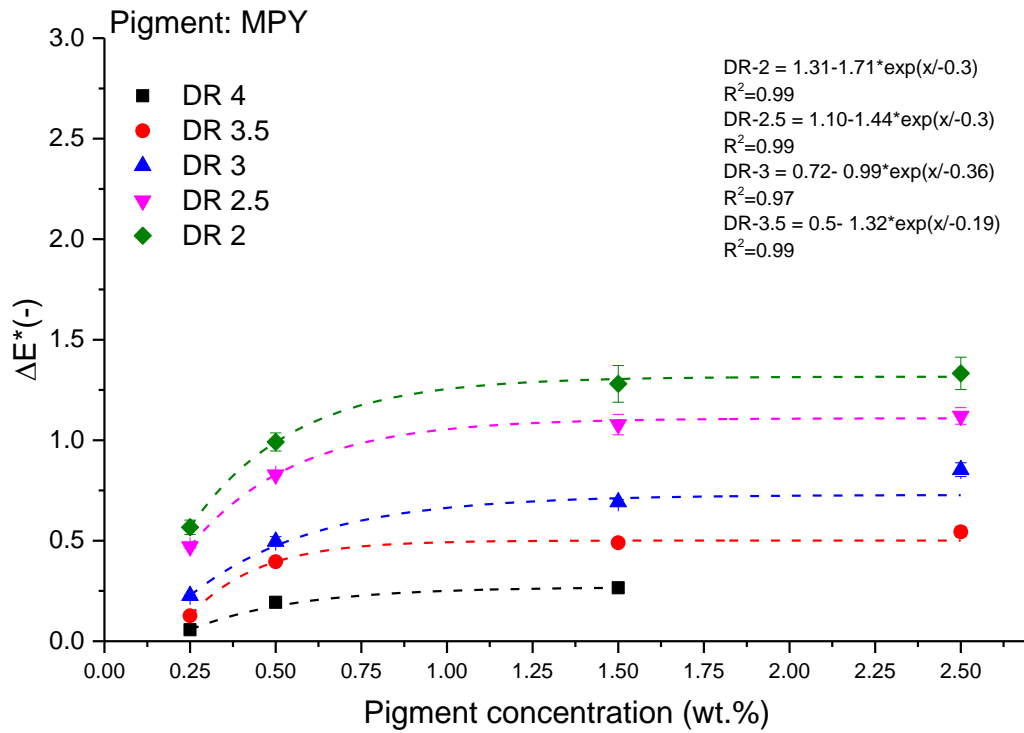


Figure 39: Residual ΔE^* values for photochromic miPP filament with MPY.

3.3.2 Physical and mechanical properties of photochromic miPP filaments

3.3.2.1 Linear density of photochromic miPP filaments

After the drawing process linear density of miPP filaments are decreased with increasing the drawing ratio, it can be seen in Figure 41. The linear density of $45.3 \pm 0.3 \text{ tex}$ for the drawing ratio of 1, and when the drawing ratio is 4, the linear density can be $14 \pm 0.17 \text{ tex}$. There is an exponential trend was observed when increasing the drawing ratio between the linear density. The linear density can be measured 20 different places of the filament and the average data was fitted with exponential functions, the goodness of fit was found $R^2=0.98$, it confirmed that there is an exponential relationship between drawing ratio and linear density. In this work, produced filaments were drawn at 120°C , which is above the glass transition temperature (T_g). The drawing process can be applied increase the tensile load on the miPP filament which is another reason for the reduction of linear density, the respective tensile load is increased with increasing the drawing ratio. However, decreasing the linear density by increasing the drawing ratio was expected. It is due to the heat and strain which was applied to the filaments during the drawing process, therefore it reduces the linear density. But it depends on the how much strain was

applied under specific temperature. In other words, during the straightening process, the macromolecules of the filament can tend to arrange themselves with respect to the filament direction, which purely caused to reduce the linear density. The structural arrangement of macromolecules during drawing process can be explained in Peterlin model, which is shown in Figure 40. There is interesting fact was observed, the addition of photochromic pigment can cause to decreasing the linear density (Figure 42). The linear density of $45.3 \pm 0.3 \text{ tex}$ for the concentration of 0 wt.% (i.e. without the addition of photochromic pigment) and when the concentration 2.5 wt.% the linear density was reduced to $34.2 \pm 0.22 \text{ tex}$, it concludes that linear density was reduced 24% by addition of pigment. In general, the introduction of additives can reduce the size of spherulites, since it cannot enter into composition of spherulites, however it can be positioned in the intercrystallite phase, therefore, the polymer supermolecular structure can be disordered, it can be extensively studied by Danilova [80], due to all these modifications there is a reduction of linear density and other physical properties of colored filaments.

3.3.2.2 Tensile strength of photochromic miPP filaments

It is a well-known effect that increasing the molecular orientation leads to increase the tensile properties. In case of molecular orientation in isotactic polypropylene will take place in the monoclinic (α), hexagonal (β) and orthorhombic (γ) [81, 82]. As discussed earlier the drawing process can lead to modify the structural arrangement of polymers in both crystal and non-crystal forms. The drawing process was carried out in two methods, they are hot and cold drawing. During the hot drawing process, the plastic deformation will take place by twinning and the phase transformation of lamellae [82], in case of cold drawing there are large plastic deformation takes place due to the neck formation, in compression of both the methods have pros and cons which already studied by many researchers [83–85]. Therefore, Peterlin model gave an idea of how the drawn fiber/filament can provide the improved tensile properties by modifying its structural orientations. According to the Peterlin model, the folded chain blocks are broken off from lamella during the drawing process, which also turns to their axes to the drawing direction, therefore, it ensures to modify the crystalline and amorphous regions of polymer structure, the proposed Peterlin model was described in Figure 40.

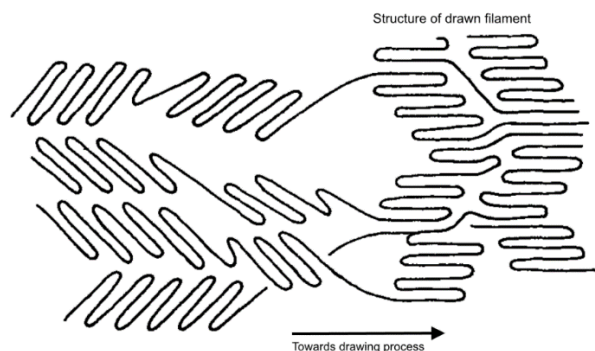


Figure 40: Filament molecular model (Peterlin model) of structure transformation during the drawing process (adopted and modified from [86, 87]).

Figure 41 shows the dependence of tensile strength on the drawing ratio, where the tensile strength of $10.51 \text{ cN.tex}^{-1}$ for the drawing ratio of 1, and when the drawing ratio is 4, the tensile strength of $31.94 \text{ cN.tex}^{-1}$, however, the limit of drawing ratio has been increased further till 5 and the results are falls slightly, this is due to the large variance in the gripping method during the sample testing, also, finer diameter of filaments were difficult to determine the elongation. The results show that non-linear relationship between the drawing ratio and tenacity, which can be fitted with exponential functions to find the goodness of fit, which shows 0.96. The goodness of fit was confirmed that there is strong relationship between the tenacity and drawing ratio. The tensile strength is the function of both crystallinity and orientation of molecular chain, as the peterlin model shows that the increasing the drawing ratio make changes in the molecular orientation which directly influenced on the tensile behavior, also it modifies the birefringence. In general, the addition of spinning additives can reduce the tenacity and elongation at break, it can be studied [88–90], in this research, results confirms that the addition of photochromic pigment causes to reduce the tensile strength and elongation at break, which is shown in Figure 42. Results of tenacity have been reduced 28 % between the concentration from 0.25 wt.% to 2.50 wt.%. The results confirm that there is a non-linear relationship between the pigment concentration and tenacity, the goodness of fit was found ($R^2=0.99$), which describes there is a strong dependence of tenacity with respect to the pigment concentrations. A possible explanation of these phenomena can be a pre-orientation of the crystalline segments of the polymeric chains are located around the photochromic pigments, which causes with slight decreasing of its melt viscosity. The melt viscosity is responsible for the backbone bonds such as chain flexibility and degree of entanglement. According to the reference [91], addition of additives like pigments are usually affects their strength and structure, which also confirmed from our research too.

3.3.2.3 Elongation at break of photochromic miPP filaments

Elongation at break is the strain at which polymer breaks during the testing under controlled temperature. To understand, the polymer with high crystallinity and orientation tends to be strong, on the contrary, the semi-crystalline polymers with low orientation have the higher elongations at the break with low modulus. Figure 41 shows results of elongation at break with respect to the drawing ratio. There is an exponential relationship between the drawing ratio and elongation at break, the goodness of fit was found $R^2=0.99$, which recommend that there is a strong relationship between the drawing ratio and elongation at break. The elongation at break 260.3% for the drawing ratio of 1, and when the drawing ratio is increased to 4, the elongation at break was found 39.9%, which confirms there is a reduction of 84%. The reason is, when the filaments to pull down in to the tensile direction causes to stretch the amorphous molecules, in depth, when the strain force is applied on the semi-crystalline polymer, first the amorphous phase of polymers are affected, nevertheless, this process is purely elastic in nature, when the force on the polymer was released to the polymeric system can be stress free, however, it is up to some extent. If the force is beyond the limit, the polymer is going to deformed, which causes to the sliding of crystallites. In general, each crystallite of the polymer can be composed of chain-folded lamellae, which are the primary reason for the low modulus as well as high elongation to the respective polymer. During the drawing process, lamellae can be orientated by themselves from a parallel direction to deformation direction, however, there is a possibility of interlamellar slipping, also the lamellae can be unfolded which causes the ultimate break. All these modifications can be increased with increasing the drawing ratio, as results elongation at break can be decreased and it confirmed from the results.

3.3.2.4 Elastic modulus of photochromic miPP filaments

The Young's modulus (i.e. elastic modulus) is one of the important parameters which helps to investigate the mechanical properties of photochromic miPP filaments. The Young's modulus of photochromic miPP filaments was plotted in the Figure 41, the data was used to fit with non-linear regression and goodness of fit was found $R^2=0.98$. Results show that significant improvement in Young's modulus, it was increased 65% from drawing ratio 1 to 4, nevertheless, it is due to the molecular arrangements and followed by the variation in the crystalline region of the filament. In other words, Young's modulus increased continuously with increasing the crystallinity. Therefore, this structural modification may cause to increase the tenacity and Young's modulus and decrease the elasticity. The Young's modulus of miPP

filaments as a function of photochromic pigments are shown in Figure 42. It is evident from this results that the photochromic pigments increased the filament flexibility, particularly in higher concentration. However, the reduction of Young's modulus with influencing of photochromic pigment is very less (i.e. 6%), and it could be within the tolerable limit. In overall the photochromic pigments having significant change in the physical and mechanical properties, particularly pigment concentration can influence the coefficient of variance (CV) for the tenacity, it decreases with increasing the pigment concentration, in some cases the results are not affected as such, for example with the drawing ratio of 2.5 at the concentration of 0.5 wt.%. The CV for the elongation and Young's modulus, there is no significant influence and the results are fluctuations. Pigment concentration and drawing ratio have a strong influence on the linear density and other physical properties of produced photochromic filaments.

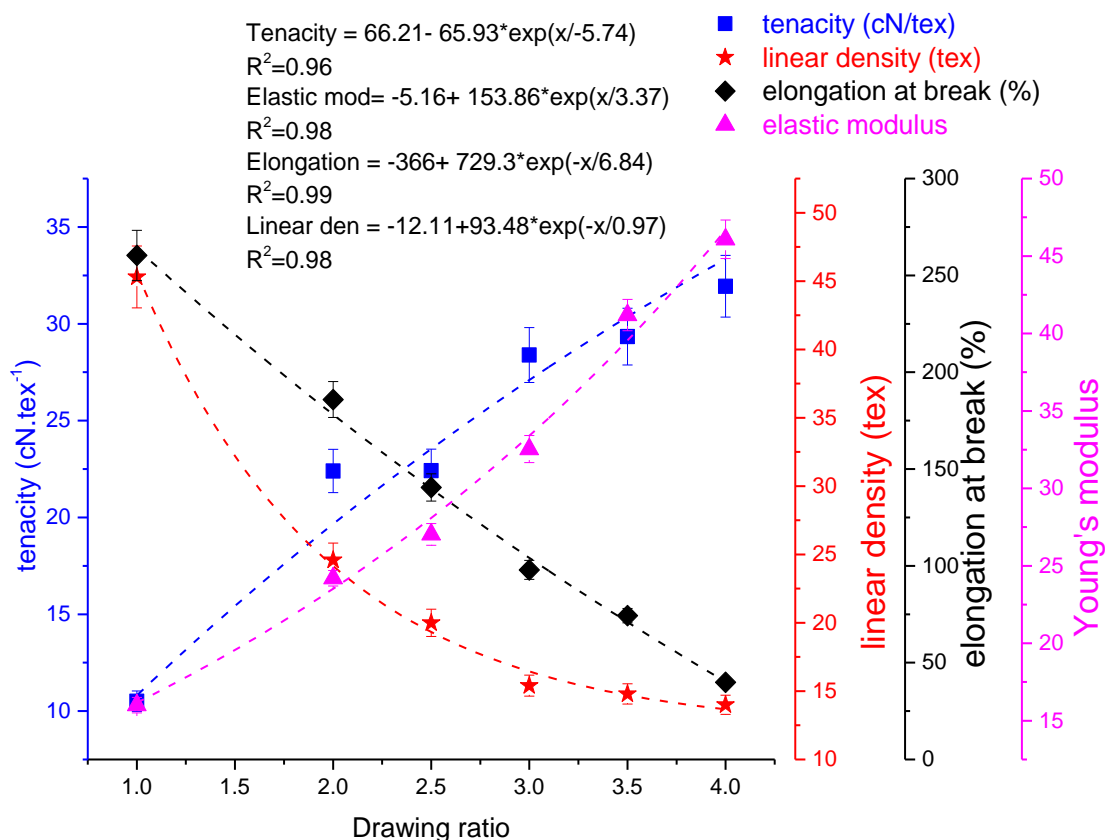


Figure 41: Effect of drawing ratio on various physical properties (MPP-0.25 wt.%).

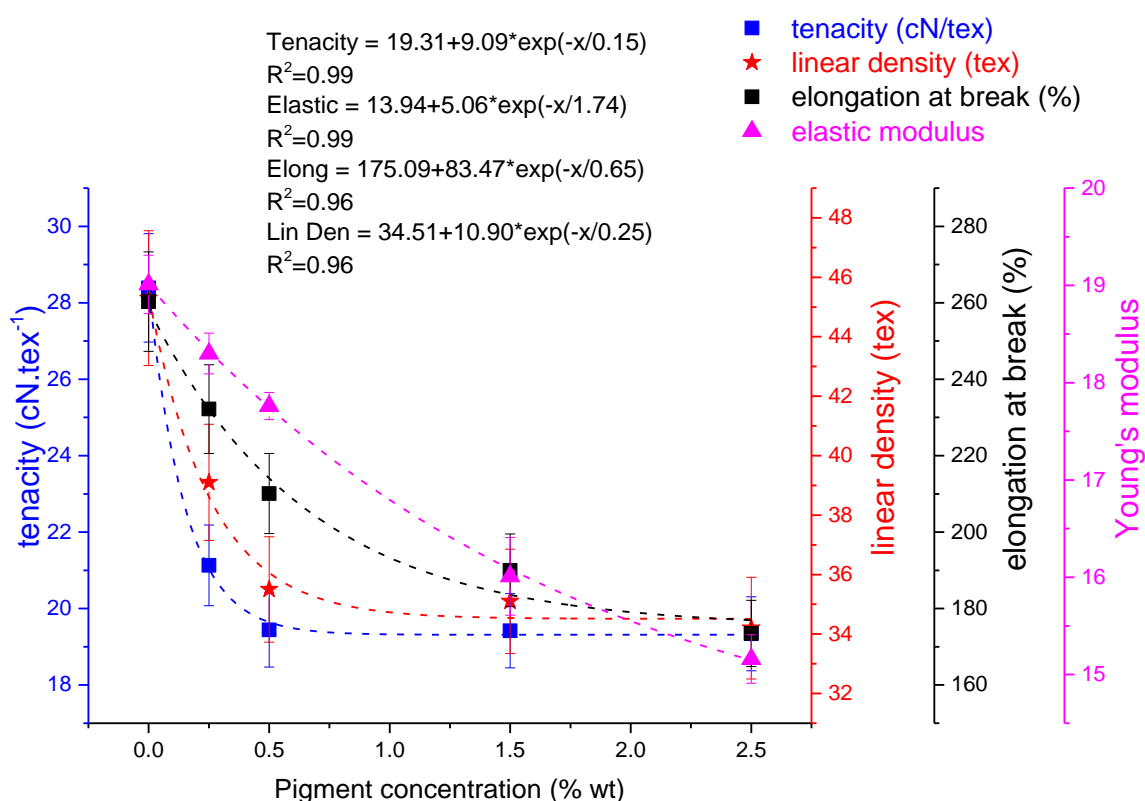


Figure 42: Impact of pigment concentration on various physical properties (DR-1).

3.3.3 Thermogravimetric Analysis of miPP filaments

Before production of photochromic miPP filaments, it is necessary to analyze the thermal degradation of photochromic pigments by thermogravimetric analysis. The purpose of this characterization is to understand how the photochromic chromophore was degraded with respect to the temperature. In this study, three different photochromic pigments were used to analyze their thermal properties and the results are shown in Figure 43. First all the pigments started degradation at 50 to 130°C, however this is due to the HALS and other residual additives present in the pigments, thereafter it sustains for higher temperature and start complete degradation, for MPY pigments degrade significantly during heating and degrade 76% of weight loss by 325°C, whereas MPB and MPP is much better and weight loss of 62% and 53% respectively.

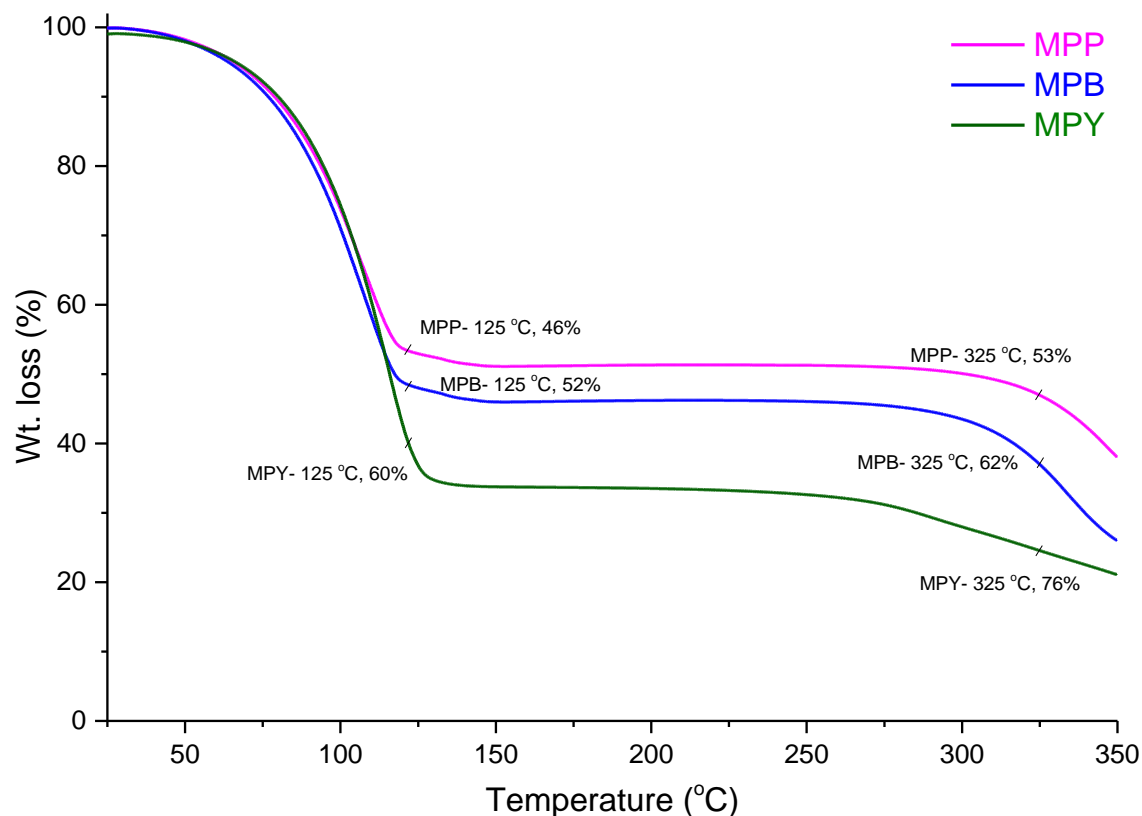


Figure 43: TGA analysis of photochromic pigments.

The value of onset degradation was obtained from the point of intersection of extrapolated pre-weight-loss baseline with the tangent to the curve produced by the decomposition reaction. However, this characterization has a small quantity of error and it was estimated around at 5°C. So, this result concludes that there is an impact of kinetic properties, since MPP shows less thermal degradation temperature, perhaps MPY shows higher degradation. Thermal degradation of the pigment is purely depending on their structure, while production of the miPP filament, the mixture of pigment and polymers are in the molten state, which stays for more than 30 minutes. Due to longer time and higher temperature may reduce dyeability of MPY pigment and the results are evident for this statement and it is shown in Figure 28 and Figure 32.

3.3.4 Differential scanning calorimetry analysis on miPP filaments

DSC is one of the most widely accepted techniques to study the thermal properties of polymeric materials. It helps to analyze the crystallization exotherm of photochromic polypropylene filaments, the results were shown in Figure 44 to Figure 49. However the polypropylene

belongs to semi-crystalline polymer and it forms the structure during the higher temperature, particularly close to their melting temperature when relaxation of polymer chain in amorphous phase is prevented mechanically, keeping fibers under tension [87, 92–94], therefore, it significantly change the thermal characteristics namely melting temperature, melting enthalpy and entropy, it is sure that these changes further influencing on their mechanical properties. The quantities structural characterization of isotactic polypropylene was studied very first by Samuel [86] and concluded as follows; isotactic polypropylene fibers are providing the higher melting temperature and enthalpy, the orientation of crystalline phase will not affected by the melting temperature of the filaments, whereas the linear dependence of melting temperature on the factor of amorphous phase, which means that melting temperature of the constrained PP fibers drawn for gradually higher drawing ratio is fully controlled by orientation of the non-crystalline phase of the filaments. The melting temperature of the polymer is known to the function of crystallization temperature, generally, it is dependence on the crystal thickness of polymeric materials. From the results, melting temperature was increased with the increasing the drawing ratio, also the heat of fusion is increased continuously with increasing the drawing ratio, this is due to the thickness of lamella can be reduced as well as the increased molecular orientation of the filaments with respect to the drawing ratio. The increasing the heat of fusion can be seen in the entropy with respect to the drawing ratio, results confirm that change in entropy can lead to increase the melting temperature along with drawing ratio was increased. The results reveal the difference in the melting peak temperature dependence on the drawing ratio. The melting temperature (T_m) of undrawn filament shows 146.08°C, whereas the drawing ratio 4 shows 150.28°C.

Table 5: Thermal and crystallinity properties of miPP filaments with respect to various drawing ratio (i.e. without the addition of photochromic pigment).

| Drawing ratio | T_m (°C) | X_c (%) | ΔH_m (J.g ⁻¹) | ΔS_m (J.g ⁻¹) |
|---------------|------------|-----------|-----------------------------------|-----------------------------------|
| 1.0 | 146.1 | 27.11 | 56.16 | 0.38 |
| 2.0 | 147.2 | 28.63 | 59.30 | 0.40 |
| 2.5 | 147.9 | 29.50 | 61.10 | 0.41 |
| 3.0 | 148.6 | 35.78 | 74.11 | 0.49 |
| 3.5 | 149.4 | 37.73 | 78.15 | 0.52 |
| 4.0 | 150.2 | 40.65 | 84.20 | 0.56 |

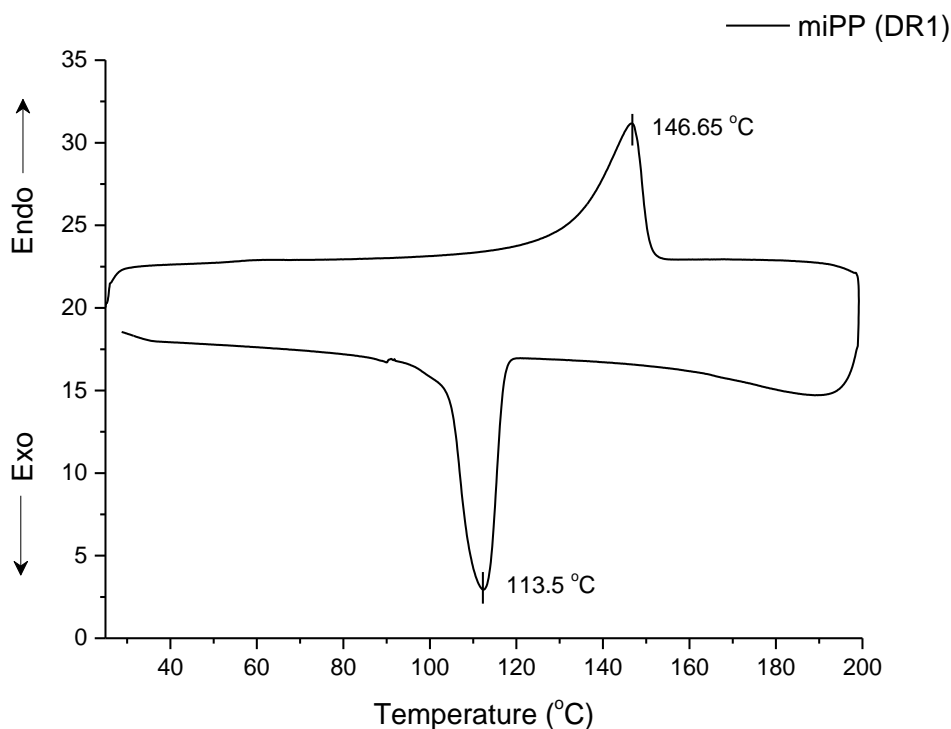


Figure 44: DSC test of miPP filament (i.e. DR-1, MPB- 0 wt.%).

The changing of melting enthalpy is increased with increasing the drawing ratio, from 56.16 to 84.20 $J.g^{-1}$ for drawing ratio 1 and 4 respectively (Table 5), this is due to the thermal demonstration of the components during the crystallization of the polymer which may create the supermolecular structure of the polymer. In general, the liquid phase may reduce the distance between adjacent chains and therefore it increases the fraction of lower energy trans conformation. The melting temperature of miPP filaments with photochromic pigments are increased $\sim 2^{\circ}C$ with increasing the photochromic pigment concentration (Figure 48). Of course, the drawing ratio is highly responsible for the increasing of melting temperature, it can be seen in Figure 49. However, it is desired and expected effects on the photochromic filaments. In the drawing ratio 4, there are two melting peaks were visible (Figure 47), it is due to the during the DSC measurement the mass colored miPP was exposure to set conditions or may be melting of less stable β crystallites formed during the measurement. The crystallinity of photochromic filaments was increased with increasing the drawing ratio, therefore, the higher rate of crystallization makes many modifications in the filament, mainly the α , β modification of morphological structure. From the results (Table 6 and Table 7), pigment concentration on crystallinity can be changed 13% on the drawing ratio of 1, in case of drawing ratio 4 does show much influence, however, this effects purely depend on the drawing ratio and slightly on

the pigment concentration too. The variation in the crystallinity can be found is higher when the drawing ratio is less and difference can be reduced in case of higher drawing ratio. Similarly, the changing in melting enthalpy and entropy was observed there is a variation with respect to the pigment concentration, however, it is due to the drawing process and slightly on the pigment concentrations.

Table 6: Thermal and crystallinity properties of miPP filaments with respect to their photochromic pigments (i.e. DR-1).

| Pigment concentration (MPP- wt.%) | T_m (°C) | X_c (%) | ΔH_m (J.g ⁻¹) | ΔS_m (J.g ⁻¹) |
|-----------------------------------|------------|-----------|-----------------------------------|-----------------------------------|
| 0.0 | 146.08 | 26.24 | 54.34 | 0.371 |
| 0.25 | 146.10 | 27.30 | 56.54 | 0.386 |
| 0.5 | 146.31 | 28.63 | 59.29 | 0.405 |
| 1.5 | 146.67 | 29.02 | 60.10 | 0.409 |
| 2.5 | 147.41 | 30.18 | 62.51 | 0.428 |

Table 7: Thermal and crystallinity properties of miPP filaments with respect to their photochromic pigments (i.e. DR-4).

| Pigment concentration (MPP- wt.%) | T_m (°C) | X_c (%) | ΔH_m (J.g ⁻¹) | ΔS_m (J.g ⁻¹) |
|-----------------------------------|------------|-----------|-----------------------------------|-----------------------------------|
| 0.0 | 149.44 | 40.55 | 83.99 | 0.566 |
| 0.25 | 149.98 | 40.44 | 83.75 | 0.558 |
| 0.5 | 150.15 | 41.48 | 85.92 | 0.567 |
| 1.5 | 150.78 | 41.76 | 86.49 | 0.567 |
| 2.5 | 151.63 | 42.54 | 88.11 | 0.577 |

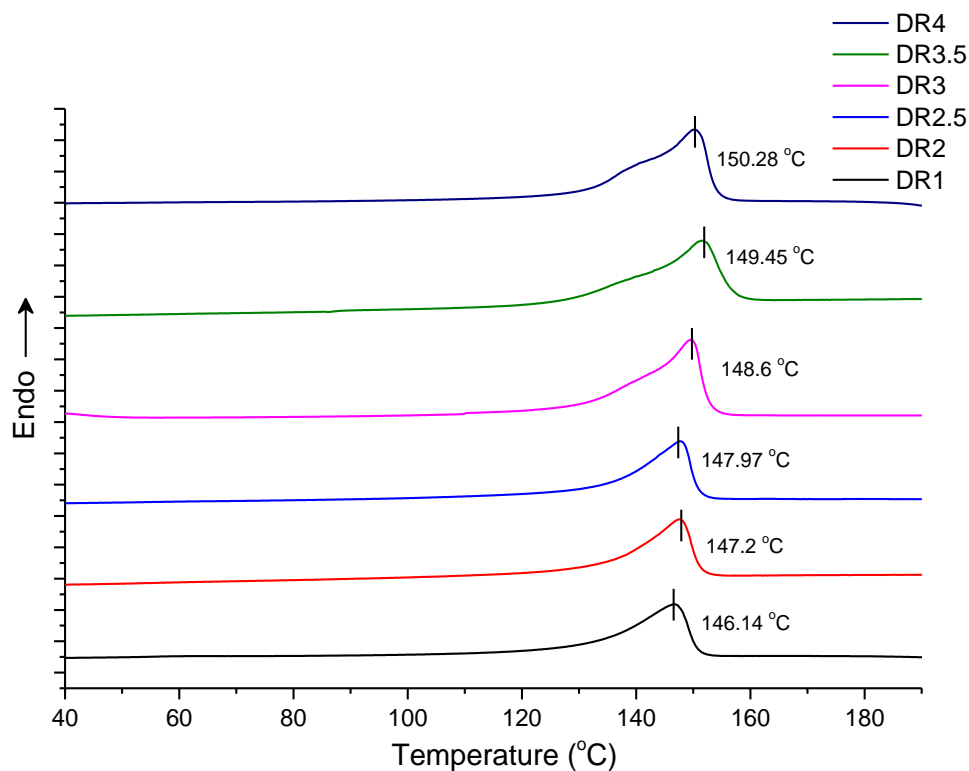


Figure 45: Normalized DSC curves for miPP filaments, (MPP=0.0 wt.%).

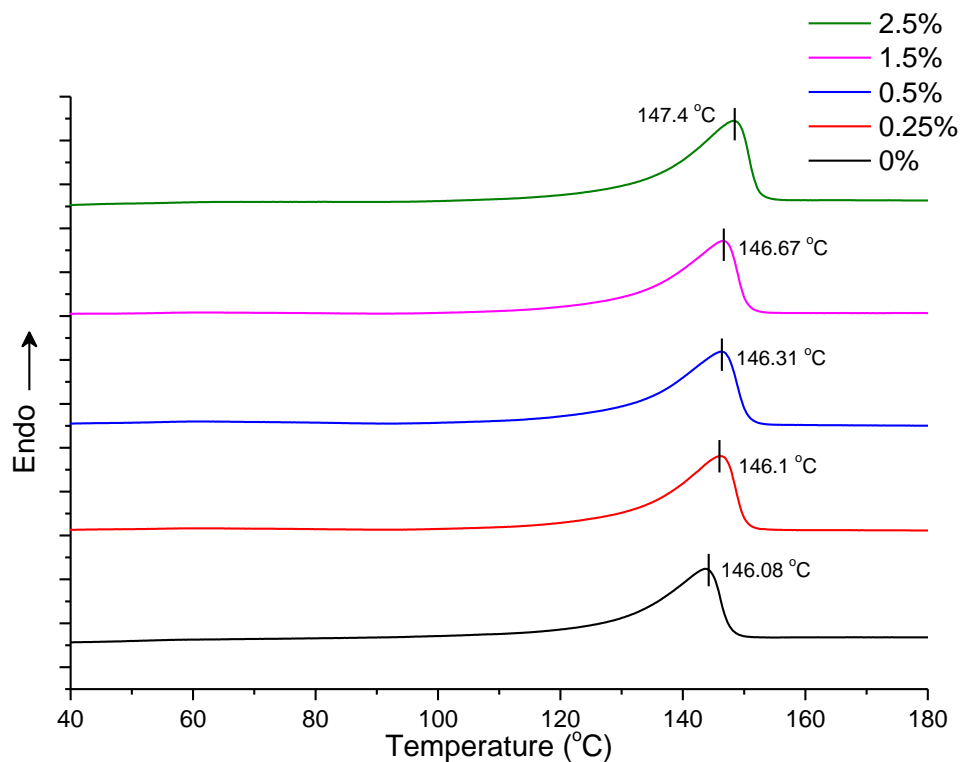


Figure 46: Normalized DSC curve of MPP incorporated miPP filament (DR-1).

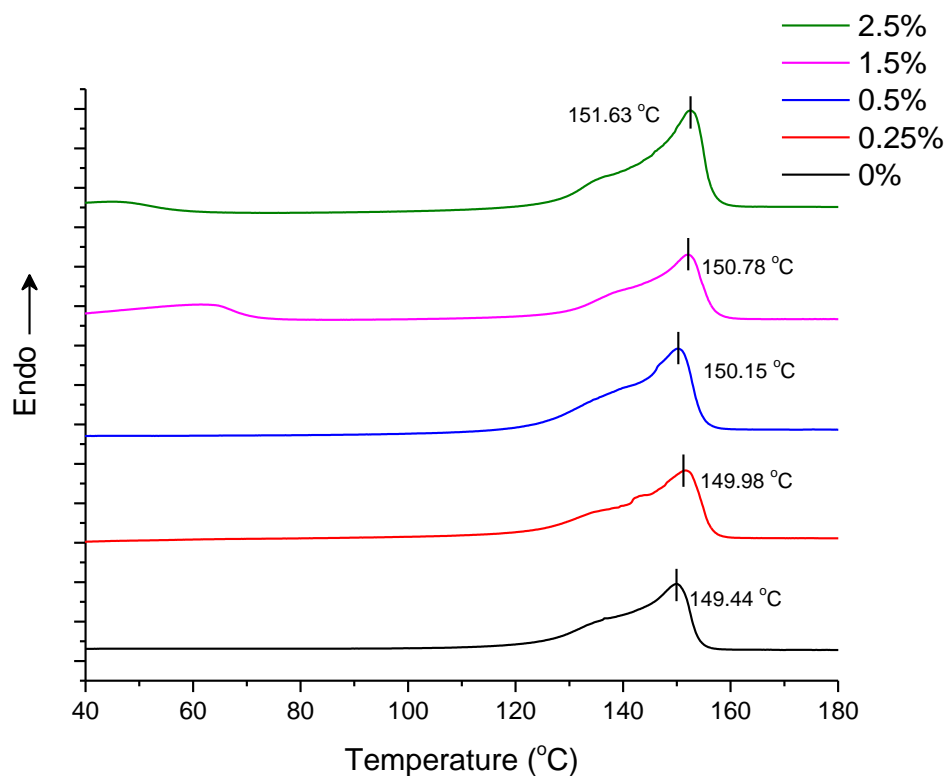


Figure 47: Normalized DSC curve of MPP incorporated miPP filament (DR-4).

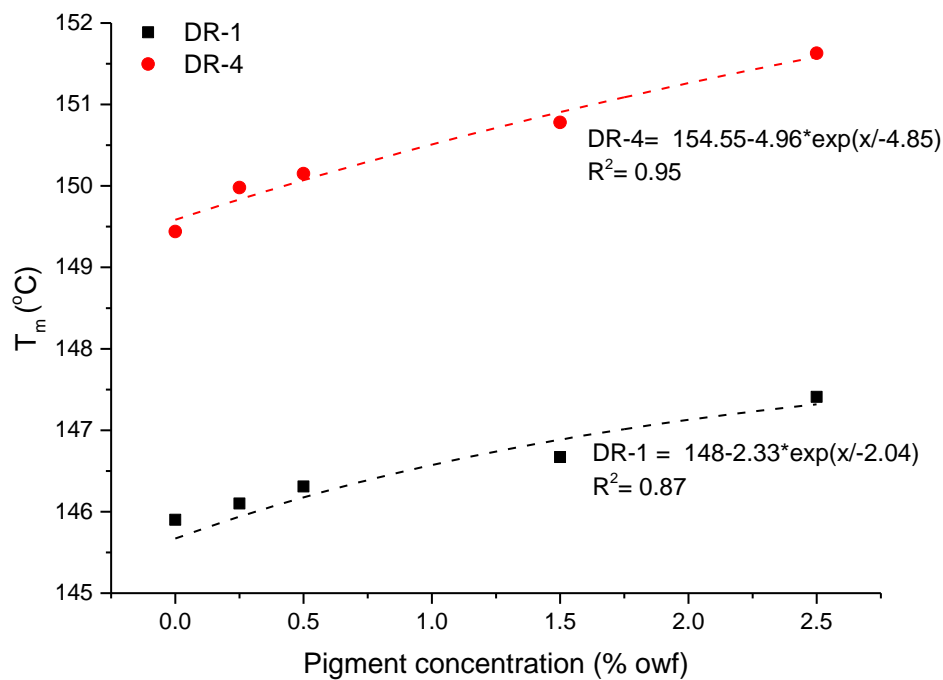


Figure 48: Effect of pigment concentration on T_m .

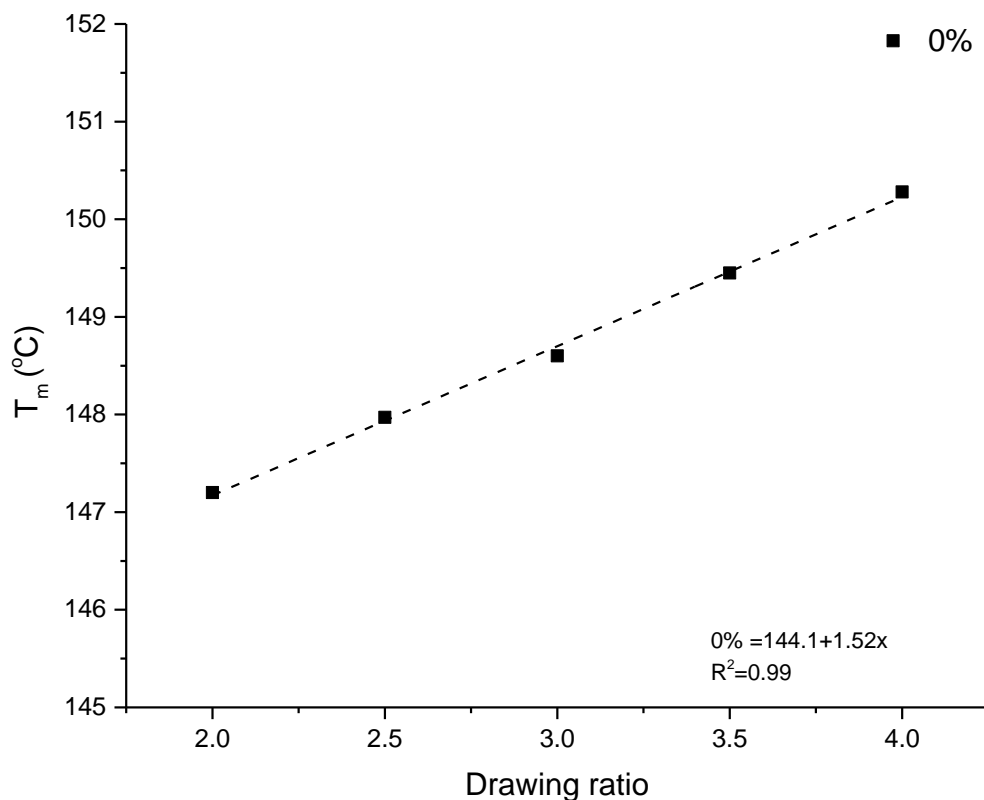


Figure 49: Effect of drawing ratio on T_m .

3.3.5 Surface morphological analysis of miPP filaments

SEM characterization was used to investigate surface characteristics of the produced photochromic miPP filaments with the influence of photochromic pigments and their distributions. In these regards, the longitudinal views were conducted to visualize the surface characteristics of mass colored filaments. For this analysis, the photochromic pigment concentration of 2.5 wt.% (i.e. all three pigments) with the different drawing ratio was selected. Since there is no special reason behind why different drawing ratio was chosen rather than availability of filaments.

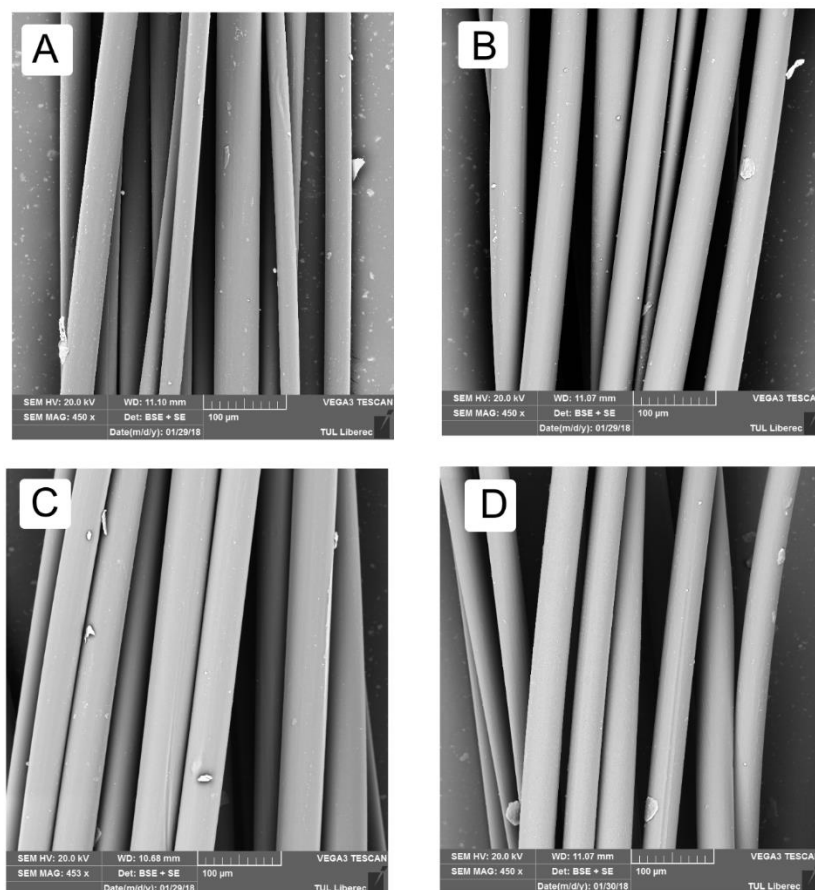


Figure 50: Longitudinal view of Photochromic miPP filaments with a circular cross-section, (A) unpigmented; (B) containing 2.5 wt.% MPP; (C) containing 2.5 wt.% MPB; (D) containing 2.5 wt.% MPY; (DR-2).

Figure 50 shows the longitudinal views of produced photochromic miPP filaments with the compression of the unpigmented filament (i.e. circular cross-sections). The outer surface for all the filaments (i.e. colored and uncolored) looks similar with a smooth surface, which means that there is no significant influence on the pigments with its distribution of filaments on surface characteristics. Also, in all the filaments does not shows any uneven and striated effects which confirm that the drawing process cannot be affected the filaments. The results are same in cross-sectional views too (Figure 51).

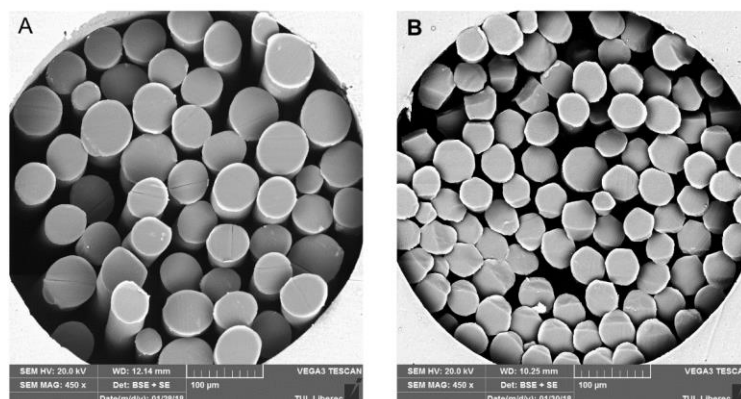


Figure 51: Cross-sectional view of photochromic miPP filaments with a circular cross-section, (A) unpigmented circular shape; (B) circular shape with 2.5 wt.% MPP;

The produced circular filaments have no melt fracture or distortion which is confirmed from these microscopical images. Therefore, it is confirmed that the process of polymer melting ability to stay together as a continuous fluid at a high shear rate. There are many intrinsic parameters were involved for fracture of miPP filaments, namely molecular weight, the degree of crystallinity, structural morphology, molecular orientation and various processing conditions, particularly drawing process and its ratio.

3.4 Results and Discussion of photochromic miPP filaments (non-circular)

3.4.1 Optical properties

Table 8 and Table 9 shows K/S (max) values to the different drawing ratio of photochromic miPP filaments on non-circular cross-sections. Due to the limited options, it manufactured with only one concentration by each pigment, therefore it is very difficult to make a graphical representation with limited independent and depended on values. Results describe the circular cross-sectional filament shows higher K/S (max) values than the non-circular filaments even in all the drawing ratios as well as in the same concentration of pigment. In over all, results of K/S (max) values were observed that it varied with respect to the cross-sectional shape of the filaments. The results of K/S (max) values on the filaments with MPP pigment, 8-star and 5-star cross-sectional filaments show 63% and 72% less K/S (max) values than the circular cross-sections in the same drawing ratios. The results trend is similar to other pigments too, so, it evidenced and confirmed that the shape of cross-sections plays a vital role in the optical properties of produced filaments. The reason behind these phenomena is, during the color

measurement the reflected light always depends on the angle of incidence, which could be modified by the substrate and its surface characteristics. Circular cross-sectional filaments typically generate the more specular reflection, on other hand, the surface reflection increased for the filament containing quadrilobe cross-section. Therefore, the refraction and the frequencies of the light intensity could change the direction, which causes to reduce the transmission coefficient of light intensity. As a result, reduce the amount of light transmission on the miPP filament with quadrilobe cross-sections. In other words, the quadrilobe cross section having the more refraction light path as compared to circular and trilobal cross-sections. Due to the above reason, circular cross-section produces more K/S (max) values than other cross-sections. However, the non-circular cross-sectional filaments have more surface area than a circular one, so it increases the air resistance and sound absorption and other handle & surface properties.

Table 8: The K/S (max) on the different cross-sections of the produced filament (DR-1) under exposure phase.

| Cross-sections | Pigment concentrations 1.5 wt. % | | | | | |
|----------------|----------------------------------|-----------------|--------|-----------------|-------|-----------------|
| | MPP | CV% K/S (max) | MPB | CV% K/S (max) | MPY | CV% K/S (max) |
| Circular | 3.230 | 82.2 | 2.835 | 112.4 | 1.397 | 229.7 |
| 5-star | 0.949 | 95.4 | 0.4969 | 249.6 | 0.544 | 160.0 |
| 8-star | 1.229 | 80.1 | 0.6024 | 67.0 | 0.948 | 183.3 |
| Triangle | - | - | - | - | 0.688 | 120.9 |

Table 9: The K/S (max) on the different cross-sections of the produced filament (DR-2) under exposure phase.

| Cross-sections | Pigment concentrations 1.5 wt. % | | | | | |
|----------------|----------------------------------|-----------------|-------|-----------------|-------|-----------------|
| | MPP | CV% K/S (max) | MPB | CV% K/S (max) | MPY | CV% K/S (max) |
| Circular | 2.523 | 135.6 | 2.201 | 90.7 | 1.229 | 190.8 |
| 5-star | 0.704 | 153.9 | 0.415 | 101.2 | 0.502 | 112.2 |
| 8-star | 0.945 | 118.2 | 0.520 | 95.1 | 0.495 | 118.7 |
| Triangle | - | - | - | - | 0.479 | 116.1 |

3.4.2 Surface morphological analysis of miPP non-circular filaments

Figure 52 shows the longitudinal views of produced miPP filaments with non-circular cross-sections. Results are evident that there is a smooth surface in case of triangular and 5-star shapes, whereas in 8-star contains some microfibers which leads to generating the fibrillation on the surface, however, there is no significant relationship with the pigment concentration with respect to these effects, it purely depends on the shape of cross-sectional. Since it contains 8-star which means there is 8-stars, due to the serrated like structure of this filament generates the microfibrils, so the 8-star shaped filament makes unevenness in the surface. Figure 53 shows the cross-sectional views of produced miPP filaments with non-circular cross-sections. Results indicate the circular and triangular shape cross-sections having no impact of addition of pigments or the drawing process, in case of 5-star some of the filaments never drawn, it can be identified by the size of the filaments by comparison of other filaments in this group, which means that some filaments are bigger than other filaments in the same groups, it can be seen in the Figure 53. However, there is no influence on the pigment for these effects. The reason may be slippage during the drawing process which leads to the particular filament to not drawn as per the respected drawing ratio, this effects only occur in the 5-star shape and not in the 8-star shape which is shown in Figure 54. In overall, there is an impact of drawing process with respect to the size of diameter, it can be seen visually, however it is well-known effects and expected results too.

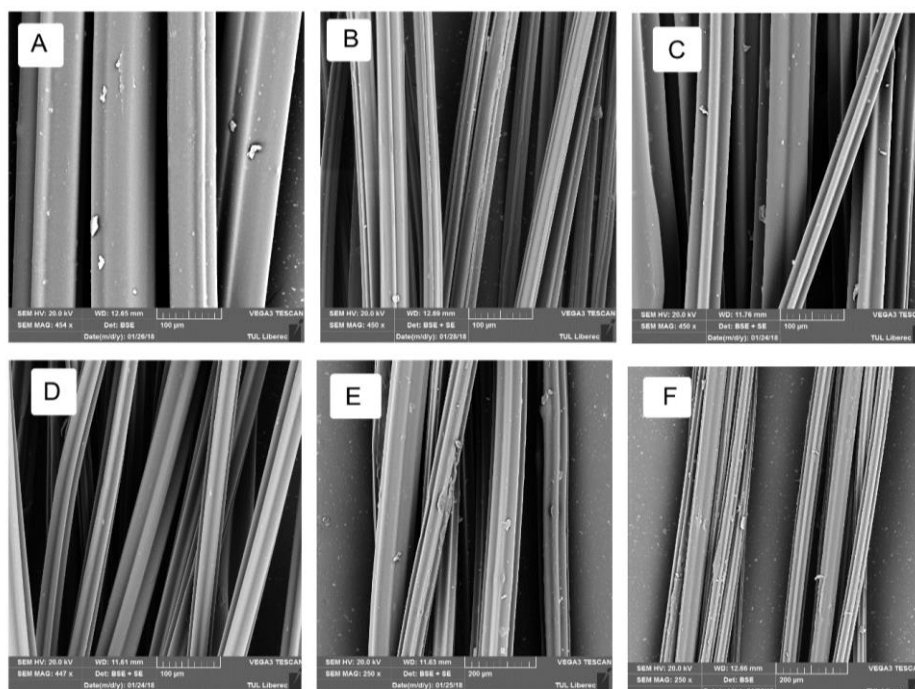


Figure 52: Longitudinal view of non-circular Photochromic miPP filaments,

(A) unpigmented triangular shape; (B) triangular shape with 2.5 wt.% MPP; (C) unpigmented 5-star shape; (D) 5-star shape with 2.5 wt.% MPP; (E) unpigmented with 8-star shape; (F) 8-star shape with 2.5 wt.% MPP (DR for unpigmented is 1 and pigmented filaments are 2).

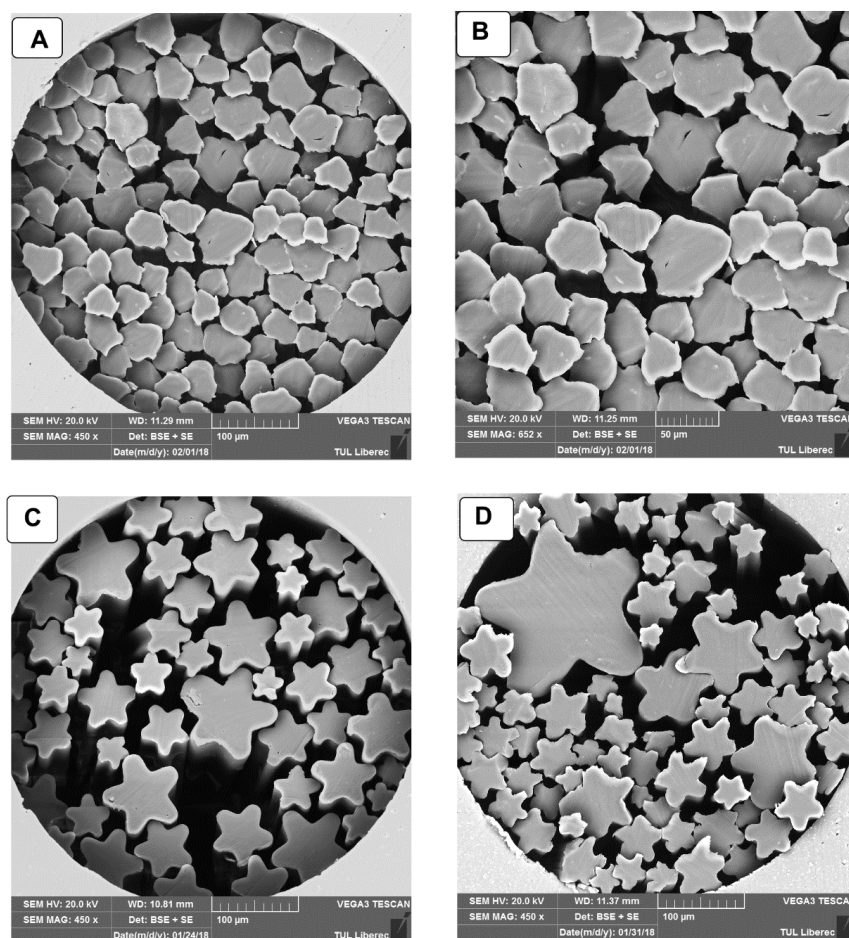


Figure 53: Cross-sectional view of non-circular photochromic miPP filaments, (A) unpigmented triangle shape (B) triangle shape with 2.5 wt.% MPP; (C) unpigmented with 5-star shape; (D) 5-star shape with 2.5 wt.% MPP (DR for unpigmented is 1 and pigmented filaments are 2).

The produced non-circular miPP filaments have no melt fracture or distortion which is confirmed from these microscopical images. Therefore, it is confirmed that the process of polymer melting ability to stay together as a continuous fluid at a high shear rate. There are many intrinsic parameters were involved for fracture of miPP filaments, namely molecular weight, the degree of crystallinity, structural morphology, molecular orientation and various processing conditions, particularly drawing process and its ratio. From the scanning electron microscopic images, it is evident that there is no microfibrils in the miPP filament structure

except the 8-star shape, However, the transition of lamellae to microfibrils can take place during the cold drawing process, it can be extensively studied in many literature.

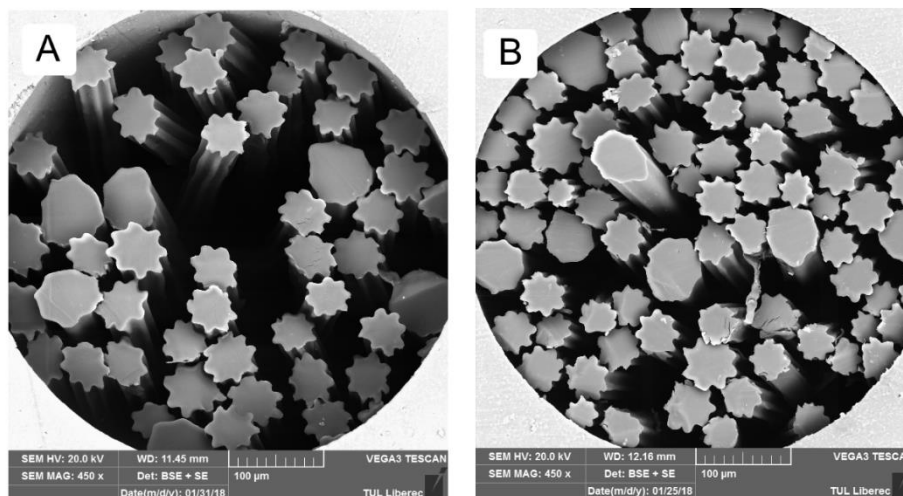


Figure 54: Cross-sectional view of non-circular photochromic miPP filaments, (A) unpigmented with 8-star shape; (B) 8-star shape with 2.5 wt.% MPP (DR for unpigmented is 1 and pigmented filaments are 2).

3.5 Conclusion

The methods and process parameters which used to produce the photochromic miPP filaments in both circular and non-circular cross-section has been discussed in this chapter. Also, it discusses the various properties which have been measured for the produced filaments. At last, various optical, structural, physical and thermal properties of produced filaments could be discussed with their obtained results, the detailed conclusion of this chapter has been given in section 6.1

Chapter 4 SOL-GEL PHOTOCHROMIC FABRIC

4.1 Introduction

In textile field, sol-gel technology has been used to provide fabrics with various functions by incorporating different functional materials such as photochromic, thermochromic, anti-microbial, water repellent, superhydrophobic, flame retardant etc. In this work, incorporation of commercial photochromic pigment (Table 10) into textile fabric by sol-gel coating. PET was chosen for the sol-gel coating since it has many advantages than other fibers except moisture absorptions. The sol-gel can be prepared by using the various precursor, then it applied to the PET fabric with different concentration of photochromic pigment (MPP). In this work, a different type of precursors is used to find the impact of precursors on the photochromic response in the coated fabric. The main aim of this study is to find the influence of precursor on photochromic response with respect to the physical and mechanical and handling properties of coated fabrics. Therefore, the first two sections are deals with the application of photochromic pigment to the fabric via sol-gel coating and the last section of this chapter is dealing with obtained results and their discussions. So, the various optical properties like color strength values (K/S functions), color strength maxima, changing in optical density, color difference by residual ΔE^* values, half-life for color change of photochromic response during exposure and reversion phase, rate constant and various color intensity, photochromic response towards to the abrasion and washing resistance has been discussed. Also, it discusses uptake% during the coating process, various physical and handling properties of coated fabric, surface morphology and surface roughness has been discussed. For all the measurement, the error can be calculated through standard uncertainty measurement

4.1.1 Sol-gel coating on PET fabric

Sol-gel coating is one of the most important emerging technology in textile industry due to its many advantages such as highly effective, adjustable coating thickness, good coating durability, easy combination with various functions and less environmental impacts. Typically, metal oxides starting from a colloidal solution (sol) that acts as the precursor for an integrated network (or gel) of either discrete particles or network polymers are used for the fabrication of materials. Typical precursors are metal alkoxides and metal salts (such as chlorides, nitrates and acetates), which undergo various forms of hydrolysis and polycondensation reactions. Both in liquid and solid phase contained in the formation of a gel-like diphasic system are evolved

by the ‘sol’ in this chemical procedure whose morphologies range from discrete particles to continuous polymer networks. A significant amount of fluid may need to be removed initially for the gel-like properties to be recognized in the case of the colloid, due to slow in the volume fraction of particles (or particle density) which can be accomplished through a number of ways. The method which is simple is to allow time for sedimentation to occur and then pour off the remaining liquid. A drying process is required in the removal of the remaining liquid (solvent) phase which is typically accompanied by a significant amount of shrinkage and densification. The distribution of porosity in the gel determines the rate at which the solvent can be removed. During this phase of processing, changes imposed upon the structural template will strongly influence the microstructure of the final component [95–103]. Figure 55 represents the deposition process of thin films using sol-gel method. In this method, a homogeneous solution of molecular reactant precursors (sol) into an infinite molecular weight three-dimensional network (gel) filling the same volume as the solution is converted by a set of chemical reactions irreversibly. In order to produce the binary or ternary systems; each molecular precursor has its own reaction rate depending on the parameters such as *pH* of the solvent, concentration and temperature in which the mixtures of precursors can also be used. In a single precursor component system, interconnected nanoscale porosity can be designed to the final material and hence a high surface area, it depends upon the precursors used and the solvent employed [52, 104–109]. Previous literature studied the silica sol-gel matrices with photochromic dyes [99, 102, 110, 111] on films and other materials, however, these studies help us to produce the photochromic fabric via sol-gel coating technology.

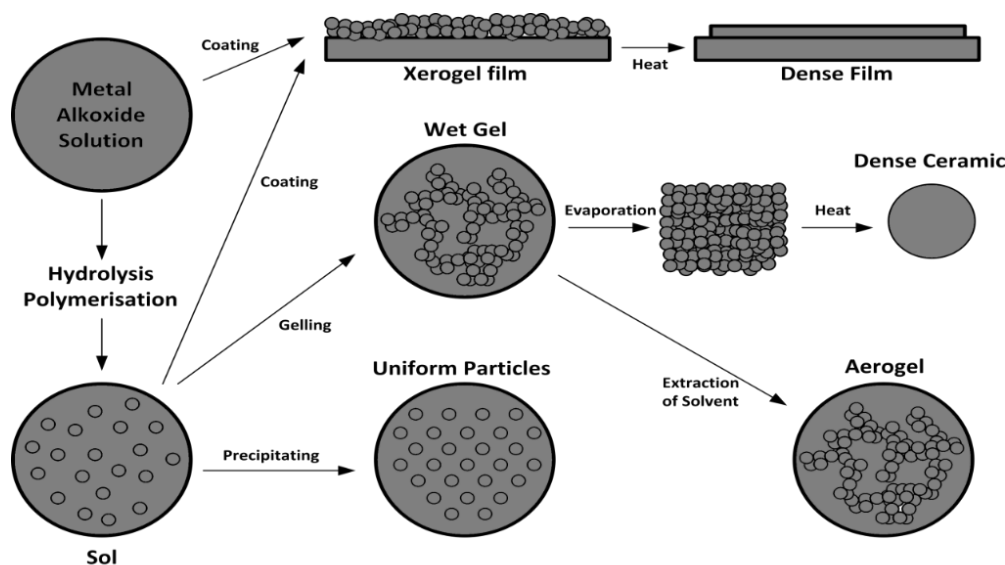


Figure 55: Schematic representation of Sol-gel coating method, (adopted and modified from [112]).

4.1.1.1 Dip coating method

The dip coating technique is a popular way of creating thin films for research purposes which ensure the uniform films onto flat or cylindrical substrates. Generally, it can be done under controlled temperature and atmospheric. In this work the photochromic pigments are integrated to the fabric through dip coating, this process can be separated into five stages.

- *Immersion*: The fabric is immersed in the solution of the coating material at a constant speed.
- *Start-up*: The fabric has remained inside the solution for a while and is starting to be pulled up.
- *Deposition*: The thin layer deposits itself on the fabric while it is pulled up. The withdrawing is carried out at a constant speed to avoid any jitters. The speed determines the thickness of the coating (faster withdrawal gives thicker coating material).
- *Drainage*: Excess liquid will drain from the surface of fabric.
- *Evaporation*: The solvent evaporates from the liquid, forming the thin layer. For volatile solvents, such as alcohols, evaporation starts already during the deposition & drainage steps.

4.2 Experimental procedure for sol-gel coating

Pre-treated, 100 % PET plain structured fabric was used for this study. Triacetoxystyrene precursor (TAS); Octyltriethoxyprecursor (OTES); Phenyltriethoxyprecursor (PhTES); aminopropyltriethoxy precursor (APS) and MPP (photochromic pigment). Since 5-chloro-1,3,3-trimethylspiro[indoline-2,3'-(3H) naphtho(2,1-b) (1,4)-oxazine] provide the better photochromic performance (in case of miPP filament), therefore it chosen for the sol-gel coating and there is no other reason for this. All the chemicals were purchased from Sigma-Aldrich, USA. Deionized water was used for the preparation of sol solutions.

Table 10: Commercial photochromic pigment used to produce photochromic fabrics.

| Color | Abbreviation | CAS | Chemical name |
|--------|--------------|------------|---|
| Purple | MPP | 27333-50-2 | 5-chloro-1,3,3-trimethylspiro[indoline-2,3'-(3H) naphtho(2,1-b) (1,4)-oxazine]. |

Table 11: Various physical properties of Raw PET fabric.

| Properties | Warp | Weft |
|--|-------|-------|
| Flexural rigidity (mg.cm) | 949.9 | 543.1 |
| Bending modulus (kg.cm ⁻²) | 330.9 | 184.1 |
| Bending length (cm) | 4.7 | 3.2 |
| Thickness (mm) | 0.326 | |
| Areal density (g.m ⁻²) | 170.7 | |

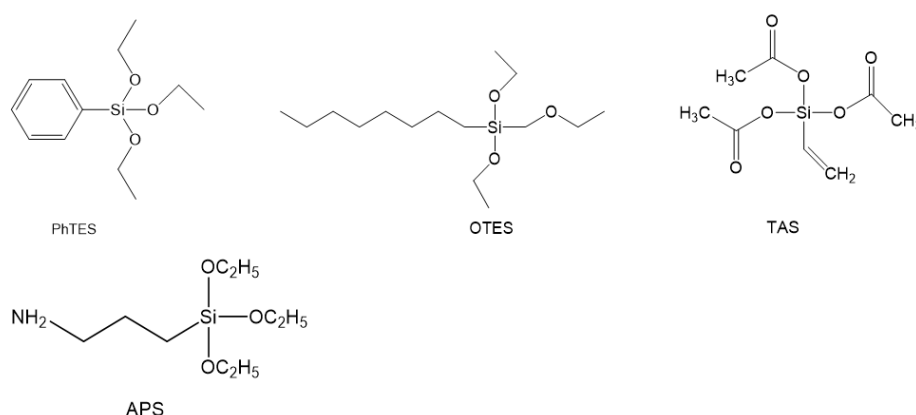


Figure 56: Chemical structure of PhTES, OTES, APS and TAS.

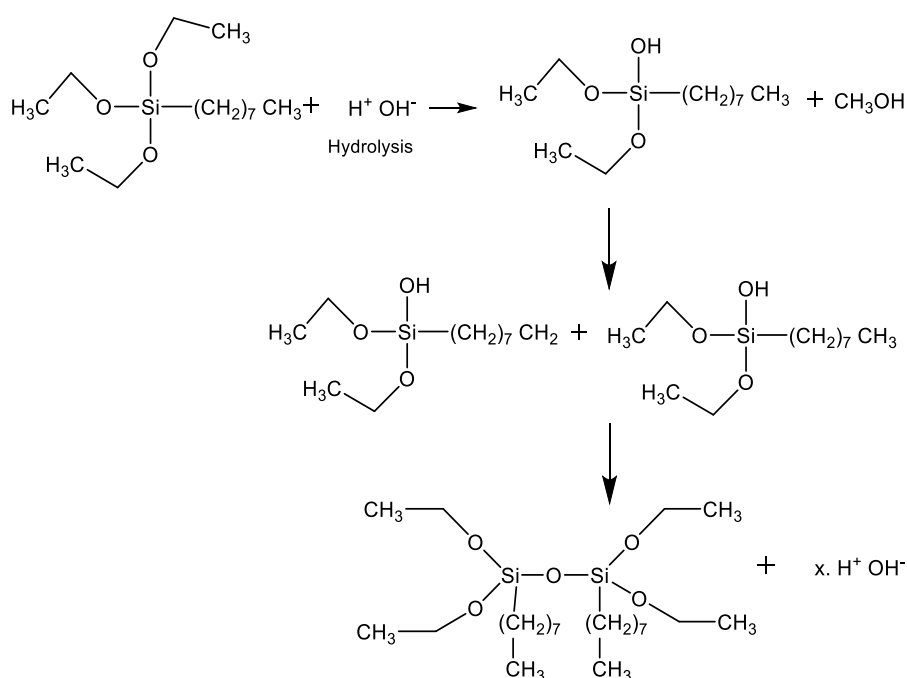
4.2.1 Silica sol-gel synthesis and coating on fabrics

The silica sols were prepared by mixing the different precursors with the catalyst and solvent, the mixing can be done with the proper proportion of silanes, catalyst, water and solvent by 32:1:100:320 molar ratios respectively, many studies could be conducted and optimize this proportions. The mixture was stirred until the crystals of the catalyst can be dissolved until a clear solution was obtained. Later, the deionized water was added to the above mixture by using the syringe pump at the speed of 1 mL.h^{-1} . Triacetoxysilane (it has the dual functions like a catalyst, certainly it will be the third precursor) was chosen as a catalyst for this study since it slowly releases the acetic acid during the hydrolysis reaction and ensures to avoid the rapid hydrolysis. The solution was continuously stirred for 24 hours at room temperature to allow the complete hydrolysis of precursors. The detailed process sequence and conditions are provided in Figure 57. The chemical structures of PhTES, OTES, APS and TAS are shown in Figure 56. The coating solution was prepared by mixing the above sol with photochromic pigments. Before mixing, the photochromic pigments were slowly added into the prepared sol and it is mixed until it is dissolved. In some cases, pigment cannot be mixed well, then the

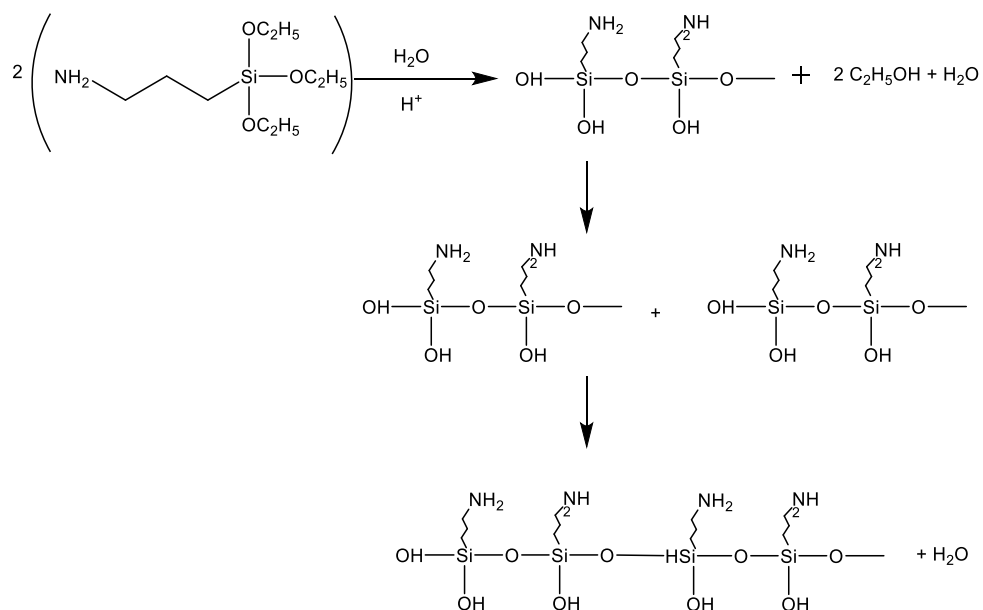
mixture can stir at 70°C until the solution was clear. Two pieces of PET fabrics (30cm×12cm) were dipped into the solution and then withdrawn vertically at a constant speed (~10mm.sec⁻¹). The fabrics were dried in atmospheric condition and then cured at 110°C for 10 minutes. Before measurement, the coated fabric was left in atmospheric condition for 24-48 hours to ensure complete stabilizing of the silica matrices, followed by washing two times as per the standard washing procedure. Samples were named as per the silica precursor's composition, which is summarized in Table 12.

Table 12: Recipe and coating conditions.

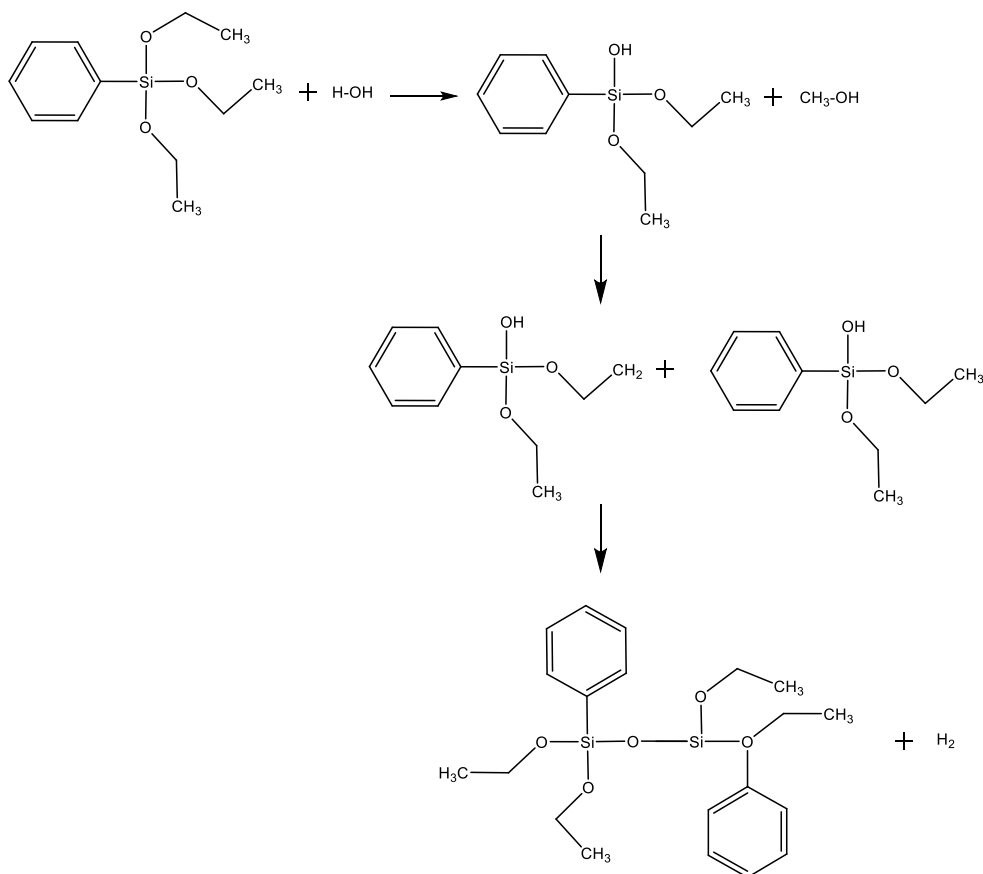
| Abbreviation | Type of precursor | MPP photochromic pigment (wt.% of fabric) | | | | | |
|--------------|---|---|------|------|------|------|------|
| OTES | Octyltriethoxy silane | 0.25 | 0.50 | 1.00 | 1.50 | 2.00 | 2.50 |
| PhTES | Phenyltriethoxy silane | 0.25 | 0.50 | 1.00 | 1.50 | 2.00 | 2.50 |
| APS | (3-Aminopropyl) triethoxy silane | 0.25 | 0.50 | 1.00 | 1.50 | 2.00 | 2.50 |
| O:P | Octyltriethoxy silane: Phenyltriethoxy silane (2:1 molar ratio) | 0.25 | 0.50 | 1.00 | 1.50 | 2.00 | 2.50 |
| P:O | Phenyltriethoxy silane: Octyltriethoxy silane (2:1 molar ratio) | 0.25 | 0.50 | 1.00 | 1.50 | 2.00 | 2.50 |



Scheme 9: Hydrolysis and condensation reaction of OTES.



Scheme 10: Hydrolysis and condensation reaction of APS.



Scheme 11: Hydrolysis and condensation reaction of PhTES.

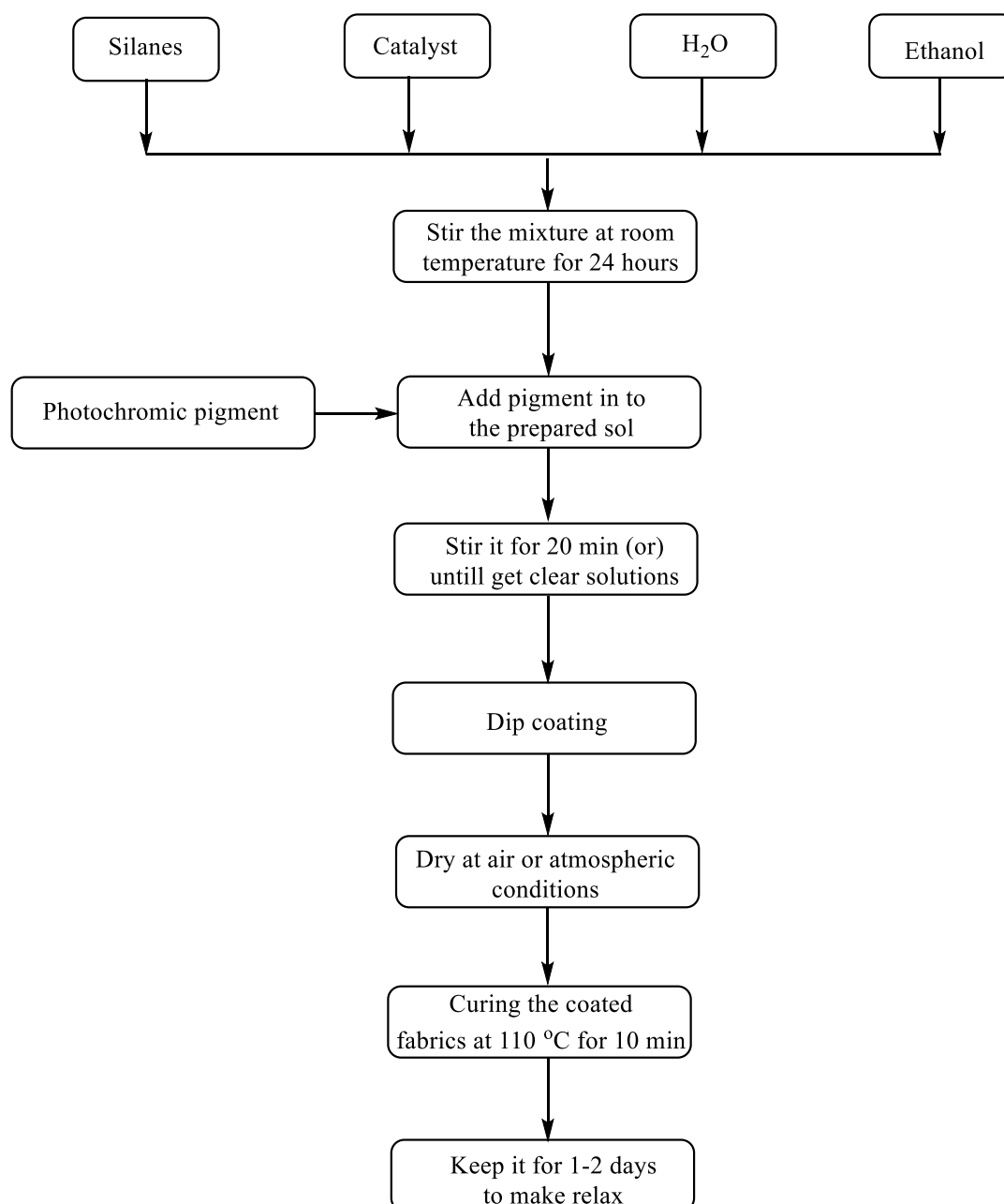


Figure 57: The sequencing process for the sol-gel coating process.

4.2.2 Measurement of kinetic properties of photochromic PET fabric

After the sol-gel coating, the fabric is measured its kinetic properties by using of Photochrom-3 with the minimum peak wavelength of 385nm. The detailed procedure for the kinetic measurement could be discussed already in the section 3.2.4. The sol-gel coated fabric has been measured five cycles both exposure and reversion phase. One measurement cycle consists of 5 min exposure under UV and 5 min of reversion phase (i.e. without UV-radiation) and totally 10 min per cycle. Average value of the five repetitive measurements was used for statistical data treatment. As discussed in the section 3.2.4, the various kinetic properties such as K/S

functions, K/S (max), change in the optical density, half-life of color change, rate constant could be calculated for the coated fabric.

4.2.3 Effect of abrasion durability on photochromic response

It is necessary to analyze the durability of the coating towards to the photochromic response; therefore, it can be determined by using simple abrasion resistance by Martindale abrasion tester. So, the coated samples were abraded for 100, 300, 500, 700 and 1000 cycles under the pressure of $9kPa$. The abrasion durability with respect to the photochromic response can be computed via the Eq. 4.1,

$$\% \text{ loss} = \left(\frac{\Delta K/S_2 - \Delta K/S_1}{\Delta K/S_1} \right) \times 100 \quad (4.1)$$

where $\Delta K/S_1$ and $\Delta K/S_2$ are the K/S (max)) before and after abrasion measurement with respect to the abrasion cycles respectively.

4.2.4 Effect of washing durability on photochromic response

The durability of coated samples against washing with respect to the photochromic response is another important property, which can be analyzed through simple washing conducted as per AATCC-61 standard. It is a test which can be able to simulate the home laundering practices as like consumer use, however, it is an accelerated washing test can be equal to five or more home commercial launderings. Before testing, the specimens (10cm to 4cm) are attached with multifiber adjacent fabric by simple sewing, then the wash liquor has been prepared by dissolving the 4g of detergent per liter of water. Later on, adding the prepared liquor on the stainless-steel container with steel balls. Close the container and operate the machine at the temperature of 60°C for 60 minutes. Later on, un-sew the adjacent fabric and test specimen. Now the test specimen has to wash twice with cold water and required to dry in the atmospheric conditions. The washing durability towards to the photochromic response can be computed the Eq. 4.1, where $\Delta K/S_1$ and $\Delta K/S_2$ are the K/S (max) before and after washing measurement cycles respectively.

4.2.5 Uptake % of the coated fabric

The amount of coating solution absorbed by the fabric can be computed by the Eq. 4. 2.

$$\text{Coating uptake (\%)} = \frac{W_2 - W_1}{W_1} \times 100 \quad (4.2)$$

where W_1 and W_2 are the weight of fabric before and after coating respectively.

4.2.6 Effect of physical properties of sol-gel coated fabrics

After the coating, the various physical properties of coated fabric can be analyzed to know the influence of precursors. First, the fabric thickness was measured by thickness gauge tester according to the ASTM D1777. Areal density was calculated based on the ASTM D3776-07. The bending properties of coated and control fabric can be measured by using SDL ATLAS (Shirley) stiffness tester, the measurement can be done as per the ASTM D1388 [113]. During the bending measurement, $2.5\text{cm} \times 20\text{cm}$ of strips made in both warp and weft directions of fabrics, while preparing the sample, the ruler was placed on the strips and slid horizontally along the designated platform of the stiffness tester, it continues until the suspended end of the strip met two parallel marks on the wall of stiffness tester, the marking point is exactly 41.5° below the horizontal plane. The length of the travelled specimen on the ruler had been recorded as the bending length (C) of both the ends as well as the front and back of the specimen can be noted an average value can be calculated for further computations [114]. From the bending length, it is possible to calculate the flexural rigidity (mg.cm) and bending modulus (kg.cm^{-2}). The above measurements were done five times and the average value was used to find the flexural rigidity and bending modulus of coated and control fabrics. The flexural rigidity and bending modulus were calculated from the Eq. 4.3 and 4.4 in mg.cm and kg.cm^{-2} respectively.

$$G = 0.1MC^3 \quad (4.3)$$

where M is the mass per unit area (g.m^{-2}) and C is the bending length (cm) of the fabric [113];

$$Q = \frac{(12G \times 10^{-6})}{g^3} \quad (4.4)$$

where Q is the bending modulus in (kg.cm^{-2}), G is the flexural rigidity and g is the fabric thickness (cm).

4.2.7 Surface morphological analysis of sol-gel coated fabric

The surface morphology of control and sol-gel coated fabrics were observed by using TS5130 Vega-Tescan scanning electron microscope (SEM). Before SEM analysis, the samples were sputter-coated with gold by using of Sputter coater to avoid the accumulation of high static electric fields. In the measurement, the electron column was kept at vacuum and other following parameters were used; 20kV accelerating voltage and $500\times$ magnification levels with a vacuum of $7.8 \times 10^{-3} \text{ Pa}$. The working distance between the sample and objective lens can be adjusted according to the image resolution.

4.2.8 Surface roughness analysis of sol-gel coated fabrics

An Olympus OLS 3100 model LSCM was employed to measure surface roughness properties of control and sol-gel coated fabrics. From this analysis, the surface roughness (which including the maximum peak height (R_p), maximum valley depth (R_v) and maximum height profile (R_z)) and other related properties were calculated as per the ISO 4287:1997 standard, the pictorial representation of analyzed surface roughness is shown in Figure 58. LSCM also generates the three-dimensional profile, which helps to find the surface modification before and after sol-gel coating. The maximum height profile (R_z) could be computed by Eq. 4.7.

$$R_p = \text{Max}(R_{p_i}) \quad (4.5)$$

$$R_v = \text{Max}(R_{v_i}) \quad (4.6)$$

$$R_z = R_p + R_v \quad (4.7)$$

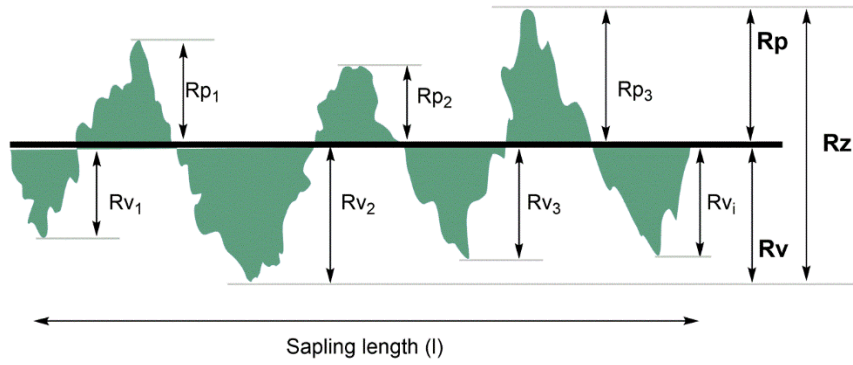


Figure 58: Schematic representation of surface roughness analysis.

4.3 Results and discussion on sol-gel coated photochromic fabrics

4.3.1 Effect of photochromic response on the sol-gel coating

4.3.1.1 Effect of K/S Values on drawing ratio of photochromic filaments

The reflectance characteristics of the photochromic pigment incorporated sol-gel coated fabric are shown in Figure 59. It was observed without UV radiation, the sol-gel coated fabric shows the flat trend of the spectrum. As discussed in the section 3.3.1.1, it is mandatory to ensure the amount of UV energy during the optical measurement and the results of UV energy are tabulated in Appendix- C. Figure 60-(A&B) shows the photographs of original color (i.e. colorless) and developed color of the photochromic fabric under the UV influence. These photographs were captured after removal of UV radiation and within 3s. However, there are

practical issues associated with the picture capturing, but it mostly with weekly developed color as well as the color with fast decay. In case of color difference is not possible to capture within the specified time limit, due to the in presence of UV radiations.

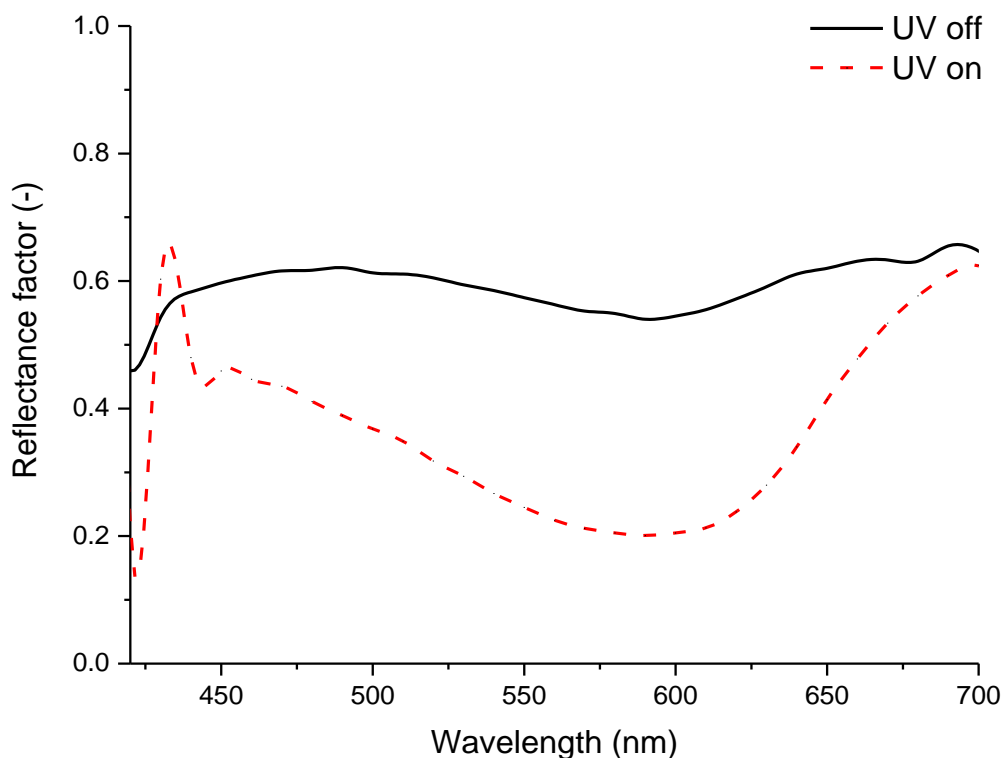


Figure 59: Visible reflection spectrum of sol-gel (OTES) coated fabric with MPP pigment.

Figure 60-(B) shows the visual observation of the color change of produced photochromic fabrics (i.e. original color of the pigment is purple). The color strength values of the photochromic fabrics with respect to different precursor compositions were shown in Figure 61. Results indicates, in the same concentration pigment derived different K/S values and it depends on the type of precursor. Therefore, K/S values are purely depending on the type of precursor used during the sol-gel coating process. From the observed results, the precursor having the strongly influence the photochromic pigment and their optical properties. Among the different precursor, OTES and its combination produce higher photochromic response than sol prepared from APS & PhTES alone or its combinations, even though at the same concentration of photochromic pigment, it can be visible in the Figure 61. The reason behind these phenomena is, the chemical structure of precursor, size & shape of silica network and available free space in the pore of sol network are the important parameters which influence on the optical properties of the photochromic pigment. Fact for why OTES based precursor

provide higher photochromic response, since it contains long flexible chains which creates more pore space along with flexible silica network, therefore it allows the photochromic pigment to undergo isomerization reactions without any interference (i.e. original to merocyanine and merocyanine to original forms), in fact APS and PhTES based precursors contains propyl and phenyl groups, which is basically rigid in nature. Therefore, it reduces the space between the pore and photochromic pigment, resulting in lower photochromic response by restricting the isomerization reaction of photochromic pigment. The lower isomerization takes to lower photochromic response, during optical measurement, it altered the light reflection, which marginally depends on the colored (isomerizes) molecules, so, results are the reduced absorption of light under UV radiations. In other words, light reflection is affected where the sol network is in a rigid manner. Another interesting fact found in the sol-gel coated fabric was the reversion phase, in case of miPP filaments, the reversion phase is almost similar trend, but in sol-gel coated fabric was varied and it depends on the precursors.



Figure 60: Photochromic sol-gel coated fabric, (A) indicates the fabric coated with APS precursor and (B) indicates the fabric coated with OTES precursor (Colored portion indicates the influence of UV radiation).

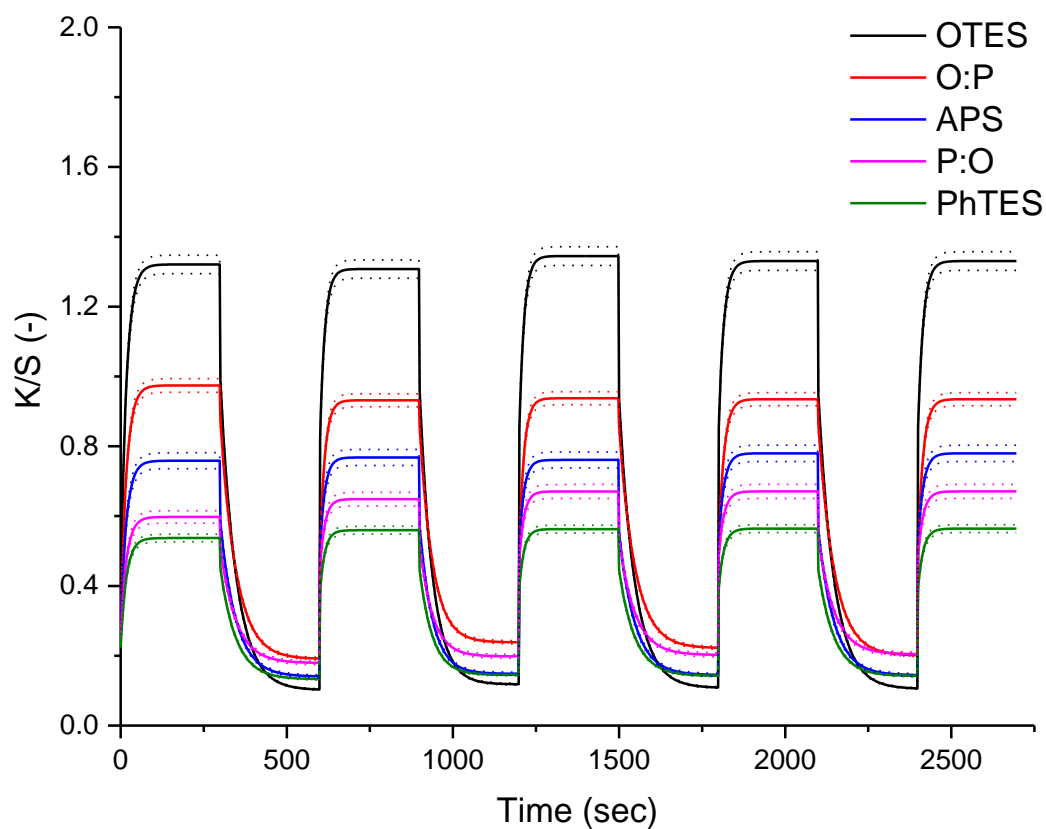


Figure 61: Effect of the precursor on the K/S values of coated fabrics (MPP-2.0 wt.%).

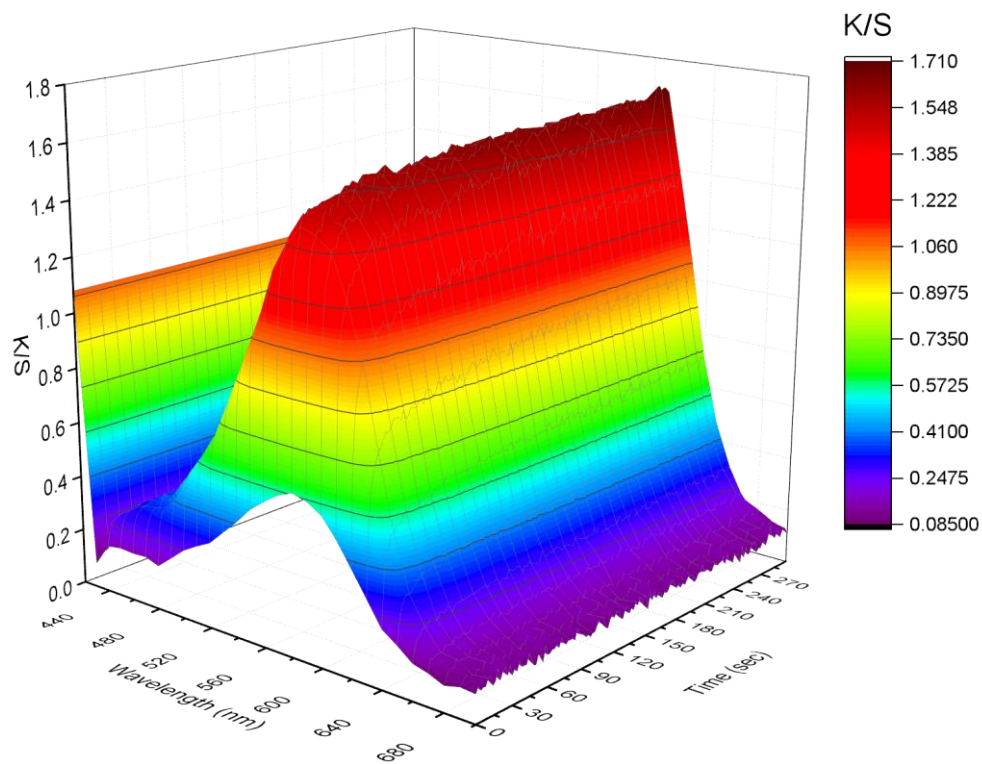


Figure 62: K/S values of OTES coated fabric (MPP-2.50 wt.%) under 5 minutes of exposure phase (UV-on).

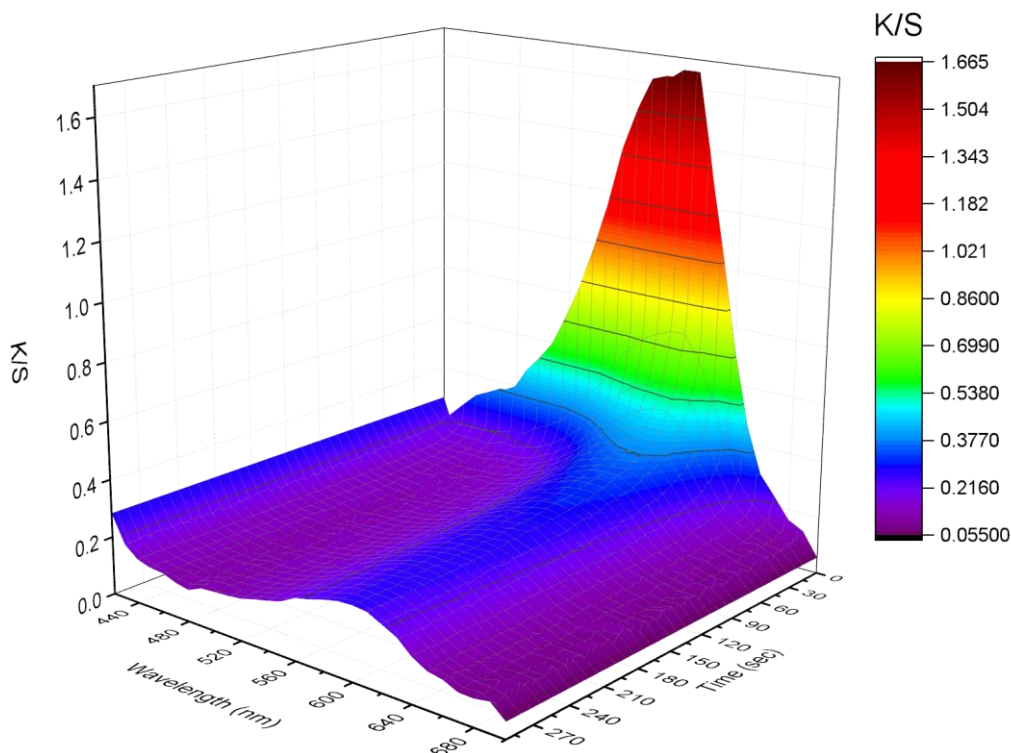


Figure 63: K/S values of OTES coated fabric (MPP-2.50 wt.%) under 5 minutes of reversion phase (UV-off).

4.3.1.2 K/S (max) functions on sol-gel coated fabrics under exposure phase

K/S (max) of produced photochromic coated fabrics with different precursor combinations was plotted in Figure 64 and the ΔOD were plotted in Figure 65. ΔOD can be calculated as per the Eq.3.2. ΔOD can be measured on the coated fabric without the addition of photochromic pigment and fabric coated with photochromic pigment. Results are significantly increasing the K/S (max) and ΔOD values with increasing the concentration of pigment. Therefore, K/S (max) and ΔOD are depending on the concentration of photochromic pigment, of course, it is a well-known effect. On other hand, K/S (max) and ΔOD is purely depended on the precursor and its combinations, since precursor has strongly influenced on the color strength values and followed by changes in the optical density. The reason behind is, the chemical groups and structure of the precursors, if the precursor is more rigid, which reduce the optical properties, it is evidently observed from these results. The combination of O:P (both 1:2; 2:1) and PhTES provided lower photochromic response than sol prepared from OTES and APS alone, even though at the same concentration of photochromic pigments. Therefore, the photochromic response is purely dependent on the chemical structure of precursor, size & shape and space of the pore of silica

network. The previous literature has been shown that the photochromic colorants were covered by sol networks during the applications [8, 115–118] and some of the literature was proposed the silica matrices along with the photochromic colorants. The data for the K/S (max) was fitted with linear regression, it concludes the goodness of fit all the precursors is above 0.98, which strongly recommend that there is a linear dependency of both the variables. Figure 66 shows K/S (max) values of different precursors with respect to the same concentrations. In this figure, two types of precursors and its combinations was used, among two, octyl based precursor shown better optical property than the phenyl based, the reason is phenyl groups in the PhTES creates a rigid network and followed by the structural transformation, which results in the reduced absorption of light under the UV radiation. However, the PET fabric (raw fabric) already have the property of scattering, once it has coated with photochromic pigment created many absorbing points. In most cases, people consider the refractive indexes of the substrate, but it is necessary to consider the refractive indexes of colorants (photochromic pigment) and its effects on the fabrics with respect to the scattering, but these scattering effects are very small and it is within tolerable and so it could be ignored. When the concentration of photochromic pigment is increased, the distance between scattering and absorption points of coated fabric have bellowed the limit of incoherence, which is nothing but, the scattering and absorption points of photochromic coated fabric are coherent [78]. The changing in optical densities of coated fabrics are given in Figure 65. There were statistically significant differences between ΔOD values of photochromic fabrics prepared by the different precursor, the data were fitted with linear regression, it shows better coefficient determination, in all the precursors shows above 0.97, which conveyed that there is a strong dependency on both ΔOD and concentration of pigment.

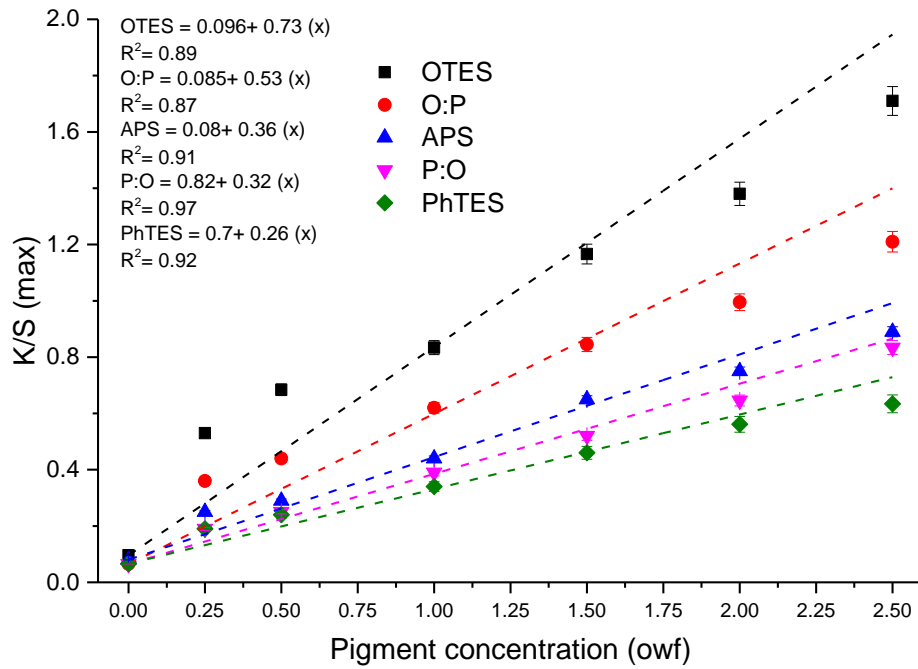


Figure 64: Dependence of K/S (max) on the sol-gel coated fabric under exposure phase.

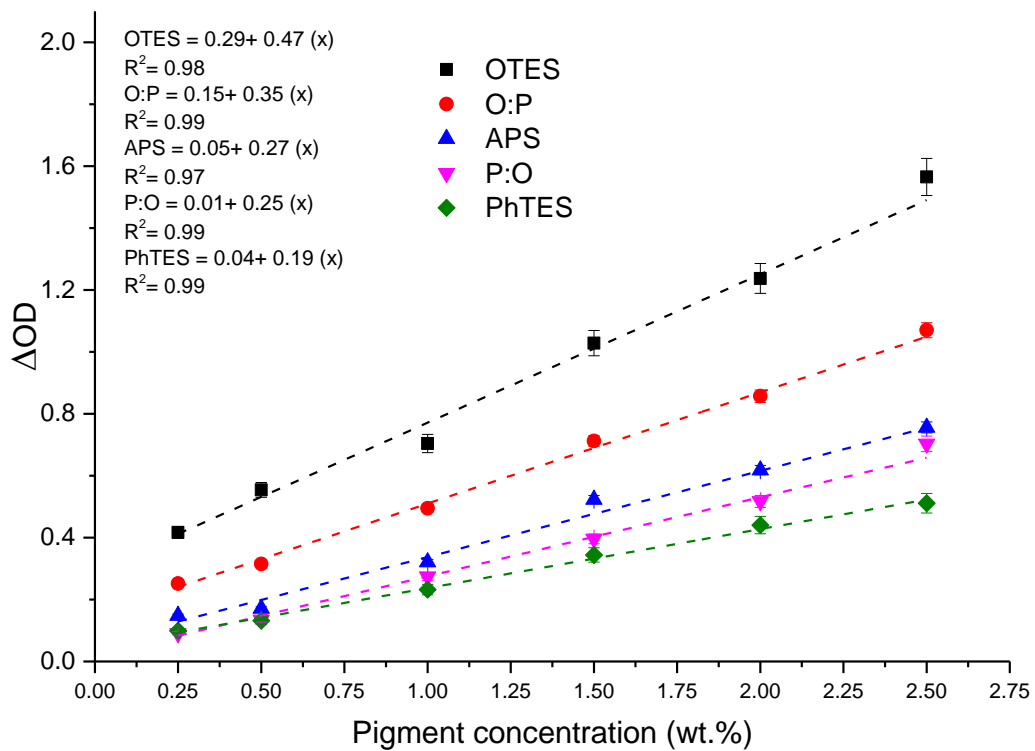


Figure 65: Dependence of ΔOD on the sol-gel coated fabric.

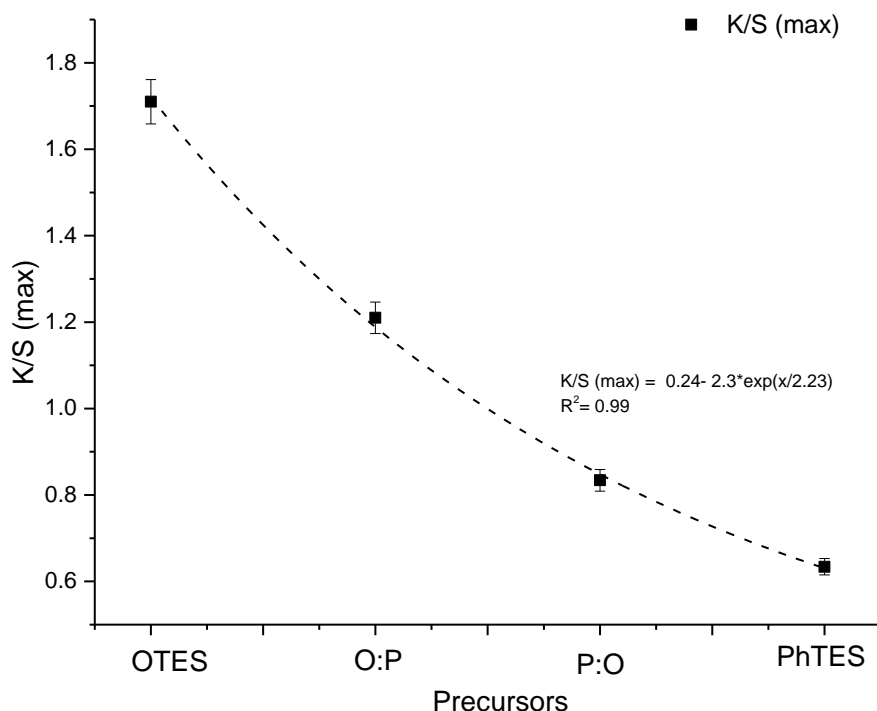


Figure 66: Dependence of K/S (max) on sol-gel coated fabric (MPP-2.50 wt.%) under exposure phase.

4.3.1.3 Half-life of color change for sol-gel coated fabric

In this research, half-life color change could be calculated as per the first-order kinetics, the equation is clearly described in the section 2.3.2. The relationship between in the half-life of color change and rate constant on the pigment concentration & precursor influences was studied, the results significantly depend on the pigment concentration & precursor combination, this trend is same for both exposure and reversion phase. Figure 67 shows the half-life of color change of sol-gel coated PET fabric with respect to the pigment concentration under the exposure phase, results are evident that purely depends on the concentration of pigments and precursor types. From the results, it is confirmed that the fabric coated with OTES, APS shows faster reaction than the PhTES & its combination. The half-life of color change for the fabric coated with PhTES shows 26s when the concentration of pigment is 0.25 wt.%, whereas it reduced to 16s at the concentration of 2.5 wt.%. In case of OTES provides the 23s at lowest and 10s at highest concentration of pigments, on other hand, APS provides 22s at lowest 14s at highest concentration, in the combination O:P (i.e. 2:1 molar ratio) has lowest half-life of color change than the combination of P:O (i.e. 2:1 molar ratio). Among the different precursors, only PhTES shows highest half-life of color change, in case of other precursors, shows the overlapping results until the pigment concentration of 1.5 wt.%. This is due to the

lowest concentration of pigment which requires almost similar time for the conversion of merocyanine form of spirooxazine. To find the statistical dependency, the data were fitted with linear regression and it shows the better coefficient determination values (<0.90). From the graph, there are some overlapping caused by the fabric coated with OTES, it shows that in lowest concentration pigment having a higher half-life, whereas the concentration is increased, the half-life is decreased as faster than its actual predicted trend. Figure 68 described the half-life of color change of photochromic fabric under the reversion phase, it is clearly described that the results are depending on the precursor types and pigment concentration. The half-life of color change during reversion phase shows higher than the exposure phase, this is due to the structural modification of pigment during the isomerization reaction. Generally, structural conversion in to merocyanine is take lower half-life than the structure of merocyanine is converting into their original structure. The half-life of color change for the fabric coated with PhTES shows 57s when the concentration of pigment is 0.25wt.%, whereas it reduced to 36s at the concentration of 2.5 wt.%. In case of OTES provides the 42s at lowest and 21s at highest concentration of pigments, on other hand, APS provides 51s at lowest 26s at highest concentration, in the combination O:P (i.e. 2:1 molar ratio) has lowest half-life of color change than the combination of P:O (i.e. 2:1 molar ratio). To find the statistical dependency, the data were fitted with linear regression and it shows the better coefficient determination values (<0.95).

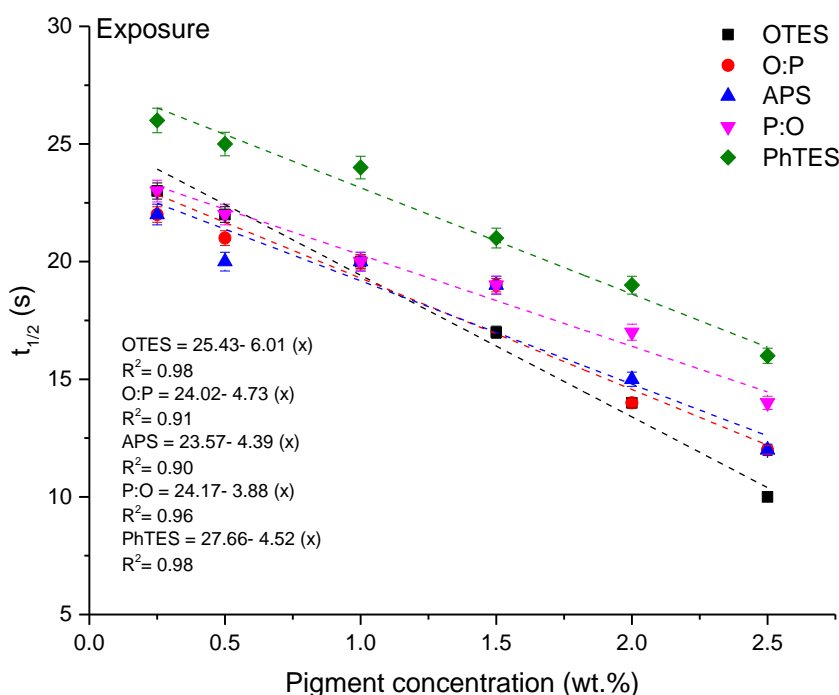


Figure 67: Half-life of color change during exposure phase of coated fabric.

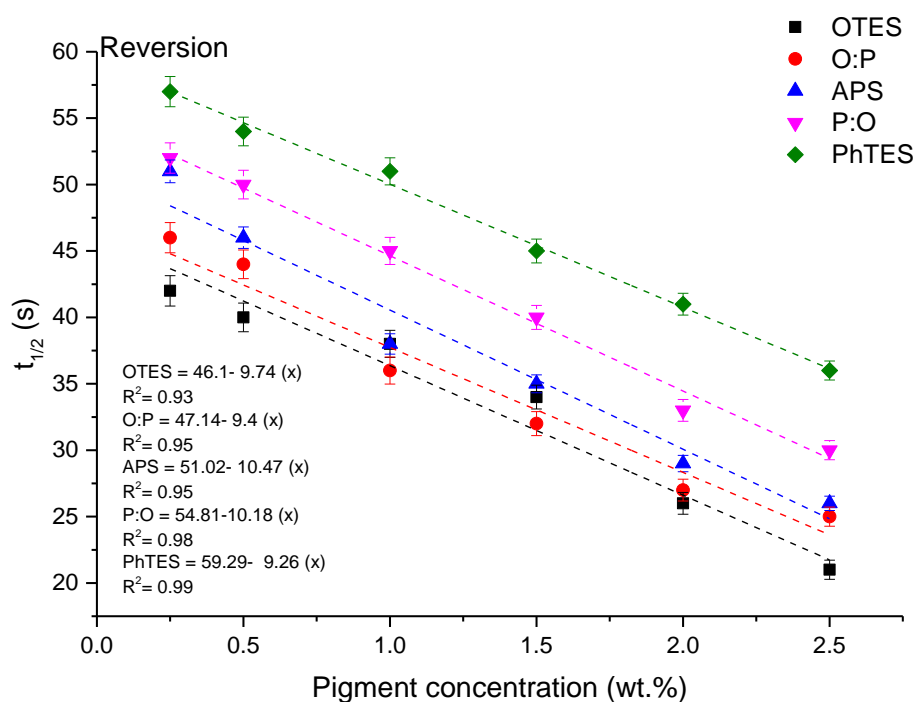


Figure 68: Half-life of color change during reversion phase of coated fabric.

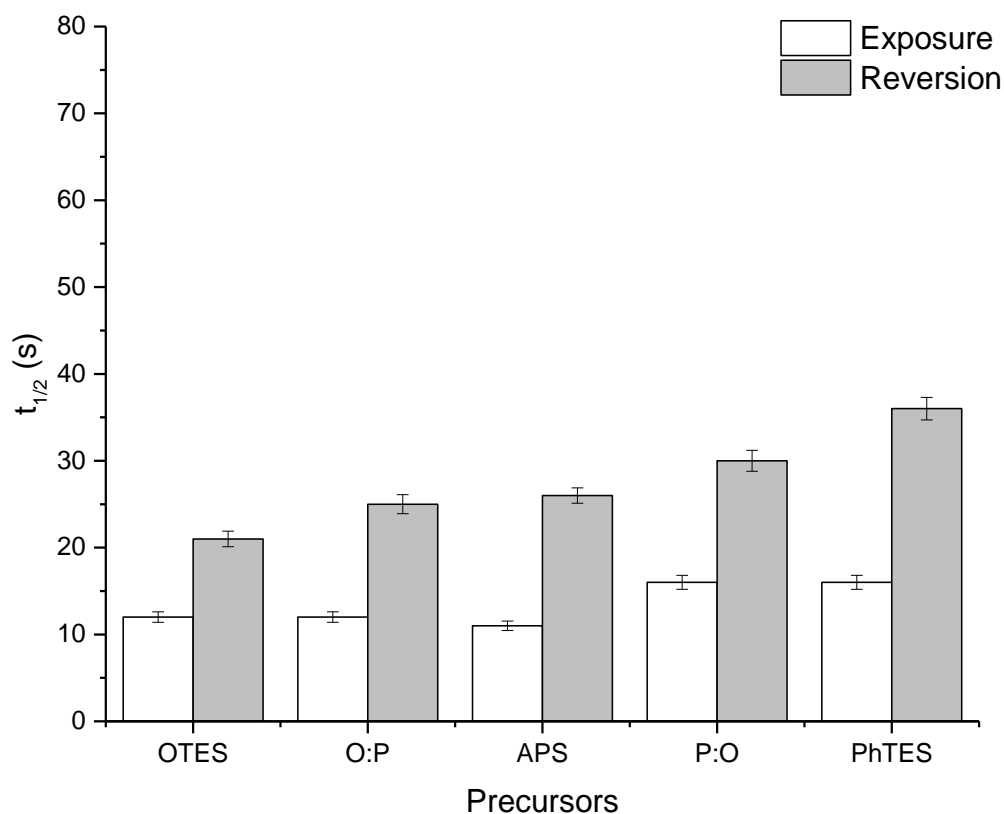


Figure 69: Impact of precursors on the half-life of color change (MPP-2.5 wt.%).

Figure 69 shows the dependence of half-life of color change on the precursors under exposure and reversion phase, the graph is made with a constant concentration (i.e. pigment concentration- 2.5 wt.%) of MPP. From this graph, the half-life of color change can be varied with respect to the precursors types, which is purely depends on it. In other words, both exposure and reversion phase, the half-life of color change, there is an influence of silica sol network, since it has been discussed in the section 4.3.1.5. Other than the silica network, there are many parameters which influence the half-life of color change, such as, UV absorption rate, concentration of photochromic colorant, available form of colorant, chemical structure of the colorant, number and type of functional groups present in the colorant, position of functional group, surface area of reactant, temperature of the system, reaction rate, level of UV energy and type of substrate. However, it generalizes the statement and it is difficult to particulate the specific parameter which influences on the half-life of color change. However, one conclusion can be proposed from these results, increasing concentration makes faster reconversion of the original form of photochromic pigment into merocyanine form. Based on the first order kinetics, the detailed kinetic parameters of photochromic coated fabrics are tabulated in the Appendix- D.

Table 13: Comparison of optical properties of photochromic filaments and fabrics.

| (MPP-2.5 wt.%) | | K/S (max) | $t_{1/2E}$ (s) | k_E (s^{-1}) | $t_{1/2R}$ (s) | k_R (s^{-1}) |
|-----------------------|----------------|-----------------|----------------|--------------------|----------------|--------------------|
| Filament | miPP filaments | 5.13 ± 0.12 | 21 | 0.03648 | 42 | 0.01650 |
| Sol-gel coated fabric | OTES | 1.71 ± 0.15 | 10 | 0.05776 | 21 | 0.02476 |
| | O:P | 1.21 ± 0.12 | 12 | 0.04951 | 25 | 0.02390 |
| | APS | 0.89 ± 0.10 | 12 | 0.04621 | 26 | 0.02166 |
| | P:O | 0.83 ± 0.09 | 14 | 0.04332 | 30 | 0.02166 |
| | PhTES | 0.63 ± 0.07 | 16 | 0.03466 | 36 | 0.01824 |

Note: K/S (max) can be calculated under exposure phase, $t_{1/2E}$ and k_E is the half-life color change and rate constant at the exposure phase respectively; $t_{1/2R}$ and k_R is the half-life color change and rate constant at the reversion phase respectively.

The comparison results of K/S (max) and half-life of color change in the exposure and reversion phase for the photochromic miPP filaments and the PET fabrics are tabulated in Table 13. The

K/S (max) values are ~4 times higher in case of miPP filaments than the sol-gel coated fabrics. On other hand, the half-life of color change has been varied, in case of miPP filaments shows two times higher than the sol-gel coated fabric with OTES. Obviously, it is due to their size of the silica structure, size of the pore of the silica, which is directly proportional to the photochromic response of coated PET fabrics, however miPP filament has slow rate than the sol-gel coated fabric, this trend is same in both exposure and reversion phase. The predicted reason could be, the sol-gel coating can provide the thin layer on the surface of PET fabric along with the photochromic pigments, which is nothing but, the fabric has the photochromic pigments only on its surface, whereas the mass coloration provides the good penetration of the colors along with the polymeric structure. Therefore, the miPP filaments required more time to undergo the molecular collision, which directly influenced on the lower speed of reaction (i.e. low rate constant) compared to the sol-gel coated fabrics. Among the sol-gel coated fabric, precursors like APS and OTES shows the highest rate than other fabrics.

4.3.1.4 Color difference analysis of sol-gel coated fabric

Based on the Eq. 2.31, color difference (ΔE^*) of photochromic coated fabric was analyzed and the results are shown Figure 70. The rate of coloration and discoloration of photochromic pigments are generally depending on the molecular structure of the pigments when it incorporated to the precursors, it is necessary to consider the sol network and other related parameters too. Also, these parameters influence on the stability and fatigue resistance of the produced photochromic fabrics. The changing of hue can be explained by the color difference (ΔE^*) and the photochromic system produces the shade intensity or shifting of the lightness of the developed color. In this work, highest residual ΔE^* was found ~3.1 units and lowest was ~0.1 units. In all the concentration photochromic fabric with OTES precursor shows highest ΔE^* , which confirms that there is a visible color difference since a human can identify the color difference if ΔE^* is more than ~0.4 units. The main objectives to produce these fabrics to determine the UV in the environment, which act as a flexible UV-sensor, therefore the residual ΔE^* values are more important to consider. The fabric coated with PhTES shows lowest ΔE^* values it can be seen in all the concentration. On other hand APS based precursor shows moderate (~1 units at maximum concentration). The fact behind these results, precursor having the strong influence, since PhTES has shown lower ΔE^* values since it has the rigid structure, which could not allow the photochromic pigments to undergo isomerization reaction, on the contrary, it shows very less uptake % during the coating (see Table 14). Therefore, it confirms

two possibilities, one is less uptake % (~65%) of photochromic pigments in the coating as well as less isomerization reaction, so it produces less color strength values which cause to lower color difference or in other words, the color difference is could not have identified since it has less than 1 units. In case of photochromic fabric produced with OTES based precursor shows higher ΔE^* values, the reason, OTES precursors allow the pigment to isomerizes as its maximum, which causes to produce more color, also this precursor allows the fabric to more uptake % (~83%). However, both OTES and PhTES produce blue color due to the hypsochromic shift whereas the original color of the pigment is purple. All the results are fitted with exponential functions to find the goodness of fit, all the results show more than 0.98, which strongly recommend that there is a significant dependency on ΔE^* values and the concentration of pigment as well as precursor types.

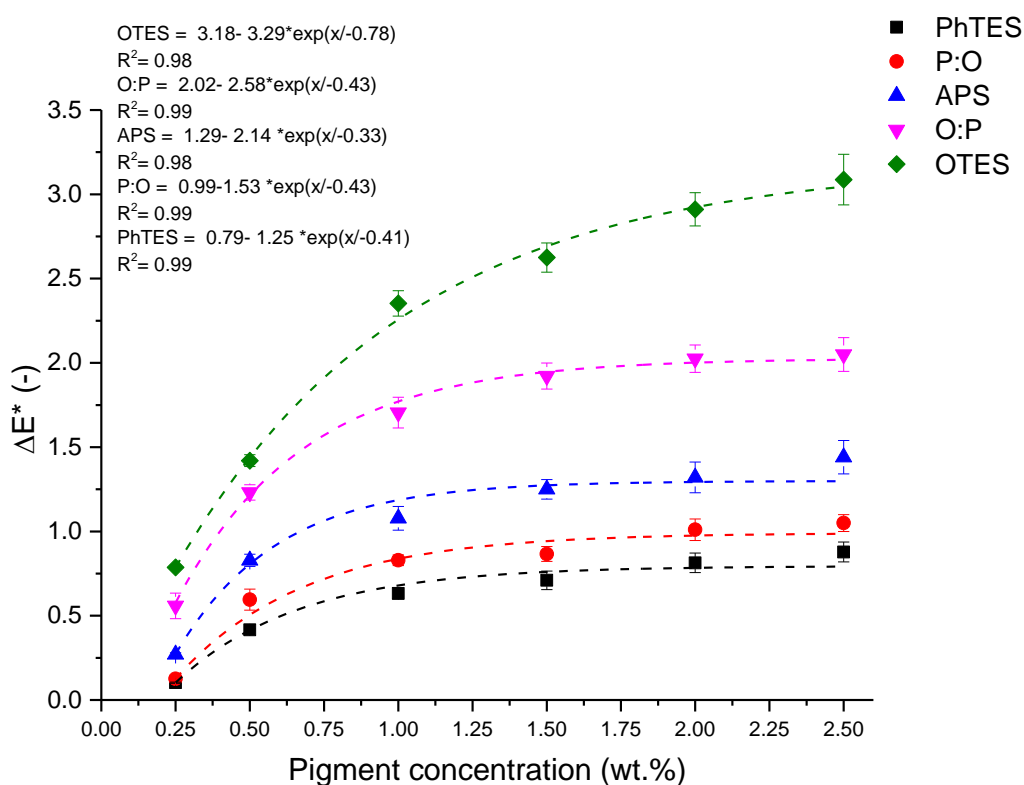


Figure 70: Residual ΔE^* for the sol-gel coated fabric.

4.3.1.5 Effect of silica sol networks on optical and physical properties

Sol-gel coating involved two basic reaction called hydrolysis and polycondensation, which is similar to the polymerization of various artificial polymers. Resulting, these reaction makes colloidal particles to the three-dimensional network, which often called sol-gel network. Generally, the physical characteristics of the sol-gel network are depending on the particle size

and cross-linking before the gelation treatment, also, the sol-gel network is deciding the physical and optical properties of coated fabric or some other substrate. Depending on the precursor types, it varies the bridging bonds which are generally created during the condensation reaction, which greatly influence the stiffness of the sol-gel network. The silica network derives the effect of sol-gel coated fabric on the optical response speed (coloration and decoloration, half-life, etc.) and physical properties, the structure of precursor determines the morphology of the coated materials. Previously, many researchers proposed predicted silica network [115, 116, 118–121], from there results, it is easy to understand the how the sol-gel matrix is formed with pore and pore size. From the OTES based precursors, obtained pores are surrounded by flexible octal chains, due to the presence of long alkyl aliphatic chain, since the phenyl groups are rigid in nature, phenyl groups in PhTES lead to a more rigid pore shell. Also, it has less steric hindrance effect on the pigments, therefore, this structural arrangement allows the pigment to undergo the photochromic reaction easily. In other words, the octyl groups produce a more flexible network with the higher surface area than other silanes, which also ensure the smaller spherical particles with more uniform distributions [122]. In a flexible shell inside a pore, a photochromic molecule can easily undergo a photochromic reaction. Also, a flexible silica coating layer is led by the flexible chain of OTES could lead to that has little effect on the fabric handle properties, which is deeply described in the upcoming sections.

4.3.1.6 Uptake % of the coated fabric and their photochromic response

The fabric uptake % of the coating process can be computed according to the Eq. 4.2, the method of determination is well described in the section 4.2.5 and the results are tabulated in Table 14. The maximum uptake was found $83.2\% \pm 0.9$ for the sol prepared with OTES, the lowest uptake was found $65.3\% \pm 0.6$ for the sol prepared with PhTES. Although in same coating conditions, PhTES and its combination absorbed lower coating solution as compared to OTES and APS, due to these facts it shows lower photochromic response and it visualized in the color strength values and K/S (max) values. The reason might be rheological properties of precursor, it could be varied with respect to the precursor. However the rheological properties of prepared sol-gel were not studied, but there is literature studied towards to the sols viscosity and its impact on the add-on % it advised that, if sol viscosity is higher might cause the lower add-on % [123].

Table 14: Uptake %, and K/S (max) (MPP-2.50 wt.%) of coated fabrics.

| Precursor | Uptake (%) after coating | | K/S (max) | $t_{1/2E}$ (s) | $t_{1/2R}$ (s) |
|-----------|--------------------------|-------|-------------|----------------|----------------|
| | % uptake | CV% | | | |
| OTES | 83.2±0.9 | 102.9 | 1.71 | 10 | 21 |
| O:P | 75.1±0.7 | 165.6 | 1.21 | 12 | 25 |
| APS | 72.3±0.7 | 66.5 | 0.89 | 12 | 26 |
| P:O | 70.6±0.6 | 47.8 | 0.83 | 14 | 30 |
| PhTES | 65.3±0.6 | 92.0 | 0.63 | 16 | 36 |

Note: K/S (max) can be calculated under exposure phase, $t_{1/2E}$ is the half-life color change at the exposure phase; $t_{1/2R}$ is the half-life color change at the reversion phase respectively.

The observed rate constant of photochromic pigment in the silica matrices is notably faster than the photochromic pigment in the filament thorough the mass coloration techniques. The half-life of color change given in Table 14, it can be clearly visible that how uptake% of coating process can affect the optical properties. Higher the uptake % by the sols like OTES and its combinations cause the higher K/S (max) values than the sols with PhTES which the lowest uptake is 65.3 ±0.6%. Another reason for the reduction of the optical properties are, the open merocyanine form of photochromic pigment largely affected by the phenyl ring of PhTES, therefore, these interactions cause the chromophore of photochromic pigment into the off-reaction. The half-life of color change has been varied with respect to the precursors types, however precursors with PhTES shows the low speed of reaction than the OTES, the reason might be the ionic interaction of precursors (cations) and the pigments (oxygen anion in the spirooxazine).

4.3.2 Hypsochromic shift on sol-gel coated fabrics

The nature and amount of the organic groups (R) in the silica matrices determine the polarity of the inner surface of the pores, in general, the photochromic properties of spirooxazine molecules are strongly depending on the polarity of the pore where the spirooxazine molecules are located. Therefore, the spectral and kinetic properties of sol-gel coated fabrics are purely affected by the polarity of precursors, which means, it affects the absorption spectrum of the colored form of merocyanine. Thus, the hypsochromic shift of ~40nm was observed (absorption maxima are shifted from 610nm to 570nm), when the fabric is coated with

OTES/PhTES or its combinations with 5-chloro-1,3,3-trimethylspiro[indoline-2,3'-(3H) naphtho(2,1-b) (1,4)-oxazine]. Since the phenyl and octyl groups made decreasing the polarity of the respective precursors. This is due to the lowering the polarity of functional groups of phenyl and octyl attached to the surface of large organic chains might hindering the influence of OH groups in the pore surface. So, the photochromic fabric with OTES/PhTES precursors is turned to Blue color instead of its original color (i.e. Purple) under the UV radiations. The reflectance spectrum of both precursors is given in Figure 71 and the produced fabric under UV radiations are given in Figure 60- (a & b).

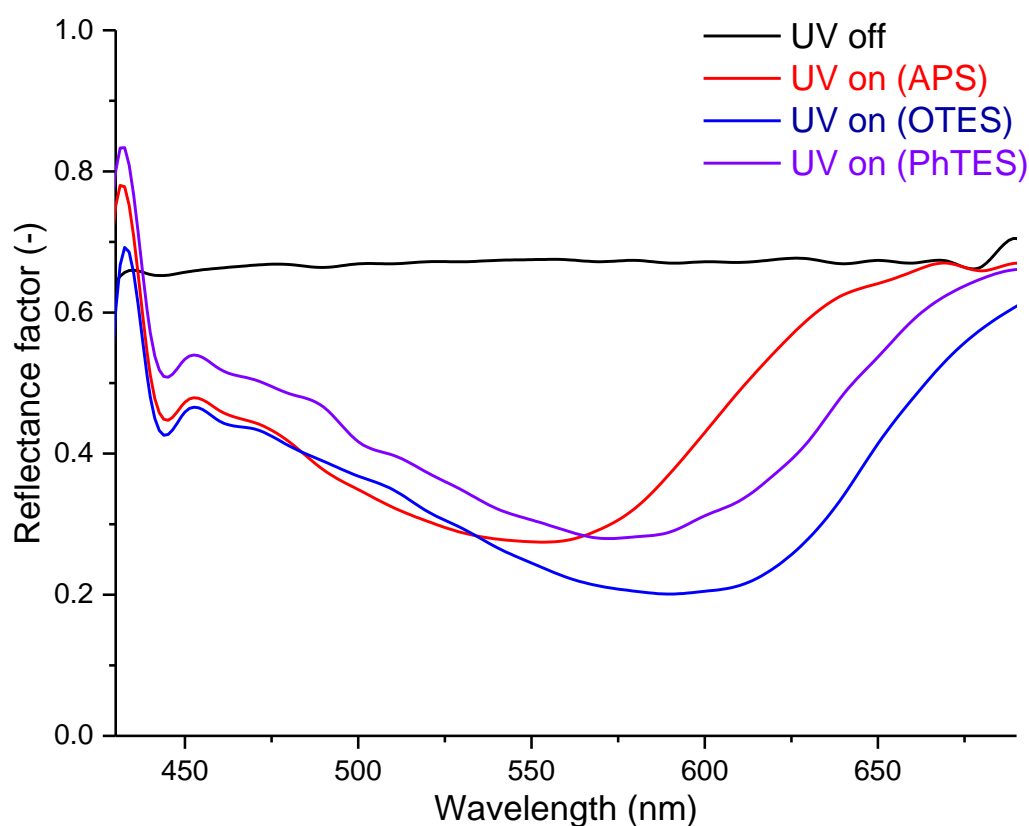


Figure 71: Reflectance spectra of coated fabric with different precursors (MPP-2.5%).

A colorless 5-chloro-1,3,3-trimethylspiro[indoline-2,3'-(3H) naphtho(2,1-b) (1,4)-oxazine] (i.e. MPP) can be isomerizes to purple colored merocyanine form in presence of APS precursor, whereas same pigment isomerizes to blue colored merocyanine when the PET fabric coated with the help of OTES or PhTES based precursor. Chemically the OTES/PhTES containing the methoxy groups which generally the electron donating in nature which are the prime reason for the hypsochromic shift of coated fabric from 610nm to 570nm. Apart from the electron donating groups, the polarity of the precursors in the OTES/PhTES major reason for the

hypsochromic shift, since it is less than the precursor APS and it confirmed by the visual appearance of fabric under UV radiations. As per the Kellmann et al. [124] hypothesis, the ground-state weakly polar molecule of 5-chloro-1,3,3-trimethylspiro[indoline-2,3'-(3H) naphtho(2,1-b) (1,4)-oxazine] could approach to the configuration of quinoid form. The polarity of both precursors OTES/PhTES plays a vital role in terms of solvatochromism and it is sensitivity towards to the precursors polarity with respect to the electron donating groups of 5-chloro-1,3,3-trimethylspiro[indoline-2,3'-(3H) naphtho (2,1-b)(1,4)-oxazine]. Due to the precursors polarity, the energy level of ground state declines more sharply than the excited state. Therefore, the result shows the energy between two different merocyanines, which has been produced during the UV radiations. The energy difference in the order of $\Delta E_1 < \Delta E_2 < \Delta E_3$ which is shown in Figure 72. This is the main reason for the observed hypsochromic shift. Generally, the λ_{max} is depended on the precursors polarity and the order of λ_{max} will be ($\lambda_1 > \lambda_2 > \lambda_3$) which is according to the $\Delta E = h\nu = hc/\lambda$. During sol-gel preparation, ethanol was added as a solvent, which also influence on the kinetics, but it is tolerable, for all these hypothesis, the molecular modeling was not done, however it can be confirmed by previous studies [124–129]. The effect kinetics and quantum yield on substitutes on 5-chloro-1,3,3-trimethylspiro[indoline-2,3'-(3H) naphtho(2,1-b) (1,4)-oxazine] are explained in Chapter 2 (Figure 6), from this we drawn that the quantum yield depending on the presence of electron in the 5-chloro-1,3,3-trimethylspiro[indoline-2,3'-(3H) naphtho(2,1-b) (1,4)-oxazine] which donates its substitutes in the 6'-position, however it controlled by the nature of the precursor, therefore, higher yield is given by the precursor with non-polar in nature [130].

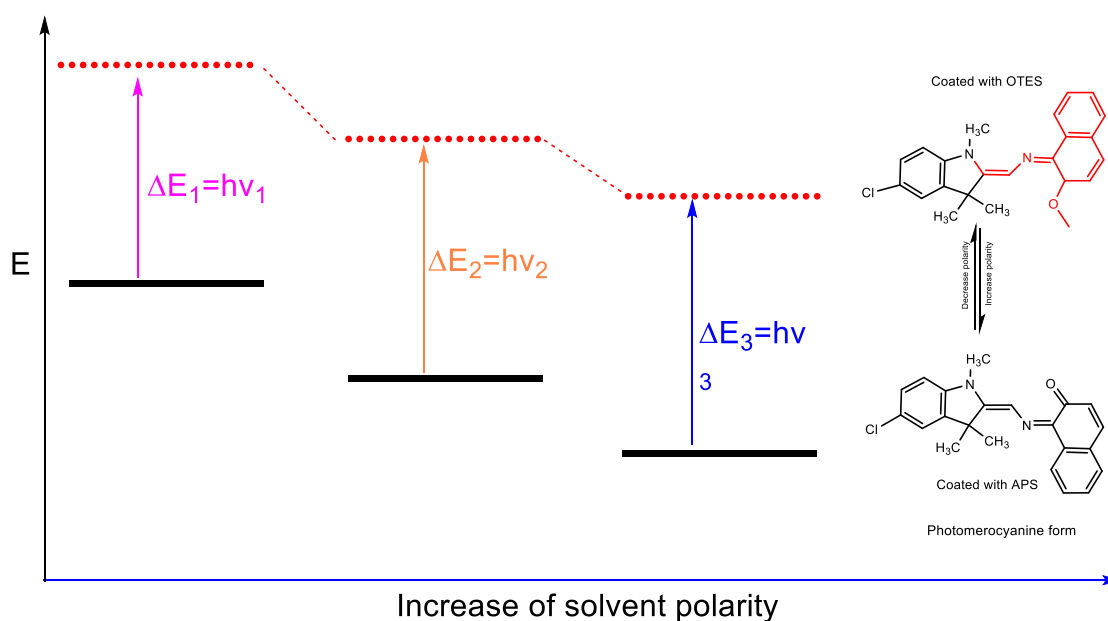


Figure 72: Schematic interpretation of hypsochromic shift on precursors polarity.

4.3.3 Effect of abrasion durability on photochromic response

The abrasion durability of sol-gel coated fabrics is investigated, the detailed method of measurement is given in the section 4.2.3. First, fabric is analyzed the photochromic response through K/S (max) values, thereafter the coated samples were abraded for 100, 300, 500, 700 and 1000 cycles under pressure of 9kPa, after the abrasion resistance the fabric again analyzed the photochromic response by computing the difference in the K/S (max) values before and after abrasion measurement. Figure 73 shows the abrasion durability of coated fabrics, which refer to the fabric samples that had been abraded various cycles and maximum for 1000 abrasion cycles. The durability of abrasion of the silica incorporated photochromic response has been reduced 17% at 1000 cycles for precursor with OTES, even though in same abrading level PhTES decreased 28%. The combination of Octyl and Phenyl in 2:1 molar ratio provides 20% and the combination of Octyl and Phenyl in 1:2 molar ratio provides 26% color loss at 1000 abrasion cycles, APS alone shows 24% color loss in the photochromic response. In case of PhTES based coating reduce the color loss % from 12%, 16%, 21%, 26%, 28% for the abrasion cycle of 100, 300, 500, 700 and 1000 respectively. The results of both before and after abrasion resistance on the K/S (max) confirm that there is a non-linear relationship on the precursors types, the goodness of fit was found $R^2=0.92$ and above, which strongly describes that there is a strong non-linear dependence on the abrasion resistance with respect to the precursor types. In overall, the coating process reduces the abrasion durability on the photochromic response, however, the overall level of abrasion durability on photochromic response is satisfactory except PhTES and its combination where PhTES is more concentrated. The results of the color loss % on the abrasion cycles (in all level) were in the order of PhTES> P:O> APS> O:P> OTES.

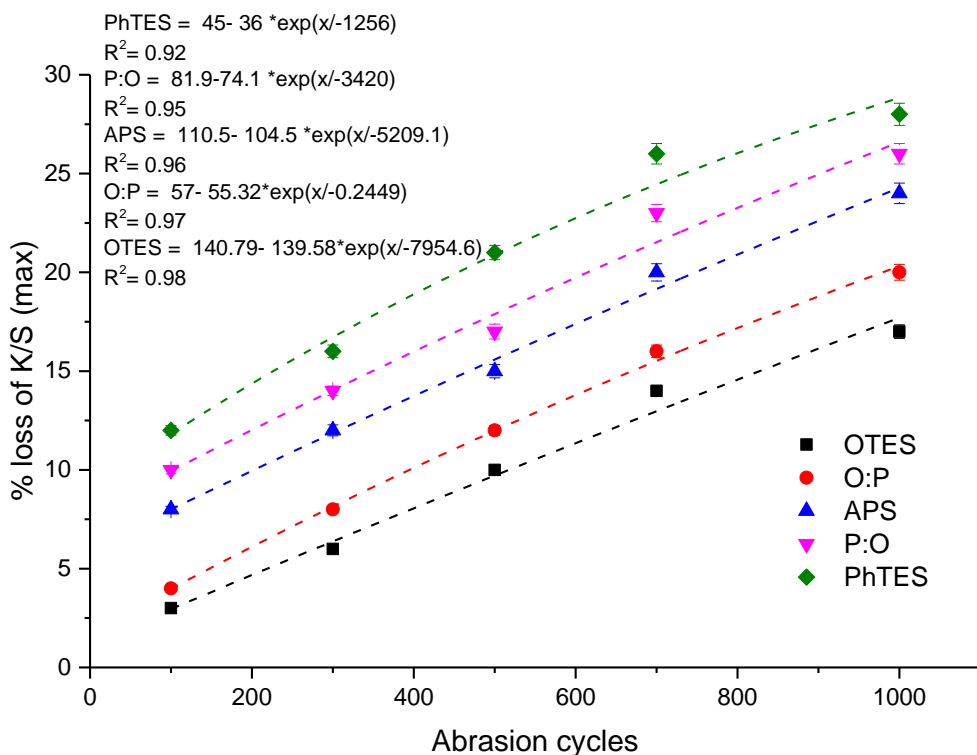


Figure 73: Abrasion durability of coated fabrics on photochromic response (MPP-2.5 wt.%).

4.3.4 Effect of washing durability on photochromic response

The assessment of washing durability of photochromic fabrics with respect to their photochromic response and results are described in Figure 74. The method of washing durability assessment was discussed in the section 4.2.4. The washing durability of sol-gel coated fabric on their photochromic response is varied with respect to the type of precursor. The poor washing durability was found in the case of OTES and its combinations whereas PhTES based precursors provide the better washing durability. This indicates that PhTES based precursors provide good washing fastness, and the reason for this phenomenon is the structure of silica matrices, in other words, K/S (max) values are decreased slightly but did not change as like the samples coated with OTES alone. Therefore, these results indicating that the photochromic effect was slightly affected due to the washing process.

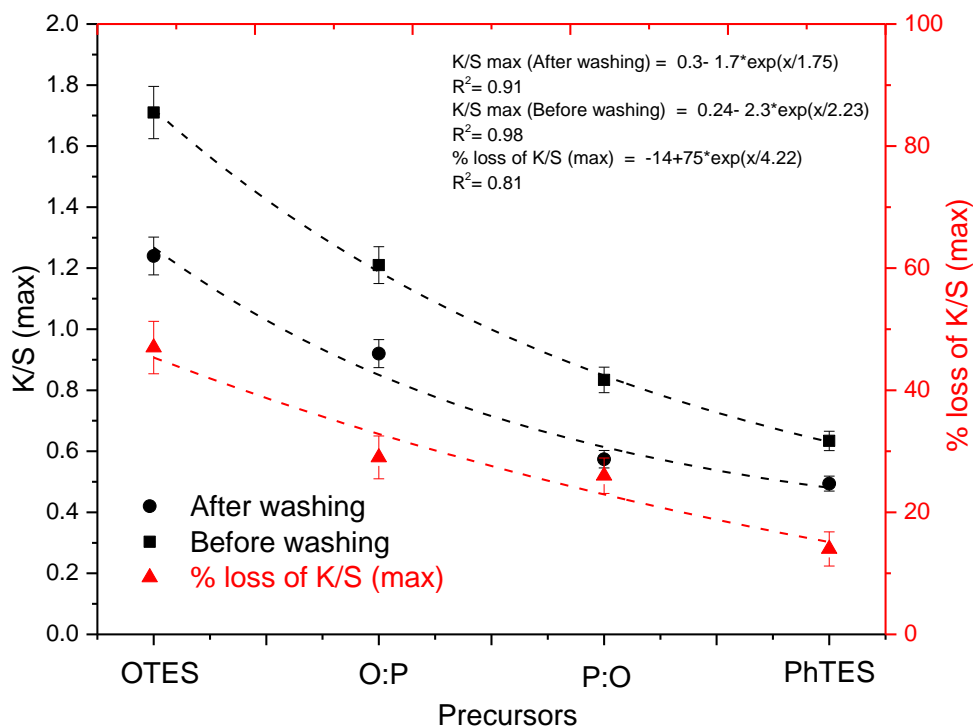


Figure 74: Washing durability of coated fabric on photochromic response (MPP-2.5 wt.%).

The durability of washing on the photochromic response of PET fabric has been reduced 47% precursor with OTES, which is very high color loss% on other hand the PhTES based PET fabric shows only 14% as color loss. The combination of Octyl and Phenyl in 2:1 molar ratio provides 29% color loss, in case of combination of Octyl and Phenyl in 1:2 shows the 26% color loss after specified washing cycles. APS alone provide the 18% loss in the photochromic response. In overall, the coating process reduces the photochromic response due to the washing, however, the overall level of washing durability is satisfactory except OTES and its combination. The reason behind for this phenomenon is the chemical structure of the sol, which has been deeply discussed in the section 4.3.1. The results of both before and after washing on the K/S (max) confirm that there is a non-linear relationship on the precursors types, the goodness of fit was found $R^2=0.91$ and above in case of K/S (max); whereas $R^2=0.81$ for the % loss of K/S (max), which describes there is a strong dependence on the washing durability with respect to the precursor types. However, the APS having the different chemical groups, therefore it is not used for statistical fit which is demonstrated in the Figure 74. The results of the color loss % on the washing cycles were in the order of OTES > O:P > APS > P:O > PhTES.

4.3.5 Effect of physical properties of sol-gel coated fabrics

4.3.5.1 Thickness and areal density of coated fabrics

The fabric thickness was analyzed and the results are tabulated in Table 15. Results shows, there is a significant relationship between fabric thickness and coating process. However, the thickness of the fabric is depending on the type of precursor used. There is no significant difference between the samples coated with OTES and control fabric (i.e. without coating treatment). Fabric coated with APS, PhTES and its combinations show increased fabric thickness, it is due to the rigid structure of silica networks, the results also confirm with surface roughness analysis.

Table 15: Physical properties of the sol-gel coated fabric (MPP-2.5 wt.%).

| Sample | Bending length | | | | Fabric thickness | | Fabric areal density | |
|---------|----------------|------|-----------|------|------------------|-------|----------------------|-------|
| | Warp (cm) | CV% | Weft (cm) | CV% | (mm) | CV% | (g.m ⁻²) | CV% |
| Control | 4.7 | 53.9 | 3.2 | 22.7 | 0.326 | 143.1 | 170.7 | 363.9 |
| OTES | 5.0 | 41.9 | 3.3 | 82.8 | 0.328 | 104.9 | 172.9 | 69.2 |
| O:P | 6.1 | 46.1 | 3.5 | 41.2 | 0.361 | 40.2 | 171.6 | 219.4 |
| APS | 6.1 | 37.7 | 3.5 | 22.8 | 0.353 | 16.0 | 173.2 | 100.2 |
| P:O | 6.5 | 19.4 | 3.6 | 67.0 | 0.375 | 25.8 | 172.4 | 109.4 |
| PhTES | 6.7 | 62.3 | 3.7 | 31.3 | 0.334 | 198.7 | 172.9 | 95.8 |

However, the thickness of the coating can be controlled by using different organic groups or may use a different molar proportion of these precursors but not sure for the expected photochromic response. Also, the viscosity of sols plays a vital role in the coating thickness, it can be reviewed by many researchers [123, 131–134]. In general, the coating thickness can be increased or decreased by introducing some functional groups, which directly influence on the coating thickness on the substrate. In some cases, with APS and PhTES coated fabric did not even bend to some extent; therefore, the coating affects other physical properties, such as drape coefficient, stiffness, bending modulus and flexural rigidity too. In general, deposition of any material on the substrate change its areal density, in our case the sol-gel coated samples show increased areal density than the control samples. The summary of the results is shown in Table 15.

4.3.5.2 Bending length, flexural rigidity and bending modulus of coated fabrics

The most significant factors in handling determination and comfort of textile are fabric stiffness. Flexural tests were conducted to the sol-gel coated fabrics, the procedure of flexural rigidity and bending modulus are explained in the section 4.2.6. Flexural rigidity and bending modulus of fabrics are calculated as per the Eq. 4.4 and 4.5 respectively, after calculation, the mean values are used to plot the graphs. The detailed results of fabric handle properties are given in the Appendix- E. The flexural rigidity and bending modulus are depicted in Figure 75 and Figure 76 respectively. As a result, a significant increase in the stiffness is caused by APS, PhTES and combination of PhTES based sol-gel treatment. OTES is the only treatment which did not cause a significant increase in the flexural rigidity and bending modulus. A higher flexural rigidity and bending modulus in the warp direction compared to uncoated fabric, while this trend was observed for all coatings in the weft directions too. Not as like precursors and its combination, the coating with OTES has the long aliphatic chain which ensures the softness of fabric without affecting the fabric bending and flexural rigidity. The most rigid fabric was observed higher when the fabric was coated with PhTES and APS coated fabric. Contrarily, O:P (2:1) combination did not show higher bending modulus and flexural rigidity, whereas, P:O (2:1) has shown higher, the reason is the higher contribution of PhTES. As a result, it increases the rigidity of coated fabric if the precursors contain PhTES, phenyl groups containing PhTES increase the rigidity of coated fabric. LSCM images have also confirmed. The results of APS coated fabric shown an increase in flexural rigidity and bending modulus, chemically APS containing the propyl groups due to its purely rigid in structure, which is the prime reason for the increasing the rigidity of fabrics. The increasing trend of flexural rigidity and bending modulus was All the treatments showed a higher flexural rigidity and bending modulus in the warp direction in comparison with the control, while this trend was observed for all coatings in the weft directions too. The coating with OTES has the long aliphatic chain which ensures the softness of fabric without affect the fabric bending and flexural rigidity as like other precursors and its combinations. PhTES and APS coated fabric were observed higher bending modulus and flexural rigidity, which says that most rigid fabric. On the contrary, O:P (2:1) combination did not show higher bending modulus and flexural rigidity, whereas, P:O (2:1) has shown higher, the reason is the higher contribution of PhTES. In overall, if the precursors contain PhTES, phenyl groups containing PhTES increase the rigidity of coated fabric. The results of both fabrics flexural and bending modulus in warp and weft way confirm that there is a non-linear relationship between the precursors types, the goodness of fit was

found $R^2=0.92$ and above in case of flexural rigidity; whereas $R^2=0.71$ and above for the bending modulus, which describes there is a strong non-linear dependence on both flexural and bending modulus with respect to the precursor types. Since, APS having the different chemical groups, therefore it is not used for statistical fit which is demonstrated in the Figure 75 and Figure 76. This results also confirmed by LSCM images. The results of APS coated fabric shown an increase in flexural rigidity and bending modulus, chemically APS containing the propyl groups which is purely rigid in structure, which is the prime reason for the increasing the rigidity of fabrics. In both the warp and weft direction, the increasing trend of flexural rigidity and bending modulus was found.

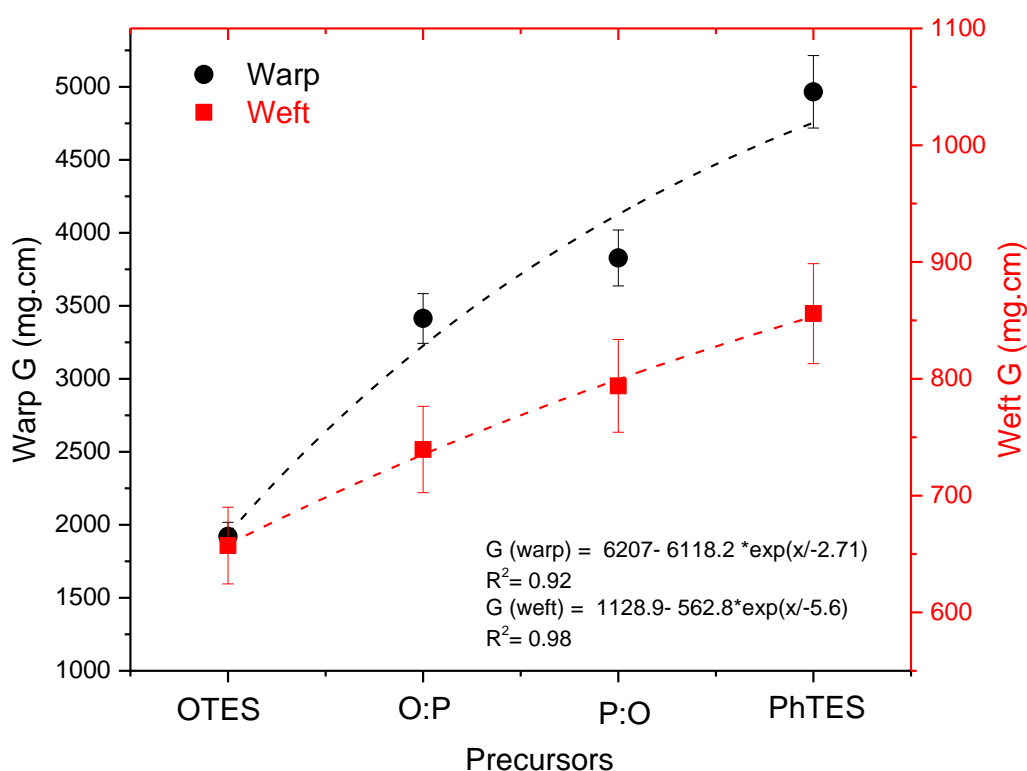


Figure 75: Flexural rigidity of sol-gel coated fabric (MPP-2.5 wt.%).

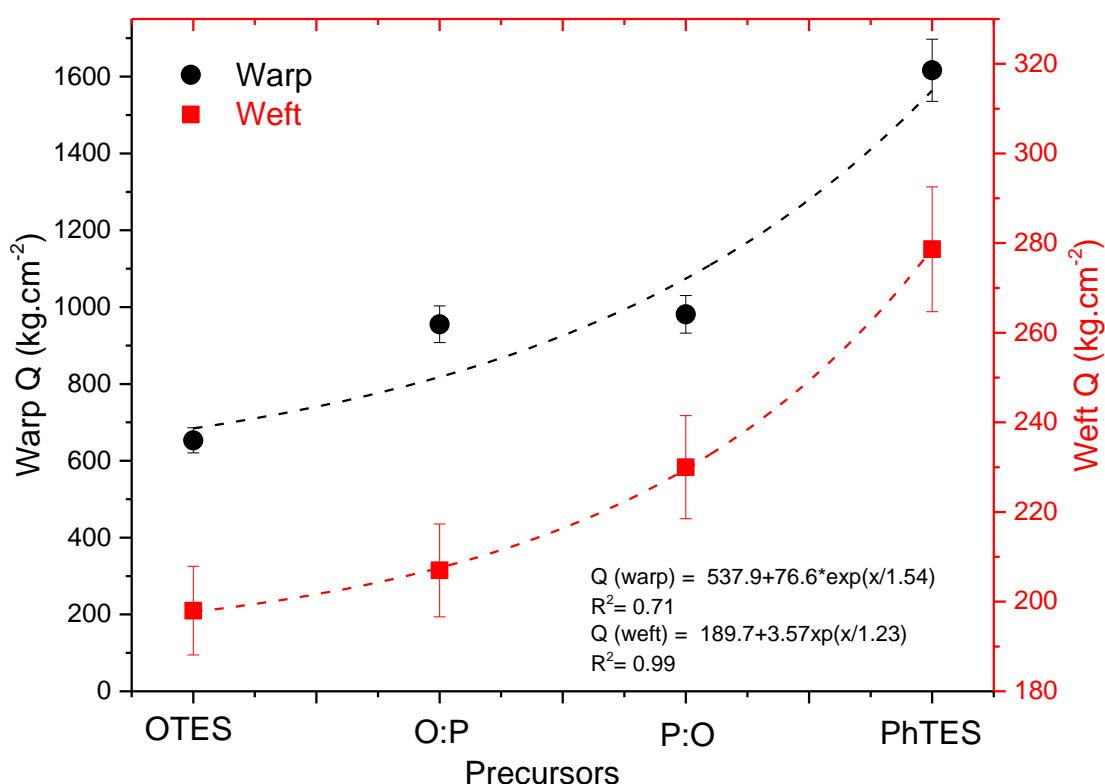


Figure 76: Bending modulus of sol-gel coated fabric (MPP-2.5 wt.%).

4.3.6 Surface morphological analysis on sol-gel coated fabric

The surface of coated and uncoated PET fabric samples was observed using SEM. Figure 77 shows the surface characteristics of PET fabrics with the different precursor. Uncoated PET (i.e. control sample) sample has plain surface without any deposition of chemicals. In contrast, such characteristic completely disappeared on the surface of coated PET samples. It is apparent from the micrographs that a thin film was formed on the coated fiber surface and the film thickness increases by changing the precursor, as compared to another precursor, PhTES shows higher deposition of sols and it formed like film, since phenyl groups in the sol networks and makes thick film formation this is the main reason why it changes the handle and other physical properties of coated samples. In fact, all coated fabrics (i.e. fibers) are covered with a continuous layer of sols, these layer formation on the fiber surface could be confirmed that the pigments containing sols were successfully coated on the PET fabrics.

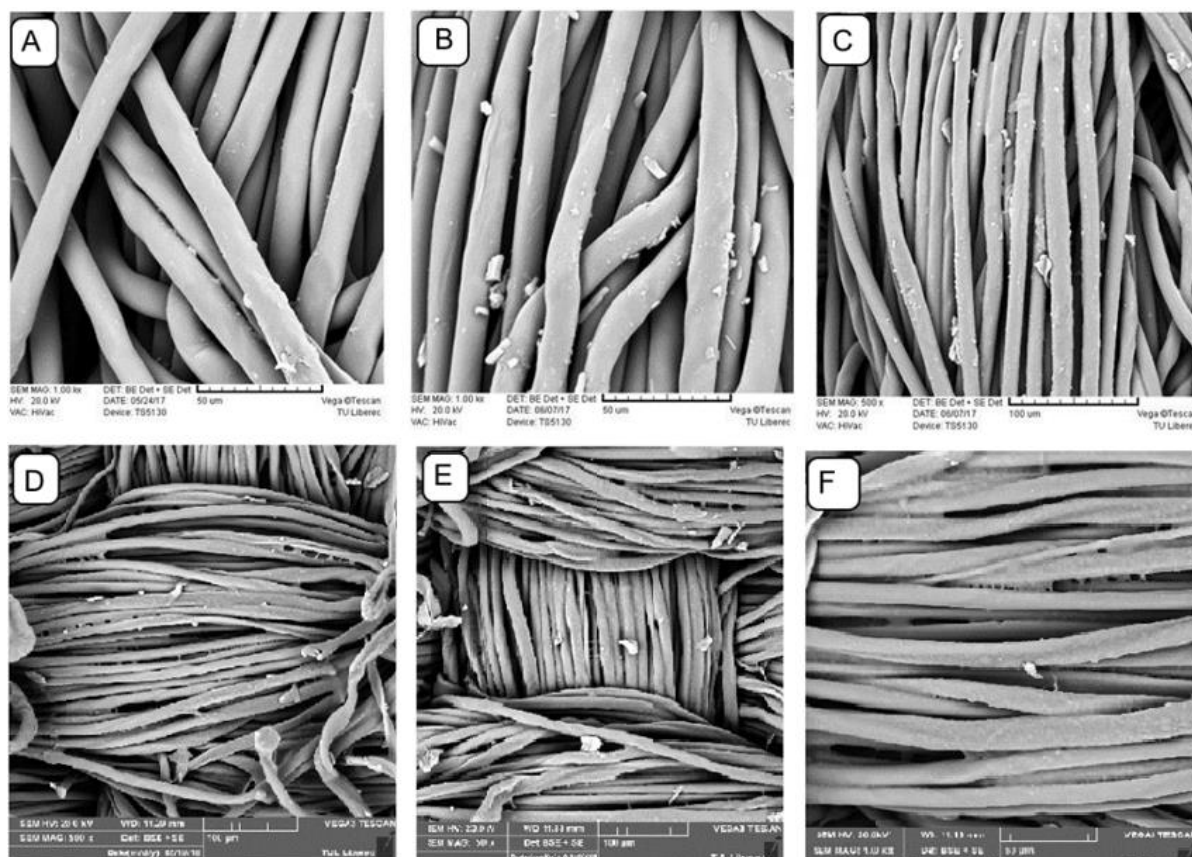


Figure 77: Surface morphological characterization of sol-gel coated fabric, (A)-control PET fabric and modified with (B) OTES; (C) O:P (2:1); (D) P:O (2:1) (E) APS and (F) PhTES precursors (MPP-2.5 wt.%).

4.3.7 Surface roughness analysis on sol-gel coated fabrics

The coated fabric shows different handle properties; consequently, it is necessary to analyze their surface characteristics. The surface roughness was analyzed by using LSCM and the various roughness data was analyzed and tabulated in Table 16. For visual scope, the LSCM images are given in Figure 78 (A-F) and it shows the surface property of fabrics before and after the sol-gel coating. These pictures and the data were confirmed that sol-gel coating made significant changes in the surface by creating the roughness. However, the images and data demonstrate that surface roughness was significantly changed and it depends on the type of precursor used, in this picture (Figure 78-F). Sols prepared with PhTES and APS containing photochromic pigment made more roughness than the sols prepared OTES alone or its combinations, which is due to the chemical groups presented in the precursor and its structure. However, OTES having the flexible long alkyl chain groups provided the significantly less roughness, although APS could not produce the roughness as like PhTES or its combinations.

Table 16 shows the roughness characteristic of the fabric before and after coating. In overall, numerical values showed there are changes in the peak height (R_p), depth valley (R_v) and the addition of both parameters (R_z). As a result, the highest numerical value indicates the more roughness, and thus significant changes in the surface roughness.

Table 16: Surface roughness characteristics of coated fabric (MPP-2.5 wt.%).

| | Max. Peak height (R_p) | | Max. Valley depth (R_v) | | Max. Depth (R_z) $R_z=R_p+R_v$ | |
|-------|----------------------------|--------------|-----------------------------|--------------|---------------------------------------|--------------|
| | R_p (μm) | CV_{R_p} % | R_v (μm) | CV_{R_v} % | R_z (μm) | CV_{R_z} % |
| Raw | 1.756 | 92.0 | 4.082 | 104.8 | 05.838 | 46.1 |
| OTES | 2.080 | 44.9 | 4.690 | 73.3 | 06.769 | 73.7 |
| O:P | 3.811 | 29.2 | 4.935 | 25.8 | 08.746 | 48.7 |
| P:O | 5.825 | 18.1 | 6.413 | 88.4 | 12.238 | 54.0 |
| APS | 4.080 | 88.4 | 4.830 | 55.6 | 08.909 | 41.4 |
| PhTES | 9.292 | 100.0 | 6.378 | 84.2 | 15.670 | 100.5 |

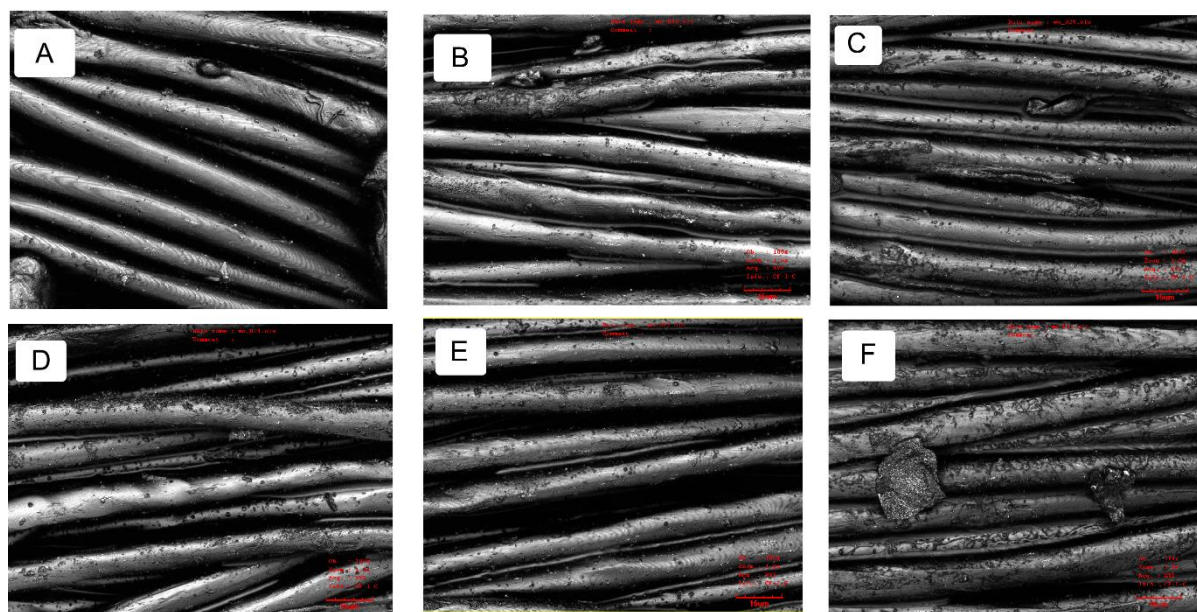


Figure 78: LSCM images photochromic fabrics with (A) control PET fabric and modified with (B) OTES; (C) O:P (2:1); (D) P:O (2:1) (E) APS and (F) PhTES precursors (MPP-2.5 wt.%).

4.4 Conclusion

This chapter described the production of photochromic fabric through the sol-gel coating. There are some issues faced during the manufacturing and the optimize the process to produce the final products. Also, the various properties which have been measured for the produced PET fabrics. At last, it discusses the various optical, physical and handling properties of produced fabric could be discussed with their obtained results, the detailed conclusion of this chapter has been given in section 6.2.

Chapter-5 COMPARISON RESULTS OF BOTH THE TECHNIQUES

5.1 Kinetics response of photochromic change on a different substrate

The photochromic pigment was incorporated on two different substrates with different techniques which they are the mass coloration of miPP filaments and sol-gel coating on PET fabrics. To get a better idea of the application technology, it is required to compare both in terms of optical characteristics, which gives an immense idea regarding the techniques involved and the type of substrate. Figure 79 describes the K/S (max) for the mass colored miPP filaments and sol-gel coated PET fabrics with respect to their relative concentrations, in this case, the same concentrations of pigment (i.e. MPP-2.5 wt.%) was used.

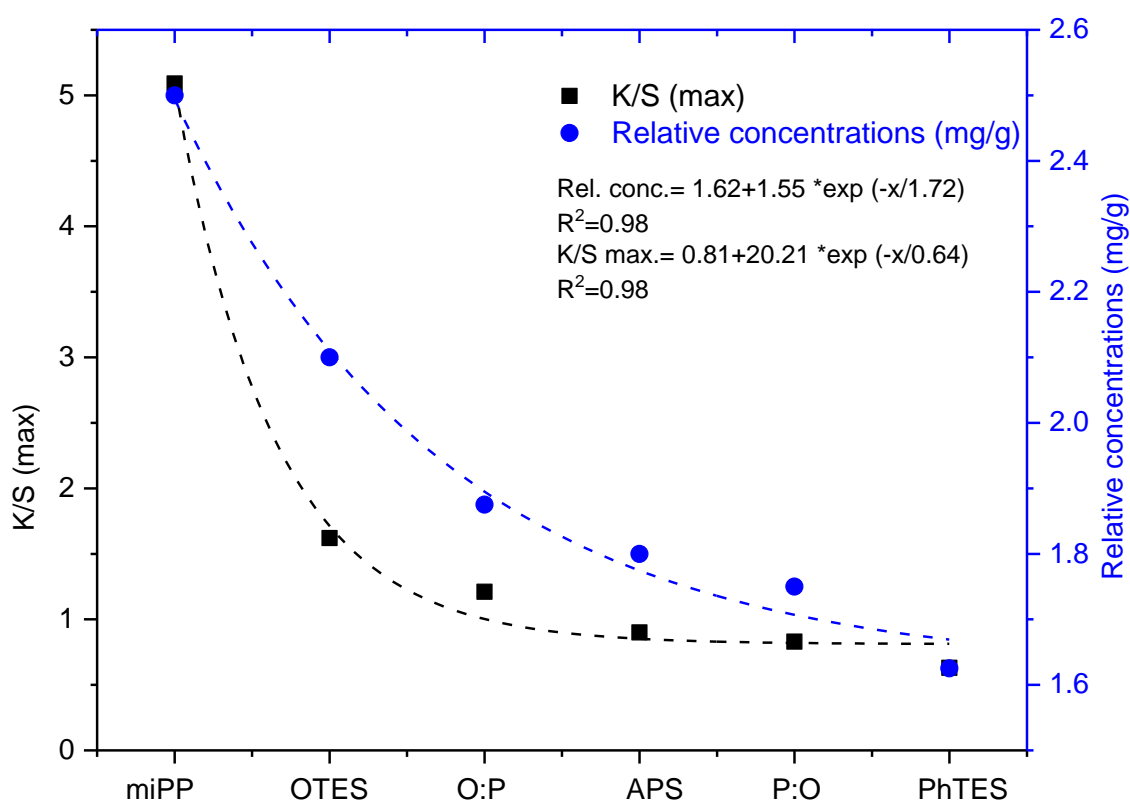


Figure 79: K/S (max) of photochromic textiles with different technique with respect to their relative concentrations.

Figure 79 shows the comparison results of photochromic textiles, among two different techniques, mass colorations produced a highest photochromic response via K/S max functions. However, the concentrations of pigment are same, perhaps the relative concentrations might

be varied with respect to the uptake % on the sol-gel coated fabrics, this is purely depends on the precursors, which used during the sol-gel preparations. Among the different precursor, the PhTES provided the lowest uptake%, the reason might be the viscosity of sol, which reduce the uptake% during the dip coating. So, the respective coated fabric has considerably lowest available pigments per mass, which compared to the coated fabric with highest uptake%. Apart from these facts, there are some other reasons which is in the mass coloration, the pigments are mixed with the molten polymer solution, whereas in the sol-gel coating it just applied on the surface, secondly, the medium of the substrate is different in terms of their optical properties.

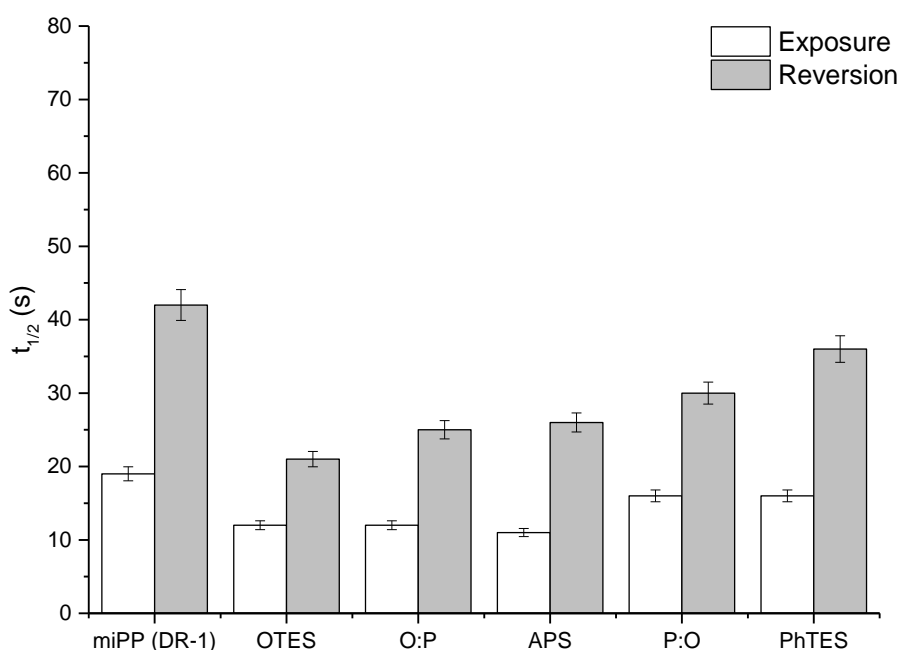


Figure 80: Half-life of color change photochromic textiles (i.e. MPP-2.5 wt.%).

Figure 80 shows the half-life of color change for the MPP incorporated textiles and results of the rate constant of various photochromic textiles have been demonstrated in the Figure 81, the rate constant of sol-gel coated fabrics varies with respect to the precursors. Obviously, it is due to their size of the structure, size of the pore, which is directly proportional to the photochromic response, rate constant is one among it, however, miPP filament has slow rate than the sol-gel coated fabric, the observed trend is same for both exposure and reversion phase. The predicted reason could be, the sol-gel coating can provide the thin layer on the surface of PET fabric along with the photochromic pigments, which is nothing but, the fabric has the photochromic pigments only on its surface, whereas the mass coloration provides the good penetration of the colors along with the polymeric structure. Therefore, the miPP filaments required more time to undergo the molecular collision, which directly influenced on the lower speed of reaction (i.e.

low rate constant) compared to the sol-gel coated fabrics. Among the sol-gel coated fabric, precursors like APS and OTES shows the highest rate than other fabrics.

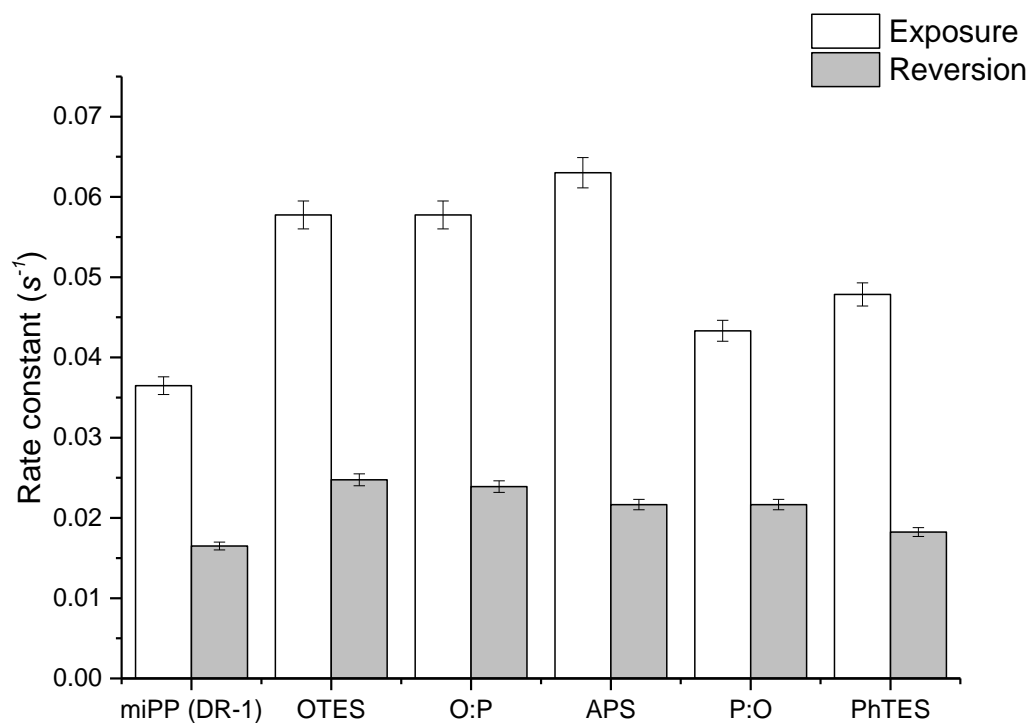


Figure 81: Rate constant of photochromic textiles (i.e. MPP-2.5 wt.%).

Chapter-6 CONCLUSION

The main aim of this chapter to conclude based on the results and its discussion of this work. The first part conclusion is the effects of drawing ratio on the optical, mechanical and physical properties of produced photochromic miPP filaments. The second part of conclusion is deals with the influence of precursor and its combination on the optical and physical properties of photochromic fabrics.

6.1 Photochromic miPP filaments

On the basis of this research, it was observed that Kubelka-Munk functions are purely depending on the drawing ratios of produced photochromic miPP filaments, it is confirmed through the K/S values, that decreased with increasing the fineness of filaments. Also, the color buildup was varied with respect to the pigment types, filaments with MPY 220% less K/S (max) values than filament with MPP even in the same concentration, it is due to the thermal degradations of pigment during the melt extrusion also MPY pigment forms two transoid isomers of the quinoid forms during the isomerization (i.e. it can be confirmed through the literature), which are the primary reason for the reduction of color build-up of MPY incorporated miPP filaments. Generally, the stabilization causes the measured errors in the exposure phase shows higher than the reversion phase, which means that the error from reversion phase is invisible, this is due to the higher variability in exposure phase and lower variability in reversion phase. The K/S (max) values for MPP incorporated miPP filaments with different cross-sectional, 8-star and 5-star cross-sectional filaments shows 63% and 72% less K/S values than the circular cross-sections respectively. The results trend is similar to all other pigments. So, it evidenced that the shape of cross-sections plays a vital role in the optical properties of produced miPP filaments. During the measurement, reflected light always depends on the angle of incidence, which could be modified by the substrate and its properties. Circular cross-sectional filaments typically generate the more specular reflection, on other hand, the surface reflection increased for the filament containing quadrilobe cross-section. The ΔOD values have been reduced with increasing the drawing ratio, it has the non-linear relationship between the drawing ratios of produced filaments. The color difference of photochromic filaments under the exposure phase was analyzed through residual ΔE^* values, from the results it concludes that the maximum residual ΔE^* values was observed ~ 2.5 units

and minimum was ~ 0.02 units. The residual ΔE^* values are decreased with increasing the drawing ratios, which confirms that lowest drawing ratio has highest residual ΔE^* values. These ΔE^* values are a significantly nonlinear relationship with respect to the concentration of pigment as well as to the drawing ratio. The residual ΔE^* values are marginally increased with increasing the concentration of pigment, it can be observed for all three pigments, this is due to the structural modifications of the pigment under the exposure phase, there are some possibilities to form some side product, which may react thermally or photochemically to form short-lived isomers (Q and U) between the singlet energy state (A^{SES}) or triplet energy state (A^{TES}) to colored isomer (B), these are all the important fact behind the higher ΔE^* values of these pigment incorporated filaments. The prime intends to determine the residual ΔE^* values can help to find the color difference, since the human vision can able to identify the color difference, if the residual ΔE^* is more than 0.4 units. Therefore, lowest drawing ratio has highest color difference, which can be easily visible by human vision. During the exposure, the color build-up was significantly increased with respect to the time, it required 30s to reach the maximum value of K/S (i.e. 6.27 ± 0.2 at 2.50 wt.% of MPP), thereafter the systems gets saturated with minor stabilization, in this position called photostationary state or photostationary equilibrium, this trend was observed in all the concentration as well as drawing ratios of the particular pigment. In case of reversion phase, it requires 128s required to reduce the maximum color build-up to a minimum it can be identified by K/S values. The observed trend is same for another pigment, only time requirement is different. Therefore, the positive acceleration of K/S values under UV exposure required less time than the negative acceleration of K/S under reversion phase, it is due to the structure of photochromic pigments which having the higher half-life. For all colored filaments, in the concentration of 0.25 wt.%, results of the half-life of color change during the exposure phase shows 34s, 24s, 15s for MPP, MPB and MPY respectively. So, it confirmed that the filament with the pigment MPY shows faster reaction which is nothing but shorted half-life as compared to other pigments. Overall the results conclude that the half-life of color change for all three pigments in both exposure and reversion phase in the order of $MPP > MPB > MPY$. The linear density has been determined and it reduced with respect to the drawing ratios, whereas $45.3 \pm 0.3 \text{ tex}$ for the drawing ratio of 1, and when the drawing ratio is 4, the linear density can be $14.2 \pm 0.17 \text{ tex}$, however, it is expected and the observed trend is exponential. Addition of pigment reduces the linear density of filaments by 24% from 0 wt.% to 2.5 wt.%. The tenacity of colored filaments was analyzed, results of tensile strength are increased with increasing the drawing ratio, whereas the tensile strength of $10.51 \text{ cN.tex}^{-1}$ for the drawing ratio of one, and when the drawing ratio is four, the

tensile strength of $31.94 \text{ cN.tex}^{-1}$. Meanwhile, the addition of pigment has been reduced 28 % for the colored filaments from 0.25 wt.% to 2.50 wt.% of the concentration, it is due to the changes in the melt viscosity caused by the addition of the pigment during the melting. The mechanical properties of colored filament have been reduced by addition of the pigment. Results confirms that significant improvement in Young's modulus, it was increased 65% from drawing ratio 1 to 4, nevertheless, it is due to the molecular arrangements and followed by the variation in the crystalline region of the filament. Results confirms that the elongation at break was reduced from 260.3% to 39.9% when the drawing ratio was increased from 1 to 4, which confirms there is a reduction of 84%. The reason is, when the filaments to pull down in to the tensile direction causes to stretch the amorphous molecules. In case of thermogravimetric analysis, it concluded that all the pigments started degradation at 120 to 140°C, however this is due to the HALS and other residual additives, thereafter it sustains for higher temperature and start complete degradation, for MPY pigments degrade significantly higher during heating and degrade 40% of weight loss by 270°C, whereas MPB and MPP is much better and degrade 25% weight loss at 310°C and 2% weight loss at 320°C respectively. The colored filaments were analyzed DSC to find out the structural modifications, the drawing ratio has a strong influence on the melting enthalpy, melting temperature which was increase with increasing the drawing ratios. The changing of melting enthalpy is increased with increasing the drawing ratio, from 56.16 to 84.20 J.g^{-1} for drawing ratio 1 and 4 respectively (i.e. without pigmentation), this is due to the thermal demonstration of the components during the crystallization of the polymer which may create the supermolecular structure of the miPP filament. The crystallinity of photochromic miPP filaments were increased with increasing the drawing ratio, therefore, the higher rate of crystallization makes many modifications in the filament, mainly the α , β modification of morphological structure (see Table 5 to Table 7), pigment concentration on crystallinity can be changed 13% on the drawing ratio of one, in case of drawing ratio four does show much influence, however, this effects purely depend on the drawing ratio and not on the pigment concentration. Addition of pigment shows that there no much influence on the melting temperature of the filaments, however, it varies the changing in enthalpy as well as the crystallinity%. SEM characterization was done, the longitudinal views of produced photo-chromic miPP filaments, the colored and uncolored filaments look similar with a smooth surface, which means that there is no significant influence on the pigments with its distribution of filaments on surface characteristics. In case of different shape of the filament, there is a smooth surface on the triangular and 5-star shape, whereas in 8-star contains some microfibers which leads to generating the fibrillation on the surface, however, there is no

significant relationship with the pigment concentration with respect to these effects, it purely depends on the shape of cross-sectional. The cross-sectional views of filament show, circular and triangular shape cross-sections having no impact of addition of pigments, in case of 5-star shape there are some effects, some of the filaments never drawn, based on the size of other filaments in this group, which means that some filaments are bigger than other filaments in the same groups. However, there is no influence on the pigment for these effects. The reason may be slippage during the drawing process which leads to the particular filament to not drawn as per the respected drawing ratio, this effects only occur in the 5-star shape and not in the 8-star shape.

6.2 Photochromic PET fabric

In this work, successfully deposited the photochromic pigments to the PET fabric through a sol-gel coating. Silica sols were prepared by different precursors and applied with different concentration of photochromic pigments. The color build-up results conclude that the same concentration of pigment derived from different K/S values and it depends on the type of precursor. Therefore, K/S values are purely depending on the type of precursor used during the sol-gel coating process. From the observed results, the precursor having the strongest influence the photochromic pigment and their optical properties. Among the different precursor, OTES and its combination produce higher photochromic response than sol prepared from APS & PhTES alone or its combinations, even though at the same concentration of photochromic pigment. Apart from this, K/S (max) and ΔOD values are significantly increased with increasing the concentration of pigment. Therefore, K/S (max) and ΔOD are depending on the concentration of photochromic pigment, of course, it is a well-known effect. On other hand, K/S (max) and ΔOD is purely depended on the precursor and its combinations, since precursor has strongly influenced on the color strength values and followed by changes in the optical density. In terms of color difference, the fabric coated with PhTES shows lowest ΔE^* values it can be seen in all the concentration. On other hand APS based precursor shows moderate (~ 1 units at maximum concentration). The fact behind these results, precursor having the strong influence, since PhTES has shown lower ΔE^* values, since it has the rigid structure, which could not allow the photochromic pigments to undergo isomerization reaction, on the contrary, it shows very less uptake % during the coating. The silica network derives the effect of sol-gel coated fabric on the optical response speed (coloration and decoloration, half-life, etc.) and physical properties, the structure of precursor determines the morphology of the coated

materials. Therefore, the chemical structure of precursor, size & shape of silica network and available free space in the pore of sol network are the important parameters which influence on the optical properties of the photochromic pigment. OTES based precursor provide higher photochromic response, since it contains long flexible chains which creates more pore space along with flexible silica network, therefore it allows the photochromic pigment to undergo isomerization reactions without any interference, also the OTES based precursors, obtained pores are surrounded by flexible octyl chains, due to the presence of long alkyl aliphatic chain, since the phenyl groups are rigid in nature, phenyl groups in PhTES lead to a more rigid pore shell. Also, OTES has less steric hindrance effect on the pigments, therefore, this structural arrangement allows the pigment to undergo the photochromic reaction easily. In other words, the octyl groups produce a more flexible network with the higher surface area than other silanes, which also ensure the smaller spherical particles with more uniform distributions. The half-life of color change of sol-gel coated PET fabric was analyzed, photochromic fabric coated with PhTES shows 26s when the concentration of pigment is 0.25 wt%, whereas it reduced to 16s at the concentration of 2.5 wt.%. In case of OTES provides the 23s at lowest and 10s at highest concentration of pigments, on other hand, APS provides 22s at lowest 14s at highest concentration, in the combination O:P (i.e. 2:1 molar ratio) has lowest half-life of color change than the combination of P:O (i.e. 2:1 molar ratio). In this work, different types of precursors used for the sol-gel coating, the interesting behaviors of hypsochromic shift of ~40nm was observed (absorption maxima are shifted from 610nm to 570nm), when the fabric is coated with OTES/PhTES or its combinations with 5-chloro-1,3,3-trimethylspiro[indoline-2,3'-(3H)naphtho(2,1-b) (1,4)-oxazine] shows Blue colored merocyanine under the UV radiations, in case of APS coated photochromic fabric shows the original color (i.e. Purple), it can be visible in the reflectance spectrum which is shown in Figure 82. Since the phenyl and octyl groups made decreasing the polarity of the respective precursors. This is due to the lowering the polarity of functional groups of phenyl and octyl attached to the surface of large organic chains might hindering the influence of OH groups in the pore surface. So, the photochromic fabric with OTES/PhTES precursors is turns to Blue color instead of its original color (i.e. Purple) under the UV radiations. The reflectance spectrum of both precursors is given in Figure 71 and the produced fabric under UV radiations are given in Figure 60-(A&B). Chemically the OTES/PhTES containing the methoxy groups which generally the electron donating in nature which are another reason for the hypsochromic shift of coated fabric from 610nm to 570nm.

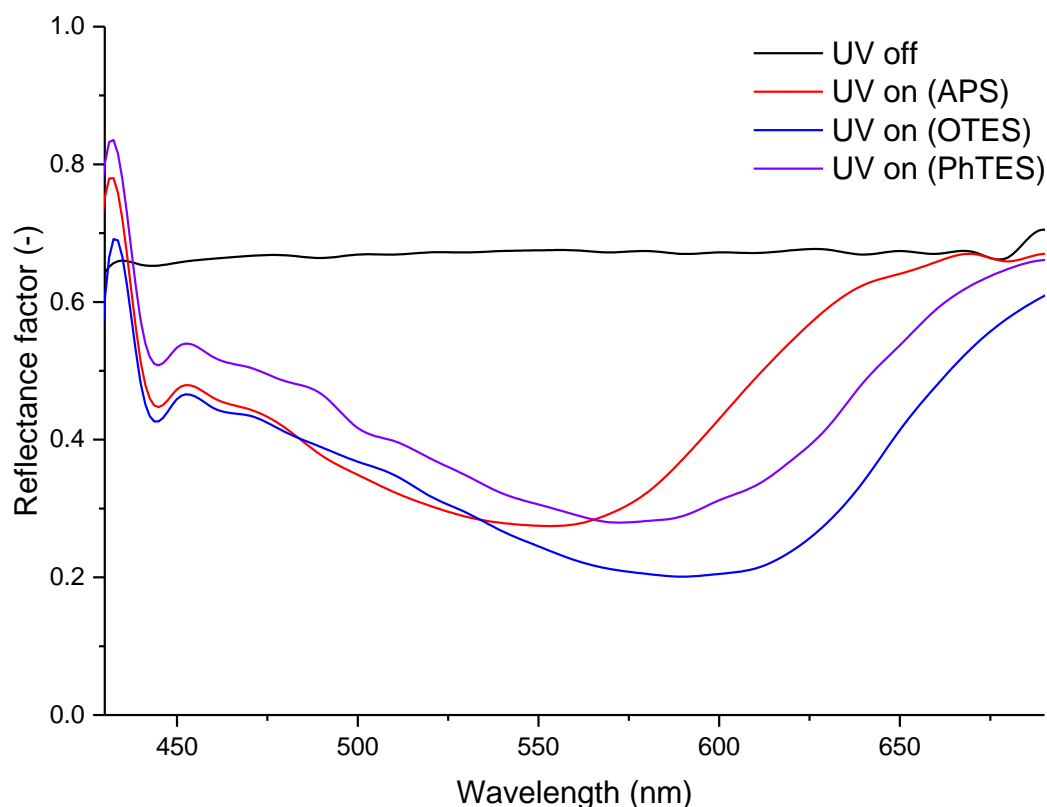


Figure 82: Reflectance spectra of MPP coated fabric with different precursors.

The durability of abrasion of the silica incorporated photochromic response has been reduced 17% at 1000 cycles for precursor with OTES, even though in same abrading level PhTES decreased 28%. The combination of Octyl and Phenyl in 2:1 molar ratio provides 20% and the combination of Octyl and Phenyl in 1:2 molar ratio provides 26% color loss at 1000 abrasion cycles, APS alone shows 24% color loss in the photochromic response. In case of PhTES based coating reduce the color loss % from 12%, 16%, 21%, 26%, 28% for the abrasion cycle of 100, 300, 500, 700 and 1000 respectively. In overall, the coating process reduces the abrasion durability on the photochromic response, however, the overall level of abrasion durability on photochromic response is satisfactory except PhTES and its combination where PhTES is more concentrated. The results of the color loss % on the abrasion cycles (in all level) were in the order of PhTES > P:O > APS > O:P > OTES. The durability of washing on the photochromic response of PET fabric has been reduced 47% precursor with OTES, which is very high color loss% on other hand the PhTES based PET fabric shows only 14% as color loss. The combination of Octyl and Phenyl in 2:1 molar ratio provides 29% color loss, in case of combination of Octyl and Phenyl in 1:2 shows the 26% color loss after specified washing

cycles. APS alone shows 18% loss in the photochromic response. In overall, the coating process reduces the photochromic response due to the washing, however, the overall level of washing durability is satisfactory except OTES and its combination. The results of the color loss % on the washing cycles were in the order of OTES>O:P>APS>P:O>PhTES. The maximum uptake was found 81% for the sol prepared with OTES, the lowest uptake was found 66% for the sol prepared with PhTES. Although in same coating conditions, PhTES and its combination absorbed lower coating solution as compared to OTES and APS, due to these facts it shows lower photochromic response and it is visualized in the color strength values and K/S (max) values. The various physical properties were analyzed, in case of thickness, there is a significant influence on the precursors. The increased stiffness of coated fabric was observed by APS, PhTES and combination. OTES is the only treatment which did not cause a significant increase in the flexural rigidity and bending modulus. A higher flexural rigidity and bending modulus in the warp direction compared uncoated fabric by all the treatments, while this trend was observed for all coatings in the weft directions too. Since, OTES has the long aliphatic chain which ensures the softness of fabric without affecting the fabric bending and flexural rigidity. The most rigid fabric was observed higher when the fabric was coated with PhTES and APS coated fabric. SEM characterization shows the surface characteristics of PET fabrics with different precursor. Uncoated PET (i.e. control sample) sample has plain surface without any deposition of chemicals. In contrast, such characteristic completely disappeared on the surface of coated PET samples. It is apparent from the micrographs that a thin film was formed on the coated fiber surface and the film thickness increases by changing the precursor, as compared to other precursor, PhTES shows higher deposition of sols and it formed like film, since phenyl groups in the sol networks and makes thick film formation this is the main reason why it changes the handle and other physical properties of coated samples. In fact, all coated fabrics (i.e. fibers) are covered with a continuous layer of sols, these layer formation on the fiber surface could be confirmed that the pigments containing sols were successfully coated on the PET fabrics. Surface roughness on the LSCM pictures and the data were confirmed that sol-gel coating made significant changes in the surface by creating the roughness. However, the images and data demonstrate that surface roughness was significantly changed and it depends on the type of precursor used, sols prepared with PhTES/APS made more roughness than the sols prepared OTES alone or its combinations, which is due to the chemical groups presented in the precursor and its structure. Advantages of sol-gel coating technique are, very simple process which does not required the special machine, can control the thickness of the coating, since it will not affect the fabric physical properties as like traditional printing on the

fabric due to the effect of binder, apart from this it produce the better durability than the printed process. On other-hand, it has a drawback like, the precursors are strongly influenced on the photochromic response and change the absorption spectrum. The comparison results of photochromic textiles show for two different techniques, mass colorations produced highest photochromic response than sol-gel coating. Overall the sol-gel coated fabric shows a lowest photochromic response in the all the case, also, the photochromic response is purely depending on the precursor types. Generally, in mass coloration, the pigments are mixed with the molten polymer solution, whereas in the sol-gel coating it just applied on the surface, secondly, the medium of the substrate is different in terms of their optical properties. The rate constant for photochromic miPP show less than the sol-gel coated fabrics, also the rate constant of sol-gel coated fabrics varies with respect to the precursors. Obviously, it is due to their size of the structure, size of the pore, which is directly proportional to the photochromic response, rate constant is one among it.

6.3 Suggestion for future work

Based on the results of research in this thesis, it can be extended further in various directions which aiming to apply the photochromic pigment into different textile materials with respect to the different techniques and on the basis of method investigated it is extended to a number of final uses, as given in the examples below.

As a synthetic fiber for textile and clothing's, polyethylene terephthalate having more advantages like more durable, dimension stability, easy to blend with other fibers, possible to modify according to the needs, therefore the future work could be preparing the mass colored polyethylene terephthalate. In these regards, photochromic pigment should have higher thermal degradation than the pigments which used in this work, it could be possible by changing the functional groups in the chemical structure, so that, it can withstand the temperature. As a regenerated cellulosic fiber Lyocell™ having many advantages than the conventional cotton fiber, which are more water absorbency, good wet strength, good dimensional stability and most important is sustainable fiber, so this research should extend to produce the mass colored Lyocell™ fibers via modified solvent spinning techniques. The new method for production of these fibers/ filaments may have the potential to replace the conventional method of colorations. However, a detailed investigation and optimization of this method would be required to evaluate the possibility to produce the photochromic polyethylene terephthalate and Lyocell™ fibers via mass coloration techniques. On other hand, the sol-gel coating techniques should extend with other textile fibers like cotton, Lyocell and polyamide etc., which can give an idea how these substrates can different than the polyethylene terephthalate fabric which has been produced in this work. In case hypsochromic effects, more combinations of precursors with different proportion has to use, therefore these proportion given an idea that how it influences to change the absorption spectra. In case of fabric optical and physical properties, the deep study is required to add some of the organic groups during the sol-gel synthesis, which help to make more flexible to the sol-gel network, as a result, shows good photochromic response and improved fabric handle properties than this work. Apart from this, required to extend this work to study on the viscosity, which plays a vital role in the sol-gel networks in terms of flexible or rigid. It could be good for application of electrochromic, thermochromic and photochromic pigment together, which stimulate the color via all these (light, temperature and electrical) stimuli, which can be some notable effects on the application point view. Hope such fabric has more demand through the various industry, fashion is one among them,

Chapter-7 NEW FINDINGS OF THE RESEARCH

On the basis of this research it was observed that, Kubelka-Munk functions are purely depending on the drawing ratios of produced photochromic miPP filaments, it is confirmed through the K/S values, that decreased with increasing the drawing ratio. The K/S (max) values for MPP incorporated miPP filaments with different cross-sectional, 8-star and 5-star cross-sectional filaments shows 63% and 72% less K/S values than the circular cross-sections respectively. The results trend is similar to all other pigments. So, it evidenced that the shape of cross-sections plays a vital role in the optical properties of produced miPP filaments. The K/S (max) and ΔOD values have been reduced with increasing the drawing ratio, it has the non-linear relationship between the drawing ratios of produced filaments. The residual ΔE^* values were observed to be maximum at ~ 2.5 units and minimum at ~ 0.02 units. With increase in drawing ratios, the residual ΔE^* values decrease and confirming that the drawing ratio which is lowest has highest residual ΔE^* values. With respect to the concentration of pigment and the drawing ratio the ΔE^* values significantly have nonlinear relationship. It is observed in all the three pigments that the residual ΔE^* values are marginally increased with increase in the concentration of pigment. In order to find the color difference, the prime intends to determine the residual ΔE^* values as the vision of humans able to identify the color difference due to the residual ΔE^* is more than 0.4 units. Henceforth, the drawing ratio which is lowest have the color difference to be highest can be easily visible by human vision. During the exposure, the color build-up was significantly increased with respect to the time, later on systems gets saturated with minor stabilization, this trend was observed in all the concentration as well as drawing ratios of the particular pigment. In case of reversion phase, significantly decreased with respect to the time. The observed trend is same for other pigment, only time requirement is different. Therefore, the positive acceleration of K/S values under UV exposure required less time than the negative acceleration of K/S under reversion phase. Generally, the stabilization causes the measured errors in the exposure phase shows higher than the reversion phase, which means that the error from reversion phase is invisible, this is due to the higher variability in exposure phase and lower variability in reversion phase. The half-life of color change for all three pigments in both exposure and reversion phase in the order of MPP>MPB>MPY. Due to the thermal degradations of pigment during the melt extrusion, with respect to pigment types the color build-up varies as then filaments with MPY 220% less K/S (max) values than filament with MPP even in the same concentration and also MPY pigment forms two transoid isomers

of the quinoid forms during the isomerization which are the essential motive for the reduction of color build-up of MPY incorporated miPP filament. In case of thermogravimetric analysis, based on the chemical structure of the pigment, the degradation % is varied and it directly influenced on the dyability of the filaments. The changing of melting enthalpy is increased with increasing the drawing ratio, from 56.16 to 84.20 $J.g^{-1}$ for drawing ratio 1 and 4 respectively (i.e. without pigmentation). Addition of pigment shows that there no much influence on the melting temperature of the filaments, however, it varies the changing in enthalpy as well as the crystallinity %. With and without pigmentation, the longitudinal views of photochromic miPP filaments produced looks similar in the micrographs. Considering the different shapes of the filament, on the triangular and in 5-star there is a smooth surface and as in 8-star, it contains some microfibers leading to generating the fibrillation on the surface. With the study of the cross-sectional view of the filament it is observed in case of 5-star shape there are some effects, some of the filaments never drawn, based on the size of other filaments in this group comparatively some filaments are larger than other filaments in the same groups.

Depending on the types of precursor the same concentration of pigment derives different K/S values. Henceforth, depending on the usage of the type of precursor the K/S values are pure which is used in the sol-gel coating process. As of the observance of the results, the photochromic pigment and their optical properties are strongly influenced by the precursor. Compared to the sol prepared from APS & PhTES alone or its combinations, OTES and its combination produce higher photochromic response even though at the same concentration of photochromic pigment. With the increase in the concentration of pigment, K/S (max) and ΔOD values are significantly increasing apart from them. As it is well known that the K/S (max) and ΔOD depends on the concentration of photochromic pigment. On other hand, K/S (max) and ΔOD is purely depending on the precursor and its combinations, due to the strong influence of precursor on the color strength values and followed by changes in the optical density. Due to the strong influence of the results, the color difference and half-life for color change of the coated fabrics depends on the precursors. The higher photochromic response is provided by the OTES based precursor based on the long flexible chains creating more pore space along with flexible silica network. Henceforth the photochromic pigment to undergo isomerization reactions without any interference is allowed by it and also flexible octal chains surround the pores obtained by the OTES based precursors. Phenyl groups in PhTES lead to a more rigid pore shell due to the presence of long alkyl aliphatic chain and due to the phenyl groups are rigid in nature. In this work, the hypsochromic shift of ~40nm was observed (absorption

maxima are shifted from 610nm to 570nm), when the fabric is coated with OTES/PhTES or its combinations with 5-chloro-1,3,3-trimethylspiro[indoline-2,3'-(3H) naphtho(2,1-b) (1,4)-oxazine], in case of APS coated photochromic fabric shows the original color. So, the coated fabric is under UV radiations, it turns to Blue color instead of its original color (i.e. Purple). From this result it is confirmed that the spectral and kinetic properties of sol-gel coated fabrics are purely affected by the polarity and the functional groups of precursors, which means, it affects the absorption spectrum of the colored form of merocyanine. With respect to the abrasion resistance and washing durability, the photochromic response was analyzed and the results depend on the precursors. By analyzing various physical properties in the case of thickness on the precursors there is a significant influence. APS PhTES and combination observed the increased stiffness of coated fabric. In the flexural rigidity and bending modulus, the treatment which does not cause a significant increase is OTES. With the different precursor surface morphology of PET fabrics is shown by the SEM characterization. Without the deposition of chemicals, the uncoated PET sample has a plain surface. On the contrary, on the surface of the coated PET samples, such characteristic completely gets disappeared. By creating the rough surface sol-gel coating made significant changes is confirmed by the LSCM pictures. It is shown that for the two different techniques of compared results of photochromic textiles, mass colorations produce the highest photochromic response than that of sol-gel coating. On the whole, in every case the sol-gel coated fabric shows lowest photochromic response and also the photochromic response depends on the precursor types purely. In general, the pigments are mixed with molten polymer solution in mass coloration, whereas in the sol-gel coating it just applied on the surface. the medium of substrate is different because of their optical properties. Comparatively, the rate constant for photochromic miPP show is less than the sol-gel coated fabrics and with respect to the precursors the rate constant of sol-gel coated fabrics varies. Evidently, it is directly proportional to the photochromic response due to their size of the structure, size of the pore at the rate constant which is one among them.

Chapter-8

8.1 Appendix

Appendix- A: Kinetic parameters of photochromic miPP filaments with respect to the first order kinetics (DR-drawing ratio).

| Photochromic pigment: MPP | | | | | | | | | |
|---------------------------|-----|----------------|------------|--------------|---------------|-----------------|------------|--------------|---------------|
| Pigment concentration | DR | Exposure phase | | | | Reversion phase | | | |
| | | I_0 | I_∞ | $k (s^{-1})$ | $t_{1/2E}(s)$ | I_0 | I_∞ | $k (s^{-1})$ | $t_{1/2R}(s)$ |
| 0.25 wt.% | 1.0 | 0.271 | 0.786 | 0.02166 | 32 | 0.850 | 0.446 | 0.01005 | 69 |
| | 2.0 | 0.233 | 0.495 | 0.02039 | 34 | 0.533 | 0.179 | 0.00976 | 71 |
| | 2.5 | 0.259 | 0.550 | 0.01824 | 38 | 0.597 | 0.223 | 0.00924 | 75 |
| | 3.0 | 0.227 | 0.469 | 0.01873 | 37 | 0.537 | 0.181 | 0.00900 | 77 |
| | 3.5 | 0.226 | 0.509 | 0.01777 | 39 | 0.537 | 0.182 | 0.00900 | 77 |
| | 4.0 | 0.207 | 0.401 | 0.01733 | 40 | 0.429 | 0.161 | 0.00889 | 78 |
| 0.50 wt.% | 1.0 | 0.387 | 1.216 | 0.02476 | 28 | 1.320 | 0.241 | 0.01284 | 54 |
| | 2.0 | 0.527 | 0.850 | 0.02310 | 30 | 0.871 | 0.185 | 0.01118 | 62 |
| | 2.5 | 0.339 | 0.830 | 0.02236 | 31 | 0.872 | 0.253 | 0.01100 | 63 |
| | 3.0 | 0.284 | 0.711 | 0.02100 | 33 | 0.758 | 0.198 | 0.01083 | 64 |
| | 3.5 | 0.289 | 0.700 | 0.02039 | 34 | 0.767 | 0.193 | 0.01035 | 67 |
| 1.50 wt.% | 1.0 | 0.755 | 3.075 | 0.02773 | 25 | 3.210 | 0.479 | 0.01475 | 47 |
| | 2.0 | 0.684 | 2.131 | 0.02476 | 28 | 2.200 | 0.387 | 0.01284 | 54 |
| | 2.5 | 0.584 | 2.039 | 0.02390 | 29 | 2.150 | 0.360 | 0.01195 | 58 |
| | 3.0 | 0.568 | 1.873 | 0.02310 | 30 | 1.959 | 0.362 | 0.01136 | 61 |
| | 3.2 | 0.491 | 1.629 | 0.02166 | 32 | 1.682 | 0.316 | 0.01155 | 60 |
| 2.50 wt.% | 1.0 | 0.511 | 3.582 | 0.03648 | 19 | 3.441 | 0.201 | 0.01650 | 42 |
| | 2.0 | 0.762 | 3.741 | 0.03301 | 21 | 3.442 | 0.199 | 0.01540 | 45 |
| | 2.5 | 0.971 | 3.744 | 0.03466 | 20 | 3.384 | 0.199 | 0.01575 | 44 |
| | 3.0 | 0.990 | 3.687 | 0.03151 | 22 | 3.350 | 0.200 | 0.01415 | 49 |
| | 3.2 | 0.997 | 3.794 | 0.02888 | 24 | 3.372 | 0.187 | 0.01284 | 54 |

Note: Color shade intensity at the beginning (I_0), Color shade intensity at the infinitive (I_∞), Half-life ($t_{1/2}$), Rate constant (k).

| Photochromic pigment: MPB | | | | | | | | | |
|---------------------------|-----|----------------|------------|--------------|------------------|-----------------|------------|--------------|------------------|
| Pigment concentration | DR | Exposure phase | | | | Reversion phase | | | |
| | | I_0 | I_∞ | $k (s^{-1})$ | $t_{1/2}$ (s) | I_0 | I_∞ | $k (s^{-1})$ | $t_{1/2}$ (s) |
| 0.25 wt. % | 1.0 | 0.154 | 0.613 | 0.03151 | 22 | 0.621 | 0.260 | 0.01612 | 43 |
| | 2.0 | 0.212 | 0.401 | 0.02888 | 24 | 0.374 | 0.157 | 0.01444 | 48 |
| | 2.5 | 0.202 | 0.357 | 0.02666 | 26 | 0.374 | 0.157 | 0.01308 | 53 |
| | 3.0 | 0.243 | 0.409 | 0.02567 | 27 | 0.357 | 0.157 | 0.01238 | 56 |
| | 3.5 | 0.264 | 0.404 | 0.02390 | 29 | 0.348 | 0.143 | 0.01136 | 61 |
| 0.50 wt. % | 1.0 | 0.328 | 0.969 | 0.03851 | 18 | 0.969 | 0.334 | 0.01925 | 36 |
| | 2.0 | 0.322 | 0.732 | 0.03301 | 21 | 0.756 | 0.243 | 0.01650 | 42 |
| | 2.5 | 0.298 | 0.656 | 0.03151 | 22 | 0.668 | 0.243 | 0.01507 | 46 |
| | 3.0 | 0.300 | 0.622 | 0.02888 | 24 | 0.637 | 0.254 | 0.01386 | 50 |
| | 3.5 | 0.266 | 0.553 | 0.02666 | 26 | 0.564 | 0.244 | 0.01333 | 52 |
| 1.50 wt. % | 1.0 | 0.662 | 2.373 | 0.04621 | 15 | 2.445 | 0.712 | 0.02166 | 32 |
| | 2.0 | 0.541 | 1.676 | 0.04332 | 16 | 1.719 | 0.609 | 0.02039 | 34 |
| | 2.5 | 0.565 | 1.269 | 0.03851 | 18 | 1.295 | 0.489 | 0.01824 | 38 |
| | 3.0 | 0.584 | 1.285 | 0.03466 | 20 | 1.599 | 0.470 | 0.01733 | 40 |
| | 3.2 | 0.475 | 1.361 | 0.03301 | 21 | 1.181 | 0.507 | 0.01733 | 40 |
| 2.50 wt. % | 1.0 | 0.889 | 3.106 | 0.05776 | 12 | 3.350 | 1.544 | 0.02476 | 28 |
| | 2.0 | 0.768 | 2.654 | 0.04951 | 14 | 2.731 | 0.949 | 0.02390 | 29 |
| | 2.5 | 0.740 | 2.478 | 0.04621 | 15 | 2.696 | 0.951 | 0.02166 | 32 |
| | 3.0 | 0.727 | 2.381 | 0.04332 | 16 | 2.523 | 0.890 | 0.02166 | 32 |
| | 3.2 | 0.668 | 2.080 | 0.03466 | 20 | 2.187 | 0.824 | 0.01824 | 38 |

| Photochromic pigment: MPY | | | | | | | | | |
|---------------------------|-----|----------------|------------|--------------|---------------|-----------------|------------|--------------|---------------|
| Pigment concentration | DR | Exposure phase | | | | Reversion phase | | | |
| | | I_0 | I_∞ | $k (s^{-1})$ | $t_{1/2} (s)$ | I_0 | I_∞ | $k (s^{-1})$ | $t_{1/2} (s)$ |
| 0.25 wt. % | 1.0 | 0.1451 | 0.354 | 0.05776 | 12 | 0.36 | 0.123 | 0.03301 | 21 |
| | 2.0 | 0.1330 | 0.312 | 0.04951 | 14 | 0.3161 | 0.134 | 0.03014 | 23 |
| | 2.5 | 0.1385 | 0.289 | 0.06301 | 11 | 0.2927 | 0.1326 | 0.02476 | 28 |
| | 3.0 | 0.1322 | 0.287 | 0.04621 | 15 | 0.289 | 0.1299 | 0.02166 | 32 |
| | 3.5 | 0.1200 | 0.255 | 0.04077 | 17 | 0.254 | 0.124 | 0.02166 | 32 |
| 0.50 wt. % | 1.0 | 0.2490 | 0.760 | 0.06931 | 10 | 0.7665 | 0.235 | 0.03466 | 20 |
| | 2.0 | 0.3176 | 0.579 | 0.06301 | 11 | 0.586 | 0.165 | 0.03151 | 22 |
| | 2.5 | 0.1877 | 0.535 | 0.06301 | 11 | 0.5422 | 0.189 | 0.03014 | 23 |
| | 3.0 | 0.1920 | 0.558 | 0.05332 | 13 | 0.5433 | 0.181 | 0.03151 | 22 |
| | 3.5 | 0.1677 | 0.477 | 0.04621 | 15 | 3.62 | 0.484 | 0.16600 | 27 |
| 1.50 wt. % | 1.0 | 0.3100 | 1.153 | 0.07702 | 09 | 1.171 | 0.612 | 0.03851 | 18 |
| | 2.0 | 0.2730 | 0.850 | 0.06931 | 10 | 0.869 | 0.248 | 0.03466 | 20 |
| | 2.5 | 0.2308 | 0.762 | 0.05776 | 12 | 0.768 | 0.247 | 0.03466 | 20 |
| | 3.0 | 0.2841 | 0.967 | 0.06301 | 11 | 0.97 | 0.274 | 0.02888 | 24 |
| | 3.5 | 0.2550 | 0.859 | 0.04951 | 14 | 0.871 | 0.244 | 0.02666 | 26 |
| 2.50 wt. % | 1.0 | 0.4771 | 1.567 | 0.08664 | 08 | 1.576 | 0.423 | 0.04332 | 16 |
| | 2.0 | 0.383 | 1.417 | 0.13863 | 05 | 1.438 | 0.3811 | 0.06301 | 11 |

Appendix- B: Mechanical properties of polypropylene photochromic miPP filaments (MPP)

| Drawing ratio | Concentration of MPP | T [tex] | σ [cN.tex ⁻¹] | CV _{σ} [%] | ε [%] | CV _{ε} [%] | E [N.tex ⁻¹] | CV _E [%] |
|---------------|----------------------|---------|----------------------------------|---------------------------------------|-------------------|--|--------------------------|---------------------|
| 1.0 | 0.00 wt.% | 44.7 | 10.51 | 22.1 | 260.3 | 16.6 | 0.56 | 23.2 |
| | 0.25 wt.% | 40.2 | 9.47 | 19.8 | 232.2 | 15.8 | 0.49 | 22.8 |
| | 0.50 wt.% | 36.4 | 9.64 | 21.3 | 210.1 | 17.2 | 0.57 | 24.1 |
| | 1.50 wt.% | 34.4 | 9.83 | 23.5 | 190.0 | 15.6 | 0.53 | 21.0 |
| | 2.50 wt.% | 32.5 | 8.55 | 24.0 | 173.5 | 15.1 | 0.48 | 23.2 |
| 2.0 | 0.00 wt.% | 24.6 | 22.40 | 14.8 | 185.9 | 8.9 | 0.99 | 16.5 |
| | 0.25 wt.% | 21.3 | 11.81 | 11.6 | 159.3 | 10.1 | 0.87 | 13.2 |
| | 0.50 wt.% | 18.1 | 12.03 | 12.8 | 142.5 | 12.1 | 1.02 | 14.9 |
| | 1.50 wt.% | 18.2 | 12.26 | 16.9 | 145.0 | 13.9 | 0.94 | 11.2 |
| | 2.50 wt.% | 18.4 | 10.67 | 18.1 | 132.4 | 9.6 | 0.84 | 15.6 |
| 2.5 | 0.00 wt.% | 20.0 | 22.41 | 15.2 | 140.5 | 9.9 | 1.50 | 17.9 |
| | 0.25 wt.% | 16.6 | 17.97 | 13.7 | 124.1 | 12.4 | 1.42 | 14.2 |
| | 0.50 wt.% | 13.9 | 15.50 | 19.2 | 119.5 | 10.2 | 1.50 | 16.7 |
| | 1.50 wt.% | 14.2 | 16.57 | 14.3 | 112.7 | 11.6 | 1.56 | 14.5 |
| | 2.50 wt.% | 16.1 | 13.17 | 11.2 | 86.8 | 12.3 | 1.39 | 13.9 |
| 3.0 | 0.00 wt.% | 15.4 | 28.39 | 11.8 | 97.9 | 11.9 | 1.54 | 12.1 |
| | 0.25 wt.% | 11.9 | 21.13 | 16.9 | 85.4 | 17.8 | 2.06 | 16.4 |
| | 0.50 wt.% | 10.4 | 19.44 | 13.5 | 80.4 | 13.6 | 1.93 | 13.2 |
| | 1.50 wt.% | 11.9 | 19.42 | 14.1 | 79.3 | 14.1 | 1.80 | 13.9 |
| | 2.50 wt.% | 14.8 | 19.34 | 15.6 | 71.7 | 15.2 | 1.78 | 14.9 |
| 3.2 | 1.50 wt.% | 13.2 | 19.03 | 14.9 | 56.8 | 15.1 | 1.84 | 15.0 |
| | 2.50 wt.% | 10.7 | 21.54 | 17.2 | 55.3 | 17.6 | 2.62 | 16.8 |
| 3.5 | 0.00wt.% | 14.8 | 29.34 | 17.4 | 61.3 | 17.2 | 2.27 | 17.6 |
| | 0.25 wt.% | 12.9 | 23.15 | 18.1 | 59.1 | 17.6 | 2.40 | 17.7 |
| | 0.50 wt.% | 10.2 | 27.59 | 16.7 | 54.9 | 16.5 | 2.61 | 17.1 |
| 4 | 0.00 wt.% | 14.0 | 31.94 | 18.6 | 39.9 | 18.9 | 2.60 | 17.8 |
| | 0.25 wt.% | 13.3 | 32.27 | 17.8 | 41.2 | 19.4 | 1.82 | 16.4 |

Note: Fineness (T), tenacity (σ), elongation (ε), Young's modulus (E).

| Drawing ratio | Concentration of MPB | T [tex] | σ [cN.tex ⁻¹] | CV _{σ} [%] | ε [%] | CV _{ε} [%] | E [N.tex ⁻¹] | CV _E [%] |
|---------------|----------------------|---------|----------------------------------|---------------------------------------|-------------------|--|--------------------------|---------------------|
| 1.0 | 0.00 wt.% | 45.5 | 10.36 | 22.2 | 261.8 | 16.8 | 0.582 | 22.99 |
| | 0.25 wt.% | 39.3 | 9.32 | 19.9 | 233.7 | 16.0 | 0.512 | 22.59 |
| | 0.50 wt.% | 35.7 | 9.49 | 21.4 | 211.6 | 17.4 | 0.592 | 23.89 |
| | 1.50 wt.% | 35.3 | 9.68 | 23.6 | 191.5 | 15.8 | 0.552 | 20.79 |
| | 2.50 wt.% | 34.4 | 8.40 | 24.1 | 175.0 | 15.3 | 0.502 | 22.99 |
| 2.0 | 0.00 wt.% | 24.8 | 22.25 | 14.9 | 187.4 | 9.1 | 1.012 | 16.29 |
| | 0.25 wt.% | 21.5 | 11.66 | 11.7 | 160.8 | 10.3 | 0.892 | 12.99 |
| | 0.50 wt.% | 18.3 | 11.88 | 12.9 | 144.0 | 12.3 | 1.042 | 14.69 |
| | 1.50 wt.% | 18.4 | 12.11 | 17.0 | 146.5 | 14.1 | 0.962 | 10.99 |
| | 2.50 wt.% | 18.6 | 10.52 | 18.2 | 133.9 | 9.8 | 0.862 | 15.39 |
| 2.5 | 0.00 wt.% | 20.2 | 22.26 | 15.3 | 142.0 | 10.1 | 1.522 | 17.69 |
| | 0.25 wt.% | 16.2 | 17.82 | 13.8 | 125.6 | 12.6 | 1.442 | 13.99 |
| | 0.50 wt.% | 14.2 | 15.35 | 19.3 | 121.0 | 10.4 | 1.522 | 16.49 |
| | 1.50 wt.% | 14.4 | 16.42 | 14.4 | 114.2 | 11.8 | 1.582 | 14.29 |
| | 2.50 wt.% | 16.3 | 13.02 | 11.3 | 88.3 | 12.5 | 1.412 | 13.69 |
| 3.0 | 0.00 wt.% | 15.6 | 28.24 | 11.9 | 99.4 | 12.1 | 1.562 | 11.89 |
| | 0.25 wt.% | 12.1 | 20.98 | 17.0 | 86.9 | 18.0 | 2.082 | 16.19 |
| | 0.50 wt.% | 10.6 | 19.29 | 13.6 | 81.9 | 13.8 | 1.952 | 12.99 |
| | 1.50 wt.% | 12.1 | 19.27 | 14.2 | 80.8 | 14.3 | 1.822 | 13.69 |
| | 2.50 wt.% | 15.7 | 19.19 | 15.7 | 73.2 | 15.4 | 1.802 | 14.69 |
| 3.2 | 1.50 wt.% | 13.2 | 18.88 | 15.0 | 58.3 | 15.3 | 1.862 | 14.79 |
| | 2.50 wt.% | 10.9 | 21.39 | 17.3 | 56.8 | 17.8 | 2.642 | 16.59 |
| 3.5 | 0.00 wt.% | 15.0 | 29.19 | 17.5 | 60.2 | 17.4 | 2.292 | 17.39 |
| | 0.25 wt.% | 13.1 | 23.00 | 18.2 | 54.2 | 17.8 | 2.422 | 17.49 |
| | 0.50 wt.% | 10.4 | 27.44 | 16.8 | 56.4 | 16.7 | 2.632 | 16.89 |
| 4 | 0.00 wt.% | 14.2 | 31.79 | 18.7 | 41.4 | 19.1 | 2.622 | 17.59 |
| | 0.25 wt.% | 15.1 | 29.99 | 16.4 | 42.2 | 19.7 | 2.32 | 17.44 |

| Drawing ratio | Concentration of MPY | T [tex] | σ [cN.tex ⁻¹] | CV _{σ} [%] | ε [%] | CV _{ε} [%] | E [N.tex ⁻¹] | CV _E [%] |
|---------------|----------------------|---------|----------------------------------|---------------------------------------|-------------------|--|--------------------------|---------------------|
| 1.0 | 0.00 wt. % | 45.5 | 10.69 | 22.0 | 264.5 | 16.8 | 0.575 | 22.87 |
| | 0.25 wt. % | 39.3 | 9.65 | 19.7 | 236.4 | 16.0 | 0.505 | 22.47 |
| | 0.50 wt. % | 35.7 | 9.82 | 21.2 | 214.3 | 17.4 | 0.585 | 23.77 |
| | 1.50 wt. % | 35.3 | 10.01 | 23.4 | 194.2 | 15.8 | 0.545 | 20.67 |
| | 2.50 wt. % | 34.4 | 8.73 | 23.9 | 177.7 | 15.3 | 0.495 | 22.87 |
| 2.0 | 0.00 wt. % | 20.4 | 22.11 | 15.4 | 143.5 | 10.3 | 1.544 | 17.48 |
| | 0.25 wt. % | 16.4 | 17.67 | 13.9 | 127.1 | 12.8 | 1.464 | 13.78 |
| | 0.50 wt. % | 14.4 | 15.20 | 19.4 | 122.5 | 10.6 | 1.544 | 16.28 |
| | 1.50 wt. % | 14.6 | 16.27 | 14.5 | 115.7 | 12.0 | 1.604 | 14.08 |
| | 2.50 wt. % | 16.5 | 12.87 | 11.4 | 89.8 | 12.7 | 1.434 | 13.48 |
| 2.5 | 0.00 wt. % | 15.6 | 28.24 | 11.9 | 99.4 | 12.1 | 1.562 | 11.89 |
| | 0.25 wt. % | 12.1 | 20.98 | 17.0 | 86.9 | 18.0 | 2.082 | 16.19 |
| | 0.50 wt. % | 10.6 | 19.29 | 13.6 | 81.9 | 13.8 | 1.952 | 12.99 |
| | 1.50 wt. % | 12.1 | 19.27 | 14.2 | 80.8 | 14.3 | 1.822 | 13.69 |
| 3.0 | 0.00 wt. % | 15.6 | 28.24 | 11.9 | 99.4 | 12.1 | 1.562 | 11.89 |
| | 0.25 wt. % | 12.1 | 20.98 | 17.0 | 86.9 | 18.0 | 2.082 | 16.19 |
| | 0.50 wt. % | 10.6 | 19.29 | 13.6 | 81.9 | 13.8 | 1.952 | 12.99 |
| | 1.50 wt. % | 12.1 | 19.27 | 14.2 | 80.8 | 14.3 | 1.822 | 13.69 |
| 3.2 | 1.50 wt. % | 13.4 | 18.88 | 15.0 | 58.3 | 15.3 | 1.862 | 14.79 |
| 3.5 | 0.00 wt. % | 15.0 | 29.19 | 17.5 | 59.8 | 17.4 | 2.292 | 17.39 |
| | 0.25 wt. % | 13.1 | 23.00 | 18.2 | 56.6 | 17.8 | 2.422 | 17.49 |
| | 0.50 wt. % | 10.4 | 27.44 | 16.8 | 51.4 | 16.7 | 2.632 | 16.89 |
| 4 | 0.00 wt. % | 10.4 | 27.44 | 16.8 | 51.4 | 16.7 | 2.632 | 16.89 |
| | 0.25 wt. % | 14.2 | 31.79 | 18.7 | 41.4 | 19.1 | 2.622 | 17.59 |

Appendix- C: Energy measurement of Phptochrom-3 (30 minutes for exposure and 40 minutes for reversion phase)

| Time (min) | UV-off (Reversion Phase) | | | UV-on (Exposure Phase) | | |
|---------------|--------------------------|---|--------------------------------|------------------------|---|--------------------------------|
| | Luminous flux (Lx) | UV energy density ($\mu\text{W.cm}^{-2}$) | Temp ($^{\circ}\text{C}$) | Luminous flux (Lx) | UV energy density ($\mu\text{W.cm}^{-2}$) | Temp ($^{\circ}\text{C}$) |
| 00 | 50500 | 2.26 | 21.25 | 55082 | 669.2 | 21.31 |
| 05 | 55300 | 2.20 | 21.37 | 55050 | 649.5 | 21.32 |
| 10 | 55277 | 2.23 | 19.89 | 55071 | 612.5 | 21.51 |
| 15 | 55084 | 2.16 | 19.99 | 55058 | 773.1 | 20.19 |
| 20 | 55099 | 2.17 | 20.15 | 55014 | 649.1 | 20.14 |
| 25 | 55125 | 2.15 | 20.95 | 55066 | 652.2 | 20.86 |
| 30 | 55130 | 2.19 | 20.95 | 55058 | 653.8 | 20.94 |
| 35 | 55078 | 2.20 | 21.09 | 55071 | 775.4 | 20.11 |

Note: Two cycles of measurement were conducted and average value has been tabulated.

Appendix- D: Kinetic parameters of photochromic fabrics with respect to the first order kinetics.

| Pigment concentration | Precursor | Exposure phase | | | | Reversion phase | | | |
|-----------------------|-----------|----------------|------------|--------------|------------------|-----------------|------------|--------------|------------------|
| | | I_0 | I_∞ | $k (s^{-1})$ | $t_{1/2}$ (s) | I_0 | I_∞ | $k (s^{-1})$ | $t_{1/2}$ (s) |
| 0.25 wt. % | OTES | 0.1052 | 0.4878 | 0.03014 | 23 | 0.5321 | 0.1005 | 0.01650 | 42 |
| | O:P | 0.1112 | 0.3325 | 0.03151 | 22 | 0.3655 | 0.1250 | 0.01507 | 46 |
| | APS | 0.1012 | 0.2242 | 0.03151 | 22 | 0.2501 | 0.1110 | 0.01359 | 51 |
| | P:O | 0.0870 | 0.1772 | 0.03014 | 23 | 0.1899 | 0.0845 | 0.01333 | 52 |
| | PhTES | 0.0880 | 0.1787 | 0.02773 | 25 | 0.1875 | 0.0825 | 0.01216 | 57 |
| | | | | | | | | | |
| 0.50 wt. % | OTES | 0.1350 | 0.5985 | 0.03151 | 22 | 0.6821 | 0.1787 | 0.01733 | 40 |
| | O:P | 0.1290 | 0.4215 | 0.03301 | 21 | 0.4325 | 0.1242 | 0.01575 | 44 |
| | APS | 0.1210 | 0.2847 | 0.03014 | 23 | 0.2954 | 0.1220 | 0.01507 | 46 |
| | P:O | 0.1222 | 0.2240 | 0.02773 | 25 | 0.2511 | 0.1114 | 0.01386 | 50 |
| | PhTES | 0.1470 | 0.2333 | 0.02666 | 26 | 0.2442 | 0.1442 | 0.01284 | 54 |
| | | | | | | | | | |
| 1.00 wt. % | OTES | 0.1425 | 0.8214 | 0.03466 | 20 | 0.8322 | 0.1358 | 0.01824 | 38 |
| | O:P | 0.1325 | 0.5480 | 0.03466 | 20 | 0.6147 | 0.1335 | 0.01925 | 36 |
| | APS | 0.1254 | 0.4214 | 0.03151 | 22 | 0.4335 | 0.1258 | 0.01824 | 38 |
| | P:O | 0.1225 | 0.3547 | 0.02888 | 24 | 0.3899 | 0.1125 | 0.01540 | 45 |
| | PhTES | 0.1198 | 0.3014 | 0.02666 | 26 | 0.344 | 0.1185 | 0.01308 | 53 |
| | | | | | | | | | |
| 1.50 wt. % | OTES | 0.1440 | 1.0121 | 0.0407 | 17 | 1.1554 | 0.1350 | 0.02039 | 34 |
| | O:P | 0.1421 | 0.7858 | 0.0364 | 19 | 0.8422 | 0.1332 | 0.02166 | 32 |
| | APS | 0.1321 | 0.6425 | 0.0346 | 20 | 0.6522 | 0.1242 | 0.01980 | 35 |
| | P:O | 0.1312 | 0.5111 | 0.0330 | 21 | 0.5211 | 0.1236 | 0.01733 | 40 |
| | PhTES | 0.1298 | 0.43542 | 0.0301 | 23 | 0.4566 | 0.1225 | 0.01386 | 50 |

Note: Color shade intensity at the beginning (I_0), Color shade intensity at the infinitive (I_∞), Half-life ($t_{1/2}$), Rate constant (k).

| Pigment concentration | Precursor | Exposure phase | | | | Reversion phase | | | |
|--------------------------|-----------|----------------|------------|--------------|------------------|-----------------|------------|--------------|------------------|
| | | I_0 | I_∞ | $k (s^{-1})$ | $t_{1/2}$ (s) | I_0 | I_∞ | $k (s^{-1})$ | $t_{1/2}$ (s) |
| 2.00 wt. % | OTES | 0.1588 | 1.2221 | 0.04951 | 14 | 1.3755 | 0.1555 | 0.02666 | 26 |
| | O:P | 0.1475 | 0.8587 | 0.04951 | 14 | 0.9954 | 0.1454 | 0.02567 | 27 |
| | APS | 0.1385 | 0.6587 | 0.04621 | 15 | 0.7445 | 0.1335 | 0.02390 | 29 |
| | P:O | 0.1309 | 0.5447 | 0.04332 | 16 | 0.6444 | 0.1384 | 0.02100 | 33 |
| | PhTES | 0.1298 | 0.4787 | 0.03648 | 19 | 0.5577 | 0.1287 | 0.01691 | 41 |
| | | | | | | | | | |
| 2.50 wt. % | OTES | 0.1772 | 1.6021 | 0.05776 | 12 | 1.7045 | 0.1652 | 0.03301 | 21 |
| | O:P | 0.1658 | 0.9898 | 0.05776 | 12 | 1.2014 | 0.1455 | 0.02773 | 25 |
| | APS | 0.1457 | 0.6875 | 0.06301 | 11 | 0.8875 | 0.1389 | 0.02666 | 26 |
| | P:O | 0.1542 | 0.7450 | 0.04332 | 16 | 0.8244 | 0.1422 | 0.02310 | 30 |
| | PhTES | 0.1454 | 0.5550 | 0.04332 | 16 | 0.6355 | 0.1295 | 0.01925 | 36 |

Appendix- E: Physical properties of sol-gel coated fabric (MPP-2.5%).

| <i>Areal density ($g.m^{-2}$)</i> | Mean | SD | CV |
|--|-------|-------|-------|
| Raw | 170.7 | 0.46 | 363.9 |
| OTES | 172.9 | 2.49 | 69.2 |
| O:P | 171.6 | 0.78 | 219.4 |
| APS | 173.2 | 1.72 | 100.2 |
| P:O | 172.4 | 1.57 | 109.4 |
| PhTES | 172.9 | 1.80 | 95.8 |
| | | | |
| <i>Thickness (mm)</i> | | | |
| Raw | 0.326 | 0.002 | 143.1 |
| OTES | 0.328 | 0.003 | 104.9 |
| O:P | 0.361 | 0.008 | 40.2 |
| APS | 0.353 | 0.022 | 16.0 |
| P:O | 0.375 | 0.014 | 25.8 |
| PhTES | 0.334 | 0.001 | 198.7 |
| | | | |
| <i>Warp bending length (cm)</i> | | | |
| Raw | 3.7 | 0.069 | 53.9 |
| OTES | 5.0 | 0.119 | 41.9 |
| O:P | 6.1 | 0.131 | 46.1 |
| APS | 6.1 | 0.161 | 37.7 |
| P:O | 6.5 | 0.333 | 19.4 |
| PhTES | 6.7 | 0.107 | 62.3 |
| | | | |
| <i>Weft bending length (cm)</i> | 3.2 | 0.143 | 22.7 |
| Raw | 3.3 | 0.039 | 82.8 |
| OTES | 3.5 | 0.085 | 41.2 |
| O:P | 3.6 | 0.053 | 67.0 |
| APS | 3.7 | 0.118 | 31.3 |
| P:O | 3.5 | 0.152 | 22.8 |
| PhTES | 3.2 | 0.143 | 22.7 |

| <i>Warp flexural rigidity (mg.cm)</i> | Mean | SD | CV |
|--|--------|-------|-------|
| Raw | 949.9 | 11.3 | 84.0 |
| OTES | 1927.9 | 15.2 | 126.8 |
| O:P | 3420.9 | 16.3 | 209.7 |
| APS | 3902.1 | 202.9 | 19.2 |
| P:O | 4061.0 | 319.7 | 12.7 |
| PhTES | 5211.6 | 336.9 | 15.5 |
| | | | |
| <i>Weft flexural rigidity (mg.cm)</i> | | | |
| Raw | 543.1 | 4.0 | 134.6 |
| OTES | 664.1 | 14.5 | 45.7 |
| O:P | 751.9 | 26.9 | 28.0 |
| APS | 801.3 | 44.0 | 18.2 |
| P:O | 781.5 | 28.7 | 27.1 |
| PhTES | 883.0 | 59.8 | 14.8 |
| | | | |
| <i>Warp bending modulus (kg.cm⁻²)</i> | | | |
| Raw | 330.9 | 10.7 | 30.9 |
| OTES | 660.7 | 16.3 | 40.3 |
| O:P | 968.4 | 28.8 | 33.6 |
| APS | 890.1 | 51.5 | 17.3 |
| P:O | 1053.5 | 102.2 | 10.3 |
| PhTES | 1710.2 | 130.8 | 13.1 |
| | | | |
| <i>Weft bending modulus (kg.cm⁻²)</i> | | | |
| Raw | 184.1 | 8.9 | 20.5 |
| OTES | 218.6 | 9.2 | 23.7 |
| O:P | 204.3 | 14.3 | 14.2 |
| APS | 176.0 | 16.2 | 10.8 |
| P:O | 193.7 | 1.3 | 142.3 |
| PhTES | 277.6 | 30.1 | 9.0 |

| <i>Peak height (μm)</i> | Mean | SD | CV |
|---|--------|----------|-------|
| Raw | 1.756 | 0.019 | 92.0 |
| OTES | 2.080 | 0.046 | 44.9 |
| O:P | 3.811 | 0.131 | 29.2 |
| APS | 4.080 | 0.046 | 88.4 |
| P:O | 5.825 | 0.322 | 18.1 |
| PhTES | 9.292 | 0.092 | 100.0 |
| | | | |
| <i>Valley depth (μm)</i> | | | |
| Raw | 4.082 | 0.038 | 104.8 |
| OTES | 4.690 | 0.063 | 73.3 |
| O:P | 4.935 | 0.191 | 25.8 |
| APS | 4.830 | 0.086 | 55.6 |
| P:O | 6.413 | 0.072 | 88.4 |
| PhTES | 6.378 | 0.075 | 84.2 |
| | | | |
| <i>Maximum depth (μm)</i> | | | |
| Raw | 5.805 | 0.12588 | 46.1 |
| OTES | 6.690 | 0.090776 | 73.7 |
| O:P | 8.739 | 0.179387 | 48.7 |
| APS | 8.799 | 0.212321 | 41.4 |
| P:O | 12.523 | 0.231967 | 54.0 |
| PhTES | 15.483 | 0.154074 | 100.5 |

8.2 References

1. Khudyakov, I. V., N. J. Turro, and I. K. Yakushenko. 1992. Kinetics and mechanism of the photochromic transformations of N-salicylidene-4-hydroxy-3,5-dimethylaniline and its complex with uranium(VI) dioxide. *Journal of Photochemistry and Photobiology, A: Chemistry* 63: 25–31.
2. Bamfield, Peter, and Michael G. Hutchings. 2010. *Chromic Phenomena*. Royal Society of Chemistry. Cambridge: Royal Society of Chemistry.
3. White, Mary Anne, and Alex Bourque. 2013. Colorant, Thermochromic. In *Encyclopedia of Color Science and Technology*, ed. Ronnier Luo, 1–12. Springer New York.
4. He, Tao, and Jiannian Yao. 2006. Photochromism in composite and hybrid materials based on transition-metal oxides and polyoxometalates. *Progress in Materials Science* 51: 810–879.
5. Suda, Masayuki, and Yasuaki Einaga. 2013. *New Frontiers in Photochromism*. Edited by Masahiro Irie, Yasushi Yokoyama, and Takahiro Seki. First. Springer International Publishing.
6. Hadjoudis, Eugene. 1995. Photochromic and thermochromic anils. *Molecular Engineering* 5: 301–337.
7. Minkin, V I, V A Bren', and A É Lyubarskaya. 1990. *Organic Photochromes*. Edited by null. *Organic Photochromes*. Vol. null. Null. Consultants Bureau, New York.
8. Pardo, Rosario, Marcos Zayat, and David Levy. 2011. Photochromic organic–inorganic hybrid materials. *Chemical Society Reviews* 40: 672.
9. Gayen, Pallab, and Chittaranjan Sinha. 2012. Effect of phenols and carboxylic acids on photochromism of 1-alkyl-2-(aryloxy)imidazoles. *Journal of Luminescence* 132. Elsevier: 2371–2377.
10. Lee, Eun Mi, Seon Yeong Gwon, Byung Chul Ji, Sheng Wang, and Sung Hoon Kim. 2012. Photoswitching electrospun nanofiber based on a spironaphthoxazine-isophorone-based fluorescent dye system. *Dyes and Pigments* 92: 542–547.
11. Rawat, M.S.M., Sudagar Mal, and Pramod Singh. 2015. Photochromism in Anils - A Review. *Open Chemistry Journal* 2: 7–19.
12. Nigel Corns, S., Steven M. Partington, and Andrew D. Towns. 2009. Industrial organic photochromic dyes. *Coloration Technology* 125: 249–261.
13. Han, Jie, and Ji Ben Meng. 2009. Progress in synthesis, photochromism and

- photomagnetism of biindenylidenedione derivatives. *Journal of Photochemistry and Photobiology C: Photochemistry Reviews* 10: 141–147.
14. Frick, Manuela. 2008. Dissertation: Photochrome Textilien - Herstellung und Eigenschaften. Edited by null. Null. Universität Stuttgart, Germany.
 15. Hertel, Ingolf V., and Claus-Peter Schulz. 2015. *Atoms, Molecules and Optical Physics* 2. Edited by William T Rhodes Richard Needs. First. Berlin: Springer-Verlag Berlin.
 16. Vikova, Martina. 2011. Photochromic textiles. Edited by null. Null. Heriot-Watt University, Scottish Borders Campus, Edinburgh, UK.
 17. Bouas-Laurent, Henri, and Heinz Dürr. 2001. Organic photochromism (IUPAC Technical Report). *Pure and Applied Chemistry* 73: 639–665.
 18. Vikova, Martina. 2009. Chromic Materials , Phenomena and their Technological Applications Methodology of measurement of chromic materials. In , ed. null, First, null:509–534. Null. Pune: Applied Science Innovations Pvt Ltd, India.
 19. Vikova, Martina, and Vik, Michal. 2013. Colorimetric Properties of Photochromic Textiles. *Applied Mechanics and Materials* 440: 260–265.
 20. E, Jacobson R. 1989. Photochromic Imaging. In *Photopolymerisation and photoimaging science and technology*, ed. N. S. Allen, 149–186. Dordrecht.
 21. Rasheed, Ayesha. 2008. Molecular Modelling Aided Design and Synthesis of Photochromic Dyes Containing a Permanent Chromophore. Heriot-Watt University.
 22. Vikova, Martina, and Vik, Michal. 2011. Alternative UV Sensors Based on Color-Changeable Pigments. *Advances in Chemical Engineering and Science* 01: 224–230.
 23. Zhang, Changrui, Zhibin Zhang, Meigong Fan, and Wenpeng Yan. 2008. Positive and negative photochromism of novel spiro[indoline-phenanthroline-oxazines]. *Dyes and Pigments* 76: 832–835.
 24. Lisyutenko, V. N., V. A. Barachevskii, A. A. Pankratov, and G. G. Konoplev. 1990. Excitation-energy relaxation in photochromic indoline spiropyranes. *Theoretical and Experimental Chemistry* 25: 390–395.
 25. Crano, John C., and Robert J. Guglielmetti. 2002. *Organic Photochromic and Thermochromic Compounds*. Vol. 1. New york, USA: Kluwer Academic Publishers, New York, USA.
 26. Ono, H, and C Osada. 1970. Photochromic spiro compounds. *Application: GB*.
 27. Arnold, G, and H. P Vollmer. 1970. Spiro[benzothiazole(or indoline)-2,3'-[3H]naphth[2,1-b][1,4]oxazines]. Germany.
 28. Heller, Harold G. 1980. Photochromic compounds. *U.S. Google Patents*.

29. Heller, Harold G. 1980. Photochromic compounds. U.S. Google Patents.
30. Vikova, Martina, Vik, Michal and Periyasamy A.P. 2015. Optical properties of photochromic pigment incorporated Polypropylene (PP) filaments:- influence of pigment concentrations & drawing ratio. In *Workshop for Ph.D Students of Textile Engineering and Faculty of Mechanical Engineering, Technical University of Liberec.*, 3:140–145. Pardubice-Czech Republic: University of Pardubice.
31. Tao, Xiaoming. 2015. Handbook of smart textiles. In *Handbook of Smart Textiles*, ed. Xiaoming Tao, 1–1058. Singapore: Springer International Publishing.
32. Billah, Shah M Reduwan, Robert M. Christie, and Renzo Shamey. 2008. Direct coloration of textiles with photochromic dyes. Part 1: Application of spiroindolinonaphthoxazines as disperse dyes to polyester, nylon and acrylic fabrics. *Coloration Technology* 124: 223–228.
33. Billah, Shah M.Reduwan, Robert M. Christie, and Keith M. Morgan. 2008. Direct coloration of textiles with photochromic dyes. Part 2: The effect of solvents on the colour change of photochromic textiles. *Coloration Technology* 124: 229–233.
34. Crano, J. C., Guglielmetti, R. J. 2002. *Organic Photochromic and Thermochromic Compounds*. First. Vol. 2. Kluwer Academic Publishers, New York, USA.
35. Lenoble, Christian, and Ralph S. Becker. 1986. Photophysics, photochemistry, kinetics, and mechanism of the photochromism of 6'-nitroindolinospiropyran. *Journal of Physical Chemistry* 90. American Chemical Society: 62–65.
36. Wyszecki, Gunter, and W. S. Stiles. 1983. *Color Science: Concepts and Methods, Quantitative Data and Formulae*. John Wiley and Sons, New York.
37. van Santen, R. A., and J. W. Niemantsverdriet. 1995. *Chemical Kinetics and Catalysis*. Edited by R. A. Van Santen and J. W. Niemantsverdriet. *Springer Science+Business Media, LLC*. First. Springer International Publishing.
38. Vorobiev, Andrey Kh, and Denis Menshykau. 2008. Kinetics of photochemical reactions in optically dense media with reagent diffusion. *Journal of Photochemistry and Photobiology A: Chemistry* 199: 303–310.
39. Appel, C, D Rhue, L Ma, and B Reve. 2002. Heats of K/Ca and K/Pb exchange in two tropical soils as measured by flow calorimetry. *Soil Science* 167: 773–781.
40. Janus, Krzysztof, Juliusz Sworakowski, Andrzej Olszowski, Aleksandra Lewanowicz, Józef Lipiński, Elzbieta Luboch, and Jan Biernat. 1999. Kinetics of a photochromic reaction in a dibenzoazo crown ether in solution and in polymer matrices. *Advanced Materials for Optics and Electronics* 9. John Wiley & Sons, Ltd.: 181–187.

41. Janus, Krzysztof, Juliusz Sworakowski, and Elzbieta Luboch. 2002. Kinetics of photochromic reactions in a 10-membered dibenzoazo crown ether. *Chemical Physics* 285: 47–54.
42. Janus, Krzysztof, Igor A. Koshets, Juliusz Sworakowski, and Stanislav Nešpůrek. 2002. An approximate non-isothermal method to study kinetic processes controlled by a distribution of rate constants: the case of a photochromic azobenzene derivative dissolved in a polymer matrix. *Journal of Materials Chemistry* 12. The Royal Society of Chemistry: 1657–1663.
43. Janus, Krzysztof, Katarzyna Matczyszyn, and Juliusz Sworakowski. 2002. Kinetics of photochemical processes in photochromic azobenzene derivatives . Effect of matrix and of the phase stability. *Materials Science- Poland* 20: 45–55.
44. Janus, Krzysztof, Juliusz Sworakowski, and Elbieta Luboch. 2002. Kinetics of photochromic reactions in a 10-membered dibenzoazo crown ether. *Chemical Physics* 285: 47–54.
45. Sworakowski, J., K. Janus, and S. Nešpůrek. 2005. Kinetics of photochromic reactions in condensed phases. *Advances in Colloid and Interface Science* 116: 97–110.
46. Rupp, Romano A., Baoli Yao, Yuan Zheng, Neimule Menke, Yingli Wang, Weibin Dong, Wei Zhao, et al. 2007. Absorbance kinetics of dye-doped systems with photochemical first order kinetics. *Physica Status Solidi (B) Basic Research* 244: 2138–2150.
47. Mancheva, I., I. Zhivkov, and S. Nešpůrek. 2005. Kinetics of the photochromic reaction in a polymer containing azobenzene groups. *Journal of Optoelectronics and Advanced Materials* 7: 253–256.
48. Vikova, Martina, and Vik, Michal. 2014. Photochromic Textiles and Measurement of Their Temperature Sensitivity. *Research Journal of Textile and Apparel* 18: 15–21.
49. Maafi, Mounir. 2008. Useful spectrokinetic methods for the investigation of photochromic and thermo-photochromic spiropyrans. *Molecules* 13: 2260–2302.
50. Gauglitz, G. 2003. Photophysical, Photochemical and Photokinetic Properties of Photochromic Systems. In *Photochromism: Molecules and Systems*, ed. Heinz Dürr and Bouas Lament Henri, 15–63. Elsevier BV.
51. Viková, Martina. 2004. Visual assessment of UV radiation by colour changeable textile sensors. In *Colour and Paints*, ed. José Luis Caivano and Hanns-Peter Struck., 129–133. Porto Alegre, Brazil: Associação Brasileira da Cor.
52. Tong Cheng, Tong Lin, Jian Fang, and R. Brady. 2006. Photochromic Wool Fabrics

- from a Hybrid Silica Coating. In *Proceedings of 2006 China International Wool Textile Conference & IWTO Wool Forum, Xi'an, China, 2006*, 33–37. Xi'an, China: China International Wool Textile Conference & IWTO Wool Forum.
53. Wilkinson, A, and A McNaught. 2009. *IUPAC Compendium of Chemical Terminology*. 2nd ed.
54. Vikova, Martina, Vik, Michal and R.M. Christie. 2014. Unique device for measurement of photochromic textiles. *Research Journal of Textile and Apparel* 18: 6–14.
55. Joshi, M, and B S Butola. 2013. Application technologies for coating, lamination and finishing of technical textiles. In *Advances in the Dyeing and Finishing of Technical Textiles*, ed. M. L. Gulrajani, 355–411.
56. Springsteen, Art. 1999. Introduction to measurement of color of fluorescent materials. *Analytica Chimica Acta* 380: 183–192.
57. Vik, Michal, and Martina Vikova. 2007. Equipment for monitoring of dynamism of irradiation and decay phase of photochromic substances. Czech Republic.
58. Viková, Martina, and Vik, Michal. 2015. The determination of absorbance and scattering coefficients for photochromic composition with the application of the black and white background method. *Textile Research Journal* 85: 1961–1971.
59. Viková, Martina, and Vik, Michal. 2015. Description of photochromic textile properties in selected color spaces. *Textile Research Journal* 85: 609–620.
60. Roy S. Berns. 2001. *Billmeyer and Saltzman's principles of color technology*. Wiley-VCH Verlag GmbH & Co. KGaA.
61. Vikova, Martina, and Vik, Michal. 2015. Description of photochromic textile properties in selected color spaces. *Textile Research Journal* 85: 609–620. doi:10.1177/0040517514549988.
62. Hamielec, Archie E, and Joao B P Soares. 1999. Metallocene catalyzed polymerization : industrial technology. In *Polypropylene : An A-Z Reference*, ed. J. Karger-Kocsis, 446–453. Dordrecht: Springer Netherlands.
63. Sterzynski, Tomasz. 1999. Lamella dimension and distribution. In *Polypropylene: An A–Z Reference*, ed. J. Karger-Kocsis, 374–382. Dordrecht: Springer Netherlands.
64. Kunugi, Toshio. 1999. High-modulus and high-strength polypropylene fibers and films. In *Polypropylene: An A–Z Reference*, ed. J. Karger-Kocsis, 295–300. Dordrecht: Springer Netherlands.
65. Spruiell, J.E., and Eric Bond. 1999. Melt Spinning of Polypropylene. In *Polymer Science and Technology Series: Polypropylene*, ed. J. Karger-Kocsis, 2:427–439. Dordrecht:

- Springer Netherlands.
66. Dubey, SatyaKesh, Naina Narang, Parmendra Singh Negi, and Vijay Narain Ojha. 2018. Measurement Results. In , ed. Satya Kesh Dubey, Naina Narang, P. S. Negi, and V. N. Ojha, 35–42. Singapore: Springer Singapore.
 67. Vik, Michal. 2017. *Colorimetry in Textile Industry*. VUTS, Liberec, Czech Republic.
 68. Shamiri, Ahmad, Mohammed H. Chakrabarti, Shah Jahan, Mohd Azlan Hussain, Walter Kaminsky, Purushothaman V. Aravind, and Wageeh A. Yehye. 2014. The influence of Ziegler-Natta and metallocene catalysts on polyolefin structure, properties, and processing ability. *Materials* 7: 5069–5108.
 69. Ujhelyiova, Anna, Eva Bolhova, Janka Oravkinova, Radovan Tiño, and Anton Marcinčin. 2007. Kinetics of dyeing process of blend polypropylene/polyester fibres with disperse dye. *Dyes and Pigments* 72: 212–216. doi:10.1016/j.dyepig.2005.08.026.
 70. Marcinčin, Anton. 1999. Dyeing of polypropylene fibers. In *Polypropylene: An A-Z reference*, ed. J. Karger-Kocsis, 172–177. Dordrecht: Springer Netherlands.
 71. Yaman, Necla, Esen Özdoğan, and Necdet Seventekin. 2011. Atmospheric plasma treatment of polypropylene fabric for improved dyeability with insoluble textile dyestuff. *Fibers and Polymers* 12: 35–41.
 72. Burkinshaw, S. M., P. E. Froehling, and M. Mignanelli. 2002. The effect of hyperbranched polymers on the dyeing of polypropylene fibres. *Dyes and Pigments* 53: 229–235.
 73. Teli, M D, R V Adivarekar, V Y Ramani, and A G Sabale. 2004. Imparting disperse and cationic dyeability to polypropylene through melt blending. *Fibers and Polymers* 5: 264–269.
 74. Kamata, Masayasu, Hiromi Suno, Toshihisa Maeda, and Ryuichi Hosikawa. 1993. Reversibly variable color patterning composition for synthetic resin articles. Japan.
 75. Kamada, Masayasu, and Shozo Suefuku. Photochromic materials. Japan.
 76. Kong, Y., and Y. N. Hay. 2002. The measurement of cristalinity of polymers by DSC. *Polymer* 43: 3873–3878.
 77. Choudhury, Asim Kumar Roy. 2014. Colour and appearance attributes. In *Principles of Colour Appearance and Measurement. Volume 1: Object Appearance, Colour Perception and Instrumental Measurement*, ed. Asim Kumar Roy Choudhury, 103–143. Woodhead Publishing.
 78. El Sherif, M., O. A. Bayoumi, and T. Z.N. Sokkar. 1997. Prediction of absorbance from reflectance for an absorbing-scattering fabric. *Color Research and Application* 22.

- Wiley Subscription Services, Inc., A Wiley Company: 32–39.
79. Bohne, Cornelia, and Reginald H. Mitchell. 2011. Characterization of the photochromism of dihydropyrenes with photophysical techniques. *Journal of Photochemistry and Photobiology C: Photochemistry Reviews* 12: 126–137.
 80. Danilova Volkovskaya G M. 2002. Technological aspects of the production of oriented polypropylene strip. *International Polymer Science and Technology* 30: 65–67.
 81. Brückner, Sergio, Stefano V. Meille, Vittorio Petraccone, and Beniamino Pirozzi. 1991. Polymorphism in isotactic polypropylene. *Progress in Polymer Science* 16: 361–404.
 82. Xu, Jun Ting, Fang Xiao Guan, Tariq Yasin, and Zhi Qiang Fan. 2003. Isothermal Crystallization of Metallocene-Based Polypropylenes with Different Isotacticity and Regioregularity. *Journal of Applied Polymer Science* 90. Wiley Subscription Services, Inc., A Wiley Company: 3215–3221.
 83. Mai, Y W, B Cotterell, and J Fante. 1982. Effect of cold extrusion and heat treatment on the mechanical properties of polypropylene. *Matériaux et Construction* 15: 99–106.
 84. De Vries, Albert J. 1983. Structure properties relationships in biaxially oriented polypropylene films. *Polymer Engineering & Science* 23: 241–246.
 85. Nadella, Hari P., Joseph E. Spruiell, and James L. White. 1978. Drawing and annealing of polypropylene fibers: Structural changes and mechanical properties. *Journal of Applied Polymer Science* 22: 3121–3133.
 86. Samuels, Robert J. 1975. Quantitative structural characterization of the melting behavior of isotactic polypropylene. *Journal of Polymer Science: Polymer Physics Edition* 13. John Wiley & Sons, Inc.: 1417–1446.
 87. Peijs, Ton, Tilo Schimanski, and Joachim Loos. 2005. Processing of single polymer composites using the concept of constrained fibers. *Polymer Composites* 26. Wiley Subscription Services, Inc., A Wiley Company: 114–120.
 88. Horrocks, Richard, Ahilan Sitpalan, Chen Zhou, and Baljinder K Kandola. 2016. Flame Retardant Polyamide Fibres: The Challenge of Minimising Flame Retardant Additive Contents with Added Nanoclays. *Polymers* 8.
 89. Gupta, V. B. 1997. Melt-spinning processes. In *Manufactured Fibre Technology*, ed. V. B. Gupta and V. K. Kothari, 67–97. Dordrecht: Springer Netherlands.
 90. Gupta, V B, and Y C Bhuvanesh. 1997. Basic principles of fluid flow during fibre spinning. In *Manufactured Fibre Technology*, ed. V. B. Gupta and V. K. Kothari, 31–66. Dordrecht: Springer Netherlands.
 91. Silberman, A., E. Raninson, I. Dolgopolsky, and S. Kenig. 1995. The effect of pigments

- on the crystallization and properties of polypropylene. *Polymers for Advanced Technologies* 6: 643–652.
92. Todoki, Minoru, and Tatsuro Kawaguchi. 1977. Origin of double melting peaks in drawn nylon 6 yarns. *Journal of Polymer Science: Polymer Physics Edition* 15. John Wiley & Sons, Inc.: 1067–1075.
 93. Loos, J., T. Schimanski, J. Hofman, T. Peijs, and P. J. Lemstra. 2001. Morphological investigations of polypropylene single-fibre reinforced polypropylene model composites. *Polymer* 42: 3827–3834.
 94. Alcock, B, N O Cabrera, N.-M. Barkoula, C T Reynolds, L E Govaert, and T Peijs. 2007. The effect of temperature and strain rate on the mechanical properties of highly oriented polypropylene tapes and all-polypropylene composites. *Composites Science and Technology* 67: 2061–2070.
 95. Wu, Linda Y.L., Q. Zhao, H. Huang, and R. J. Lim. 2017. Sol-gel based photochromic coating for solar responsive smart window. *Surface and Coatings Technology* 320: 601–607.
 96. Chen, Zhong, and Linda Y.L. Wu. 2013. Scratch damage resistance of silica-based sol-gel coatings on polymeric substrates. In *Tribology of Polymeric Nanocomposites: Friction and Wear of Bulk Materials and Coatings: Second Edition*, 467–511. Oxford: Elsevier.
 97. Yi, G.-C., T. Yatsui, M. Ohtsu, and RJ. Groarke. 2016. ZnO Nanorods and their Heterostructures for Electrical and Optical Nanodevice Applications. In *Reference Module in Materials Science and Materials Engineering*, 335–374. Elsevier.
 98. Hou, L., and H. Schmidt. 1996. Photochromic properties of a silylated spirooxazine in sol-gel coatings. *Materials Letters* 27: 215–218. doi:10.1016/0167-577X(95)00287-1.
 99. Tomonaga, Hiroyuki, and Takeshi Morimoto. 2001. Photochromic coatings including silver halide microcrystals via sol-gel process. *Thin Solid Films* 392: 355–360.
 100. Hu, J. L., and J. Lu. 2016. Memory polymer coatings for smart textiles. In *Active Coatings for Smart Textiles*, 11–34. Elsevier.
 101. Hu, J.L. 2016. Introduction to active coatings for smart textiles. In *Active Coatings for Smart Textiles*, 1–7. Elsevier.
 102. Wang, C., and Y. Yin. 2016. Functional modification of fiber surface via sol-gel technology. In *Active Coatings for Smart Textiles*, 301–328. Elsevier.
 103. Sahoo, P., S. K. Das, and J. Paulo Davim. 2016. Surface Finish Coatings. In *Comprehensive Materials Finishing*, 3–3:38–55. Oxford: Elsevier..

104. Tong Cheng, Tong Lin, Jian Fang, and Rex Brady. 2007. Photochromic Wool Fabrics from a Hybrid Silica Coating. *Textile Research Journal* 77: 923–928.
105. Parhizkar, M, Y Zhao, X Wang, and T Lin. 2014. Photostability and Durability Properties of Photochromic Organosilica Coating on Fabric. *Journal of Engineered Fibers and Fabrics* 9: 65–73.
106. Zhang, Qiu Ping, Bin Jie Xin, and Lan Tian Lin. 2013. Preparation and Characterisation of Electrochromic Fabrics Based on Polyaniline. *Advanced Materials Research* 651. Trans Tech Publications: 77–82.
107. Parhizkar, M, Y Zhao, X Wang, and T Lin. 2014. No Title. *J. Eng. Fibers Fabrics* 9: 65.
108. Tao, Xiaoming. 2015. *Handbook of smart textiles*. Edited by null. *Handbook of Smart Textiles*. Vol. null. Null.
109. Cheng, Tong, Tong Lin, Rex Brady, and Xungai Wang. 2008. Fast response photochromic textiles from hybrid silica surface coating. *Fibers and Polymers* 9: 301–306.
110. Shim, E. 2013. Bonding requirements in coating and laminating of textiles. In *Joining Textiles*, 309–351. Woodhead Publishing.
111. Meirowitz, R. 2010. Microencapsulation technology for coating and lamination of textiles. In *Smart Textile Coatings and Laminates*, 125–154. Elsevier.
112. Sol-gel process. 2017. *wikipedia*. https://en.wikipedia.org/wiki/Sol-gel_process. Accessed July 10.
113. Lammens, Nicolas, Mathias Kersemans, Geert Luyckx, Wim Van Paepegem, and Joris Degrieck. 2014. Improved accuracy in the determination of flexural rigidity of textile fabrics by the Peirce cantilever test (ASTM D1388). *Textile Research Journal* 84: 1307–1314.
114. Peirce, F. T. 1930. The handle of cloth as a measurable quantity. *Journal of the Textile Institute Transactions* 21. Taylor & Francis: T377–T416.
115. Pardo, Rosario, Marcos Zayat, and David Levy. 2006. Temperature dependence of the photochromism of naphthopyrans in functionalized sol-gel thin films. *J. Mater. Chem.* 16. The Royal Society of Chemistry: 1734–1740.
116. Pardo, Rosario, Marcos Zayat, and David Levy. 2012. Stability against photodegradation of a photochromic spirooxazine dye embedded in amino-functionalized sol-gel hybrid coatings. *Journal of Sol-Gel Science and Technology* 63: 400–407.

117. Pardo Martínez, Clara Inés. 2010. Energy use and energy efficiency development in the German and Colombian textile industries. *Energy for Sustainable Development* 14: 94–103.
118. Alvarez-Herrero, Alberto, Daniel Garranzo, Rosario Pardo, Marcos Zayat, and David Levy. 2008. Temperature dependence of the optical and kinetic properties of photochromic spirooxazine derivatives in sol-gel thin films. *physica status solidi (c)* 5. WILEY-VCH Verlag: 1160–1163.
119. Pardo, Rosario, Marcos Zayat, and David Levy. 2009. Reaching bistability in a photochromic spirooxazine embedded sol-gel hybrid coatings. *J. Mater. Chem.* 19. The Royal Society of Chemistry: 6756–6760.
120. Li, Fengyan, Yanjun Xing, and Xin Ding. 2008. Silica xerogel coating on the surface of natural and synthetic fabrics. *Surface and Coatings Technology* 202: 4721–4727.
121. Pardo, Rosario, Marcos Zayat, and David Levy. 2008. Effect of the chemical environment on the light-induced degradation of a photochromic dye in ormosil thin films. *Journal of Photochemistry and Photobiology A: Chemistry* 198: 232–236.
122. Chambers, R Carlisle, Wayne E Jones, Yair Haruvy, Stephen E Webber, and Marye Anne Fox. 1993. Influence of steric effects on the kinetics of ethyltrimethoxysilane hydrolysis in a fast sol-gel system. *Chemistry of Materials* 5: 1481–1486.
123. Gallo, T A, and LC Klein. 1986. Apparent Viscosity of Sol - Gel Processed Silica. *Journal of Non-Crystalline Solids* 82: 198–204.
124. Kellmann, A., F. Tfibel, R. Dubest, P. Levoir, J. Aubard, E. Pottier, and R. Guglielmetti. 1989. Photophysics and kinetics of two photochromic indolinospirooxazines and one indolinospironaphthopyran. *Journal of Photochemistry and Photobiology, A: Chemistry* 49: 63–73.
125. Billah, Shah M Reduwan, Robert M Christie, and Keith M Morgan. 2008. Direct coloration of textiles with photochromic dyes. Part 2: The effect of solvents on the colour change of photochromic textiles . *Coloration Technology* 124: 229–233.
126. Christie, R.M., Christian K.Agyako, and Kevin Mitchell. 1995. An investigation of the electronic spectral properties of the merocyanines derived from photochromic spiroindolinonaphth[2,1-b][1,4]oxazines. *Dyes and Pigments* 29: 241–250.
127. Hoten, Masanobu, Yukio Kojima, and Taisuke Ito. 1992. Halochromism of acrylic fibres dyed with some disperse dyes. *Journal of the Society of Dyers and Colourists* 108. Blackwell Publishing Ltd: 21–28.
128. Partington, Steven M., and Andrew D. Towns. 2014. Photochromism in

- spiroindolinonaphthoxazine dyes: Effects of alkyl and ester substituents on photochromic properties. *Dyes and Pigments* 104. Elsevier Ltd: 123–130.
129. Van Der Schueren, Lien, Karen Hemelsoet, Veronique Van Speybroeck, and Karen De Clerck. 2012. The influence of a polyamide matrix on the halochromic behaviour of the pH-sensitive azo dye Nitrazine Yellow. *Dyes and Pigments* 94: 443–451.
130. Christie, Robert M., Keith M. Morgan, Ayesha Rasheed, Mohanad Aldib, and Georgina Rosair. 2013. The molecular design, synthesis and photochromic properties of spirooxazines containing a permanent azo (hydrazone) chromophore. *Dyes and Pigments* 98: 263–272.
131. Guglielmi, Massimo, and Stefano Zenezini. 1990. The Thickness of Sol-Gel Silica Coating Obtained by dipping. *Journal of Non-Crystalline Solids* 121: 303–309.
132. Pierre, Alain C. 1998. Gelation. In , ed. Alain C. Pierre, 169–204. Boston, MA: Springer US.
133. Pierre, Alain C. 1998. Applications of Sol-Gel Processing. In , ed. Alain C. Pierre, 347–386. Boston, MA: Springer US.
134. Cisneros-Zevallos, L, and J M Krochta. Dependence of Coating Thickness on Viscosity of Coating Solution Applied to Fruits and Vegetables by Dipping Method. *Journal of Food Science* 68: 503–510.

List of Publications

Research Manuscripts

- [1] Periyasamy Aravin Prince, Vikova Martina, Vik Michal. 2016. Optical properties of photochromic pigment incorporated into polypropylene filaments. *Vlakna a Textil* 23:171–178. [Impact factor=0.3]
- [2] Viková Martina, Periyasamy Aravin Prince, Vik Michal and Ujhelyiová Anna. 2017. Effect of drawing ratio on difference in optical density and mechanical properties of mass colored photochromic polypropylene filaments. *Journal of Textile Institute* 108:1365–1370. [Impact factor=0.8]
- [3] Periyasamy Aravin Prince, Vikova Martina, Vik Michal. 2017. A review of photochromism in textiles and its measurement. *Textile Progress* 49:53–136. [Scopus and Thomson Reuters included]
- [4] Seipel Sina, Yu Jhu, Periyasamy Aravin Prince, et al. 2017. Characterization and optimization of an inkjet-printed smart textile UV-sensor cured with UV-LED light. *IOP Conference Series of Material Science Engineering* 254:1–4. [Scopus and Thomson Reuters included]
- [6] Periyasamy Aravin Prince, Vikova Martina, Vik Michal. Photochromic polypropylene filaments: Impacts of physical and mechanical properties on kinetic properties. *Fibers Textile Eastern Europe*. Under review [Impact factor =0.45]
- [7] Periyasamy Aravin Prince, Vikova Martina, Vik Michal. Organosilica coated photochromic polyethylene terephthalate (PET) fabrics with their kinetic and physical properties. *Journal of Sol-Gel Science Technology*. Under review [Impact factor =1.68]
- [8] Seipel Sina, Yu Jhu, Periyasamy Aravin Prince, et al. Optimization of an inkjet-printed smart textile UV-sensor cured with UV-light using production process parameters. *Applied Surface Science*. Under review [Impact factor =3.44]
- [9] Seipel Sina, Yu Jhu, Periyasamy Aravin Prince, et al. Inkjet printing and UV-LED curing of a smart textile UV-sensor using photochromic dye. *Journal of Materials Chemistry C*. 0Under review [Impact factor =5.96]

Book Chapter

- [10] Seipel Sina, Yu Jhu, Periyasamy Aravin Prince, et al. 2018. Resource-Efficient Production of a Smart Textile UV Sensor Using Photochromic Dyes: Characterization

and Optimization. In: Kyosev Y, Mahltig B, Schwarz-Pfeiffer A (eds) *Narrow Smart Textile*. Springer International Publishing, Cham, pp 251–257

Book

- [11] Vik Michal, Periyasamy Aravin Prince, Vikova Martina (ed). 2018. *Chromic Materials: Fundamentals, Measurements, and Applications.*, Apple Academic Press (Under CRC press), New Jersey, USA.





International Conferences / Workshops

- [12] Vik Michal, Vikova Martina, Periyasamy Aravin Prince. Influence of SPD on Whiteness value of FWA treated samples. *21st International Conference Light SVĚTLO 2015*, Brno Univ. Technol. Czech Republic, Vol. 1; 2015, p.5.
- [13] Vikova Martina, Vik Michal, Periyasamy Aravin Prince. Optical properties of photochromic pigment incorporated Polypropylene (PP) filaments:- influence of pigment concentrations & drawing ratio. *Work. PhD Students Textile Engineering and Mechanical Engineering*, Technical University Liberec, Liberec.; 2015, p. 140–145.
- [14] Periyasamy Aravin Prince, Vikova Martina, Vik Michal. Problems in kinetic measurement of mass dyed Photochromic Polypropylene filaments with respect to different color space systems. *4th CIE Expert Symposium Color Visual Appearance.*, Prague: CIE- Austria; 2016, p. 325–333.
- [15] Periyasamy Aravin Prince, Vikova Martina, Vik Michal Optical properties of photochromic pigment incorporated polypropylene filaments:- Influence of pigment concentrations and drawing ratios. *24th International Federation Association of Textile Chemistry Color Congress.*, Pardubice-Czech Republic: University of Pardubice; 2016.
- [16] Seipel S, Yu Jhu, Nierstrasz V, Periyasamy AP et al. Characterization and optimization of an inkjet-printed smart textile UV-sensor cured with UV-LED light. *AUTEX World Textile Conference.*, Corfu, Greece: 2017.
- [17] Vikova Martina, Periyasamy Aravin Prince, et al. Color-changeable sensorial fibers, fastness and dynamic properties. *Asia Africa Science Platform Program Seminar Series 10*, Kyoto: Kyoto Institute of Technology, Japan; 2017.
- [18] Periyasamy Aravin Prince, Vikova Martina, Vik Michal. Sol-gel photochromic fabrics. *9th Central European Conference, Liberec*: Technical University Liberec, Liberec.; 2017, p. 94–98.

Curriculum Vitae

PERSONAL INFORMATION

Aravin Prince Periyasamy

 Harur, Dharmapuri, TN, India.
 +420 775 48 60 50
 aravinprince@gmail.com
 <http://aravinprince.weebly.com/>
Sex Male | Date of birth 10/06/1983 | Nationality Indian

WORK EXPERIENCE

- | | |
|----------------------|--|
| Aug 2011- Nov 2014 | <i>Assistant Professor</i> DKTE Textile Engineering Institute, Ichalkaranji, MH, India <ul style="list-style-type: none">Teaching and Research in the field of Textile chemical processing.Color chemistry, Chromic materials, Denim processing. |
| July 2007- July 2009 | <i>Production Executive</i> Texport Syndicate, Bangalore, India <ul style="list-style-type: none">Production & Research activities on denim processing textile dyeing.Sustainability in wet processing, LCA on denim processing. |
| May 2003- June 2004 | <i>Production Executive</i> MS Dyeing House, Tirupur, India <ul style="list-style-type: none">Handling with textile fabric dyeing and finishing. |
-
- | | |
|-------------------------|---|
| December 2014 - Present | <i>Ph.D in Textile Techniques and Material Engineering</i> <i>Technical University of Liberec, Czech Republic.</i> <ul style="list-style-type: none">Working on the photochromic materials and their kinetics.Sol-gel coating, properties of photochromic materials. |
| Aug 2009 - July 2011 | <i>Masters in Textile Technology</i> <i>Anna University, Chennai, India.</i> <ul style="list-style-type: none">Developments in fiber formation, Advanced chemical processing.Sustainability in textiles, LCA, Green fashion.Defibrillation on Lyocell fiber. |
| July 2004 - July 2007 | <i>Bachelors in Textile Technology</i> <i>Anna University, Chennai, India.</i> <ul style="list-style-type: none">Fiber formation, Spinning, Weaving, Chemical processing, Garmenting.Sustainable processing. |
-

PERSONAL SKILLS

- | | |
|----------------------------------|---|
| Communication skills | <ul style="list-style-type: none">Good communication skills gained through my previous experiences. |
| Organizational managerial skills | <ul style="list-style-type: none">Leadership (Motivating & Inspiring my teams through positive attitude)Mentoring (Conducted the mentoring activity to group of my students).Organization (Conducted technical symposium and conference). |
| Digital competence | <ul style="list-style-type: none">Good command of office suite.Good command of statistical and analytical software's like Originlab, MATLAB, SPSS, Minitab, Graph pad and ANSYS.LCA software's like Umberto, GaBi, SimaPro and openLCA. |